MECHANISMS OF GLUCAGON SECRETION

IN MOUSE PANCREATIC α-CELLS

by

Sylvain Jacques Le Marchand

Dissertation

Submitted to the Faculty of the

Graduate School of Vanderbilt University

in partial fulfillment of the requirements

for the degree of

DOCTOR OF PHILOSOPHY

in

Molecular Physiology and Biophysics

May, 2011

Nashville, Tennessee

Approved:

Professor Albert H. Beth

Professor Roger J. Colbran

Professor Anne K. Kenworthy

Professor Owen P. McGuinness

Professor Alvin C. Powers

A mes parents, Jacqueline et Patrice,

A ma soeur Bérénice, à ma nièce Willa,

A ma femme Elena.

Je vous remercie pour votre amour.

ACKNOWLEDGEMENTS

I am heartily thankful to my mentor, Dave Piston, who provided me with the opportunity to perform cutting edge research in the diabetes field. I am proud to have achieved this fantastic voyage within pancreatic islets. I really enjoyed observing cellular events by fluorescence microscopy. Nature is truly beautiful!

I also owe my deepest gratitude and admiration to Dave for fostering a positive and constructive environment in the lab. His support and his inveterate optimism were invaluable for the completion of this project.

I am grateful to the fellow members of the Piston laboratory for sharing their expertise and for their enthusiasm. Likewise, I would like to thank my thesis committee for challenging my knowledge and helping me to develop as a researcher.

I acknowledge the Islet Procurement and Analysis core for helping me with the perifusion assays presented in this thesis, the Flow Cytometry core for sorting my fluorescent cells, and the Hormone Assay core for measuring the amount of glucagon and insulin contained in my samples.

The work presented in this dissertation would not have been possible without the continuous support, belief and love from my family. I love you so much.

TABLE OF CONTENTS

Page

LIST OF FIGURES

Figure *Page*

LIST OF TABLES

Table *Page*

CHAPTER I

GENERAL INTRODUCTION

Introductory comments:

My doctoral project explores the physiology of pancreatic neuroendocrine cells (α-cells) that secrete a peptide hormone (glucagon) under hypoglycemic conditions. Glucagon-secreting α-cells are part of pancreatic micro-organs called islets of Langerhans. My research was mainly conducted on both isolated α-cells and on α-cells present within intact islets harvested from mouse pancreata.

First, this introduction describes how proper blood glucose levels are maintained and how glucagon helps to regulate glucose homeostasis. Impairment of glucagon secretion and its consequences in the setting of diabetes are discussed. Then, I examine the physiology of pancreatic islets in terms of cytoarchitecture, developmental origin, vascularization and innervation. Because insulin-secreting β-cells, the most abundant cell type within the islet, are believed to profoundly influence α-cell secretory activity, their physiology is also discussed. Lastly, I focus the discussion on α-cells with the intention of providing an in-depth presentation of their physiology, and, in particular, on the proposed mechanisms underlying glucagon secretion in low-glucose conditions and glucagon suppression in high-glucose levels.

1- Bi-hormonal regulation of blood glucose homeostasis and diabetes

1-1 Bi-hormonal regulation of blood glucose homeostasis

Glucose constitutes a fundamental source of energy for the cells, and its concentration in the blood is normally around 4 to 5.5 mM, and up to 8 mM during the first hour after a meal (1). These concentrations are mainly regulated by the endocrine function of the islets of Langerhans. In response to an increase in blood glucose concentration, insulin (a 51 amino acid peptide) is secreted into the bloodstream by β-cells. Insulin secretion lowers blood glucose level mainly by stimulating glucose uptake in muscles and adipose tissues, and by inhibiting glucose release from the liver. Temporary hyperglycemia is often benign, asymptomatic, and induces tissue dehydratation as a result of the osmotic effect of glucose. However, chronic hyperglycemia, as seen in the setting of diabetes mellitus, can lead to serious complications over a period of years, including kidney failure, neurological problems, cardiovascular damage, loss of vision, etc (2).

Glucagon (a 29 amino acid peptide hormone) is the metabolic counterpart of insulin, and its secretion by α-cells is increased under hypoglycemic conditions (glucose levels below 3.8 mM), typically during fasting or physical exercise (1). Glucagon raises the blood glucose level by stimulating hepatic glucose output via glycogenolysis and gluconeogenesis. It ensures that the minimal energetic supply is available to the body, and particularly to the brain, which is the main consumer of glucose and relies almost entirely on a continuous supply of glucose from the arterial circulation (3). Not surprisingly, dizziness, disorientation, blurred vision and even loss of consciousness are

common neuroglycopenic symptoms when the blood glucose level is abnormally low (4). As a result, severe and prolonged hypoglycemia can cause irreversible brain damage and even death. A large body of evidence suggests that the counterregulatory (glucose-raising) response to hypoglycemia is gradual. First, insulin secretion decreases drastically below 4.5 mM glucose, and glucagon secretion is increased at glucose levels lower than 3.8 mM. If the glucagon response is not sufficient to restore proper glycemia other counterregulatory systems become activated: the sympathetic autonomic nervous system and the hypothalamic-pituitary-adrenal axis (5, 6). However, the relative contribution of the different autonomic inputs is still debated.

Besides the central role played by insulin and glucagon, other systems modulate blood glucose concentration. These include control of energy balance, glucose reabsorption by the kidneys, release of incretins from the gastrointestinal tract, and hepatic glucose autoregulation.

1-2 Glucagon and diabetes mellitus

1-2-1 Diabetes in numbers

In 2007, over 8% of the US population had diabetes mellitus (7). Diabetes contributed to 235,000 deaths in 2005, and the total cost of diabetes in 2007 was estimated to be $218 billion in the United States (8). In 2000, the World Health Organization estimated that the worldwide prevalence of diabetes would rise from 171 to 366 million in 30 years (9). Factors contributing to this increased prevalence are modern diets, obesity, physical inactivity, and an increase in the number of individuals older than 65 years (9). The exact etiology of the disease is unclear and is still under intense

investigation, but accumulating evidence suggests an interaction between genetic predisposition and environment (10).

1-2-2 Diabetes and impairment of the bi-hormonal regulation of blood glucose homeostasis

Insulin deficiency is the cornerstone of diabetes mellitus and leads to a chronic hyperglycemic state (i.e. glucose levels greater than 7 mM) responsible for long-term complications including kidney failure, blindness, nerve damage, and cardiovascular problems (2). Insulin deficiency results from autoimmune destruction of β-cells in type-I diabetes (~ 5% of the total diabetic cases) and from concomitant insulin resistance and defective insulin secretion in type-II diabetes (~ 95% of total cases). Consequently, most of the research has been devoted to the secretion and action of insulin. However, glucagon release and action are also impaired in the setting of diabetes (11).

In 1975, Unger R.H. and Orci L. proposed, in what they called the "bihormonal hypothesis", that diabetes-associated hyperglycemia originates from both hypoinsulinemia and hyperglucagonemia (11). Since then, type-I and advanced type-II diabetes have been associated with elevated levels of glucagon (13-16) as well as enhanced hepatic sensitivity to glucagon (17) that exacerbate chronic hyperglycemia. Also, diabetic patients under treatment with insulin or insulin secretagogues (i.e. a sulfonylurea or a "glinide") often fail to secrete sufficient amounts of glucagon during hypoglycemic episodes. As a result, hypoglycemia induced by therapy (iatrogenic hypoglycemia) is responsible for ~ 2-4% of the fatalities in type-I diabetes (18).

1-2-3 Glucagon secretion and action as targets for the treatment of diabetes

Pharmacological control of glucagon secretion or action represents a promising therapeutic strategy for the treatment of excess glucose production in diabetic patients (19-21). For instance, biguanide compounds such as metformin, a widely-used anti-diabetic drug, counteract glucagon action by blocking hepatic glucose production, likely via gluconeogenesis inhibition (22). In addition, emergency glucagon kits are prescribed to diabetic patients that are particularly exposed to severe hypoglycemic shocks. When one of these episodes occurs, the persons in contact with the patient (family members, school personnel, etc.) should administer glucagon to the patient to help him regain consciousness (2, 23).

Cell replacement therapy via islet transplantation represents another promising strategy to cure type-I and advanced type-II diabetes (24-26). Infusing islets into the liver via the portal vein has been the site of choice for clinical islet transplantation (27). However, this surgical method is perfectible: 2 years after transplantation, only 15% of the patients remain insulin-independent (28). Furthermore, glucagon responses to insulin-induced hypoglycemia are absent from islets transplanted intrahepatically (29). Improving our knowledge of islet function may be translated into a better chance of success for islet transplants.

2- The islet of Langerhans

2-1 Islet architecture

The pancreas accomplishes two main functions: an exocrine one and an endocrine one. The exocrine function is ensured by acinar cells that produce pancreatic juice (alkaline fluid containing a variety of digestive enzymes such as trypsinogen, chymotrypsinogen, elastase, carboxypeptidase, pancreatic lipase, and amylase) (30). The pancreatic effluent is secreted into the small intestine through a network of pancreatic ducts in response to the intestinal hormones secretin and cholecystokinin. The digestive enzymes help further breakdown of carbohydrates, proteins and lipids present in the chyme.

The endocrine function of the pancreas is mediated by "micro-organs" called "islets of Langerhans". The secretion of pancreatic hormones into the bloodstream is pivotal to maintain proper glycemia, as discussed in Section 1. The human pancreas contains millions of islets that are scattered throughout the exocrine tissue. Altogether, islets represent around 1-2% of the total pancreatic weight. An islet is mainly spherical, typically 100-200μm in diameter, and is composed of 1,000 to 10,000 cells (31). At least five distinct cell types are present in an islet. 55-65% of the cells are insulin-secreting β-cells, 25-35% are glucagon-secreting α-cells, 5-10% are somatostatin-secreting δ-cells, and a small number of other cells secrete pancreatic polypeptide or ghrelin (32, 33). The roles of somatostatin, pancreatic polypeptide and ghrelin in overall islet function are not currently well understood.

In mice, the model we have been using for our studies, the islet is composed of 70-80% of β-cells, 10-15% of α-cells, and a few representatives of the other cell-types mentioned above. Besides the proportion of the different cell-types, the cytoarchitecture of rodent islets differs from human islets (32). For instance, rodent α-cells are found in the periphery of the entire islet while human α-cells appear to surround smaller regions of β-cells that cluster together to make an islet (34). The fact that human α-cells represent a larger percentage of the islet and may have increased interactions with multiple β-cells suggests that paracrine signaling from β-cells could play a greater role for human α-cell physiology than for rodent α-cells.

2-2 Islet development and transcriptional control of cell differentiation

Islet morphogenesis is a complex process resulting from the differentiation, proliferation, and migration of pancreatic endocrine cells. The embryonic pancreas develops by fusion of dorsal and ventral protrusions of the primitive gut epithelium (35). In the mouse, the first glucagon-producing α-cells appear on embryonic day 9.5 (E9.5) and insulin-producing cells are detected the following day (36). At this stage, all the insulin positive cells are also positive for glucagon immunoreactivity (37). The presence of several hormones within one premature cell suggests that the different islet cell-types originate from common multipotential precursors that evolve into fully differentiated cells during development (38). At E14.5, most of the β-cells are fully differentiated and by E18.5 typical islets are formed with centrally located β-cells (36). Ghrelin-expressing cells are found as early as E10.5 (39), whereas somatostatin-expressing cells appear on E15.5 and pancreatic polypeptide-producing cells differentiate shortly before birth (37).

Several transcription factors have been identified in pancreatic development. Pancreatic duodenal homeobox-1 (Pdx-1, also known as insulin promoter factor 1 or Ipf-1) was the first transcription factor to be ascribed in pancreatic development in mice (40) and humans (41). Pdx-1 expression is vital for pancreatic formation from ductal epithelial cells and for the proper maturation of islet cells (42). Similarly, deletion of the transcription factors Ptf1a and Isl-1 from "knock-out" mice results in complete absence of pancreas development (43, 44). Neurogenin-3, a member of a family of basic helix–loop–helix transcription factors, has been implicated in the development of the islets, as illustrated by the absence of endocrine cells in pancreata from mice lacking this transcription factor (45). Another member of the basic helix–loop–helix group, Beta2/NeuroD, likely participates in proliferation of endocrine cells and their proper organization as a three-dimensional structure (46).

The different islet cell-types originate from common multipotential precursors that evolve into fully differentiated cells during development. Transcription factors such as Nkx2.2 (47) and Arx (48) are involved in endocrine differentiation, while Brain-4 (49), Pax-6 (50), MafB (51, 52) and Foxa2 (53) appear to control more specifically the α-cell differentiation.

Studying islet development is important to understand the etiology of some genetically-based diseases related to the pancreas. For instance, humans carrying a homozygous single-nucleotide deletion in the Pdx-1 gene coding region fail to develop a pancreas (41). The heterozygous state of this mutation has also been linked to early-onset type-II diabetes development, designated as maturity-onset diabetes of the young 4 (MODY-4) (54). Furthermore, missense mutations in the Pdx-1 coding region predispose

to late-onset type-II diabetes mellitus (55, 56). Pdx-1 is a transcription factor that binds to the insulin gene promoter (among other genes) and mutations in the insulin promoter also increase the susceptibility to type-II diabetes (57). Mutations in Beta2/NeuroD have also been associated with the development of type-II diabetes (58).

The determination of the spatial and temporal expression of transcription factors involved in cell differentiation, as well as the interaction of their signaling pathways, will likely help the development of alternative therapeutic approaches to treat some forms of diabetes. For instance, treatment of diabetes by islet transplantation is hampered by the shortage of donor organs. Alternative sources of β-cells could become available from embryonic stem cells (59) or from duplication of differentiated β-cells (60, 61).

2-3 Islet microvasculature

In order to fulfill their endocrine function, pancreatic islets are densely vascularized. Islets only represent 1-2% of the pancreas weight but receive 5-15% of the organ's blood supply (62). An islet is highly vascularized; it is supplied by one to five arterioles that branches into a dense network of capillaries. These capillaries are supplemented with a large number of fenestrations closed by diaphragms (63, 64) that allow direct exchanges between blood and endocrine cells. Thanks to this direct interface, the islet responds acutely to changes in blood glucose concentration by secreting proper amounts of hormone into the bloodstream. In addition, islets are connected in parallel to the arterial circulation: arterioles from the splenic artery perfuse the islets while venules drain the secretory products into the splenic vein and then exit the pancreas into the portal vein (65). This organization ensures that all the islets are exposed to the same

concentration of nutrients and hormones.

The direction of the blood flow within the islet has profound physiological implications for its endocrine activity since products secreted from one cell-type can alter the function of other cell-types. For instance, anterograde (arterial) perfusion of isolated pancreata from rats, dogs and humans with anti-somatostatin antibodies (somatostatin is a potent inhibitor of both insulin and glucagon secretion) did not affect the α- and β-cell secretory activity. In contrast, the retrograde (veinal) perfusion of anti-somatostatin antibodies increases both insulin and glucagon secretion, suggesting that somatostatin-secreting δ-cells are downstream of both α- and β-cells. From these physiological studies, it was concluded that the order of perfusion was β → α → δ (66-71). However, two other models have been proposed to describe the direction of the blood flow within an islet (72). One model argues that the non-β-cell mantle is perfused first, followed by the β-cell core (73-75). A third model proposes that blood flow perfuses one pole of the islet first, traverses the islet regardless of the cell-type and exits by the opposite pole (76). Recent technical advances such as the development of fast line-scanning confocal microscopes allow high speed imaging of the blood flow *in vivo* (77). All three models of microcirculation actually coexist, although it was found that the first model (order of perfusion: β → α → δ) was prominent in mice (60% of the total number of islets analyzed). One careful note from this study is the fact that only islets from the tail of the pancreas have been imaged. Previous anatomical studies from the head of pancreas tended to support the third model (mantle to core to mantle). It is therefore possible that islets are differently vascularized according to their location in the pancreas.

The cytoarchitecture of human islets being different than in rodents (no β-cell

core, no non-β-cell mantle), its microvasculature organization may differ from rodents (34). In addition, some evidence indicates that glucose stimulates the rate of blood flow through the islets (78). Future studies on islet microvasculature should shed light on its structural organization and on the regulation of blood flow rate by glucose and other nutrient or hormonal stimuli.

2-4 Islet innervation

Islets of Langerhans are extensively innervated by the autonomic nervous system (79). Sympathetic, parasympathetic as well as sensory nerves project deeply into the islet. Activation of sympathetic and parasympathetic nervous systems is controlled by glucose-sensing neurons within the ventromedial hypothalamus (80, 81). Sympathetic nerves release several neurotransmitters into the islets: norepinephrine, galanin and neuropeptide Y (82-85). Parasympathetic neurotransmitters comprise acetylcholine (86), as well as several neuropeptides (vasoactive intestinal polypeptide (87-89), gastrin releasing peptide (90-92), and pituitary adenylate cyclase activating polypeptide (93-95)). Sensory nerves contain substance P (96) and calcitonin gene-related polypeptide (97). Other types of neurotransmitters have been found in the endocrine pancreas: GABA (98), nitric oxide (99), cholecystokinin (100), ATP (101), L-glutamate (102), glycine (103), dopamine and serotonin (104). Finally, the presence of nerve fibers projecting from the duodenum to the islets suggests a direct entero-pancreatic neural communication (105). While considerable progress has been made to characterize the different types of nerves present in the pancreas, their respective physiological roles for the endocrine function of the pancreas remain largely unknown.

Most of the research on islet innervation has been dedicated to the sympathetic nervous system which is activated during hypoglycemia, exercise or stress. Norepinephrine, a sympathetic neurotransmitter, is an inhibitor of both insulin (106, 107) and somatostatin (108, 109) secretion while being a potent secretagogue for glucagon (107, 110) and pancreatic polypeptide (109). Furthermore, sympathetic neuropeptides such as galanin and neuropeptide Y inhibit insulin secretion (111, 112). *In vivo* research in humans has suggested that the sympathetic stimulation of glucagon secretion was the ultimate counterregulatory (glucose-raising) response to severe glucose deprivation (113) (114). However, other studies on human recipients of pancreas transplantation (115), and on denervated pancreata from conscious dogs (116), demonstrated that glucagon was normally secreted in response to acute hypoglycemia besides impaired pancreatic innervation.

In contrast, the parasympathetic nervous system is activated during hyperglycemia and stimulates the overall islet secretory response, as demonstrated by enhanced insulin, as well as glucagon, somatostatin and pancreatic polypeptide secretion following parasympathetic stimulation (117, 118). Furthermore, parasympathetic neurotransmitters such as acetylcholine, vasoactive intestinal polypeptide, pituitary adenyl cyclase-activating polypeptide, and gastrin-releasing polypeptide are able to stimulate both insulin and glucagon secretion *in vitro* as well as *in vivo* (89, 91-93, 95). However, their relative contribution to islet hormone response remains to be determined.

Several studies propose that the autonomic nervous system is important for islet synchronization and pulsatile insulin release. Sampling from the hepatic portal vein in humans, dogs, and rats revealed that insulin is secreted in pulses with a periodicity of ~ 4-

10 minutes (119-121). Also, oscillations of insulin secretion are present in isolated perifused islets (122). It is therefore likely that most of the islets are synchronized within the pancreas to allow pulsatile insulin release. The loss of pulsatile insulin release following inhibition of pancreatic ganglia suggests that the autonomic nervous system underlie this synchronization (123). Furthermore, insulin pulsatility disappears after islet transplantation but the synchronization of insulin secretion returns once the transplant is reinnervated (124). Mathematical models of the islet function and an *in vitro* study suggest that a single cholinergic pulse applied to all the islets is enough to synchronize their oscillations (125, 126).

3- β-cell physiology

3-1 The standard model of glucose-stimulated insulin secretion

Insulin being so important in the setting of diabetes, most of the research in the islet field has been devoted to the study of β-cell physiology. At the level of a single isolated β-cell, the mechanisms underlying glucose-stimulated insulin secretion are fairly well understood and involve a multistep process. Upon an elevation in extracellular glucose concentration over the range of 5 to 30 mM, glucose is passively transported into β-cells by glucose transporters type 2 (GLUT-2) (127-129). Phosphorylation of glucose by glucokinase (i.e hexokinase IV) ensures that glucose enters the glycolytic pathway (130-132). Glucokinase is a low affinity enzyme (apparent K_M ~ 8 mM) and is the rate-limiting step of glucose metabolism in β-cells. Together, GLUT-2 and glucokinase constitute the β-cell glucose sensor that allows these cells to respond to changes in glucose in the millimolar range.

Each molecule of glucose transported into the cells yields up to 36 molecules of ATP. The resulting increase in [ATP] to [ADP] ratio closes ATP-sensitive inward-rectifying K^+ channels (K_{ATP}) (133-135). The decrease in K^+ efflux depolarizes the plasma membrane and activates L-type voltage-gated calcium channels. The subsequent influx of Ca^{2+} triggers exocytosis of insulin-containing granules (136-138). Granule fusion stops after repolarization of β-cell membrane and closure of L-type voltage-gated Ca^{2+} channels. Several non-exclusive models describe the mechanism underlying membrane repolarization: activation of voltage-dependent K^+ channels (outward current) (139), activation of Ca^{2+} dependent K^+ channels (140), and re-opening of K_{ATP} channels following the transient decrease in [ATP] to [ADP] ratio due to oscillations in the rate of glycolysis (141). This sequence of depolarization and repolarization causes intracellular calcium oscillations that likely contribute to pulsatile release of insulin.

3-2 Glucose-stimulation of insulin secretion is biphasic

The first phase of insulin secretion refers to the strong secretory response that occurs within the first 5-10 minutes of glucose stimulation. In humans and rats, the second phase begins after the nadir of the first phase, the rate of insulin release increases slowly until reaching a higher plateau after a further 25 to 30 minutes (142). In contrast, the slow rising phase is absent in isolated mouse islets so that the second phase is essentially a plateau that starts from the nadir of the first phase (143). However, the slow rising phase was observed *in vivo* in the conscious mouse (144).

The first phase of insulin secretion is almost invariably lost in patients with impaired glucose tolerance or with type-II diabetes mellitus (145, 146). In normal

physiology, the acute phase involves the exocytosis of a small pool of insulin-containing granules, termed the readily releasable pool (147, 148). On average an isolated mouse β-cell contains ~ 10,000 granules, but only 50-100 granules constitute this releasable pool. It is estimated that when β-cells are exposed to a step-increase in glucose concentration (from 3 to 16.7 mM), around 20 granules are released per cell per minute at the peak of the first phase. This rate falls at ~5 granules per minute during the second phase (149) (150). The standard model of glucose-stimulated insulin secretion previously described in Section 3-1 accounts for the first phase but does not explain the increasing rate of insulin release observed during the rising phase in rat islets and humans. This second phase is under intense investigation and is often referred to as the "K_{ATP}-independent pathway" or simply "amplifying pathway" (as opposed to "K_{ATP} pathway" or "triggering pathway" for the first phase) (151). Indeed, this phase appears to improve the rate of insulin secretion without modifying the cytoplasmic calcium levels. In other words, the second phase amplifies the triggering action of calcium ions. Despite several candidates such as ATP (152, 153), cyclic AMP (154), citrate cycle intermediates exported to the cytosol (155), and granule translocation by the cytoskeleton (156, 157), no consensus has been reached on the mechanism responsible for this amplification. A good illustration of the importance of these "K_{ATP}-independent pathways" is the fact that transgenic mouse islets lacking functional K_{ATP} channels (either through deletion of Kir6.2 or Sur-1 subunits) still exhibit glucose-stimulated insulin secretion (158-160).

The amount of insulin secreted during both phases depends on the number of releasable granules. For instance, this pool of granules can be enlarged by previous exposure to glucose (time-dependent potentiation) (161), or by agents such as glucagon

(162) and glucagon-like peptide 1 (GLP-1) that activate protein kinase A (PKA), or acetylcholine that activate protein kinase C (PKC) (149, 163, 164). In addition, other metabolic pathways are able to amplify glucose-stimulated insulin secretion; as shown for free fatty acid (165, 166) and amino acid metabolism (167, 168). In summary, β-cell secretory activity involves the interplay of different signaling pathways (e.g. nutrient metabolism, endocrine and paracrine effects) that modulate the rate of insulin release.

3-3 Glucose-stimulation of insulin secretion is pulsatile

Isolated β-cells exposed to glucose stimulation exhibit irregular intracellular calcium oscillations with different waveforms, durations and amplitudes. In contrast, when β-cells are present within the islet, they respond to glucose in a coordinated way, as illustrated by synchronized calcium oscillations that spread throughout the islet (169, 170). Two main types of regular and repeating oscillations have been reported in rodents: fast oscillations (duration: ~20-40 s, frequency: 2 min^{-1}) and slow oscillations (duration: 4-10 min, frequency: 0.25 min^{-1}). In addition, mixed patterns of oscillations are occasionally observed where fast oscillations are superimposed on slow oscillations (141, 169, 171). Synchronous oscillations are induced at glucose concentrations over 7 mM (172), a subsequent increase in glucose levels tends to lengthen the duration of slow oscillations (173) and to enhance the amplitude of fast oscillations (174). However, it is unclear what mechanisms determine the oscillatory pattern displayed by the islet. Mathematical models propose that fast oscillations are electrical in nature and involve calcium and potassium channels. In contrast, slow oscillations would originate from slow metabolic processes possibly mediated by a feedback inhibition loop on

phosphofructokinase by ATP (175, 176).

Synchronous calcium oscillations spreading throughout the rodent islet generate in-phase pulses of insulin secretion (141, 177, 178). Slow and fast secretory pulses have been measured from single murine islets (179). Intercellular communication through gap junctions made of connexin-36 (Cx36) subunits serves to synchronize electrical activity and secretion among β-cells, as demonstrated by loss of coordination in islets treated with gap junction blockers, or in transgenic mouse islets lacking Cx36 (180, 181). Gap junctions are membrane channels that allow the direct exchange of small molecules (< 1 kDa) between adjacent cells. Gap junctions are not specific so that a wide variety of ions, metabolites, second messengers can pass through them (182). Homotypic channels made of Cx36 display low voltage sensitivity and remain open under basal and stimulated conditions (183, 184). Cx36 channels have a low conductance (185) and preferentially exchange cationic molecules (186). However, what molecules are transferred between β-cells and how they affect β-cell physiology remains to be established.

Pulsatile insulin release has also been measured in the portal vein in rats (187) and in mice (188). *In vivo* pulses of insulin secretion were slow with a period of 5-10 minutes. Fast insulin pulses were not reported but the low sensitivity of the method did not allow the detection of 30-second pulses. However, both plasma insulin pulses and calcium oscillations measured in islets harvested from the same mouse exhibited a similar periodicity (188). This observation suggests that the rhythmicity of insulin measured in the portal vein is intrinsically determined by the islet rhythmicity. The majority of the islets must be synchronized together for pulses of secretion to occur from the whole pancreas. As briefly discussed in Section 2-4, cholinergic innervation from the autonomic

nervous system is the leading hypothesis to account for this inter-islet synchronization (123-126).

Pulses of insulin secretion have also been measured in the portal vein in humans (189, 190). However, unlike islet rodents, calcium oscillations spreading throughout the islet were not detected in human islets stimulated by glucose. Nonetheless, discrete regions of the human islet were oscillating but these clusters of oscillating β-cells were not synchronized together *ex vivo* (32, 191). This distinct behavior likely emanates from differences in islet cytoarchitecture. Indeed, rodent β-cells form a continuous cell population in the islet core whereas human β-cells are grouped in clusters separated by other cell-types (32, 34). The presence of gap junctions made of Cx36 in human β-cells (192) likely explains why discrete regions of the human islet were oscillating. As a cautionary note, it should to be pointed out that human islet studies carry some inherent limiting factors that may complicate the interpretation of the results. For instance, human islets being larger than rodent islets, the core of the islet suffers from the limited diffusion of oxygen (hypoxia) and nutrients in culture. Other limiting factors involve the quality of islet isolation from cadaveric pancreata, their cryo-preservation and their transport (193, 194).

Pulsatile release of insulin from the pancreas is altered in humans with type-II diabetes, as well as in relatives of both type-I and type-II diabetic patients. Irregular oscillations and reduced amplitudes have been reported (195-197). Pulsatile insulin therapy, which mimics normal periodicity and amplitude of insulin release by the pancreas, has been effective in reducing the progression of diabetes complications (198). The exact mechanisms involved behind this improvement are not yet understood,

however pulsatile insulin therapy reduces hepatic glucose production in type-I diabetic patients (199) and increases insulin sensitivity in adipose tissue in type-II diabetics (200).

4- α-cell physiology

4-1 Historical perspectives

Paul Langerhans (1847-1888), a German physician and anatomist, discovered the pancreatic islets in 1869 by histochemical staining of the rabbit pancreas (201). Islets were called "points folliculaires" (202), "intertubular cell-clumps" (203), "secondary cell groups" (204), and "pseudofollicles" (205). It was in 1893 that Laguesse G.E. called these cell clusters: "islets of Langerhans", in honor to their discoverer. In 1907, Lane M. described two histologically distinct cell populations in the islet (206). The group with the greater number of cells was called β-cells, whereas the smaller group was referred to as A-cells. Unraveling the function of the islet had been quite challenging. Langerhans himself believed that islets were nerve endings structures. Islets were later on presented as lymphatic tissue (203), as part of the exocrine tissue (207), or as endocrine cells essential for normal carbohydrate metabolism. The latter hypothesis was mainly based on the observation that islets in diabetic individuals were often diseased and/or scarce (208).

In 1889, Minkowski O. and von Mering J.V. achieved the first total pancreatectomy in dogs. During the following weeks after the surgery, they noticed that the depancreatized dogs were developing "diabetes-like" symptoms, such as glycosuria, polyuria, thirst, hunger, weight loss, in spite of ample supply of nutrients (209). This seminal experiment provided the first proof that diabetes could arise from the lack of a pancreatic substance secreted into the bloodstream. In 1916, this internal secretion of the

pancreas was called “insulin” by Shaffer P.A., but attempts to isolate this active component from pancreatic extracts were inconclusive. In 1921, Banting F. and Best C. hypothesized that the presence of trypsin or other digestive enzymes in the pancreatic extract could deactivate insulin (210, 211). They took advantage of the fact that exocrine tissues degenerate after ligation of the pancreatic ducts, while islets are unaffected. Extracts from degenerated pancreas reduced blood sugar in diabetic animals (depancreatized dogs) and prolonged their lifespan.

In 1923, Murlin J.R. *et al.* found that injection of a fraction of these pancreatic extracts strongly raised the blood sugar in normal and diabetic dogs (212, 213). They called this hyperglycemic substance “glucagon”. In 1948, Sutherland E.W. and de Duve C. provided the first demonstration assigning α-cells as the source of glucagon (214). Several observations supported their hypothesis: 1) Glucagon was more concentrated in extracts from the splenic portion of the pancreas, where the highest concentration of islets is found. Also, extracts from degenerated pancreata following ductal ligation (degeneration of the exocrine tissue) yielded a greater amount of glucagon per unit weight. These experiments suggested that glucagon was produced in the islets. 2) β-cell destruction by alloxan did not reduce the amount of glucagon present in the extracts (as opposed to insulin), indicating that glucagon originated in α-cells (at that time, the only other cell-type known to constitute the islets besides β-cells). In 1952, Foa P.P. *et al.* provided the first physiological evidence that glucagon is secreted in response to hypoglycemia (215). Cross-circulation experiments between two dogs showed that lowering blood glucose in one dog by intravenous injection of insulin induces an increase in blood glucose in the recipient dog. In the mid-1950s, improvement in the purification

of glucagon (216) and determination of its amino acid sequence (217) allowed the study of its biophysical properties and biological roles.

In 1961, Unger R.H. *et al.* developed glucagon antibodies and radioactive immunoassays that allowed the measurement of glucagon release (218). In 1962, immunofluorescence staining identified α-cells as the source of glucagon (219). In 1967, Lacy P.E. and Kostianovsky M. described a method based on collagenase digestion for isolating intact islets from the pancreas (220). Over the last 40 years, these technical breakthroughs have been helping the study of α-cell physiology.

4-2 Transcriptional control and processing of proglucagon

The region coding for glucagon is part of the preproglucagon gene. The proximal promoter of the preproglucagon gene carries a minimum promoter region (G1) and at least four enhancer elements (G2–G5) (221). A variety of transcription factors are able to interact with the promoter region and regulate proglucagon expression in temporal and spatial manners. G2, G3, G4 and G5 control the transcription levels of the gene (e.g. Pax-6 and Pbx-Prep1 interact with G3 (222)). In contrast, G1 restricts its expression in the α-cells with little activation potential (223) through interactions with Pax-6, Cdx-2/3, Isl-1, Brain-4 and Foxa2 (224-227). In addition, preproglucagon transcription can be regulated by cyclic AMP (228).

The preproglucagon nucleotide sequence was determined in rodents and humans in the early 1980s by Bell G.I. *et al*. (229, 230). Analysis of the preproglucagon cDNA revealed that it encodes not only glucagon but also two glucagon-like peptide hormones, namely glucagon-like peptide-1 (GLP-1) and GLP-2, and a few other peptides (231). The

gene is translated into the endocrine precursor preproglucagon (180 amino acids) in pancreatic α-cells (232), in L cells from the intestinal mucosa (233), in the brain (234) and in the submandibular glands (235). After cleavage of the signal peptide in the rough endoplasmic reticulum, proglucagon (160 amino acids) is post-translationally processed in a tissue-specific manner (236). In pancreatic α-cells, proglucagon processing yields glucagon (29 amino acids), and other peptides with unknown biological functions: an intervening peptide IP-1 (6 amino acids), glicentin-related polypeptide (30 amino acids) and the major proglucagon fragment (87 amino acids) that contains the unprocessed GLP-1, IP-2 and GLP-2 sequences. In contrast, proglucagon processed in the intestinal L cells generates GLP-1 (36 amino acids) and GLP-2 (33 amino acids) along with glicentin (69 amino acids), glicentin-related polypeptide, oxyntomodulin (37 amino acids, also called "enteroglucagon") and IP-2 (12 amino acids).

Cell specificity of proglucagon processing originates from cell-specific expression of prohormone convertases (PC) that cleave the precursor protein (237). PC2 is present in α-cells (238, 239) while PC1/3 processes proglucagon in the L cells (240). The transcription regulation of the PC gene is not fully understood, but PC2 gene has been reported to be regulated by: Egr1 (241), repressor element 1/neuron restrictive silencer element (242), thyroid hormone receptor α1 and retinoid X receptor (243), Beta2/NeuroD1 (244), and Pax-6 (245). Prohormone convertases are themselves synthesized as inactive precursors that are proteolytically activated along their transport through the endoplasmic reticulum, the Golgi apparatus, the trans-Golgi network, up to the secretory granules where fully activated PCs will cleave the prohormones at cleavage sites characterized by multibasic residues (246).

4-3 Physiological fates of glucagon

4-3-1 Glucagon receptor and associated signaling pathways

Once released into the bloodstream, glucagon signals its physiological effects on the target tissues displaying glucagon receptors on their plasma membrane. In 1971, glucagon receptors were first described in the rat liver by Rodbell M. and coworkers as binding sites that activate adenylyl cyclase (247). In 1993, cloning of the glucagon receptor cDNA formally identified this receptor as a seven transmembrane-spanning protein of the G protein-coupled receptor (GPCR) family (248). Based on sequence homology, glucagon receptors belong to a subset of the GPCR family (i.e. the class B) that includes, among others, receptors for GLP-1, GLP-2, GIP (gastric inhibitory polypeptide), secretin, VIP (vasoactive intestinal polypeptide), and growth hormone-releasing hormone (249, 250).

The binding of glucagon to the extracellular domains of the glucagon receptor triggers downstream signaling pathways. The concentration of glucagon required for half maximal effects is in the 2-4 nM range (251). Interaction of glucagon with its receptor changes the conformation of the receptor and thus allows its interaction with an associated G protein. Glucagon receptor activation has been linked to at least two types of G proteins, namely Gsα and Gq. Activation of Gsα increases, via activation of adenylyl cyclase, the intracellular levels of cyclic AMP and the activity of protein kinase A (PKA). In contrast, Gq activates phospholipase C, that in turn hydrolyzes phosphatidylinositol 4,5-bisphosphate (PIP2) to diacyl glycerol (DAG) and inositol triphosphate (IP3). These second messengers lead to protein kinase C (PKC) activation and elevation in the free cytoplasmic calcium concentration, respectively (252). These

signal transduction cascades initiate the activation/inhibition of a variety of downstream effector proteins that are temporally and spatially regulated. Activation of these signaling pathways can initiate fast responses such as opening of ion channels in the plasma membrane, activation of metabolic enzymes, or direct effect on exocytosis, as well as slow responses mediated by modulations in gene transcription. For instance, glucagon triggers the internalization of the glucagon receptor while repressing the expression of the glucagon receptor gene (253, 254).

4-3-2 Biological functions of glucagon

Glucagon receptors are mainly expressed in the liver and in kidneys, and to a lesser extent, in the heart, adipose tissues, spleen, thymus, adrenal glands, pancreatic islets, cerebral cortex, lungs, and throughout the gastrointestinal tract (251, 255). Thus, glucagon likely modulates multiple responses in these tissues, including effects on ion transport and glomerular filtration rate in kidneys (256), cardiotonic effects in the heart (257), increased lipolysis in adipose tissues (258), and action as a satiety factor in the brain (259). Glucagon also increases amino acid degradation and inhibits protein synthesis (260). Although all of the biological functions of glucagon have not been revealed, considerable progress has been made in understanding its primary role as a regulator of glucose homeostasis. Thus, the main function of glucagon as a hyperglycemic hormone is to stimulate hepatic glucose output by potentiating both glycogenolysis (from glycogen stores) and gluconeogenesis (from lactate, glycerol and amino acids) and by inhibiting both glycogenesis and glycolysis (for review, see (20)).

Besides its endocrine function, glucagon exerts both paracrine and autocrine

effects within the pancreatic islets. It stimulates insulin and somatostatin secretion from β- and δ-cells, respectively (69, 261). Glucagon also exhibits an autocrine effect on α-cell secretory activity by potentiating its own secretion (162). In addition, glucagon likely controls α-cell proliferation, as illustrated by the presence α-cell hyperplasia in transgenic mice that are unable to secrete glucagon or to express glucagon receptors (262, 263).

4-3-3 Glucagon degradation

The half-life of glucagon in plasma is approximately 3 to 6 minutes (264, 265). Glucagon degradation begins in the blood where it is hydrolyzed by the serine protease dipeptidyl-peptidase IV (DPP-IV), a majority of which being membrane bound (on intestinal epithelial cells, kidney, liver etc.) (266). However, clearance of glucagon from the circulation is mainly accomplished by target tissues, the more important of them being the liver and kidneys. It is estimated that the liver accounts for more than a third of glucagon degradation rate (264). Several mechanisms have been identified for hepatic glucagon degradation; some of them involve plasma membrane glucagonases, such as the glucagon-degrading aminopeptidase, or the receptor-linked glucagonase, whereas other mechanisms are associated with endocytosis of glucagon bound to its receptor (251). Interestingly, the metabolites resulting from glucagon cleavage may have their own biological functions, as illustrated by the production of miniglucagon (fragment 19-29) that inhibits hepatic plasma membrane Ca^{2+} pumps without interfering with the adenylyl cyclase activity (267). Miniglucagon is also present in α-cell granules and is proposed to exert a paracrine inhibitory effect on insulin-secreting β-cells (268).

4-4 Physiological levels of glucagon in the blood

4-4-1 Fed state

In healthy humans, a high-carbohydrate meal induces a rise in blood glucose from ~5 mM to glucose levels greater than 8 mM within a period of 30 minutes to 1 hour. This elevation in glucose stimulates insulin secretion from β-cells (310). After blood glucose concentration has reached a maximum, it begins to decline due to the secretion of insulin. Insulin stimulates glucose uptake in muscles and adipose tissues by mediating the translocation of glucose transporters (GLUT-4) to their cell surface. Glucose is oxidized in these tissues and serves as fuel to meet their energy needs. In addition, insulin helps to store excess of glucose in the form of glycogen in the liver and skeletal muscles (1). Protein ingestion also participates in the induction of β-cell secretory activity, but its effect is less pronounced compared to the ingestion of carbohydrates (310).

In parallel to the β-cell response, α-cell secretory activity can increase or decrease, depending on the content of the meal. Blood glucagon concentration modestly decreases after a high-carbohydrate meal (e.g. ~10-15% decrease in (310), and ~20-25% in (534)). In contrast, glucagon secretion is strongly enhanced after a protein-rich meal (e.g. ~50% increase in (310), and ~100% in (534)). Similar results have been reported in dogs (535) and in rodents (536). Insulin and glucagon act in concert to metabolize amino acids: insulin enhances amino acid uptake and protein synthesis, while glucagon stimulates gluconeogenesis from amino acids (1). Finally, glucagon secretion is relatively constant after a standard meal containing carbohydrates, proteins and fats (534).

4-4-2 Fasted state and starvation

Within two hours after a meal, blood glucose concentrations return to normal fasting levels (4.5 to 5.5 mM) (310). In humans, the fasting plasma glucagon concentrations have been reported to range between 100-200 pg/mL (310, 534). The portal vein contains greater amount of glucagon (300-500 pg/mL) because the vein drains glucagon secreted from the pancreas to the liver, the major target organ for glucagon (269, 535).

During fasting, as well as during exercise, as blood glucose levels decrease, insulin levels decrease, and glucagon levels rise. These hormonal changes cause the liver to produce and release glucose so that blood glucose levels are maintained. During the first 12 hours after a meal, glycogenolysis is the main source of blood glucose. By ~16 hours of fasting, both glycogenolysis and gluconeogenesis contribute equally. After 30 hours, the glycogen stores are depleted and normal blood glucose levels are primarily maintained by gluconeogenesis (from lactate, glycerol and amino acids) (12). Even a prolonged fast lasting between 3 days to 5 weeks does not dramatically reduce blood glucose levels (3.5 to 4 mM) (12). The maintenance of blood glucose levels is mainly achieved by the breakdown of triacylglycerol stores, a source of high energy fuel located predominantly in adipose tissues. Also, more ketone bodies, a by-product of free fatty acid metabolism, are released by the liver into the bloodstream. During prolonged starvation, ketone bodies become the main source of energy for the brain (in place of glucose). Thus, the oxidation of ketone bodies by the brain reduces the need for blood glucose during prolonged starvation (1).

4-5 Mechanisms of glucagon secretion

4-5-1 Biphasic secretion of glucagon

A step-increase from low to high glucose levels induces biphasic secretion of insulin, as previously described in Section 3-2. A similar pattern is observed with glucagon following a step-decrease in glucose concentrations, as reported in rats (270), dogs (271) and humans (272). In the perfused rat pancreas, the acute first phase occurs rapidly within 5 minute of the glucose switch and lasts less than 5 minutes. The second phase is essentially a plateau that starts from the nadir of the first phase and is maintained at a higher level compared to high-glucose conditions. In mouse isolated islets, a switch from high to low glucose induces a monophasic glucagon response (a slow-rising phase has been reported (306), as well as an acute response that plateaues at the same level (448).

Stimulation of the perfused rat pancreas in low-glucose concentrations with epinephrine and norepinephrine results in the same biphasic secretory pattern (270), although the peak of the first phase and the plateau are higher compared to a step-decrease in glucose. The stimulatory effect of the catecholamines is greatly reduced in pancreas perfused at higher glucose levels.

Arginine and glutamate also induce a biphasic secretion of glucagon in the perfused rat pancreas, and the amplitude of the response is inversely related to the glucose concentration (273).

4-5-2 Pulsatile glucagon release

Regular pulses of glucagon secretion have been observed in 16h-fasted rhesus

monkeys and baboons (274) with oscillations displaying a period averaging 9 minutes. The study also reports regular insulin pulses in phase with oscillations in blood glucose concentration. Glucagon oscillations were antisynchronous with insulin and blood glucose oscillations. The same pattern was observed in isolated dog pancreata perfused at a constant glucose level (5 mM), suggesting that an intrinsic rhythm of hormone secretion is present in the pancreas (275). In addition, somatostatin pulses were found to oscillate in phase with the pulses of insulin (275-277). Hormonal pulses were also described in isolated perfused pancreata from rhesus monkeys, although the oscillations were less regular and more frequent (period ~6 minutes) than *in vivo* (276). This observation suggests that factors extrinsic to the pancreas modulate the frequency of hormonal pulses.

Regular pulses of glucagon, antisynchronous with insulin pulses, are also observed in high-glucose conditions from perfused rat pancreata (278) and perifused human islets (277). These studies did not describe any oscillatory activity in low-glucose conditions (3 mM), but a step-increase to 20 mM glucose induced regular oscillations with a period of ~5 minutes. The nadirs between the glucagon pulses were lower than the basal secretion at 3 mM glucose, resulting in ~20% suppression of average glucagon release (277).

Pulses of glucagon are more efficient over continuous delivery at enhancing glucose production from isolated rat hepatocytes (279, 280). Continuous perifusion of glucagon increased the EC_{50} of glucose production ~5-fold compared to pulsatile glucagon delivery (279). In addition, the amplitude of glucagon pulses is decreased in baboons with β-cell deficiency following streptozotocin treatment (281). These observations suggest that pulsatile release is likely important for proper glucose

homeostasis and may be altered in the diabetic state.

4-5-3 Electrophysiological model of glucagon secretion at low glucose levels

The cellular mechanisms leading to insulin secretion by β-cells are fairly well understood, as described previously in Section 3-1. In contrast to the secretion of insulin, the mechanisms underlying the secretion of glucagon from α-cells are largely unknown. Similarly to β-cells, α-cells contain comparable secretory machinery: glucose transporter (in this case GLUT-1), glucokinase, K_{ATP} channels, L-type voltage-gated calcium channels and secretory granules (282-287). However, α-cell secretory activity is opposite to β-cells: glucagon is released maximally at low glucose levels (< 4 mM), whereas β-cells increase their secretion of insulin at glucose levels greater than 7 mM. It is not clear how a glucose-dependent depolarizing pathway as seems to be present in the α-cell leads to the inhibition of glucagon release.

Electrophysiological recordings have identified a variety of ion channels in α-cells. For instance, a voltage-gated Na^+ channel is proposed to play a major role in the occurrence of action potentials observed in low or absence of glucose. This depolarizing current is activated around -40 mV and is inhibited by tetrodotoxin (TTX). TTX inactivation of the Na^+ channel abolishes the action potentials and strongly inhibits glucagon secretion (285). In addition to the Na^+ channels, there are at least four different types of K^+ channels: K_{ATP} channels, G protein-gated K^+ channels (K_I channel), delayed rectifying K^+ channels (K_{Dr}), and transient K^+ channels (A-channel). It has been proposed that K_I channel activation is induced by somatostatin and that the subsequent hyperpolarization of the membrane inhibits glucagon secretion (288). However, another

study questions the importance of the K_I channel by reporting that somatostatin mediates its inhibition by depriming of secretory granules, without modifying α-cell $[Ca^{2+}]_i$ (intracellular free calcium concentration) (289). K_{Dr} and A-channels are voltage-gated channels proposed to be involved in the repolarization of the membrane following the outcome of an action potential (285).

Four types of voltage-gated Ca^{2+} channels (T-, N-, R-, and L-type) have also been described in α-cells. The T-type channel is a low-voltage-activated channel that opens at membrane potentials as negative as -65 mV, whereas N- and R-type channels are activated between -30 and -40 mV (290). Further depolarization above -20 mV opens the L-type high-voltage-activated channels. However, their relative importance for the secretion of glucagon is still debated. Some argue that N-type channel inhibition prevents glucagon secretion (286, 291-293), some found a prominent role for L-type channels (294-297). These contradictory observations are difficult to explain, but one study reports a differential role for the two channels: N-type channels would be prominent for basal secretion whereas L-type channels would be more important when cyclic AMP level rises, as observed after epinephrine stimulation (286). Another study proposes that α-cells can be divided into distinct populations characterized by the type of calcium channels they predominantly express (298).

One model of glucagon secretion at low glucose proposes that T-type Ca^{2+} channels act as pacemaker channels (285, 299). The small depolarization resulting from the influx of Ca^{2+} would activate Na^+ channels and subsequently triggers high-voltage-activated Ca^{2+} channel opening (mainly L- and N-types), eventually culminating in exocytosis of glucagon granules. The action potential is then inactivated by opening of

K_{Dr} and A-channels. However, this nascent model is likely oversimplified and needs to be further refined to fully explain how glucagon is secreted. For instance, T-type channels appear to be inactivated before activation of Na^+ channels (285), and their expression in rodent α-cells is debated (295).

Lastly, another ion channel, the hyperpolarisation-activated cyclic nucleotide-gated (HCN) channel, is expressed in α-cells. HCN channels are members of a superfamily of voltage-gated cation channels that are permeable to both Na^+ and K^+ ions and produce a slowly activating inward current. Unlike most voltage-dependent channels, HCN channels are activated by membrane hyperpolarization and may play a role in the generation of spontaneous action potentials in low-glucose conditions (300).

4-5-4 The "switch-off" hypothesis

Type-I and advanced type-II diabetic patients under exogenous insulin treatment or treatment with insulin secretagogues fail to secrete proper amounts of glucagon during hypoglycemic episodes (Section 1-2-2). A leading hypothesis to explain this dysfunction is referred to as the "intraislet insulin hypothesis" (301-303). This hypothesis postulates that the rapid decrease in insulin secretion after a switch from high to low glucose levels is the trigger for maximal glucagon response. This hypothesis is based mainly on streptozotocin-induced diabetic rats exhibiting impaired insulin responses at high glucose and reduced glucagon secretion at low glucose. A near-normal glucagon response to low glucose levels could be artificially restored by switching off an exogenous insulin infusion in the portal vein (302). The same result was obtained in perifused intact islets from rats and humans (303). In addition, α-cell-specific insulin receptor (IR) knockout

mice display a blunted glucagon response to fasting-induced hypoglycemia (304). Similarly, mouse islets and murine tumor α-cell lines (αTC1-6 cells) with reduced expression of IRs following small interference RNA transfection secrete reduced amounts of glucagon under low-glucose conditions (305). Defects in glucagon response to insulin were associated with disruption of the IR – IR substrate 1/2 – phosphatidyl inositol -3 kinase (PI3K) - protein kinase B / Akt pathway (304, 305). However, it is not understood how this signaling pathway modulates glucagon secretion.

More recently, reestablishment of glucagon secretion during glucose deprivation was also obtained by turning off zinc in streptozotocin-treated mouse islets (306) and diabetic-induced rats (307). Zinc would mediate its triggering effect by closing of K_{ATP} channels (306). Also, the importance of insulin for the switch-off model was challenged by the observation that zinc-free insulin infusion did not initiate glucagon secretion during hypoglycemia (307). In addition, somatostatin infusion in diabetic-induced rats was also able to induce an elevation of the glucagon response during glucose deprivation (308).

The exact molecular mechanisms involved in the switch-off model have not been clearly established; however mathematical modeling of the pancreatic network describing cell-cell interactions predicts some of the defects observed in the setting of diabetes (309). Also, mathematical modeling of a network based on the stimulatory effect of glucose on insulin and somatostatin secretion, and on the inhibitory effect of theses hormones on glucagon release predicts that a switch-off signal enhances the amplitude of glucagon pulses (308). However, no experimental data are yet available to confirm this prediction.

4-5-5 The "calcium store-operated" hypothesis

This hypothesis postulates that glucagon secretion is governed by a calcium store-operated mechanism (294). In this model, intracellular calcium stores in the endoplasmic reticulum are depleted at low glucose levels. The release of calcium stores would activate a depolarizing store-operated influx of cations, which eventually triggers voltage-dependent Ca^{2+} influx and glucagon secretion. This hypothesis is mainly based on the observation that inhibition of the sarcoplasmic-endoplasmic reticulum Ca^{2+} ATPase pump (SERCA) by cyclopiazonic acid (CPA) depolarizes isolated mouse α-cells and causes $[Ca^{2+}]_i$ oscillations. However, another report failed to observe any effect in isolated rat α-cells following SERCA blockade by thapsigargin (311). Also, the identity of the channels responsible for depletion of calcium stores and for membrane depolarization remains to be established.

4-5-6 Glucagon secretagogues

i) Amino acids

Unlike glucose, which inhibits glucagon secretion and stimulates insulin release from islets, amino acids induce the release of both hormones, but are generally more effective at stimulating glucagon secretion (312). Circulating amino acids play an important role for glucagon secretion and blood glucose homeostatis. For example, a protein-rich meal would cause hypoglycemia if insulin was the only hormone to be released (313).

Individual amino acids differ in their ability to enhance glucagon secretion. Arginine is the most potent glucagon secretagogue, alanine and glycine are less effective,

while leucine, isoleucine, lysine and valine are inactive (314, 315). The mechanisms of action of each of these amino acids are not known but are likely different and synergistic. For instance, a mixture of 20 amino acids releases more glucagon than equimolar concentration of one amino acid alone (316). Three non-exclusive mechanisms have been proposed for L-arginine stimulation of glucagon secretion (317): 1) α-cell uptake of the positively charged arginine followed by depolarization of the plasma membrane and activation of high-voltage gated calcium channels; 2) arginine metabolism through the action of arginase that hydrolyzes arginine to urea and ornithine. Ornithine is then further metabolized and feeds the citric acid cycle. The increase of ATP/ADP ratio closes K_{ATP} channels and depolarizes the plasma membrane; and 3) exocytotic stimulation by nitric oxide (NO) derived from the metabolism of arginine through the action of NO synthase. Based on the immediate glucagon response following arginine stimulation and on the ability of the non-metabolized amino acid α-amino-isobutyric acid to induce a fast $[Ca^{2+}]_i$ increase in α-cells, mechanism 1) has become the leading hypothesis (318). However, transgenic mice that lack functional K_{ATP} channels display blunted response to arginine at low-glucose conditions. This observation supports mechanism 2) where an elevation in metabolic state increases ATP levels, blocks K_{ATP} channels and depolarizes the membrane (319).

ii) Fatty acids

Circulating fatty acids are a source of energy for islets and play an important role for insulin secretion (166). Short-term application (< 3 h) of fatty acids potentiates glucose-stimulated insulin secretion, whereas long-term exposure (6-24 h) results in

elevated basal insulin secretion and reduced response to glucose (320). Less is known about the role of fatty acids on glucagon secretion. Conflicting results have been reported, likely due to species differences and experimental conditions. For instance, short-term application of the free fatty acid (FFA) palmitate inhibits the secretion of glucagon from guinea pigs (321, 322), whereas it stimulates glucagon secretion from murines (323-325). It was found that the longer the chain length of saturated FFAs, the greater is the rodent glucagon response. Also, saturated fatty acids were more effective in stimulating glucagon secretion than unsaturated fatty acids; and *trans*-fatty acids were more potent than their *cis* isomers (325). The stimulatory effect of palmitate is correlated with an increase in α-cell $[Ca^{2+}]_i$ and has a direct effect on the exocytosis rate (324). In addition, palmitate reduces somatostatin secretion from δ-cells by ~50% at high glucose levels. The relief of paracrine somatostatin inhibition likely contributes to palmitate effect on glucagon secretion in high-glucose conditions.

Long-term exposure of FFAs results in decreased total glucagon content by ~65% and elevates glucagon secretion (13-fold) in rat islets perifused with low-glucose levels, whereas the basal insulin and somatostatin secretions were only marginally increased (~1.6-fold) (326). Long-term stimulatory effects have also been reported on murine tumor cell line αTC1-6 (327). This effect raises the question whether elevated plasma FFA levels may in part explain the hyperglucagonemia associated with type-II diabetes.

iii) Epinephrine

The hypothalamic-pituitary-adrenal axis is activated under advanced hypoglycemia (< 3.8 mM glucose). Epinephrine, which is produced in the adrenal glands,

is secreted into the bloodstream and stimulates glucagon secretion (5, 113, 114). Epinephrine mediates its positive effect on α-cells by binding to β-adrenergic receptors. The resulting activation of adenylyl cyclase elevates cyclic AMP levels and activates PKA, which induces a stimulation of Ca^{2+} influx through L-type voltage-gated calcium channels and an acceleration of granule mobilization (286). An alternative model, based on the "calcium store-operated" hypothesis proposes that epinephrine mobilizes intracellular calcium stores, thereby inducing a store-operated current sufficient for α-cell activation (294). However, the effect of epinephrine on $[Ca^{2+}]_i$ is controversial since it has been reported that epinephrine does not affect α-cell $[Ca^{2+}]_i$ (361).

iv) Norepinephrine

The autonomic nervous system is activated under advanced hypoglycemia and releases the neurotransmitter norepinephrine (107, 110). One study provides evidence that norepinephrine mediates its positive effect on glucagon secretion by activation of α-adrenergic receptors (328). The authors used phentolamine, a non-selective α-adrenergic receptor antagonist, to block the effect of norepinephrine. Blockade of the β-adrenergic receptors with propanolol did not affect norepinephrine stimulation of glucagon secretion. Because binding of norepinephrine to α2-adrenergic receptors inhibits adenylyl cyclase, the authors propose that norepinephrine mediates its positive effect by binding to α1-adrenergic receptors, which activate phospholipase C, and thus elevate IP3 and $[Ca^{2+}]_i$.

v) Positive autocrine feedback by glucagon and L-glutamate

Glucagon secretion stimulates its own secretion following binding of the hormone to glucagon receptors in α-cell plasma membrane (162). Glucagon application to batches of isolated rat α-cells induces an elevation in both cyclic AMP levels and exocytosis rates with an EC_{50} of 1.6-1.7 nM. The stimulation plateaues at concentrations beyond 10 nM, where a more than 3-fold enhancement in exocytosis rate is observed. Application of the PKA inhibitor Rp-cAMPS reduces the rat α-cell response by ~50% indicating than both PKA-dependent and PKA-independent mechanisms are involved. The authors propose that the PKA-independent mechanism involves a cAMP-guanidine nucleotide exchange factor II (GEFII). In β-cells, cAMP-GEFII interacts with the Rab-interacting molecule Rim2 (329), which has been implicated in vesicle exocytosis (330). In contrast to rat α-cells, no PKA-independent pathway was found in mouse α-cells (162).

L-glutamate is the major excitatory neurotransmitter in the central nervous system. α-cells express vesicular glutamate transporters that facilitate glutamate uptake into vesicles (102), and glutamate is normally secreted together with glucagon (331). Rat α-cells express ionotropic glutamate receptors, including the AMPA and kainate subtypes (332), and metabotropic glutamate receptors (333, 334). Ionotropic glutamate receptors are ion channels that are permeable to Na^+, K^+, and sometimes Ca^{2+}. Their activation in low-glucose conditions triggers glucagon secretion in both rodents (335) and humans (336), likely by plasma membrane depolarization and activation of voltage-gated calcium channels. G protein-coupled metabotropic receptors modulate cellular cAMP levels in neurons and are typically associated with autocrine feedback inhibition of L-glutamate signaling. Stimulation of metabotropic receptors in low-glucose conditions inhibits

glucagon secretion from rat α-cells (333, 334), but has no effect in humans (336). Thus, glutamate likely exerts a positive autocrine signal for human glucagon release; however its physiological effect remains to be determined in rodents since glutamate has been associated with both stimulatory and inhibitory effects on glucagon secretion (334, 335).

4-6 Glucose-mediated suppression of glucagon secretion

α-cells contain much of the same secretory machinery as β-cells: glucose transporters, glucokinase, K_{ATP} channels, voltage-gated calcium channels and dense core secretory granules. However, unlike β-cells that are activated in response to an increase in glucose levels above 6 mM, α-cell secretion is inhibited at glucose concentrations above 4 mM. The mechanisms underlying the suppression of α-cell secretory activity are poorly understood, but two non-exclusive types of models have been proposed: direct inhibition by glucose, and paracrine inhibition from non α-cells within the islet of Langerhans.

4-6-1 Direct inhibition by glucose

i) The pros and cons

Several lines of evidence suggest that glucose inhibits the secretion of glucagon directly. First, secretion from mouse islets and perfused rat pancreas occurs in the absence of glucose or in low-glucose conditions and is inhibited when the glucose concentration reaches 4-6 mM (314, 337). This observation undermines a prominent role for β-cell secretory products in this inhibition because such concentrations are generally below the threshold for β-cell activation and insulin release. Also, glucose dose-

dependently reduces the stimulatory effect of amino acids on glucagon secretion from human diabetic patients without any substantial change in β-cell function (338), and from isolated rat α-cells (316). In addition, secretion from clonal α-cell lines (αTC1-6 and αTC1-9) is dose-dependently inhibited by glucose (305, 339). The same effect was reported from dispersed hamster islets when cell-cell contacts were abolished and paracrine effects greatly reduced (340).

In contrast, significant data argue against direct inhibitory action of glucose on glucagon secretion. First, glucose stimulates glucagon secretion from a pure population of isolated rat α-cells sorted by fluorescence-activated cell sorting (311, 341). Interestingly, non-sorted dispersed rat islets still respond to glucose by inhibiting the secretion of glucagon (341). The stimulatory effect of glucose on sorted α-cells is mediated by a β-cell-like mechanism involving glucose metabolism, closure of K_{ATP} channels and activation of voltage-gated calcium channels (311, 341). Second, observations suggesting a direct effect of glucose, as described previously, were obtained without the total absence of potential inhibitors from neighboring cell-types. Third, one should be cautious with data from clonal cell lines, because they rarely display a pure phenotype (342-344). Lastly, the known inhibitory effects of β-cell secretory products (insulin, zinc, GABA) and δ-cell somatostatin undermine the hypothetical direct inhibition by glucose (discussion in Section 4-6-2).

ii) Proposed mechanisms for the suppression of glucagon secretion by glucose

The present consensus is that glucose is dose-dependently transported into α-cells by GLUT-1, a lower capacity (Vmax) and higher affinity (low K_M) isoform than GLUT-

2, expressed in β-cells. The low expression of GLUT-1 results in glucose uptake rates 10-fold lower than in β-cells, but these are still an order of magnitude greater than overall metabolic flux (282), suggesting that glucose transport is not rate-limiting for α-cell metabolism. Thus, GLUT-1 and glucokinase likely form the glucose-sensor that initiates α-cell glucose metabolism (283). Rates of glucose metabolism have been reported to represent only 20-40% of what is observed in β-cells (345-347). Accordingly, small increases in ATP to ADP ratios were reported in α-cells (339, 348, 349). In contrast, one study failed to detect any change in ATP or ADP levels (347), and attempts to measure α-cell NAD(P)H or flavoprotein autofluorescence response to glucose have been unsuccessful with fluorescence microscopic techniques (191, 296, 350, 351).

K_{ATP} channels are expressed in mouse (352, 353) and rat α-cells (284, 311), in αTC1-6 cells (354), and in human α-cells (291), but have not been found in guinea pig α-cells (355). Rat α-cell K_{ATP} channels have an ATP sensitivity comparable to mouse and rat β-cell K_{ATP} channels ($0.85 < K_I < 0.95$ mM), but mouse α-cell K_{ATP} channels are much more sensitive for ATP ($K_I \sim 0.2$ mM). The reason for this greater sensitivity is not known (353). In addition, the K_{ATP} channel density is similar in mouse α- and β-cells (353). Similar to β-cells, glucose metabolism should depolarize the plasma membrane upon K_{ATP} closure. This effect was reported from α-cells in intact mouse islets (285) (356) and from isolated rat α-cells (341). However, the effect of glucose on α-cell membrane potential is still debated because membrane hyperpolarization after glucose stimulation has been observed from isolated mouse α-cells (352) and from α-cells in mouse and rat islets (357, 358).

Since glucagon release from islets is inhibited at elevated concentrations of

glucose, one would naïvely expect the α-cell $[Ca^{2+}]_i$ to drop concomitantly. Several models of glucose-mediated suppression of glucagon secretion rely on this assumption and incorporate reports describing a glucose-mediated decrease in α-cell cytoplasmic calcium levels or a slowing down of oscillation frequencies in intact mouse and human islets (191, 359, 360) and in dispersed guinea pig α-cells (361). Thus, one model proposes that α-cells are spontaneously activated in low-glucose conditions, as described in the electrophysiological model (Section 4-5-3). In this model, glucose metabolism leads to inactivation of K_{ATP} channels, membrane depolarization and inactivation of voltage-dependent channels important for spontaneous generation of action potentials (285, 291, 356, 362). In particular, these authors argue that glucose-mediated α-cell membrane depolarization inactivates voltage-gated Na^+ channels, T-type Ca^{2+} channels and A-type K^+ channels.

Supporters of the calcium store-operated current model (Section 4-5-5) propose that depletion of intracellular calcium stores in low-glucose conditions would activate a depolarizing store-operated influx of cations, which eventually triggers voltage-dependent Ca^{2+} influx and glucagon secretion (294). After an increase in glucose concentration, metabolism is accelerated and the intracellular calcium stores are refilled, leading to reduction of conductance, membrane repolarization, and suppression of glucagon secretion (337). However, this mechanism is not likely to govern glucagon secretion because inhibition of the SERCA pump by thapsigargin does not affect the ability of glucose to stimulate secretion from flow-sorted rat α-cells (311).

Models of glucagon suppression by glucose often postulate that $[Ca^{2+}]_i$ and calcium oscillations (either their amplitude, frequency, or both) are reduced at inhibiting

concentrations of glucose. However, calcium dynamics are difficult to measure in intact islets due to the difficulty of distinguishing α-cells among other cell-types. Nonetheless, besides studies reporting a increase in calcium dynamics in intact mouse islets (359, 360), intact human islets (191), single rat α-cells (363), dispersed guinea pig α-cells (361) and dispersed mouse α-cells (319, 337), other studies report a weak or negligible inhibitory effect of glucose in dispersed mouse α-cells (296, 339), whereas others describe glucose-mediated increases in $[Ca^{2+}]_i$ in isolated rat α-cells (311) and in α-cells within intact mouse islets (364).

4-6-2 The paracrine model of glucagon inhibition

The paracrine model refers to the inhibition of α-cell secretory activity by products released from other cell-types within an islet. Whether interactions occur via the interstitium or via the microvasculature is difficult to discern *in vivo*, although one study reports that β-cell secretory products are mainly released towards the interstitial space, away from blood vessels (365). The direction of blood microcirculation goes predominantly from β-cells to α-cells to δ-cells (Section 2-3). This order of perifusion is propitious for intraislet paracrine modulation of glucagon secretion by β-cell products. Compared to rodent islets, the human islet contains a greater proportion of α-cells and α-cells are not only located in the periphery of the islet (32). This particular cytoarchitecture predisposes human islets to intense paracrine signaling.

Accumulating evidence suggests that paracrine signals from β- and δ-cells are important for the suppression of glucagon secretion in high-glucose conditions. For instance, glucagon secretion from isolated rat α-cells is dose-dependently increased by

glucose, and this effect was counteracted by addition of potential paracrine inhibitors such as insulin, Zn^{2+}, GABA and somatostatin (311). However, these agents did not inhibit glucagon secretion below the basal rate observed at 1 mM glucose. Another argument for the paracrine hypothesis is the fact that α-cells become hyperactive in high-glucose conditions when β-cells are deficient. This hyperglucagonemic effect is observed in patients with type-I and advanced type-II diabetes (13-16, 366), and in alloxan-induced diabetic dogs (367). In contrast, overactive β-cells inhibit the α-cell secretory response (348). In addition, the pulsatile release of glucagon is antisynchronous to pulses of insulin and somatostatin in high-glucose conditions (278, 277). This opposite synchronicity suggests that α-cells are negatively coordinated with other cell-types, probably by paracrine signaling.

Paracrine signals are likely essential for proper regulation of glucagon secretion; however, it is not known which paracrine factor is prominent for glucagon suppression under physiological conditions, and the molecular mechanisms leading to this inhibition remain to be clearly established. Several potential candidates have been proposed, such as insulin, zinc ions, GABA, ATP and somatostatin. The evidence supporting the involvement of each of the potential paracrine inhibitors is discussed, as well as their proposed mechanism of action.

i) Insulin

Within the β-cell secretory granule, insulin is found at high concentration (~40 mM) and packaged into insoluble crystalline hexamers (368). Upon release into the circulation, the hexamer dissociates into bioactive monomers resulting in high local

concentrations of insulin that likely influence neighboring cells. Insulin has long been considered as the most likely β-cell products responsible for glucagon inhibition (369). Addition of exogenous insulin reduces glucagon secretion in humans, provided that glucose is co-infused to prevent hypoglycemia (370). The same inhibition is obtained from the isolated chicken perfused pancreas (371), the perfused pancreas of streptozotocin-treated rats (372), alloxan-treated dogs (367, 373), streptozotocin-treated hamsters (340), islets of streptozotocin-treated guinea pigs (349), isolated rat and mouse islets perifused in low-glucose conditions (339, 374), isolated rat α-cells (311, 341) and clonal mouse α-cells (375). Also, anti-insulin antibodies perfused in the isolated rat pancreas lead to a ~3-fold increase in the amount of glucagon secreted at 5.5 mM glucose (376). A similar positive effect was also reported with anti-insulin antibodies in humans (261).

High levels of insulin receptor transcripts have been identified in rat α-cells (341) and receptor expression has been reported in clonal mouse α-cells (375). α-cell-specific insulin receptor knockout mice exhibited mild glucose intolerance, hyperglycemia, and hyperglucagonemia in the fed state and enhanced glucagon secretion in response to L-arginine (304). Furthermore, small interference RNA-mediated knockdown of insulin receptor in glucagon-secreting InR1G clonal cells (from hamster glucagonoma) promoted enhanced secretion following glucose stimulation (304).

Few studies provide some mechanistic insight regarding the inhibitory effect of insulin on α-cells. Electrophysiological studies report a hyperpolarizing effect of insulin mediated by a greater K_{ATP} channel activity. Measurements of K_{ATP} channel currents demonstrate that high concentration of insulin (3 μM) is able to reduce the channel

sensitivity to ATP block in single mouse α-cells. The authors report that the K_I for ATP was shifted from 0.2 to 0.5 mM and that this effect was mediated by activation of PI3K (353). Another study on isolated rat α-cells also describes an elevation in K_{ATP} currents with "zinc-free" insulin (17 nM) but the effect was transient (~5 minutes) and was not mediated by PI3K activation (341).

In addition, the insulin receptor – PI3K – PKC / Akt pathway has been implicated in the translocation of GABA-$_A$ receptor channels (ligand-gated chloride channels) to the α-cell plasma membrane (377). This mechanism will be further discussed in the section related to GABA inhibition.

The proposed models for insulin inhibition of glucagon are based on the hypothesis that α-cell membrane is hyperpolarized in intact islets at inhibiting concentrations of glucose. However, this postulate is still debated ((285, 356) vs (357)), as is the overall effect of the hexose on $[Ca^{2+}]_i$ dynamics, as previously discussed in Section 4-6-1. Studies of the effect of insulin on α-cell $[Ca^{2+}]_i$ dynamics are scarce. One study reports a ~25% decrease in the frequency of calcium oscillations in αTC1-9 cells perifused in the absence of glucose or in 0.5 mM glucose. This effect was mediated by PI3K activation. However, insulin lost its inhibitory effect when glucose was greater or equal than 1 mM (339). Another study reports a small, if any, inhibitory effect on $[Ca^{2+}]_i$ in dispersed mouse α-cells (296).

ii) Zinc ions

β-cell secretory granules contain crystals of insulin hexamers, each hexamer being centrally coordinated with two Zn^{2+}. High concentrations of Zn^{2+} (~20 mM) are found

within the granules (368) and zinc is co-released with insulin (341); thus, zinc is another candidate for paracrine signaling. α-cells are equipped with a set of transporters (i.e. Zip1, Zip10, Zip14) allowing the uptake of Zn^{2+}, as well as transporters (i.e. ZnT4, ZnT5, ZnT8) responsible for extracellular efflux or accumulation into organelles (378). Zn^{2+} is also likely transported into α-cells in part through calcium channels (378).

The inhibitory effect of zinc on glucagon secretion was observed in isolated perfused rat pancreata (348), intact mouse islets (378), isolated rat α-cells (311, 341), and αTC1-6 cells (378). However, another report failed to observe any effect of exogenous Zn^{2+} on glucagon secretion from intact mouse islets and αTC1-9 cells (339). The mechanism of Zn^{2+}-mediated inhibition of α-cells is largely unclear. One electrophysiological study demonstrates that Zn^{2+} can reversibly activate K_{ATP} channels (EC_{50} = 2.2 μM) in isolated rat α-cells. K_{ATP} channel opening reduces α-cell electrical activity, and glucagon secretion (IC_{50} = 2.7 μM) (341). Few studies relate the effect of exogenous Zn^{2+} on α-cell calcium activity. Knowing that Zn^{2+} opens K_{ATP} channels, and that it reduces electrical activity and glucagon secretion, one could assume that α-cell $[Ca^{2+}]_i$ dynamics are inhibited. However, Zn^{2+} was found to slightly stimulate the frequency of calcium oscillations in dispersed mouse α-cells and in αTC1-9 cells (339), and another group failed to observe any effect of Zn^{2+} on dispersed mouse α-cell $[Ca^{2+}]_i$ (296).

iii) GABA

γ- aminobutyric acid (GABA) is an important inhibitory neurotransmitter in the central nervous system but several lines of evidence support a role of the neurotransmitter

for normal pancreatic endocrine function. GABA is produced in β-cells from glutamate by the enzyme glutamate decarboxylase, and is transported into synaptic-like microvesicles that are secreted in a regulated manner (379). Compared to insulin-containing large-dense core vesicles, microvesicles are much smaller in size. They constitute a different pool of vesicles and their exocytosis is differently regulated (380) (381-383). The reported effects of glucose on GABA release are controversial. One study reported a glucose-dependent increase of GABA secretion from the β-cell line βTC6 (384). Another did not notice any change from the β-cell line MIN6 (385). However, a majority of studies indicate that less GABA is secreted in high-glucose conditions from reaggregated rat β-cells (386, 387), rat islets (331), and βTC6 cells (388). It is notable that *in vivo* pancreatic islets are innervated by GABAergic neurons (98).

The ligand-gated chloride channel, $GABA_A$ receptor, is expressed in human (377), rat (293, 377) and guinea pig α-cells (389), as well as in αTC6 and In-R1G9 cells (377), but not in β- or δ-cells (293, 389). It has been demonstrated that insulin secretion induces $GABA_A$ receptor translocation to the α-cell plasma membrane (377). This potentiatory effect of insulin on GABA- $GABA_A$ receptor signaling is mediated by the insulin – insulin receptor – PI3K – Akt pathway (377). $GABA_A$ receptor activation by GABA leads to α-cell membrane hyperpolarization, as shown in dispersed guinea pig α-cells (389), rat islets (293, 377), and αTC6 cells (377). Putatively by this mechanism, GABA inhibits glucagon secretion from the perfused rat pancreas (390), guinea pig, rat and mouse islets (293, 389-391), αTC1-9 cells (391) and isolated rat α-cells (311). In addition, the use of an antagonist for the $GABA_A$ receptor increases glucagon secretion from intact mouse and rat islets, in both low- and high-glucose conditions (291).

Interestingly, the secretion of glucagon at high glucose was still less than at low glucose, suggesting that GABA is likely not entirely responsible for glucagon inhibition by glucose. The authors also report that the $GABA_A$ receptor antagonist did not stimulate glucagon secretion from human islets, and that $GABA_A$ receptors are scarcely expressed in human α-cells. Lastly, exogenous GABA application does not alter $[Ca^{2+}]_i$ dynamics in dispersed mouse α-cells (296).

iv) ATP

ATP is a recent addition to the list of potential paracrine inhibitors of glucagon secretion (392). ATP is concentrated in synaptic vesicles of nerve terminals within the islet. ATP is also found in insulin secretory granules (101, 368) and is co-released with insulin (393). Additionally, ATP molecules can be converted by plasma membrane ectonucleotidases into ATP metabolites or adenosine, and induce opposite effects depending on the type of purinergic receptor activated (394). Mouse α-cells express ATP and adenosine purinergic receptors $P2Y_1$, A_1, and A_{2A} (392, 395). Extracellular addition of ATP was found to reduce α-cell calcium dynamics and to inhibit the secretion of glucagon from intact mouse islets (392). In contrast, adenosine had the same inhibitory effect on calcium signals but did not modify the amount of glucagon secreted. These effects are unlikely mediated by concomitant stimulation of β-cell secretory activity because both ATP and adenosine lower the secretion of insulin (395, 396).

The inhibition of glucagon secretion by ATP in mouse islets (392), contrasts with previous findings in perfused rat pancreata (278, 395), and rat islets (278) where ATP and adenosine had a stimulatory effect on glucagon secretion. The reason for this discrepancy

is unclear and may reflect species differences. The effects of α-cell purinergic activation in humans have not been reported.

v) Somatostatin

In 1973, somatostatin (SST), a peptide hormone, was isolated in the hypothalamic tissue of the sheep and characterized as a suppressor of growth hormone secretion (397). SST is not only produced in the hypothalamus but throughout the central nervous system and most of the peripheral organs, including in the pancreatic islet δ-cells (398, 399). Thus, SST has two functions: one as a neurotransmitter and one as a hormone. *In vivo* and *in vitro* studies have shown that exogenous application of SST, or SST analogues, potently inhibits both insulin and glucagon secretion (400, 401). All five SST receptor subtypes are expressed in human, rat and mouse islets (402, 403), but it appears that α-cells predominantly express type-2 SST receptors and β-cells are mostly associated with type-5 SST receptors (401, 404). Interestingly, SST secretion is dose-dependently stimulated by glucose in pancreatic islets and the threshold concentration for δ-cells (4-5 mM) to respond to glucose is lower than that for β-cells (6-7 mM) (324, 337, 359, 405). This observation makes SST a good candidate for an important role in glucose-mediated inhibition of glucagon secretion.

All SST receptors characterized to date are coupled to inhibitory G proteins. Three different mechanisms have been proposed for the inhibition of glucagon secretion. Electrophysiological studies have reported that SST mediates its effect by activating a G protein-gated K^+ channel, which hyperpolarizes the plasma membrane and inhibits the α-cell electrical activity (289, 406). Somatostatin is also involved in a Gαi2 protein-

dependent pathway where activation of the protein phosphatase calcineurin leads to depriming of docked glucagon-containing granules belonging to the readily releasable pool (407). Interestingly, no decrease in $[Ca^{2+}]_i$ was observed, suggesting that the inhibition was not mediated by hyperpolarization of the membrane. Lastly, SST receptor activation inhibits adenylyl cyclase activity, thereby reducing cAMP levels and PKA stimulation of glucagon secretion (408).

Convincing arguments in favor of a prominent role of SST for glucagon inhibition in high-glucose conditions come from studies in SST $^{-/-}$ mice (405). Islets from these mice do not secrete SST, and in turn, glucagon secretion is no longer inhibited under high-glucose conditions, despite elevated insulin secretion. However, this result contrasts with a previous study where pertussis toxin was used to abolish somatostatin signaling in mouse islets (292). Those authors showed that pertussis toxin pretreatment did not alter the inhibition of glucagon secretion by glucose. Also, it has been documented that the hyperglucagonemia associated with diabetes persists in spite of elevated SST levels during hyperglycemia in humans, rats and dogs (409-414). Lastly, perifusion of mouse islets with an inhibitor of type-2 SST receptors stimulates glucagon secretion in low glucose but does not affect secretion at 7 mM glucose (337). These results argue against a prominent effect of SST in glucose suppression of glucagon secretion.

Chapter I wrap-up:

This first chapter is meant to introduce the physiology of pancreatic islets and to provide an in-depth presentation of glucagon-secreting α-cells. The α-cell research field is very controversial. The mechanisms of glucagon secretion in low-glucose conditions, as well as the mechanisms of glucagon suppression by glucose are still debated. For instance, it is not known if glucose mediates its inhibition directly on α-cells or indirectly via paracrine inhibition from other islet cell types. Such controversies likely reflect in part interspecies (humans, dogs, guinea pigs, rats, mice) and intraspecies (e.g. C57BL6 vs. NMRI mice) differences. In addition, the α-cell physiology is likely different *in vivo* (whole animal and perfused pancreas), compared to *ex vivo* (intact islets and isolated α-cells), or *in vitro* (tumoral α-cell lines).

The primary objective of our research was to investigate the mechanisms of glucagon secretion in low-glucose conditions and its suppression by glucose. We were particularly interested in determining the relationship between α-cell $[Ca^{2+}]_i$ and glucagon secretion. *In vivo* measurement of α-cell calcium dynamics by fluorescence microscopy is currently not possible due to technical limitations such as loading of the islets with a calcium indicator and light scattering in the tissues. Since hormonal responses to glucose are conserved in *ex vivo* mouse islets (Fig. IV-1), and harvested islets can be easily loaded with the calcium indicator Fluo-4, we used the intact pancreatic islet as a model for studying the mechanisms of glucagon secretion. In addition, we used flow-sorted α-cells to compare the α-cell physiology from islet α-cells with α-cells retrieved from their intraislet environment.

Ex vivo studies have been hindered by the lack of reliable methods to identify α-cells among other cell types in the living islet. Chapter II addresses this issue and presents a fluorescent-based visualization method whereby transgenic mice specifically express fluorescent proteins in α-cells. This α-cell identification strategy is utilized in Chapter III, IV and V. Chapter III investigates the role of ion channels (i.e. sodium, calcium and potassium channels) thought to be important for normal α-cell $[Ca^{2+}]_i$ oscillations and glucagon secretion in low-glucose conditions. Chapter IV reports the effect of glucose on α-cell metabolism and on glucagon secretion from sorted α-cells. Chapter V presents the effects of glucose and candidate paracrine inhibitors on α-cell $[Ca^{2+}]_i$. Chapter VI presents an innovative fluorescent-based method to study intercellular chemical communication through gap junctions. However, the method could not be applied on islets because the fluorescent tracer leaks out of the cells. Chapter VII summarizes the main results of our study of the mechanisms of glucagon secretion, and proposes future directions. Overall, our research supports a paracrine inhibitory model whereby non-α-cells would suppress glucagon secretion without decreasing α-cell $[Ca^{2+}]_i$, or inhibiting α-cell $[Ca^{2+}]_i$ oscillations.

CHAPTER II

α-CELL IDENTIFICATION WITHIN LIVING INTACT MOUSE ISLETS

1- Introduction

The first description of α-cells was achieved in 1907 by Lane M.A. using histochemical staining ((206), Fig.II-1). It was only in 1962 that α-cells were unequivocally ascribed as the source of glucagon, thanks to the development of immunofluorescence (219). Since then, α-cell research has been lagging behind β-cell research. Insulin deficiency being pivotal for the occurrence of diabetes, most of the research in the islet field has focused on β-cells. Thus, while the mechanisms of glucose-stimulated insulin secretion by β-cells are fairly well understood, the mechanisms underlying glucagon secretion under hypoglycemic conditions as well as its inhibition under hyperglycemic levels remain largely unknown.

A major impediment in the study of α-cells has been the lack of reliable methods to identify them within the intact living islet. In mice, only 10 to 15% of islet cells are α-cells, the remaining of the islet is composed of β-cells (~75 to 80% of the cells), δ-cells (5-10%), plus a few pancreatic polypeptide cells and ghrelin cells. Most previous research has been based on post hoc immunostaining analyses (359, 360, 364, 415-417), electrophysiological properties (285, 286, 292), or cell sorting based on size and autofluorescence (284, 316, 341, 348, 418). These identification methods suffer from several technical issues that interfere with the interpretation of the results. It is

challenging to trace a single cell within an intact islet before and after immunostaining treatment because of the morphological changes that inevitably follow tissue fixation. Electrophysiological identification can be misleading given the variability of reported electrical properties of different islet cell types (290, 419). Sorting by size or by autofluorescence yield significant overlap of different cell types and does not discriminate well between α- and other non-α-cells (418). In addition, the high number of islets required by this method makes it difficult to sort mouse α-cells. Consequently, sorting has only been applied on rat cells (311, 316, 341, 418).

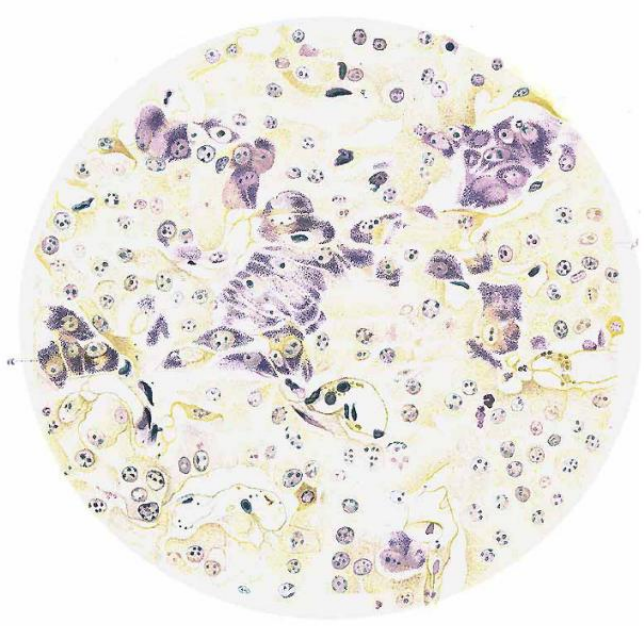

Figure II-1. The first visualization of α-cells in an islet by Lane M.A. in 1907 (from (206)). Section of an islet of Langerhans of the guinea pig, fixed in 70% alcohol, and stained with Bensley's Neutral Gentian, showing α-cells in violet and β-cells in orange.

At the onset of this thesis research, there was no rigorous method to distinguish α-cells from β-cells within a living islet. In this chapter, I describe a successful fluorescence-based visualization method whereby transgenic mice specifically express fluorescent proteins in α-cells (Section 3-1). This strategy will be used for investigating the mechanisms of glucagon secretion (Chapter III) and suppression by glucose (Chapter IV and V). In contrast, Section 3-2 presents an unsuccessful transgenic attempt to express fluorescent proteins specifically in α-cells. In the following sections, I discuss several other possible fluorescence-based strategies for identifying α-cells. I hypothesized that cell-specific differences in biophysical properties could be used to locate α-cells within the islet. Thus, I investigated potential cell differences in glucose uptake (Section 3-3), plasma membrane potential at low glucose levels (Section 3-4), intracellular calcium dynamics at low glucose (Section 3-5), and intracellular calcium responses to epinephrine (Section 3-6). These methods were assessed on transgenic islets expressing fluorescent proteins in α-cells (described in Section 3-1) to determine their respective specificity and reliability. Lastly, I discuss the main outcomes of the study in Section 4.

2- Materials and methods

2-1 Materials

Fluo4-AM, fetal bovine serum, penicillin, streptomycin, Hanks' balanced salt solution, phosphate buffer saline (PBS) and Roswell Park Memorial Institute (RPMI) 1640 medium were purchased from Invitrogen (Carlsbad, CA). Antibodies were purchased from Millipore (Billerica, MA). Unless specified, all other products were

purchased from Sigma-Aldrich (St. Louis, MO).

2-2 Transgenic mice

All work with animals was conducted in compliance with the Vanderbilt University Institutional Animal Care and Use Committee (IACUC). Transgenic mice (C57BL/6 genetic background) that specifically express Enhanced Yellow Fluorescent Proteins (EYFP) in α-cells have been designed and described by Quoix *et al*. (420). Transgenic mice are identified by polymerase chain reaction (PCR) on mouse-tail DNA (Puregene Mouse Tail Kit, Gentra Systems, Minneapolis, MN). EYFP-specific oligonucleotide primers: 5'-TGA CCC TGA AGT TCA TCT GCA CCA-3' (forward) and 5'- TGT GGC GGA TCT TGA AGT TCA CCT-3' (reverse), expected fragment size: 384bp. Cre-specific primers: 5'- TGC CAC GAC CAA GTG ACA GC-3' (forward) and 5'- CCA GGT TAC GGA TAT AGT TCA TG-3' (reverse), expected size: 675bp.

Fluo4-AM is the most suitable fluorescent Ca^{2+}-indicator dye for studying calcium dynamics in islets (170, 421). However, this fluorescent indicator dye cannot be used with EYFP-labeled α-cells since their emission spectra overlap. We therefore used ROSA26-tandem-dimer Red Fluorescent Protein (ROSA26-tdRFP) mice (422) obtained from the European Mouse Mutant Archive (EMMA, Munich, Germany) to perform Fluo-4 imaging.

2-3 Islet isolation and culture

Male mice (2 to 6 month-old) were anesthetized by intraperitoneal injection of 0.05 ml ketamine/xylazine (VedCo, St. Joseph, MO) at 80 mg/ml and 20 mg/ml,

respectively. We used a modified version of the collagenase digestion method described elsewhere (220, 423). Briefly, the pancreas was excised from the peritoneal cavity and placed in cold Hanks' balanced salt solution. The tissue was chopped into small pieces with a pair of scissors and Collagenase P (Roche Applied Science, Indianapolis, IN) was added at a concentration of 3 mg/mL. The solution was shaken vigorously in a 37ºC water bath for 12 minutes and the digested tissue was centrifuged at ~1,000 rpm (revolutions per minute). The pellet was washed three times in cold Hanks' balanced salt solution. The tissue was then placed into culture dishes and islets were hand-picked under a stereomicroscope. The digestion method yields ~150-200 islets per mouse.

Islets were cultured in islet medium composed of RPMI 1640 medium supplemented with 10% fetal bovine serum, penicillin (100 units/ml), streptomycin (100 µg/ml) and glucose (11 mM) at 37ºC under 5% humidified CO_2.

2-4 Immunofluorescence

Freshly isolated islets were attached on gelatin (0.1%) coated 35-mm glass-bottomed dishes (MatTek Corp., Ashland, MA) and cultured overnight. Islets were then fixed in PBS containing 2% of paraformaldehyde for 20 minutes, and permeabilized overnight at 4ºC in PBS with 0.3% Triton X-100, 5 mM sodium azide, 1% BSA and 5% goat serum (from Jackson ImmunoResearch Laboratories, West Grove, PA). Islets were incubated in permeabilization solution supplemented with primary guinea pig (GP) anti-glucagon antibodies (1:500) for 24-48 hours at 4ºC, washed with PBS three times, incubated with secondary anti-GP antibodies conjugated with Alexa Fluor 488 (1:1000) and rabbit anti-GFP antibodies conjugated with Alexa Fluor 555 (1:250 from a stock of 2

mg/ml) for another 24-48 hours, and washed three times before imaging. Alexa 488 and 555 were excited at 488 and 543nm, and their emission collected through a short (520-560nm) and a long-pass filter (>560nm), respectively.

2-5 Imaging conditions under the confocal microscope

Living intact islets were studied in imaging solution (i.e. filtered aqueous solution containing: 125 mM NaCl, 5.7 mM KCl, 2.5 mM $CaCl_2 – 2H_2O$, 1.2 mM $MgCl_2$, 10 mM HEPES (i.e. 4-(2-hydroxyethyl)-1-piperazineethanesulfonic acid) and 0.1% bovine serum albumin (BSA), pH7.4).

Islets were imaged in a poly(dimethylsiloxane) (PDMS) microfluidic device placed on the microscope stage, in a temperature controlled chamber at 37ºC and 5% CO_2. The fabrication of the device has been previously described (180, 424). The microfluidic chip holds the islet stable for imaging purposes and allows rapid reagent change. As shown in Fig. II-2, the device consists of a Y-shaped channel (height ~100 μm and width ~600 μm).

2-6 Glucose uptake measurements by confocal 2-NBDG imaging

Transgenic islets expressing tdRFP in α-cells were placed in a microfluidic device and perifused in imaging solution at 1 mM glucose. The fluorescent D-glucose analog, 2-NBDG (i.e. 2-[*N*-(7-nitrobenz-2-oxa-1,3-diazol-4-yl)amino]-2-deoxy-D-glucose), was supplemented to the islets through the Reagent Well during 5 min. The islets were then washed with the imaging solution for 1 min, and confocal z-stacks were collected. 2-NBDG was excited at 458nm and its emission collected between 490 and 560nm. α-cell RFP was excited at 561nm and its emission collected between 565 and 730nm.

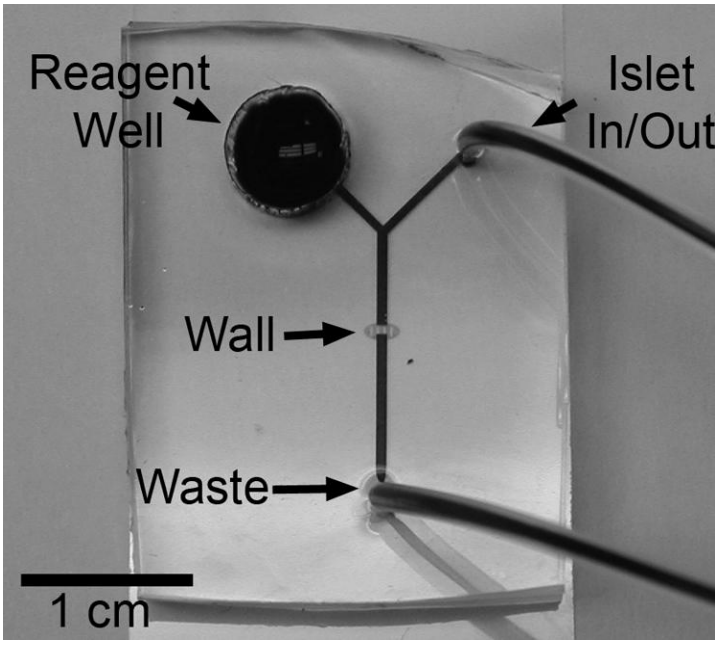

Figure II-2. A dye-loaded microfluidic device (from (180)). Islets are transported by gravity flow from the In/Out port to the Wall where they are trapped. The Reagent Well is used to quickly change the solution in the channel. A constant flow (~15 μL/min) is held between the reagent Well and the Waste port. The islets remained stationary after long periods of flow time (minutes to hours) and during reagent solution changes.

2-7 Plasma membrane potential measurements by confocal $DiBAC_4(3)$ imaging

Islets were perifused in imaging solution supplemented with 200 nM of bis - (1,3 - diethylthiobarbituric acid)trimethine oxonol), also called $DiBAC_4(3)$. An increase in fluorescence intensity is the consequence of dye accumulation into depolarizing cells (425, 426). After 30 minutes, confocal z-stacks were acquired by exciting the fluorescent dye at 488nm and by collected the emission between 490nm and 560nm. Meanwhile, α-cell RFP was excited at 561nm and its emission collected between 565 and 730nm.

2-8 Intracellular free calcium measurements by confocal Fluo4-AM imaging

The acetoxymethyl ester group (AM) allows the hydrophilic calcium indicator to cross the plasma membrane. Endogenous esterases cleave the AM group, trapping Fluo-4 in the cytosol. An increase in Fluo-4 intensity relates to greater $[Ca^{2+}]_i$ and the response is linear to physiological free calcium concentrations (421).

Islets were labeled with 5 μM of Fluo4-AM for one hour in imaging solution containing 1 mM glucose, at 37°C. After washing, islets were allowed to equilibrate on the microscope stage for 15 minutes. Time-series Fluo4 imaging was used for recording calcium oscillations within RFP islets. Fluo-4 was excited at 488nm and its emission was recorded between 490 and 560nm. tdRFP was excited at 561nm and its fluorescence collected between 565 and 730nm (LSM710, Zeiss).

2-9 Data analysis

Data collected by the LSM710 microscope were analyzed using Metamorph 7.6.1 (MDS Analytical Technologies, Downingtown, PA) and Excel 2007 (Microsoft, Redmond, WA). For analysis of single cells within pancreatic islets, regions of interest were chosen to exclude cell edges in order to best ensure that none of the neighboring cell fluorescence was collected. Background signal was subtracted from all images analyzed.

3- Results

3-1 Trangenic mice expressing fluorescent proteins under the glucagon promoter

In 2000, Herrera P.L. successfully designed a transgenic mouse line expressing a human growth hormone (hGH) specifically in α-cells (427). He used a Cre (cyclization recombinase) /loxP (locus of crossover of P1) system (428), whereby a reporter transgene is activated in a tissue specific manner. The strategy relies on the generation of mice expressing two transgenes. The "reporter" transgene (hGH) contained a loxP-flanked stop codon cassette upstream of the hGH coding region that blocks its expression. A second, or "tagger" transgene, consisted of the Cre recombinase gene placed under the control of a 2.1kb rat glucagon promoter fragment. Cre recombinase expression results in the excision of the STOP site in the reporter transgene, thus allowing hGH synthesis. This strategy was used to permanently label glucagon-expressing progenitor cells. Post hoc immunostaining on fixed pancreatic tissues was used to confirm that hGH was specifically expressed in α-cells, and that α- and β-cell lineages arose independently during ontogeny (427).

One advantage of generating double transgenic animals, over single transgenic mice expressing a reporter protein directly controlled by the glucagon promoter, is that the Cre/loxP strategy permits stronger expression of the reporter. Indeed, the glucagon promoter is known to be weak (compared to the insulin promoter (429)) and low expression of the reporter would be expected. In contrast, even if the expression of the Cre recombinase driven by the glucagon promoter is low in the Cre/loxP system, it is sufficient to allow excision of the loxP-flanked STOP sequence and to drive the expression of the reporter protein placed under the control of a stronger promoter.

In 2007, Quoix *et al.* bred mice bearing the tagger transgene expressing Cre recombinase under the control of the rat glucagon promoter (420) with conditional reporter mice containing a loxP-flanked stop codon cassette between the ROSA26 promoter (430) and a fluorescent protein (EYFP) gene (431). Transgenic mice shared a C57BL/6 genetic background. The authors showed that there were no statistical deviations in physiological parameters between transgenic and wild type mice in terms of body weight, islet architecture, plasma glucagon levels, blood glucose responses to insulin injection as well as blood glucose responses to fasting and refeeding (420).

The specific expression of fluorescent proteins in α-cells renders possible their identification within an islet and is particularly well-suited for fluorescence microscopy. We decided that the Cre/loxP system was the best method to study α-cells and Dr. Pedro Herrera (Department of Genetic Medicine and Development, University of Geneva, Geneva, Switzerland) and Dr. Alvin Powers (Department of Medicine, Vanderbilt University, Nashville, TN) generously provided us with Glucagon-Cre and ROSA26-EYFP mice, respectively. In order to assess the cell specificity of the fluorescent protein expression, we isolated the islets from double transgenic mice and performed immunofluorescence on islets fixed with paraformaldehyde. Immunofluorescence confirms that expression of fluorescent proteins is specific to α-cells (Fig. II-3). We found that ~63% of α-cells (132 of 210 cells), as determined by anti-glucagon antibodies, were labeled with fluorescent proteins (anti-GFP antibodies). Importantly, all of the fluorescent protein-expressing cells are glucagon-positive, although 35-40% of the α-cells are not labeled. It is not clear why fluorescent proteins are not expressed in all of the α-cells. This mosaic expression has been reported in other studies based on the Cre/loxP

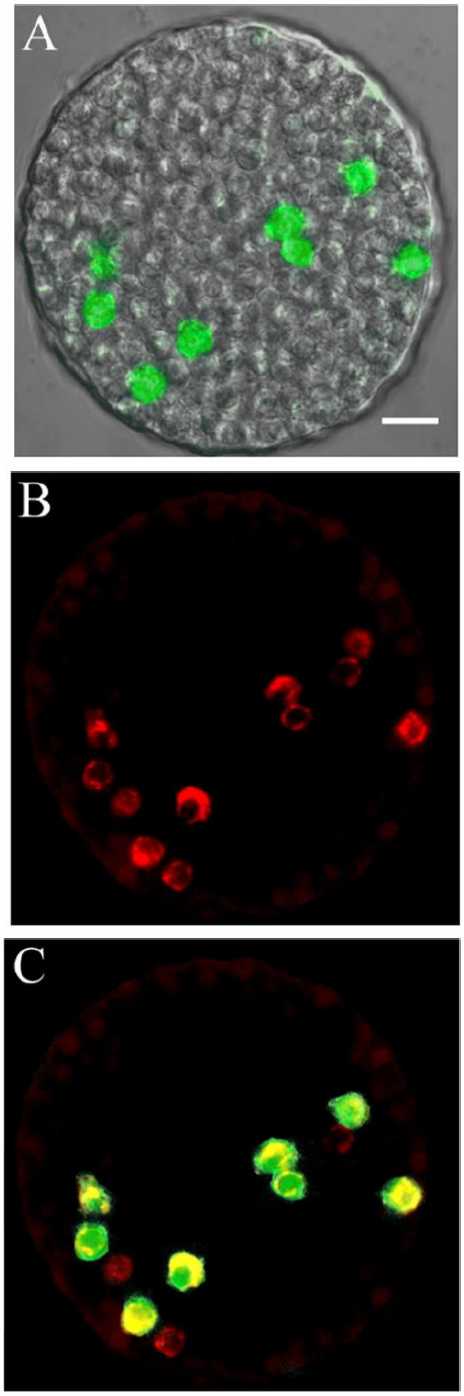

Figure II-3. Fluorescence-based visualization of α-cells within an islet. A, overlay of differential interference contrast and anti-GFP antibodies (green) images from a fixed permeabilized islet harvested from a EYFP-labeled α-cell animal. B, same islet stained with anti-glucagon antibodies (red). C, overlay of anti-GFP (green) and anti-glucagon (red) antibodies, co-localization presented in yellow. Scale bar = 20 μm. Bar in A is valid for A-C.

strategy (432) and is likely the consequence of position-effect variegations in the expression of the Glucagon-Cre transgene whereby inactivation of the transgene in some cells is caused by abnormal juxtaposition with heterochromatin (428). Alternatively, the transgene could become hypermethylated in some cells and remain silent (432).

The Cre/loxP system is a flexible method and other fluorescent proteins can be expressed instead of EYFP. For instance, the expression of EYFP is not suitable for calcium imaging, as measured by Fluo-4 imaging, because both EYFP and Fluo-4 emission spectra overlap. Thus, ROSA26-tdRFP mice were bred with Glucagon-Cre mice to perform Fluo-4 imaging on α-cells expressing red fluorescent proteins. Similar to transgenic islets containing EYFP-labeled α-cells, we sought to determine the percent of α-cells expressing RFP by fluorescence immunostaining. However, we were not able to obtain antibodies against tdimer2(12), which is the RFP expressed in our transgenic animals (422, 433). Since tdimer2(12) is a modified version of DsRed, a fluorescent protein isolated from corals (i.e *Discosoma sp.*), we tested monoclonal antibodies against DsRed (D.s. Peptide Antibody, Clontech) without success, as previously reported (434). To overcome staining RFP-labeled cells, we selected the islets by counting the number of RFP cells they contained and compared the result with the number of glucagon-positive cells revealed by immunostaining α-cells. We acquired confocal sections of the islets to carefully count the number of RFP-cells, and selected 26 islets that contained a total of 54 α-cells. Using glucagon antibodies, we immunostained the islets and found a total of 252 α-cells. We conclude that ~21% of the α-cells express RFP in our transgenic animals. This result differs from the ~63% of α-cells expressing EYFP from our Glucagon-Cre / ROSA26-EYFP mice. This difference is likely due to lower expression of the ROSA26-

tdRFP gene or to silencing of the Glucagon-Cre gene in later generations (435).

3-2 Trangenic mice expressing EYFP under the transthyretin (TTR) promoter

Several attempts were made to design transgenic animals that specifically express fluorescent proteins in α-cells. One hurdle to overcome was the weakness of the glucagon promoter to drive the expression of fluorescent reporters in sufficient amount to be detected. As previously discussed, the Cre-loxP strategy used by Dr. Herrera helped to amplify the expression of the reporter. Another issue was to determine what fragment of the glucagon promoter bears important consensus sequences for cell-specificity. Thus, smaller fragments of the glucagon promoter were used to drive the expression of transgenes, but the specificity was lost and the transgenes were also expressed in other cell-types (429).

Since the use of the glucagon promoter was unsuccessful, the Bell laboratory from the University of Chicago tried another approach based on the transthyretin (TTR) promoter. TTR is a serum and cerebrospinal fluid carrier protein involved in the transport of retinol and the thyroid hormone thyroxine. TTR is mainly synthesized in the liver where it is released, but other sites of production, such as the choroid plexus and pancreatic islets, are also involved (436, 437). Interestingly, patients with glucagonoma syndrome, a rare tumor of the α-cells, exhibit high serum concentrations of glucagon and TTR, suggesting that TTR production from the islets might be mostly ascribed to glucagon-producing cells (438-440). Immunohistochemical analyzes of slices of human pancreata showed that α-cells were strongly TTR immunoreactive, compared to β-cells that were slightly immunoreactive (437). These findings were the likely rationale for

designing transgenic mice with fluorescent proteins controlled by the TTR promoter.

When I joined Dr. Piston's laboratory, there were no rigorous methods available for distinguishing α-cells from other non-α-cells in the islet. We had previously received these TTR mice from the Bell's group and my first task was to breed them and confirm that the TTR promoter was mostly active in α-cells, as claimed by their conceivers. Unfortunately, fluorescent proteins were expressed in most of the islet and the brightest cells were not necessarily α-cells (Fig. II-4). Consequently, the TTR strategy was not successful in achieving α-cell specificity.

3-3 α-cell identification based on cell-specific glucose uptake characteristics

3-3-1 Rationale

α- and β-cells are thought to be equipped with different sets of glucose transporter isoforms. Northern blots as well as Western blots from dispersed rat islets suggest that GLUT-1 and GLUT-2 are expressed in β-cells, GLUT-2 being predominant (282). In contrast, rat non β-cells (mostly α-cells purified by fluorescence-activated cell sorting based on size and autofluorescence properties) only express GLUT-1 albeit at low abundance. Radio-isotopic measurements confirmed that β- and non β-cells exhibited different uptake rates for D-glucose and 3-*O*-methyl-D-glucose (a nonmetabolizable glucose analog) (128, 282, 345). α-cell GLUT-1 has a high affinity for glucose (Km ~3 mM) while β-cell GLUT-2 transports the sugar more efficiently around 15 mM (441, 442). This difference suggests cell-specific glucose transport properties in the islet.

The fluorescent D-glucose analog, 2-NBDG, has been used to study the rates of glucose uptake in rat pancreatic endocrine cells by fluorescence microscopy (441). The

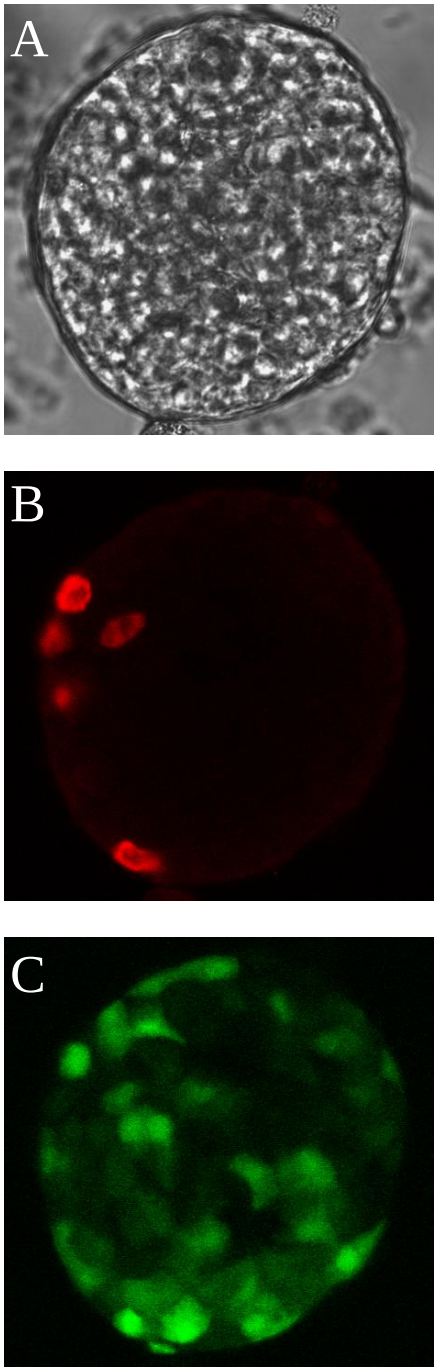

Figure II-4. Immunofluorescence of islets from transgenic mice expressing EYFP under the TTR promoter. A, differential interference contrast image of a fixed and permeabilized islet harvested from transgenic animals. B, same islet stained with anti-glucagon antibodies (red). C, same islet stained with anti-GFP (green) antibodies. The expression of fluorescent proteins is not restricted in α-cells, but is spread throughout the islet. Scale bar: 20 μm.

authors report that 2-NBDG was readily taken up by a majority of dispersed islet cells, and that a subset (~20%) of the cells only weakly transported the fluorescent glucose analog. Immunofluorescence staining confirmed that bright cells were β-cells, whereas weak cells were associated with α-cells and possibly other non-α-cells. Thus, cell differences in 2-NBDG uptake could potentially be used to readily distinguish α-cells from other cell types within an islet, provided that only α-cells exhibit slow transport rates.

3-3-2 Expected results

We tested the fluorescent glucose analog 2-NBDG in intact mouse islets from transgenic animals, whose α-cells express tdRFP (see Section II-3-1). We hypothesized that α-cells could be identified over other islet cell-types based on differences in 2-NBDG uptake. We expect that all the RFP α-cells will slowly transport 2-NBDG, compared to the majority of the islet cells (mostly β-cells). In Section 3-1, we found that only ~21% of α-cells are expressing RFP in our transgenic animals. Thus, we expect that only ~21% of the cells exhibiting slow 2-NBDG uptake would be RFP positive.

3-3-3 Results

Figure II-5 provides an example of confocal section of a mouse islet that was perifused with 2-NBDG (500 μM) for 5 minutes. This example illustrates the fact α-cells, as identified by RFP expression, are only weakly fluorescent for 2-NBDG compared to most of the islet. Overall, all the RFP-labeled cells (17 α-cells from 5 islets) were weakly fluorescent for 2-NBDG compared to most of the non-RFP cells that were ~2 to 3 fold

brighter. This observation demonstrates that, besides expressing glucose transporters that are more efficient at transporting glucose, α-cells are globally less effective than β-cells at taking up submillimolar concentrations of the sugar. The weak transport associated with α-cells is likely the result of low GLUT-1 expression in this cell type (282). The physiological relevance of cell-specific differences in glucose transport is not clear since the rate of glycolysis is limited by glucokinase in both cell types and this rate is more than 10-fold greater than that of glucose transport (282).

Figure II-5 also illustrates the fact that 2-NBDG is slowly transported into non-RFP cells. Overall, only ~21% (14 out of 68 cells) of the cells that were weakly fluorescent for 2-NBDG were RFP-positive. This number is similar to the percent of α-cells that are labeled with RFP. Since all the α-cells are associated with weak 2-NBDG fluorescence, this observation suggests that the remaining 79% of the weak cells are also α-cells.

3-3-4 Discussion

Using 2-NBDG to identify α-cells is a promising method but further controls are necessary for its validation. Direct α-cell identification by RFP fluorescence reveals that all the α-cells slowly transport 2-NBDG, compared to most of the islet cells. In order to use 2-NBDG as a method of identifying α-cells in wild-type islets, it is important to demonstrate that α-cells are the only cell-type to exhibit slow 2-NBDG uptake. Our observation that the percent of α-cells expressing RFP closely matches the proportion of RFP cells associated with slow 2-NBDG uptake suggests that α-cells can be discriminated from other islet cell-types based on differences in 2-NBDG uptake.

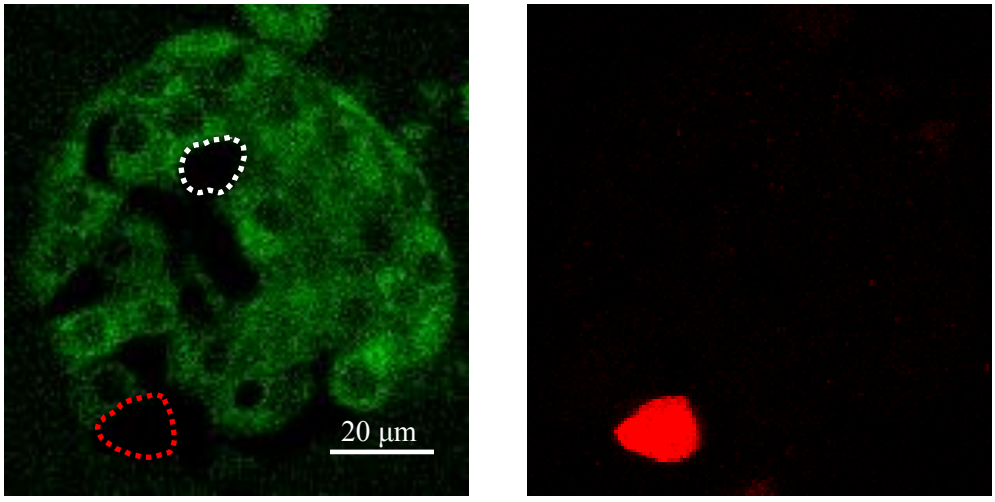

Figure II-5. Fluorescence-based visualization of cell differences in glucose transport. Left panel, representative confocal image of an islet (from a tdRFP-labeled α-cell mouse) that has been previously perifused for 5 minutes in 500 μM of 2-NBDG (green). The red dashed trace indicates the localization of one RFP-expressing α-cell, as shown in the right panel. Compared to most of the cells in the islets, the glucose analog, 2-NBDG, is slowly transported into α-cells. However, non-RFP cells were also weakly fluorescent for 2-NBDG, as illustrated by the white dashed trace.

A similar approach could be performed on wild-type mouse islets in which the number of cells that are weakly labeled by 2-NBDG could be determined by confocal sectioning of the islet. Post hoc immunostaining for α-cells from the same islets should yield the same number of cells. However, this strategy does not prove directly that the method is specific for α-cells. It is conceivable that some other cell-types such as somatostatin-secreting δ-cells, pancreatic polypeptide cells, ghrelin cells, or a subset of β-cells could exhibit the same 2-NBDG response than α-cells. The problem is circular since there is no rigorous way of discriminating between different cell-types in the living wild-type islet. One

possible approach would be to disperse wild-type islets into single cells and perform 2-NBDG imaging. Post hoc immunostaining for the different cell-types should directly test for the specificity of the method, assuming that cell-specificity of 2-NBDG transport is not altered during dispersion. Alternatively, 2-NBDG uptake could be assessed on islets which β-cells express GFP (e.g. MIP-GFP transgenic mouse (443)). This control should confirm that all the β-cells are brightly labeled with 2-NBDG.

2-NBDG imaging could provide an easy and fast method for discriminating α-cells within intact islets under the microscope. Such a method could be performed on wild-type mouse islets and thus, would avoid the inconvenience of transgenic animals (i.e. cost, maintenance, genotyping). In addition, the method could be applied on other islet species in which transgenic lines are more difficult or impossible to obtain, such as rats and humans. However, further studies would be necessary to validate the method in these species. For instance, one possible limitation is the fact that human β-cells predominantly express GLUT-1 instead of GLUT-2 (442). In addition, it is not known how GLUT-1 expression compares between human α- and β-cells. Thus, it could be possible that 2-NBDG uptake would not be significantly different between human α- and β-cells.

3-4 α-cell identification based on cell-specific differences in membrane potential

3-4-1 Rationale

$DiBAC_4(3)$ is a fluorescent anionic probe used for assessing changes in the plasma membrane potential (425, 426). Increased depolarization leads to accumulation of the dye within the depolarized cells, and thus an increase in fluorescence; whereas

hyperpolarization results in decrease in fluorescence. Hjortoe *et al.* (358) applied this membrane potential indicator on intact mouse islets. The authors report the presence of bright depolarized cells at low glucose levels and identify them as α-cells by post-hoc immunofluorescence. In contrast, the fluorescence intensity associated with β-cells was much lower. This difference in membrane potential at low glucose, as measured by $DiBAC_4(3)$, could be used as a method to identify and monitor α-cells in an islet.

3-4-2 Results / discussion

We used $DiBAC_4(3)$ on transgenic islets expressing tdRFP in α-cells perifused at 1 mM glucose to determine if the depolarized cells were indeed α-cells (see Fig. II-6). We found that $DiBAC_4(3)$ fluorescence was on average 175.4 ±17.6% brighter in RFP-labeled α-cells (42 α-cells from 7 islets) than in the remaining non-labeled cells (mostly β-cells). Also, ~75% of RFP α-cells exhibited fluorescence intensities 2-fold greater than β-cells. This observation suggests that most of the α-cells are more depolarized than β-cells at low glucose levels. Importantly, only ~26% of the bright cells were expressing RFP (23 RFP-labeled cells out of 87 bright cells). Since we cannot distinguish between the different islet cell-types, it is not possible to determine the cell composition of the remaining ~74% of bright cells. In Section 3-1, we found that only ~21% of the α-cells express RFP in our transgenic animals. Similar to our 2-NBDG study previously presented, if all the bright cells were α-cells, it would imply that ~21% of the bright cells express RFP in our transgenic islets. Consequently, the result suggests that most of the bright cells are α-cells. Similar to 2-NBDG, validation of the $DiBAC_4(3)$ method as a rigorous way to identify α-cells within intact living islets would require development of

further control experiments.

3-5 α-cell identification based on cell-specific $[Ca^{2+}]_I$ dynamics

3-5-1 Rationale

Glucagon-secreting α-cells exhibit intracellular calcium oscillations at low glucose levels in intact mouse islets (359, 360), and dispersed mouse α-cells (319, 337, 420). In contrast insulin-secreting β-cells are silent below 6 mM glucose (172). This cell-specific difference in calcium dynamics could constitute a simple assay for identifying α-cells in an intact islet.

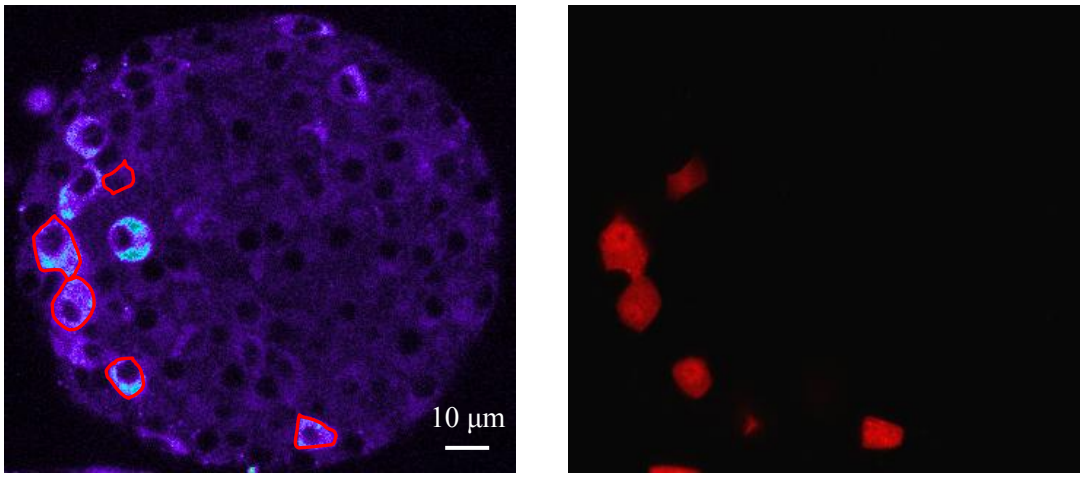

Figure II-6. Fluorescence-based visualization of cell differences in membrane potential. Left panel, representative confocal image of an islet (from a tdRFP-labeled α-cell mouse) perifused at 1 mM glucose in $DiBAC_4(3)$ (pseudocolor). The red traces indicate the localization of RFP-expressing α-cells, as presented in the right panel.

3-5-2 Results / discussion

We used transgenic islets expressing tdRFP in α-cells and performed Fluo-4 imaging at 1 mM glucose to determine if α-cell $[Ca^{2+}]_i$ was oscillating (Fig. II-7). We found that ~77% of islet α-cells were oscillating during a 5-minute observation period (41 out of 53 RFP-labeled cells in 7 islets from 2 mice). Consequently, α-cell identification based on calcium oscillations would not apply for the remaining ~23% of silent α-cells. In addition, we noticed that most of the cells exhibiting calcium oscillations at low glucose were not labeled with RFP. Only ~25% (41 out of 163 cells) of the oscillating cells were RFP positive. Since ~21% of the α-cells are RFP positive (Section 3-1), the results suggests that most (if not all) of the oscillating cells at low glucose are α-cells. Further validation of the method would require more control experiments to determine if some non-α-cells also oscillate at low glucose levels. Importantly, one disadvantage of the method over 2-NBDG or $DiBAC_4(3)$ imaging is that Fluo-4 is only restricted to the first layer of the islet. As a result, Fluo-4 imaging could not identify α-cells located deeper inside the islet.

3-6 α-cell identification based on cell-specific responses in $[Ca^{2+}]_i$ to epinephrine

3-6-1 Rationale

Epinephrine is a potent glucagon secretagogue and has been reported to cause elevation of $[Ca^{2+}]_i$ in a majority of mouse islet α-cells exposed to low glucose levels, while having no effect on β-cell $[Ca^{2+}]_i$ (294). This difference in intracellular calcium responses could be used as a tool for identifying α-cells.

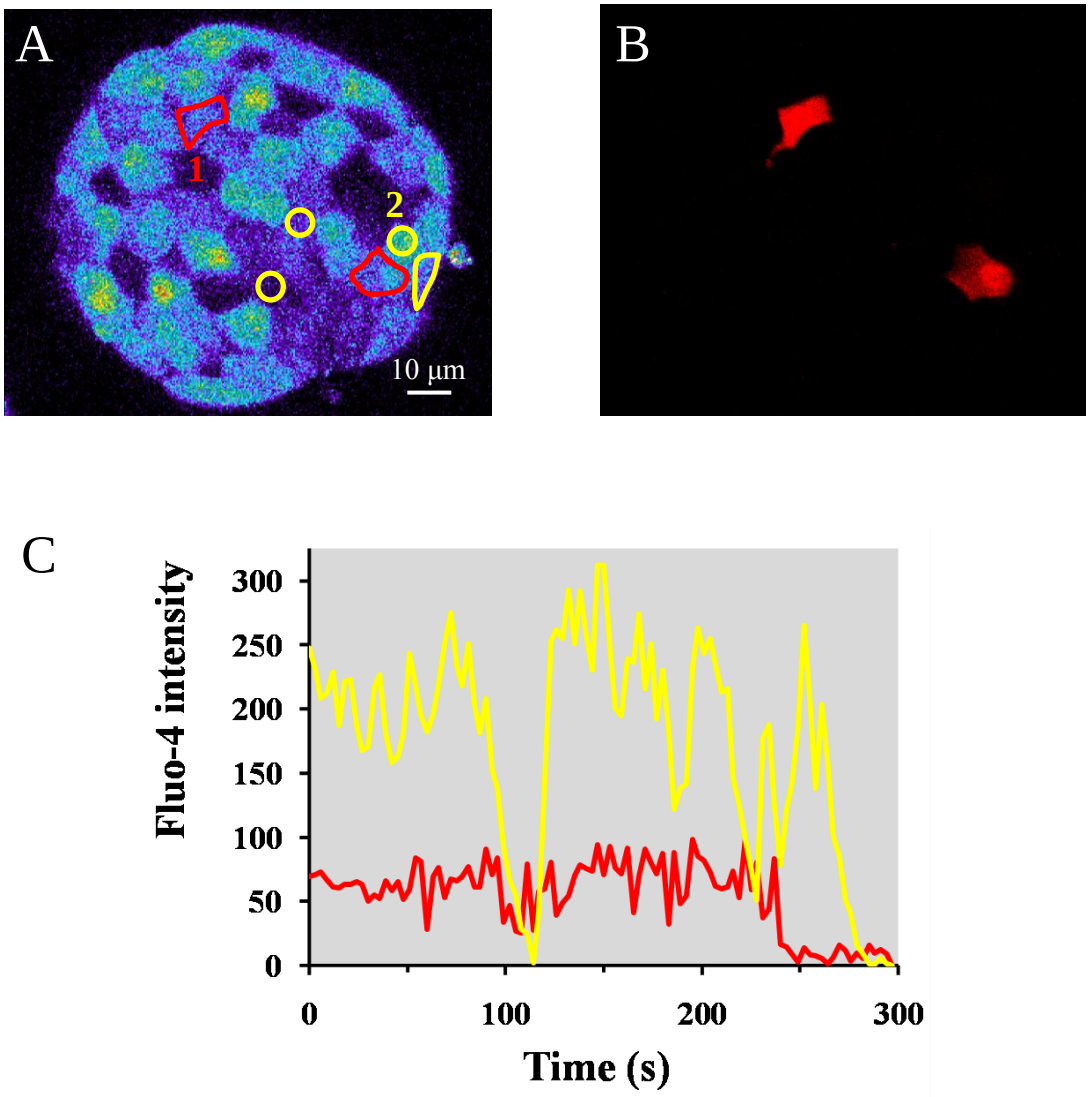

Figure II-7. Cell-specific visualization of intracellular calcium dynamics by Fluo-4 imaging. A, representative confocal image of an islet (from tdRFP-labeled α-cell mouse) loaded with Fluo-4 (pseudocolor) in 1 mM glucose. The confocal section was taken at the bottom of the islet. The red traces indicate the localization of two RFP-expressing α-cells, as presented in B. The yellow traces outline oscillating cells that do not express RFP. C, time-series acquisitions of Fluo-4 intensity (A.U.) over a period of 5 minutes at 1 mM glucose. The red and yellow plots refer respectively to the cells #1 and #2 presented in panel A.

3-6-2 Results / discussion

We perifused transgenic islets expressing tdRFP in α-cells at 1 mM glucose and measured the effect of epinephrine on α-cell $[Ca^{2+}]_i$ using the calcium indicator Fluo-4, (Fig. II-8). We found that application of 1 μM epinephrine did not significantly change α-cell $[Ca^{2+}]_i$ (-9.3 ±12.4% change in Fluo-4 intensity for 5 minutes following the application of the drug, n=8 α-cells from 3 islets). Longer incubation (>10 minutes) did not alter the averaged $[Ca^{2+}]_i$ either. Furthermore, epinephrine had no effect on β-cell $[Ca^{2+}]_i$ (-1.6 ±1.4%, n=3 islets). Figure II-8 shows representative traces of α- and β-cell $[Ca^{2+}]_i$ responses to epinephrine. Greater concentrations of epinephrine (i.e. 10 μM) also did not alter $[Ca^{2+}]_i$ responses.

The effect of epinephrine on α-cell $[Ca^{2+}]_i$ is controversial since it has been argued that epinephrine stimulates glucagon secretion mainly by a cAMP-dependent pathway leading to acceleration of the rate of granule mobilization from a reserve pool to a readily releasable pool (286, 361). Our results support this model and indicate that epinephrine enhances glucagon secretion without elevating $[Ca^{2+}]_i$.

4- Conclusion and future directions

One reason why research on α-cell physiology has lagged behind β-cell research is the lack of reliable methods to unequivocally identify them within intact living islets. This limitation is likely one source of controversies in the field. We describe a successful approach of visualizing α-cells in Section 3-1. The method relies on the specific expression of fluorescent proteins in α-cells from double transgenic mice.

The Cre/loxP strategy used for driving the expression of fluorescent proteins in α-

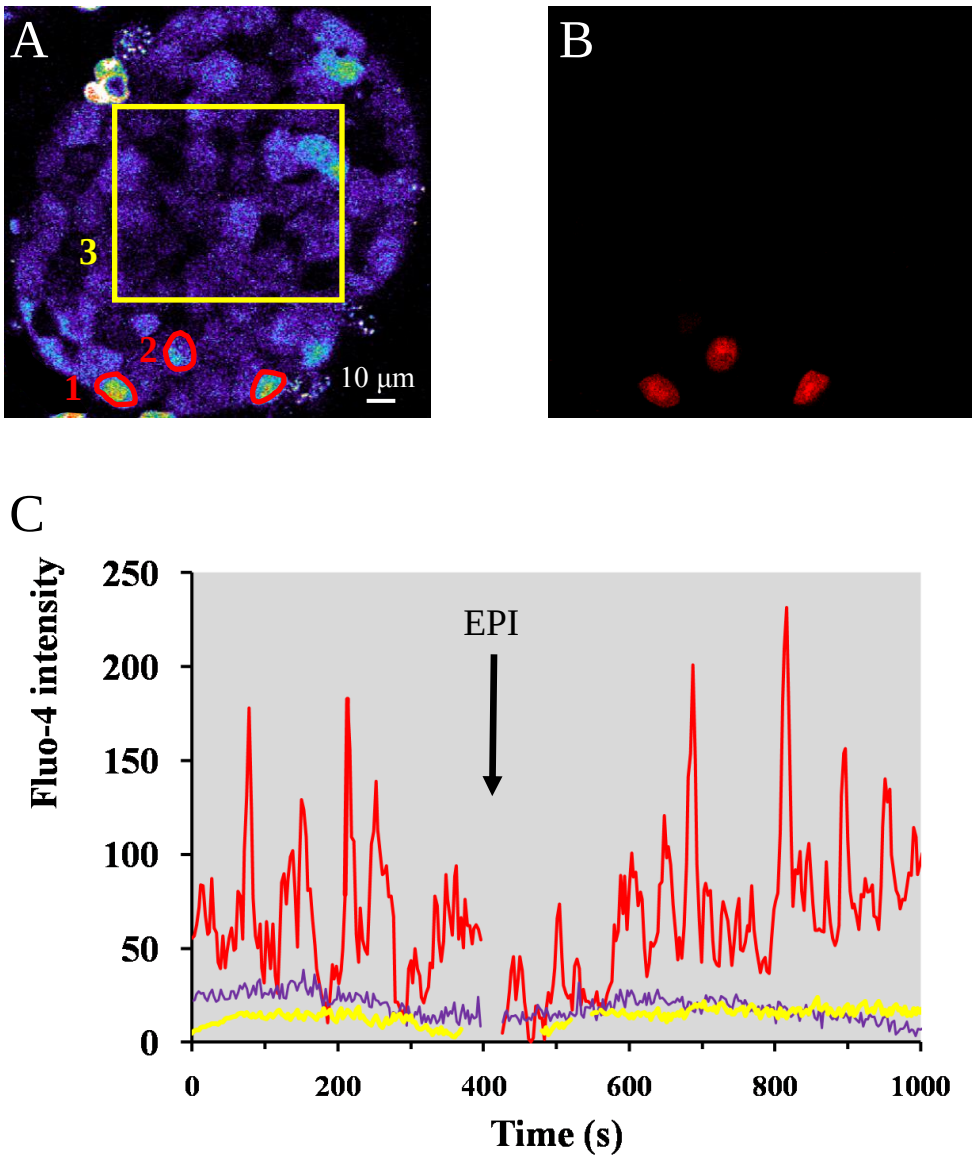

Figure II-8. Epinephrine does not affect $[Ca^{2+}]_i$ at low glucose. A, representative confocal image of an islet (from tdRFP-labeled α-cell mouse) loaded with Fluo-4 (pseudocolor) in 1 mM glucose. The confocal section was taken at the bottom of the islet. The red traces indicate the localization of three RFP-expressing α-cells, as presented in B. The yellow rectangle represents β-cells. C, time-series acquisitions of Fluo-4 intensity (A.U.). The black arrow shows when 1 µM of epinephrine (EPI) has been perifused to the islet. The red, violet and yellow plots refer respectively to the regions #1, #2 and #3 presented in panel A. On average, epinephrine does not change α-cell $[Ca^{2+}]_i$ (in text).

cells will likely help the study of α-cell physiology since it is now possible to perform quantitative fluorescence imaging on well-identified α-cells within the living pancreatic islets. For instance, we used this strategy to perform 2-NBDG imaging (Section 3-3), $DiBAC_4(3)$ imaging (Section 3-4), Fluo-4 imaging (Section 3-5 and 3-6, Chapter III and V), FuraRed imaging (Chapter V), NAD(P)H imaging (Chapter IV) and TMRE imaging (Chapter IV – Section 3-7). In addition, the expression of fluorescent proteins in α-cells allows the constitution of pure population of α-cells isolated by fluorescence-activated cell sorting (Chapter IV, Section 3-1). The method will also greatly facilitate the electrophysiological study of α-cells. Besides issues concerning the specificity of α-cell identification based on electrophysiological properties, only 7% of the cells hit during patch-clamp experiments are identified as α-cells (357). Furthermore, the tagger transgene (Cre-Glucagon) can be used with different reporter trangenes (in place of ROSA26-FPs) to drive the expression of genes of interest. For instance, this strategy has been recently utilized for creating transgenic mice with α-cell-specific conditional knockout of insulin receptors (444) and L-type calcium channels (Cav1.2 subunits) (419).

Transgenic-based identification of α-cells suffers from a few disadvantages. First, the technology is currently available only in the mouse, thus the method only applies for the study of mouse α-cells. In addition, not all the α-cells are labeled by fluorescent proteins, only ~20% of α-cells were identifiable in our Glucagon-Cre / ROSA26-tdRFP mice. Furthermore, acquiring and maintaining double transgenic animals are expensive and time-consuming. We therefore investigated several possible fluorescence-based strategies for identifying α-cells based on cell-specific differences in biophysical properties, such as glucose uptake (Section 3-3), plasma membrane potential at low

glucose (Section 3-4), intracellular calcium dynamics at low glucose (Section 3-5), and intracellular calcium responses to epinephrine (Section 3-6). We used RFP-labeled α-cells from transgenic animals to unequivocally identify α-cells in the islet and compared their biophysical responses to non-labeled cells. We found that all the RFP-cells were slowly transporting glucose, that more than 75% of them were more depolarized than β-cells at low glucose levels, and that ~75% of them exhibited $[Ca^{2+}]_i$ oscillations at low glucose. The relationship between membrane potential and $[Ca^{2+}]_i$ oscillations is further studied in Chapter III. Importantly, the percent of α-cells expressing RFP closely matches the percent of RFP cells among the islet cells characterized on their biophysical properties. Although further control experiments are necessary, this observation suggests that these methods could potentially help to distinguish α-cells from the other cell-types.

Lastly, we are currently developing a lentiviral-based method for expressing genes of interest in α-cells. We are particularly interested in expressing fluorescent biosensors to measure cAMP, Ca^{2+}, and ATP (445). The biosensor coding region will be driven by the glucagon promoter for specific expression in α-cells, and the genetic material will be transduced into isolated intact islets or dispersed islet cells. Fluorescent biosensors can also be genetically targeted to distinct locations within α-cells, such as organelles and membranes.

CHAPTER III

MECHANISMS OF GLUCAGON SECRETION UNDER LOW GLUCOSE CONDITIONS

1- Introduction

1-1 The electrophysiological model of glucagon secretion

Glucagon is secreted by the islets of Langerhans under hypoglycemic conditions to promote glucose output from the liver (20). The molecular mechanisms of glucagon secretion from α-cells are not known and are a matter of controversy, as detailed in Chapter I, Section 4-6. Electrophysiological measurements on mouse islets and isolated mouse α-cells have identified a number of membrane channels potentially important for the release of glucagon (285, 356). The "electrophysiological model" of glucagon secretion (Fig. III-1) proposes that, at low glucose levels (Fig. III-1A), K_{ATP} channels are partially open, resulting in an intermediate resting membrane potential (~ -45mV). Tetrodotoxin (TTX)-sensitive voltage-gated Na^+ channels are therefore activated and depolarize the membrane enough to maximally activate high-voltage sensitive calcium channels (above -20mV) that generate calcium activity transients and stimulate granule exocytosis. The model also proposes an explanation for the inhibition of glucagon secretion by glucose (Fig. III-1B). Similar to β-cells, glucose metabolism increases the ATP to ADP ratio, closing K_{ATP} channels and thus depolarizing the plasma membrane. Unlike β-cells, α-cell membrane depolarization by glucose (to ~ -30mV) would inactivate

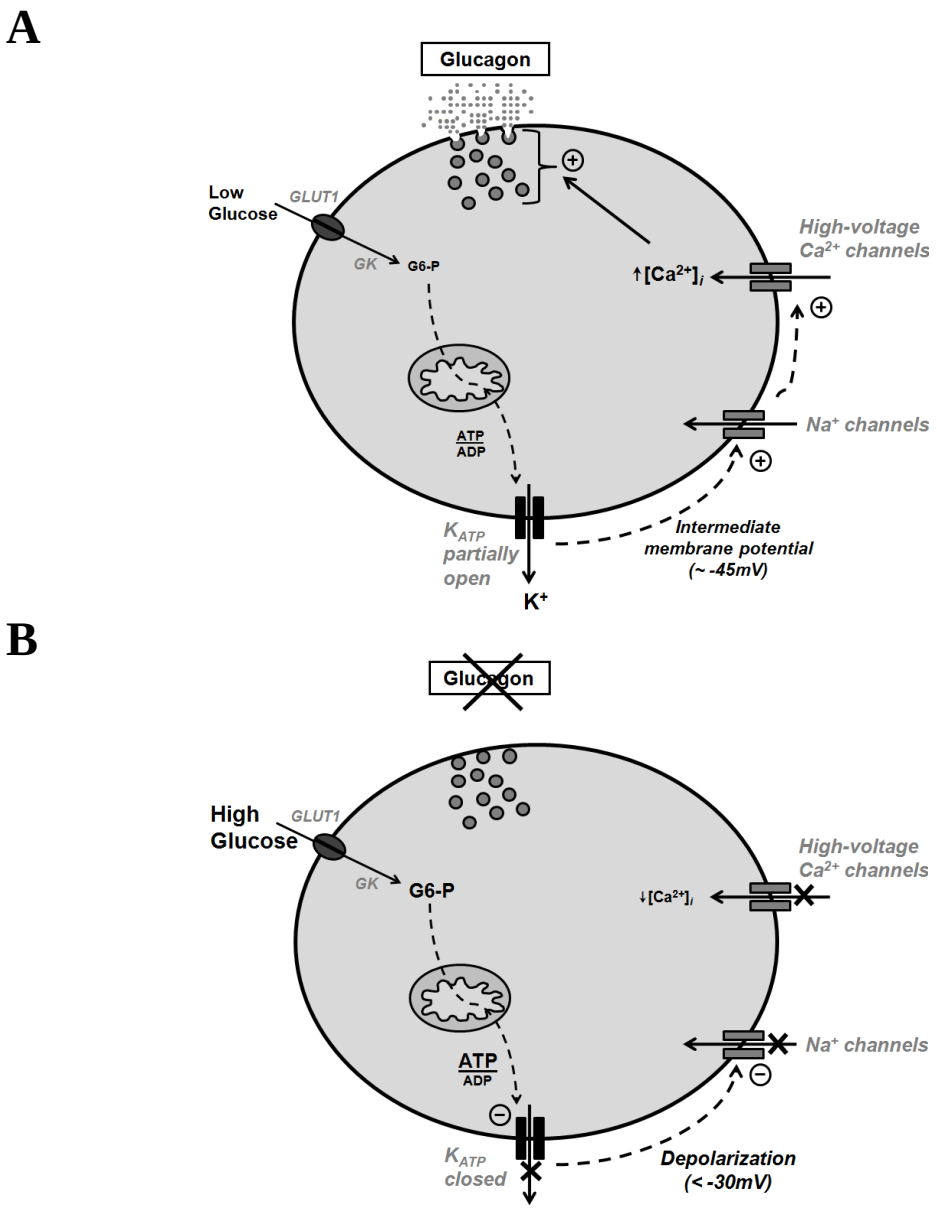

Figure III-1: Electrophysiological model of glucagon secretion, modified from (356). A, under low glucose conditions, K_{ATP} channels are partially open and set the plasma membrane to an intermediate resting potential (~ -45mV). At this resting potential, voltage-gated Na^+ channels are activated and depolarizing action potentials occur. Such depolarizing events activate more high-voltage sensitive calcium channels (> -20mV). Calcium channel activation stimulates exocytosis of glucagon-containing granules. B, at glucose concentrations higher than 4 mM, glucose metabolism increases the ATP to ADP ratio, closing K_{ATP} channels and thus depolarizing the plasma membrane (to ~ -30mV). α-cell membrane depolarization by glucose would inactivate voltage-gated Na^+ channels. As a result, action potentials are lost and less high-voltage calcium channels are recruited, leading to suppression of granule exocytosis.

TTX-sensitive voltage-gated Na^+ channels. As a result, less high-voltage calcium channels are activated and calcium oscillations are suppressed (285, 291, 356).

1-2 Limitations of the model

The electrophysiological model provides an attractive description of glucagon secretion, but suffers from several issues. First, the model implies that glucose directly inhibits the secretion of glucagon. However, the literature describes an increase in glucagon secretion from isolated rat α-cells (311, 341). Likewise, the model predicts that glucose slightly depolarizes the α-cell membrane, as reported in intact mouse islets (285, 356) and from isolated rat α-cells (341). However, membrane hyperpolarization has also been observed from isolated mouse α-cells (352) and from α-cells in both mouse and rat islets (357, 358). In addition, the identity of high-voltage sensitive calcium channels involved in the generation of α-cell calcium oscillations is still debated. Some studies support a prominent role for the N-type channels (286, 291-293), whereas others favor the L-type isoform (294-297). As discussed in Chapter II, a major impediment in the study of α-cells has been the lack of reliable methods to identify them within the intact living islet (Chapter II). The proponents of the electrophysiological model have identified α-cells based on electrophysiological properties such as the presence of TTX-sensitive currents at physiological membrane potentials (285, 291, 356). However, electrophysiological identification can be misleading since TTX-sensitive currents are also present in β-cells (295, 446, 447). In addition, other studies failed to detect the residual sodium currents used for α-cell identification (295, 353). Furthermore, only 7% of the cells hit during patch clamp experiments in intact islets are identified as α-cells

based on electrophysiological properties (357). Since α-cells account for ~15% of islet cells, and an even greater percentage of those on the surface of the islet, the representativeness of the selected population is questionable.

1-3 Objectives of the study

In Chapter II – Section 3-1, we described a fluorescence-based identification method to unequivocally distinguish α-cells from other cell-types in the mouse islet. The present study tests the electrophysiological model in well-identified α-cells by investigating the role of ion channels thought to be important for glucagon secretion under hypoglycemic conditions (i.e. TTX-sensitive voltage-gated Na^+ channels, high-voltage sensitive calcium channels and K_{ATP} channels). We were particularly interested in determining how pharmacological modulation of these channels affects α-cell intracellular calcium dynamics and glucagon secretion.

2- Materials and methods

2-1 Materials – Transgenic mice - Islet isolation and culture (as described in Chapter II – Section 2). Tetrodotoxin was purchased from Tocris Bioscience.

2-2 Islet perifusion and hormone analysis

The day after isolation, islets were split into groups of 150 islets. Each group was placed into one of the individual glass chambers for simultaneous study. Islets were settled in the perifusion chambers on top of mesh filters small enough (25 μm) to prevent

islets from escaping into the effluent. Each experiment was preceded by a 30-minute stabilization period using a perifusion of 0.1% Dulbecco's Modified Eagle Medium (DMEM) containing 0.1% BSA, 0.111% HEPES, 38.1 mM $NaHCO_3$, 4 mM L-glutamine, 1 mM sodium pyruvate and 1.5 ‰ phenol red. Additional glucose and/or drugs were added to the perifusion medium as indicated in the text. Samples were collected every 3 minutes by the Islet Procurement and Analysis Core and the amount of hormone secreted was measured by radio-immunoassays in the Vanderbilt Hormone Assay Core.

2-4 Confocal fluorescence microscopy

Imaging conditions under the microscope and intracellular free calcium imaging by Fluo4-AM are described in Chapter II, Section 2-5 and 2-8, respectively.

3- Results

3-1 Glucose effects on hormone secretion from perifused islets

The hormonal response of perifused intact mouse islets exposed to a 15-minute step-increase in glucose concentration is presented in Figure III-2. The temporal response of glucagon secretion indicates that high concentrations of glucose strongly inhibit α-cell secretory activity. Glucagon release is reduced by ~60% from 1 to 12 mM glucose, as expected (356). Interestingly, inhibition of glucagon secretion by glucose is much faster than its recovery when glucose is switched back to low levels. Thus, glucagon release is maximally inhibited 10 minutes after glucose elevation, whereas maximal secretion is

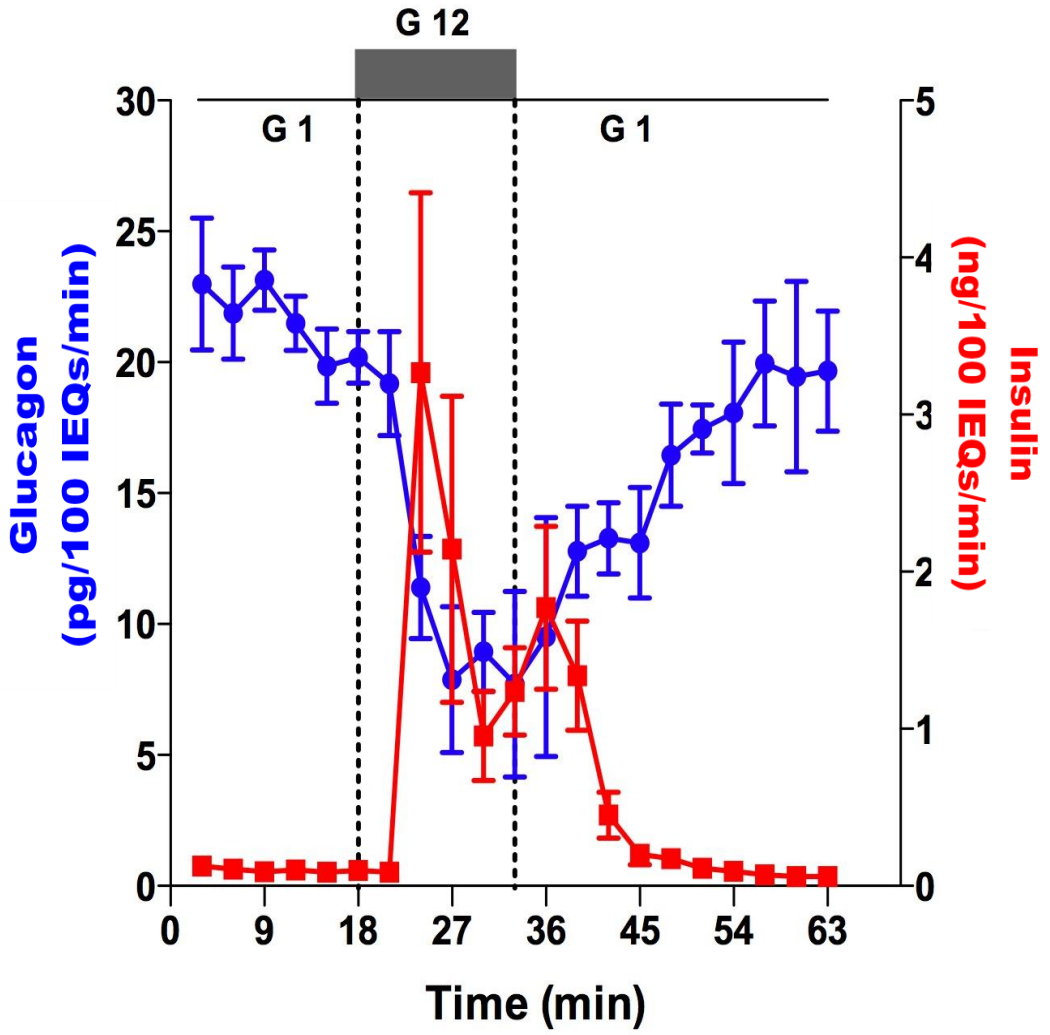

Figure III-2: Glucose effects on hormone secretion from intact perifused islets. Isolated islets were exposed to 1 mM glucose for 30 minutes (from -30 to 0 min). Then, both glucagon and insulin responses (blue and red traces, respectively) were measured for 18 minutes at 1 mM glucose (G1). The perifusion was changed to 12 mM (G2) for 15 minutes, and switched back to 1 mM. Responses from low to high glucose, and from high to low glucose, are statistically significant for both hormones ($p<0.01$ – Student's *t* test). The experiment was repeated 3 times, error bars represent the standard error of the mean.

To compare the volume of islets with different diameters and volumes, individual islets are mathematically converted to standard islet equivalents (IEQs) with a diameter of 150 µm (449).

only reached 30 minutes after return to low glucose levels. The slow rising phase resulting from a switch from high to low glucose has also been reported in mouse islets (306). However, this result contradicts other perifusion assays describing a first phase characterized by an acute glucagon response followed by a second phase that starts after the nadir of the first phase (rat and human islets (303)), or alternatively an acute response that plateaued at the same level (mouse islets (448)). The reason for these differences is not known and could arise from different experimental conditions, such as islet isolation or culture medium, or from species differences. The glucagon response to a-step decrease in glucose has been attributed to switch-off of paracrine inhibition by insulin, zinc and somatostatin (302, 303, 306, 308), as previously discussed in Chapter I – Section 4-6-2.

The insulin response presented in Figure III-2 is almost opposite to glucagon. Insulin release is inhibited under hypoglycemic conditions, whereas addition of glucose (12 mM) strongly stimulates its secretion. A step-increase in glucose leads to a biphasic insulin response composed of an acute first phase that lasts ~10 minutes followed by a second phase plateau that starts at the nadir of the first phase, as previously reported (143). The mechanisms behind this biphasic response are discussed in Chapter I – Section 3-2. Exogenous application of insulin is a strong inhibitor of glucagon secretion; however, it is unclear whether intra-islet insulin secretion suppresses glucagon (Chapter I – Section 4-6-2). The time resolution (3 minutes) of our perifusion assays was not sufficient for discriminating which cell-type is first affected by a step-increase in glucose. For instance, if glucagon was suppressed before the secretion of insulin, the result would have supported a direct inhibitory effect of the sugar, as opposed to an indirect effect mediated by insulin.

Similar to *in vivo*, glucagon secretion from *ex vivo* islets is maximal under hypoglycemic conditions. It is worth noting that isolated islets constitute a simpler model to study than *in vivo* islets since inputs from the sympathetic autonomic nervous system and the hypothalamic-pituitary-adrenal axis stimulate the secretion of glucagon under advanced hypoglycemia (Chapter I – Section 1-1). The present chapter focuses on the mechanisms of glucagon secretion under low-glucose conditions, when β-cell secretory activity is inhibited. In particular, we study the effects of pharmacological modification of ions channels on the secretion of glucagon. Since insulin secretion from β-cells potentially suppresses glucagon secretion, insulin was therefore simultaneously measured with glucagon to avoid any misinterpretation.

3-2 Role of high-voltage-gated calcium channels

3-2-1 Rationale

Influx of calcium is a trigger for the exocytosis of neuroendocrine vesicles (450, 451). For instance, pulsatile insulin release likely originates from coordinated calcium oscillations among β-cells, and calcium influx is mediated by L-type calcium channels (136-138). α-cells are known to exhibit calcium oscillations at low glucose levels (Chapter II – Section 3-5, (364, 415, 452)) but the identity of the calcium channels responsible for such oscillations remains controversial. Two channel subtypes, namely L- and N-type, have been proposed to drive α-cell calcium oscillations and glucagon secretion. Proponents of the electrophysiological model of glucagon secretion support a prominent role for N-type channels (286, 291-293), but other groups contradict this view and favor the L-type isoform (294-297). To determine which subtype is involved in our

isolated mouse islets, we tested the effect of selective calcium channel antagonists on α-cell calcium oscillations and on glucagon secretion.

3-2-2 Results

Transgenic islets containing RFP-labeled α-cells were loaded with the calcium indicator dye Fluo-4. Islet $[Ca^{2+}]_i$ signal was recorded during 5 minutes at 1 mM glucose, then calcium channel antagonists were added to the perifusion solution. Nifedipine and ω-conotoxin were used to selectively block L-type and N-type calcium channels, respectively (453). In Figure III-3A, a representative Fluo-4 experiment shows that ω-conotoxin at 1 μM does not have any apparent effect on both α- and β-cell $[Ca^{2+}]_i$ at low glucose levels. Greater concentrations were also tested (up to 10 μM) and no effect was observed. In contrast, nifedipine (20 μM) strongly inhibits α-cell calcium oscillations. Overall, nifedipine reduces α-cell Fluo-4 signal by -18.2±3.7% (13 α-cells from 5 islets, $p<0.01$ – Student's *t* test). Lower concentrations of nifedipine also reduce the amplitude of calcium oscillations (Fig. III-3B).

We next sought to confirm the inhibitory effect of nifedipine on glucagon secretion from perifused islets (Fig. III-4). Similar to glucose (Fig. III-2), nifedipine suppresses glucagon secretion by ~55% ($p<0.01$ – Student's *t* test). These results suggest that L-type calcium channels play a prominent role for α-cell calcium oscillations and secretory activity. In contrast, ω-conotoxin did not affect glucagon secretion from intact islets in static incubation experiments at 1 mM glucose (data not shown).

We used a maximal level of 20 μM of nifedipine in our experiments on α-cell calcium oscillations and glucagon secretion. Equal or greater concentrations of the drugs

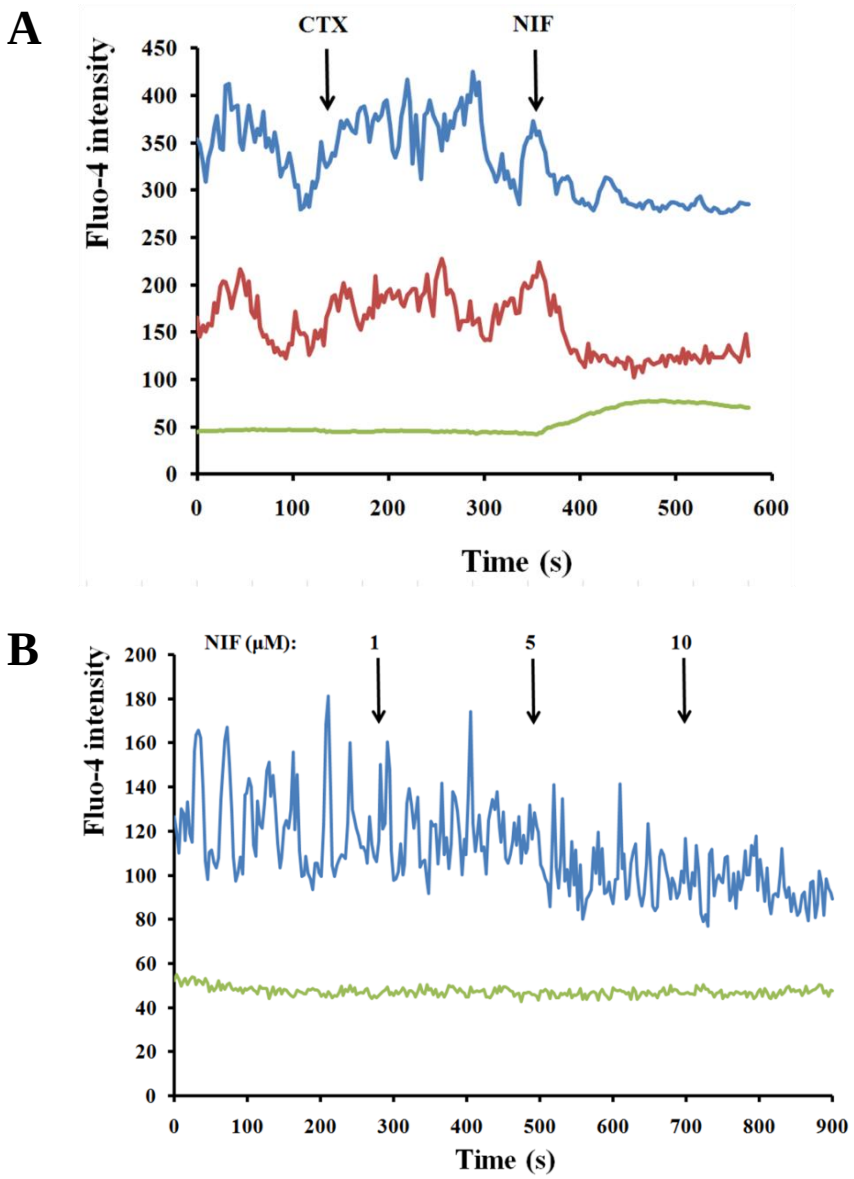

Figure III-3: Representative intracellular calcium responses to blockade of high-voltage-gated calcium channels in intact mouse islets. An islet from a transgenic mouse expressing RFP in α-cells has been loaded with Fluo-4 at 1 mM glucose and placed in a microfluidic device for imaging purposes. Blue and red traces represent α-cell $[Ca^{2+}]_i$, and the green traces indicate β-cell $[Ca^{2+}]_i$. Fluo-4 intensity is expressed in arbitrary units. A, the calcium responses from two α-cells in the same islet are presented. ω-conotoxin (CTX) and nifedipine (NIF) were perifused at 1 μM and 20 μM, respectively. B, increasing concentrations of nifedipine were perifused to another islet at times indicated by the arrows. Nifedipine reduces calcium activity in α-cells while having no noticeable effects on β-cells. The figure is representative of 18 α-cells from 7 islets harvested from 3 mice.

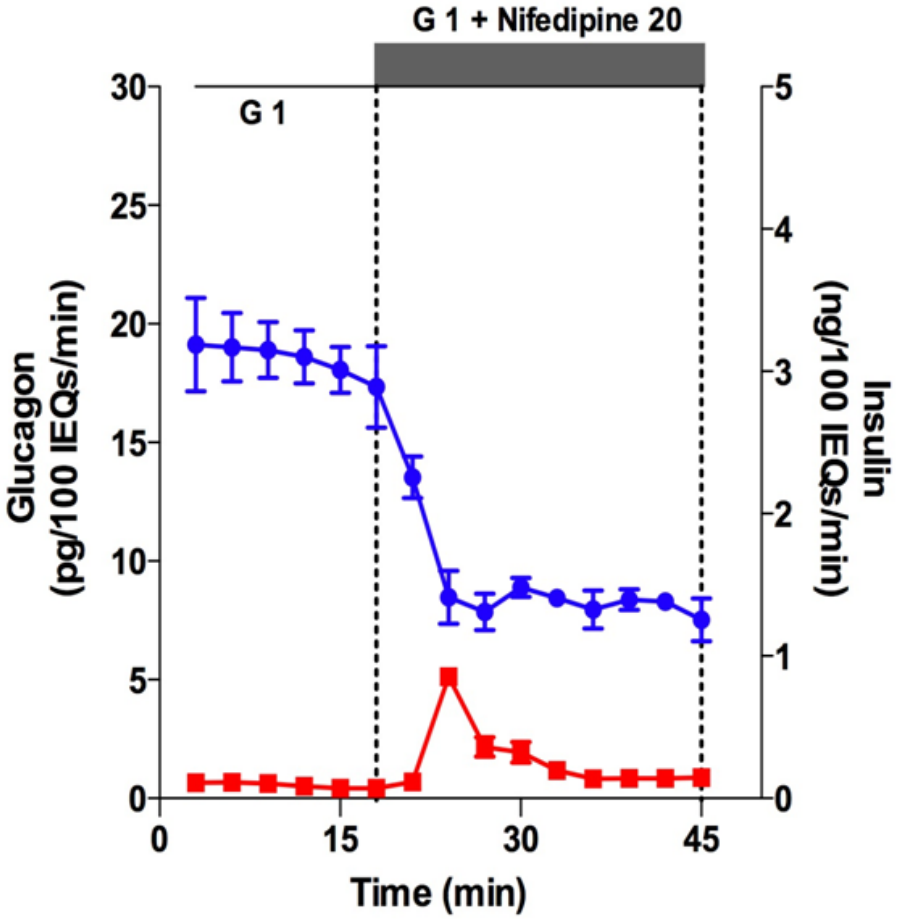

Figure III-4: Effects of nifedipine on hormone secretion from intact perifused islets. Isolated islets were exposed to 1 mM glucose for 30 minutes (from -30 to 0 min). Then, glucagon and insulin responses (blue and red traces, respectively) were measured for 15 minutes at 1 mM glucose (G1), and with 20 μM nifedipine was perifused for 30 minutes. Nifedipine suppression of glucagon secretion is statistically significant (p<0.01 – Student's t test). The experiment was repeated 4 times, error bars represent the standard error of the mean.

have been used to study the role of L-type calcium channels in islets (291, 292, 454). However, 20 μM of nifedipine induces an increase in β-cell $[Ca^{2+}]_i$, whereas lower concentrations have no effect (Fig. III-3). This observation likely reflects non-specific effects of the drug on potassium channels (455, 456). The depolarizing effect on β-cells is also apparent from the insulin response in which a transient stimulation is observed (Fig. III-4), but this effect is unlikely responsible for the suppression of glucagon since glucagon suppression occurs before the small rise in insulin release.

3-3 Role of tetrodotoxin-sensitive Na^+ channels for α-cell $[Ca^{2+}]_i$ and glucagon secretion

3-3-1 Rationale

Activation of TTX-sensitive voltage-gated Na^+ channels has been proposed to play a primary role for the secretion of glucagon at low glucose levels (285, 291, 356). The authors report that TTX inhibits both electrical activity and $[Ca^{2+}]_i$ oscillations in α-cells within intact mouse islets, and measure a ~50% inhibition in glucagon secretion. One important limitation in their studies was the lack of a reliable method for distinguishing α- from β-cells. The authors identified α-cells based on electrophysiological properties, and in particular via the presence of TTX-sensitive currents. However, electrophysiological identification can be deceptive given the variability of reported electrical properties of different islet cell types and the presence of TTX-sensitive currents in β-cells (290, 295, 457). We decided to test the effect of TTX on transgenic islets containing RFP-labeled α-cells (as described in Chapter II - Section 3-1).

3-3-2 Results

Transgenic islets were loaded with Fluo-4 and then transferred into a microfluidic device perifused at 1mM glucose, as described in Chapter II – Section 2-5. We applied TTX at low glucose levels to determine if inhibition of TTX-sensitive Na^+ channels would lead to reduction of α-cell $[Ca^{2+}]_i$ oscillations. Surprisingly, we did not observe any decrease in α-cell $[Ca^{2+}]_i$ activity under application of TTX in the range of 0.1 to 1 μg/mL (i.e 0.3 to 3 μM) (Figure III-5). On the contrary, TTX has a stimulatory effect on α-cells, as indicated by a small increase in the frequency of $[Ca^{2+}]_i$ oscillations; while having no effect on β-cell $[Ca^{2+}]_i$. The reason for such effect is presently unknown.

Since our results contradict the putative inhibitory effect of TTX on α-cell calcium oscillations, we measured the secretion of glucagon from islets exposed to TTX (Figure III-6). In our hands, TTX did not inhibit glucagon secretion. On the contrary, TTX increases glucagon secretion by ~25% ($p<0.01$, Student's *t* test). Meanwhile, TTX did not affect insulin secretion (Figure III-6).

3-4 Pharmacological modulation of K_{ATP} channels

3-4-1 Rationale

β-cell K_{ATP} channels couple cell metabolism to electrical activity and are therefore pivotal in triggering glucose-stimulated insulin secretion (458). K_{ATP} channels are also functional in mouse (352, 353) and rat α-cells (284, 311), in mouse cultured αTC-6 cells (459, 460), and in human α-cells (291), but may be absent in guinea pig α-cells (355). However, their role for glucagon secretion is a matter of controversy in the α-cell physiology research field.

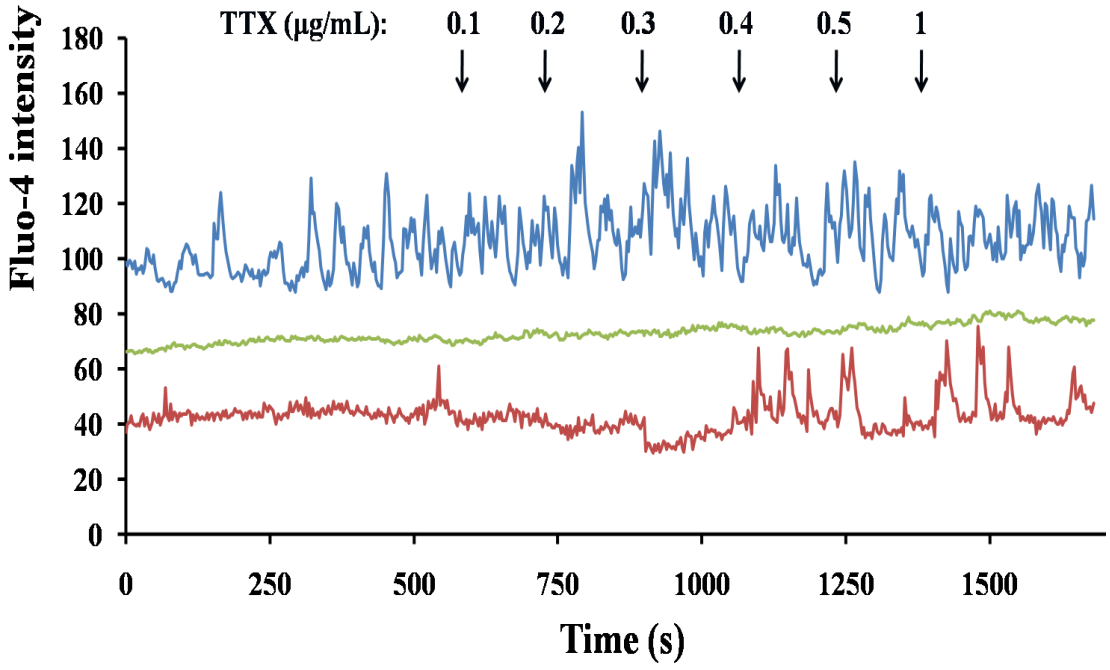

Figure III-5: Representative intracellular calcium responses to tetrodotoxin in intact mouse islets. Blue and red traces represent α-cells and the green trace indicates β-cells. An islet from a transgenic mouse expressing RFP in α-cells has been loaded with Fluo-4 at 1 mM glucose and placed in a microfluidic device for imaging purposes. Increasing concentrations of tetrodotoxin (TTX) were perifused in the device at times indicated by the arrows. TTX stimulates calcium activity in α-cells while having no noticeable effects on β-cells. Fluo-4 intensity is expressed in arbitrary units. The figure is representative of 14 α-cells analyzed from 6 islets harvested from 2 mice.

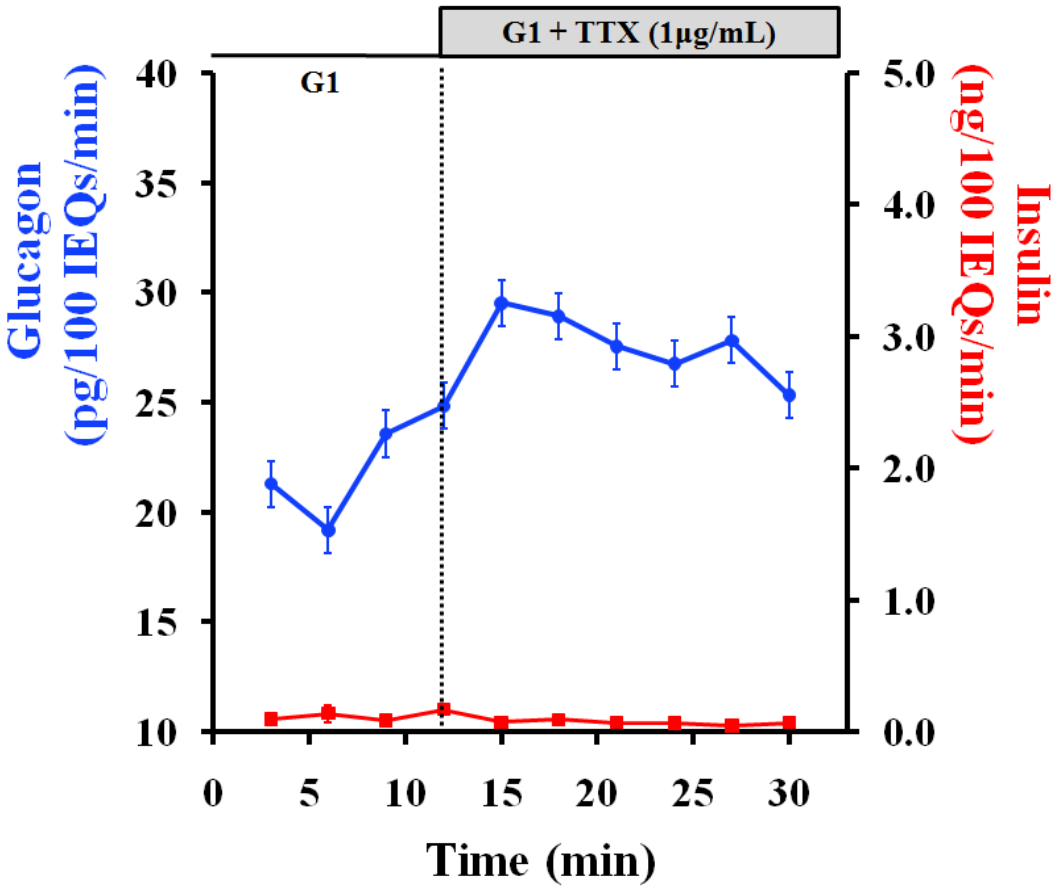

Figure III-6: Tetrodotoxin effects on glucagon secretion from intact perifused islets. Isolated islets were exposed to 1 mM glucose for 30 minutes (from -30 to 0 min). Then, glucagon response (blue trace) was measured for 9 minutes at 1 mM glucose (G1), and tetrodotoxin (TTX) was perifused for 21 minutes. TTX stimulation of glucagon secretion is statistically significant ($p<0.01$ – Student's *t* test). The experiment was repeated 6 times, error bars represent the standard error of the mean.

The pancreatic K_{ATP} channel is a heterooctameric protein composed of four inward rectifier K^+ subunits (Kir6.2) that generate the channel pore, and four sulphonylurea receptor subunits (SUR1), each Kir6.2 being associated with one SUR1 (461). In support of a prominent role for K_{ATP} channels in glucagon secretion, SUR-1-knockout mouse islets secrete less glucagon than wild-type islets under hypoglycemic conditions, and glucagon secretion is not suppressed by glucose anymore (356, 448, 462). However, the global knockout of K_{ATP} channels makes the results difficult to interpret since β-cell physiology is also altered in this strategy. Thus, it cannot be discerned whether the defects in glucagon secretion are due to lack of K_{ATP} channels in α-cells or to loss of paracrine regulation by other islet cell-types. However, islets from Kir6.2-deficient mice exhibit normal glucagon responses (463). The reason for this discrepancy is presently unknown.

Pharmacological modulation of K_{ATP} channel activity has been a valuable strategy for assessing its role in α-cell electrical activity, calcium oscillations, and secretory activity. Sulphonylureas, such as tolbutamide, are potent K_{ATP} channel blockers that are used in the treatment of type-II diabetes because of their ability to stimulate insulin secretion (464). Some studies on intact mouse islets report that high levels of tolbutamide, like glucose, inhibit glucagon output (285, 356). A dual effect of tolbutamine on glucagon secretion has also been observed where low concentrations (0.1-1 μM) are stimulatory, and greater concentrations (10-100 μM) are inhibitory (291). This observation is central for the electrophysiological model of glucagon secretion since it suggests that a small membrane depolarization activates high-voltage-gated calcium channels, whereas a stronger depolarization would inactivate voltage-gated channels

important for calcium oscillations. However, it is not clear why tolbutamide-mediated depolarization would not set the membrane potential to a level sufficient for calcium channel activation, as seen in β-cells. Furthermore, inhibition of glucagon secretion from islets at high tolbutamine levels could also be explained by enhanced paracrine inhibition from neighboring β-cells.

The electrophysiological model of glucagon secretion describes a direct inhibitory effect of high concentrations of tolbutamide on glucagon secretion. Thus, the model predicts that single α-cells retrieved from their islet environment should also be inhibited by tolbutamide. However, isolated rat α-cells exhibit a β-cell-like behavior in response to tolbutamide (i.e. K_{ATP} channel closure, increase in $[Ca^{2+}]_i$ and in secretory activity) (284, 311, 341). These observations strongly support a prominent role for paracrine inhibition in intact islets. This hypothesis is further supported by the demonstration that both insulin (341, 353) and zinc ions (341) are able to increase α-cell K_{ATP} channel activity. β-cell secretory products could arguably overcome the closure of α-cell K_{ATP} channels by tolbutamide and hyperpolarize the membrane so that high-voltage-gated calcium channels become inactivated.

Diazoxide, a K_{ATP} channel opener, has been consistently associated with inhibition of electrical activity, calcium oscillations and glucagon secretion in dispersed rat α-cells (284, 311, 341), and mouse islets (285, 291, 296). These observations suggest that membrane hyperpolarization following K_{ATP} channel opening inactivates high-voltage-gated calcium channels critical for glucagon secretion.

In contrast to the previously described studies, pharmacological modulation of K_{ATP} channel activity has also been reported to not affect α-cell calcium activity in mouse

islet α-cells and dispersed mouse α-cells (294, 360, 465), undermining a potential role for the channel in α-cell physiology.

Given the controversy on the role of K_{ATP} channels in α-cells, we investigated how modulation of K_{ATP} channel activity affects α-cell $[Ca^{2+}]_i$ in our positively-identified mouse α-cells, and how it relates to glucagon output.

3-4-2 Results

Diazoxide effects on α-cell $[Ca^{2+}]_i$ and glucagon secretion

In Section 3-2, we demonstrated the importance of L-type calcium channels for α-cell calcium oscillations and glucagon secretion at low glucose levels. These high-voltage-gated channels are maximally activated when the membrane is depolarized above -30 to -20 mV (291, 457). Thus, hyperpolarizing the membrane by opening K_{ATP} channels should inactivate L-type calcium channels. Similar to nifedipine blockade of calcium channels, inactivation should inhibit glucagon secretion.

Transgenic islets containing RFP-labeled α-cells were loaded with Fluo-4 and then transferred into a microfluidic device perifused at 1mM glucose. Fluo-4 fluorescence as an indicator of $[Ca^{2+}]_i$ activity was monitored for 5 minutes, and then diazoxide was perifused to the islets. We observed a clear inhibition (reduction in the frequency and/or amplitude of calcium oscillations) in ~50% of 20 oscillating α-cells. Representative calcium responses are presented in Figure III-7. Comparing the averaged Fluo-4 intensity before and after diazoxide application, we found that 100 μM diazoxide significantly reduced Fluo-4 signal by -22.6 ±5.2% (n=25) in α-cells, whereas β-cell intensity was not affected (+9.8 ±9.7% in β-cells, n=5 islets). In addition, diazoxide had no effect on 5 α-

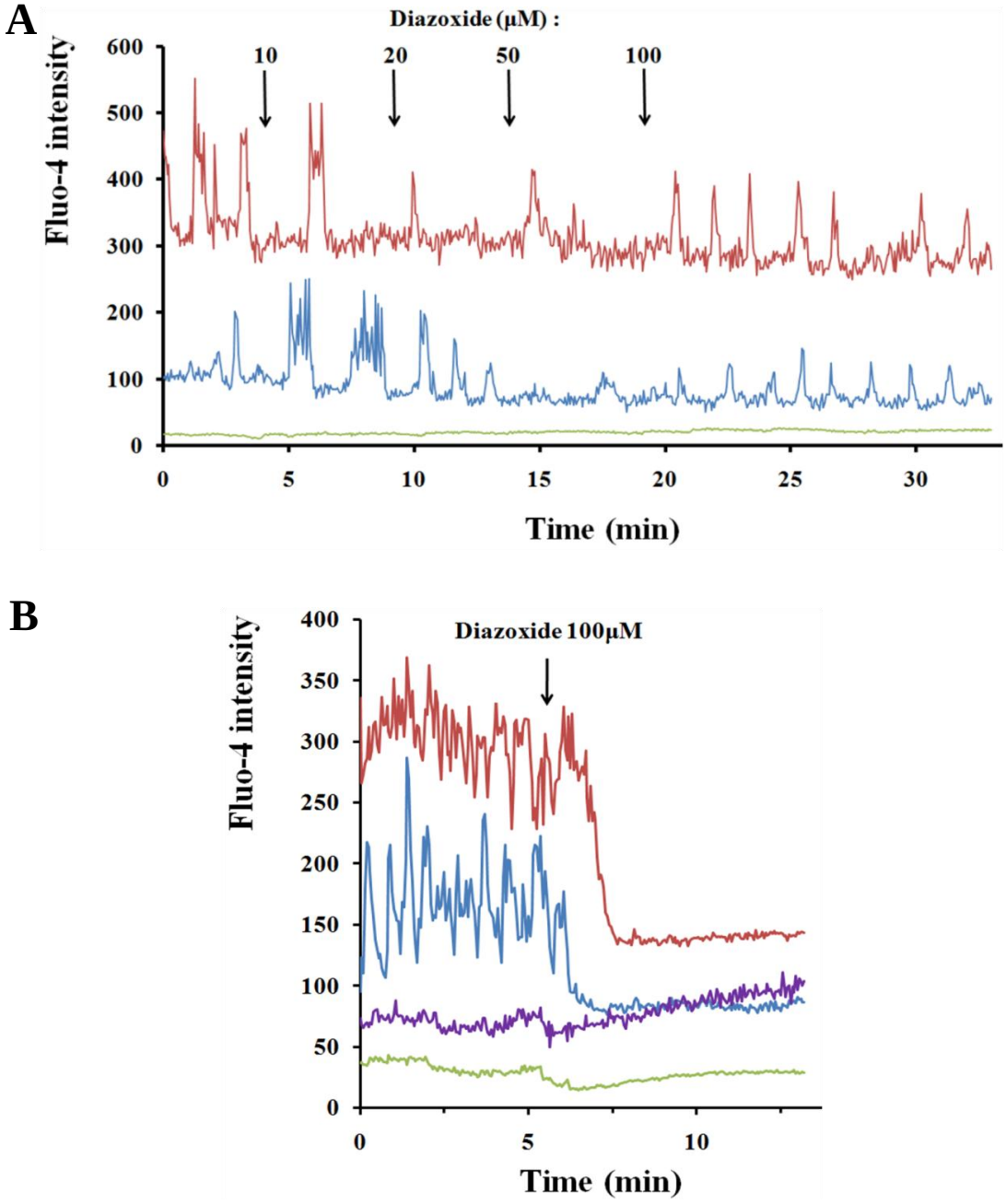

Figure III-7: Representative intracellular calcium responses to K_{ATP} channel opening by diazoxide. A, an islet from a transgenic mouse containing RFP-labeled α-cells has been loaded with Fluo-4 at 1 mM glucose and placed in a microfluidic device for imaging purposes. Blue and red traces represent two α-cells and the green trace indicates β-cells. Fluo-4 intensity is expressed in arbitrary units. Increasing concentrations of diazoxide were perifused at times indicated by the arrows. B, $[Ca^{2+}]_i$ responses from another islet. Diazoxide strongly inhibits α-cells with intense calcium activity (red and blue traces). In contrast, diazoxide does not affect silent α-cells and β-cells (violet and green traces, respectively). The figure is representative of 25 α-cells from 7 islets isolated from 2 mice.

cells that were not oscillating, likely because these cells were already too hyperpolarized for high-voltage-gated calcium channel activation. In addition, lower diazoxide concentrations (< 20 μM) were also found to inhibit calcium activity in 12 out of 15 oscillating α-cells from 2 islets isolated from 2 mice.

We measured the glucagon secretion response from intact islets perifused at 1 mM glucose and exposed the islets to 100 μM diazoxide (Fig. III-8). As expected, diazoxide suppresses glucagon secretion. We observed a ~45% ($p<0.01$, Student's t test) reduction in glucagon secretion, similar to perifusion of glucose and nifedipine (Fig. III-2 and III-4, respectively). Meanwhile, diazoxide did not affect insulin secretion (Fig. III-8). Since β-cell secretory activity is barely detectable in these conditions, α-cell inhibition is likely the consequence of direct activation of α-cell KATP channels by diazoxide, and not by indirect paracrine effects.

Tolbutamide effects on α-cell $[Ca^{2+}]_i$ and glucagon secretion

Similar to the study of diazoxide effects on α-cell calcium activity, we perifused RFP-α-cell transgenic islets at 1 mM glucose and applied tolbutamide (K_{ATP} channel blocker) to the perifusion chamber (Fig. III-9). Out of 34 α-cells analyzed (10 islets from 3 mice), ~45% of them exhibited an increase in calcium activity after application of 100μM tolbutamide. The effect of tolbutamide is heterogeneous from cell to cell. Some α-cells behave like β-cells and quickly respond by a strong rise in $[Ca^{2+}]_i$, whereas others responded more slowly (Fig. III-9A).

We noticed that ~25% of α-cells exhibited transient inhibition in the frequency/amplitude of calcium oscillations for 5-10 minutes before recovering

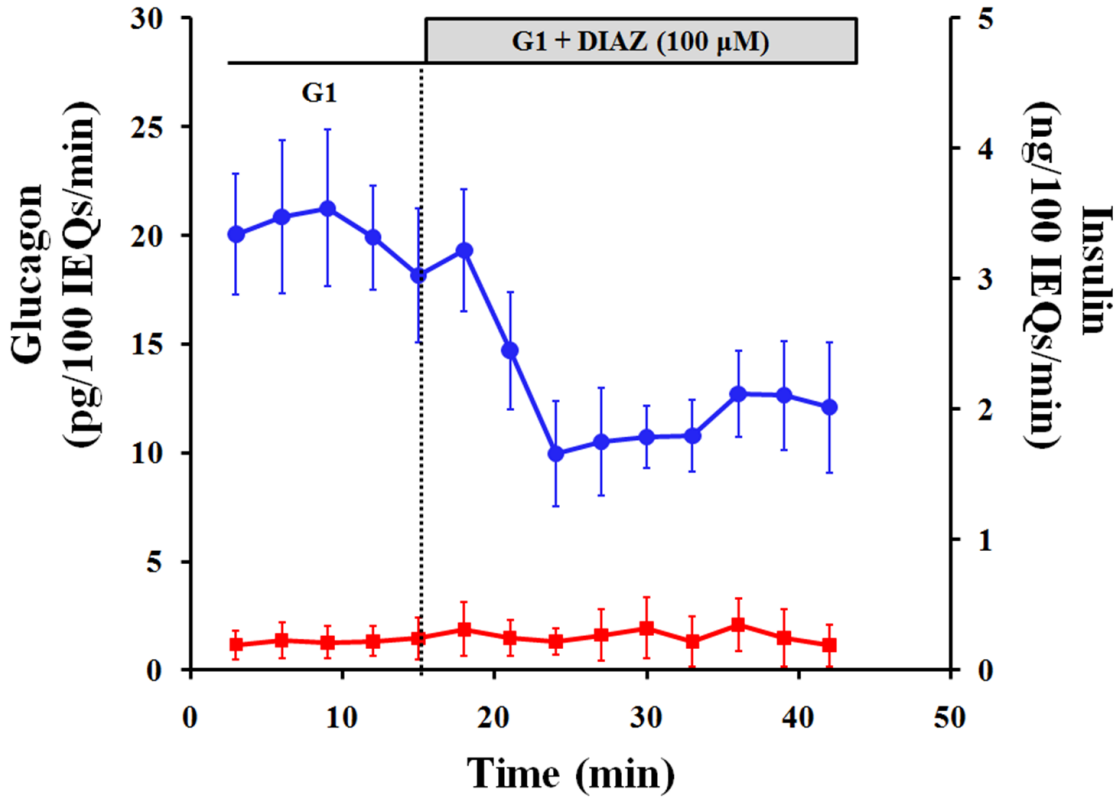

Figure III-8: Diazoxide effects on hormone secretion from intact perifused islets. Isolated islets were exposed to 1 mM glucose for 30 minutes (from -30 to 0 min). Then, glucagon and insulin responses (blue and red traces, respectively) were measured for 12 minutes at 1 mM glucose (G1), and diazoxide (DIAZ) was perifused for 30 minutes at 100 µM. Diazoxide suppression of glucagon secretion is statistically significant ($p<0.01$ – Student's *t* test). The experiment was repeated 3 times, error bars represent the standard error of the mean.

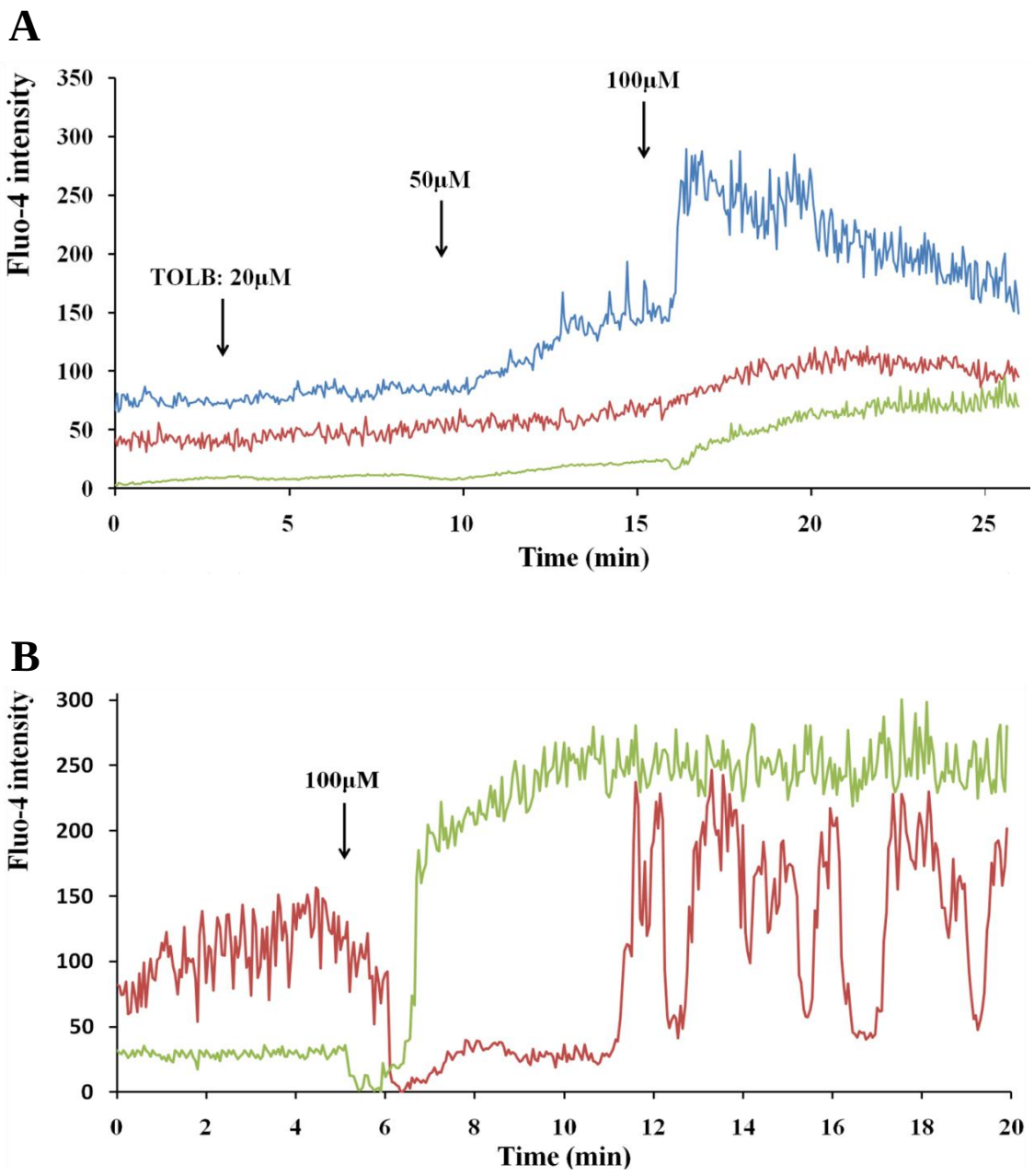

Figure III-9: Representative intracellular calcium responses to K_{ATP} channel blockade by tolbutamide. A, an islet from a transgenic mouse containing RFP-labeled α-cells has been loaded with Fluo-4 at 1 mM glucose and placed in a microfluidic device for imaging purposes. Blue and red traces represent α-cells and the green traces indicate β-cells. Fluo-4 intensity is expressed in arbitrary units. A, increasing concentrations of tolbutamide (TOLB) were perifused at times indicated by the arrows. Similar to β-cells (green trace), two α-cells in the same islet (blue and red traces) augment their $[Ca^{2+}]_i$ in response to high concentrations of tolbutamide. B, imaging of another islet shows that unlike β-cells, one α-cell exhibits a transient inhibition in calcium activity. The figure is representative of 34 α-cells from 10 islets harvested from 3 mice.

(Fig. III-9B). Interestingly, α-cells associated with fast $[Ca^{2+}]_i$ activation were often silent or weakly active before tolbutamide stimulation, whereas transient inactivation was mostly observed in cells harboring intense calcium activity. It is not clear how blockade of K_{ATP} channels would suppress calcium oscillations in a subset of α-cells. According to the electrophysiological model of glucagon secretion, tolbutamide could depolarize non-active cells so that high-voltage calcium channels activate. In contrast, active α-cells are already depolarized and further depolarization would inactivate calcium channels (285, 291, 356). However, this inhibitory effect on calcium oscillations is only transient, and electrophysiological measurements failed to detect such a temporary effect on electrical activity perhaps because tolbutamide was only applied for a short period of time (10s to 2 min) (285, 291). Recovery of calcium oscillations could involve membrane repolarization by voltage-gated channels activated at depolarized membrane potentials, such as K_{Dr} and A-channels (285). Finally, tolbutamide had no significant effect on ~25% of the α-cells, and inhibited calcium activity in only ~5% of the α-cells.

In a separate experiment, we compared Fluo-4 intensity before and 30 minutes after application of 100 μM tolbutamide by acquiring z-stacks (similar to our NAD(P)H measurements described in Chapter IV – Section 2-4). We calculated an average increase in Fluo-4 signal of 36.9 ±11.5% in 46 α-cells (7 islets from 2 mice). In comparison, β-cell Fluo-4 signal rose by 140.8 ±27.0%. The majority of α-cells (~60%) responded by an increase in Fluo-4 signal greater than 15%, with an average of 74.5±17.2%. However, we observed a subpopulation representing ~25% of α-cells that exhibited a decrease greater than 15% with an average of -24.1±4.7%. Fluo-4 intensity was stable in the remaining ~15% of α-cells (-1.4±4.8). The different responses to tolbutamide (and diazoxide)

application indicate that α-cells constitute a heterogeneous cell population in which some cells are in an excited state at low glucose, while others are inactive.

Our study of the effects of tolbutamide on calcium dynamics shows that closure of K_{ATP} channels stimulates α-cell calcium activity at low glucose levels. We next sought to determine how this effect is translated in terms of glucagon output. We measured the secretion of glucagon from perifused islets in response to tolbutamide (100 μM) at 1 mM glucose (Fig. III-10). We found that tolbutamide enhances glucagon secretion by ~95% ($p<0.01$, Student's *t* test). Meanwhile, insulin secretion from β-cells was strongly stimulated. The time-response of hormone outputs indicates that insulin release is quickly stimulated, whereas glucagon secretion is only enhanced after ~15 minutes following tolbutamide application. This time-lag between insulin and glucagon responses corroborate our calcium measurements describing transient suppression of calcium activity in some α-cells. The observed stimulatory effect of tolbutamide on glucagon secretion contrasts with previous studies of inhibition of glucagon secretion from mouse islets (285, 291, 356). Such a discrepancy is difficult to explain, but differences in mouse islet isolation procedure, culture condition, perifusion medium composition, are all possible sources of divergence. Nonetheless, our observation that tolbutamide stimulates glucagon secretion is supported by other studies in isolated rat α-cells (311), perfused rat pancreas (466) and perfused dog pancreas (467).

Similar to isolated rat α-cells (284, 311, 341, 468), our study suggests that closure of α-cell K_{ATP} channels stimulate both α-cell calcium activity and glucagon secretion in intact mouse islets. This observation implies that membrane depolarization is one way to enhance α-cell secretory activity at low glucose levels, and contradicts the

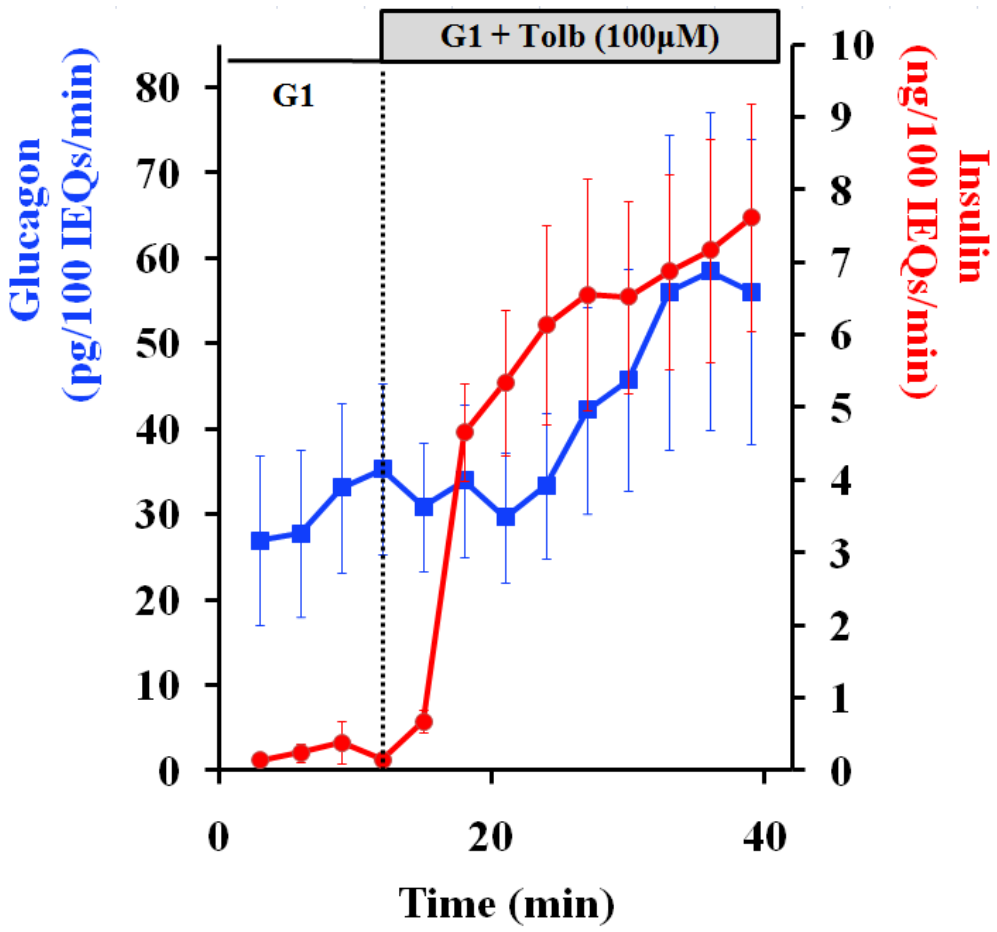

Figure III-10: Tolbutamide effects on hormone secretion from intact perifused islets. Isolated islets were exposed to 1 mM glucose for 30 minutes (from -30 to 0 min). Then, glucagon and insulin responses (blue and red traces, respectively) were measured for 18 minutes at 1 mM glucose (G1), and tolbutamide (Tolb) was perifused for 27 minutes at 100 µM. Tolbutamide stimulates the secretion of both glucagon and insulin ($p<0.01$ – Student's *t* test). The experiment was repeated 6 times, error bars represent the standard error of the mean.

electrophysiological model stating that strong membrane depolarization suppresses glucagon secretion. The stimulatory effect of tolbutamide also challenges the paracrine description of glucagon suppression. Indeed, β-cells are strongly activated by tolbutamide, and paracrine products such as insulin, zinc and GABA could potentially inhibit the secretion of glucagon. Somatostatin, another paracrine candidate secreted by δ-cells, is also released in greater amounts when stimulated by tolbutamide (405). Paracrine inhibitory products are thus unable to overcome tolbutamide stimulation of glucagon secretion. This description is not unique to tolbutamide since both arginine and KCl strongly depolarize α-cell membrane and raise α-cell $[Ca^{2+}]_i$, while stimulating both glucagon and insulin secretion (318, 469). We confirmed the stimulatory effect of 10 mM arginine on islet α-cells by measuring a 52.3 ±15.7% increase in $[Ca^{2+}]_i$, compared to 22.1 ±5.4% in β-cells (Fig. III-11).

4- Discussion

The hormonal response to glucose from isolated mouse islets is similar to that seen *in vivo* (Fig. III-2). Under hypoglycemic conditions, glucagon is maximally released while insulin secretion is minimal. The response is opposite at hyperglycemic levels: glucagon secretion is suppressed and insulin release is strongly stimulated. Thus, we utilized isolated islets to study the mechanisms of glucagon secretion at low glucose levels. We were particularly interested in determining how pharmacological modulation of ion channels affects α-cell $[Ca^{2+}]_i$ and glucagon secretion, and use these results to test the predictions of the electrophysiological model of glucagon secretion.

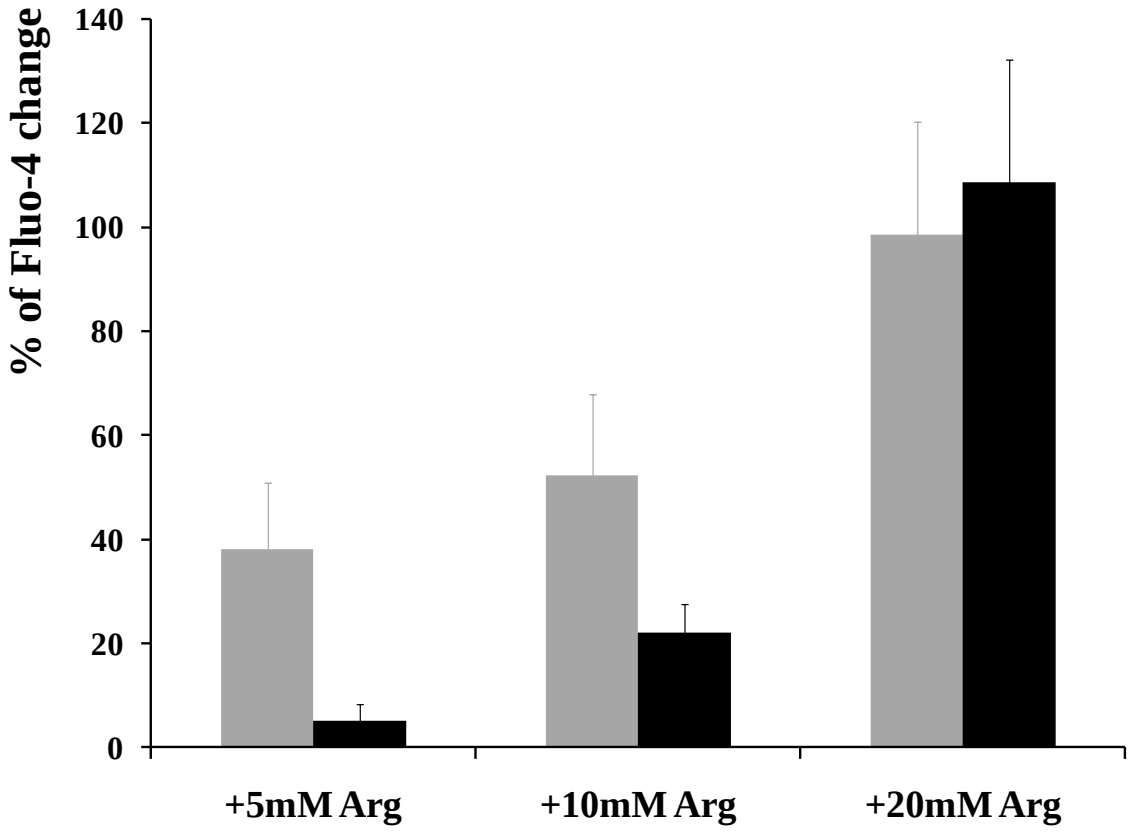

Figure III-11: Arginine effects on cellular calcium concentration in intact perifused islets. Isolated islets incubated 1 mM glucose were exposed to step-increases in arginine (Arg) concentrations. The change in $[Ca^{2+}]_i$ is assessed in % change in Fluo-4 signal compared to baseline signals at 1 mM glucose. Gray and black columns represent α- and β-cells, respectively. Arginine elevation of α-cell $[Ca^{2+}]_i$ is already significant at 5mM, whereas β-cell $[Ca^{2+}]_i$ increases significantly above 10mM arginine ($p<0.01$ – Student's *t* test). 16 α-cells from 6 islets harvested from 2 mice were utilized for this experiment. Error bars represent the standard error of the mean.

The use of selective blockers of high-voltage-gated calcium channels demonstrates that L-type channels are critical for normal α-cell calcium oscillations and glucagon release in islets from C57BL6 mice (Fig. III-3 and III-4), supporting other reports from C57BL6 (295-297) and NMRI mouse islets (294, 352). However, blocking N-type channels was ineffective in inhibiting α-cells, contrary to results from NMRI mice (291, 292) and rats (286, 293, 311). Thus, species differences, as well as differences in islet isolation procedure and islet culture condition, are possible explanations for this discrepancy.

We next investigated the effect of TTX-sensitive voltage-gated sodium channels thought to be important for activating high-voltage gated calcium channels (285, 291, 311, 356). In our hands, neither α-cell calcium oscillations nor glucagon secretion were inhibited by TTX (Fig. III-5 and III-6). This result indicates that activation of TTX-sensitive sodium channels is not necessary for L-type calcium channel activation at low glucose levels. In contrast to the expected inhibitory effect of TTX, we actually observed an increase in α-cell calcium activity and a stimulation of glucagon secretion. One possible explanation is that action potentials usually driven by voltage-gated Na^+ currents transiently depolarize the membrane to positive potentials and activate voltage-gated K^+ channels (352). K^+ channel activation would rapidly repolarize the membrane and inactivate L-type calcium channels. "L" stands for long-lasting currents, once activated, L-type channels stay open for more than >400ms (537). It is possible that blockade of TTX-sensitive Na^+ channels suppresses the activation of K^+ repolarizing currents responsible for the inactivation of L-type calcium channels.

K_{ATP} channels play a prominent role in glucose-stimulated insulin secretion, but

their role in glucagon secretion is unclear. Similar to β-cells, some argue that glucose metabolism closes K_{ATP} channels, but unlike β-cells, membrane depolarization inactivates calcium channels (285, 291, 356). Other groups argue that paracrine inhibitors open α-cell K_{ATP} channels and membrane hyperpolarization inactivates calcium channels (341, 353). Lastly, others failed to detect any function for K_{ATP} channels (292, 360, 465). Fluo-4 imaging on well-identified α-cells reveals that closure of K_{ATP} channels by tolbutamide stimulates calcium activity (Fig. III-9), and our glucagon secretion assays confirm this effect (Fig. III-10). Since glucose inhibits the secretion of glucagon (Fig. III-2), the result indicates that glucose may not mediate its inhibitory effect by closing K_{ATP} channels. In addition, tolbutamide also stimulates the secretory activity of β- and δ-cells (Fig, III-10, (405)). The lack of paracrine inhibition by tolbutamide challenges the paracrine model of glucagon inhibition by glucose. Likewise, depolarizing agents, such as arginine and KCl, enhance both glucagon and insulin secretion (318, 469). It could be argued that the effects of glucose or paracrine inhibitors are overcome when the membrane is forced to depolarize.

Activation of K_{ATP} channels by diazoxide increases the outward current of K^+ and hyperpolarizes the membrane. The inhibitory effect of diazoxide on α-cell calcium activity (Fig. III-7) suggests that membrane hyperpolarization inactivates L-type voltage gated calcium channels. As a result, glucagon secretion is blunted (Fig. III-8). Interestingly, both diazoxide and nifedipine (calcium channel blocker) inhibit the secretion of glucagon by ~60%, to the same extent that it is inhibited by glucose (Fig. III-2, III-4 and III-8). It is therefore tempting to hypothesize that glucose mediates its inhibition by opening K_{ATP} channels and inactivating L-type calcium channels, either

directly or via paracrine effectors.

Overall, our results indicate that α-cell calcium oscillations are mediated by L-type calcium channels that drive the secretion of glucagon at low glucose. In contrast to the electrophysiological model predictions, TTX-sensitive sodium channels are not necessary for L-type calcium channel activation, and membrane depolarization mediated by closure of K_{ATP} channels does not inactivate L-type calcium channels. In β-cells, glucose metabolism closes K_{ATP} channels that depolarize the resting membrane potential from ~ -60mV in low-glucose conditions to ~ -35mV in high-glucose conditions (538). This increase in membrane potential activates L-type calcium channels. These calcium channels start to open at membrane potential higher than -50mV; they are maximally activated between -20mV and +10mV; and they are fully inactivated at potentials greater than +40mV (447). We showed that α-cell L-type calcium channels do not require the depolarizing effect of Na^+ channels to be activated. This result suggests that α-cell membrane should be fairly depolarized at low glucose concentrations (> -50mV) to allow L-type channel activation. Comparable resting membrane potential levels have been reported in rat and mouse islet α-cells (357) and in isolated rat α-cells (352). In addition, the use of membrane potential dyes reveals that a majority of α-cells are likely more depolarized than β-cells at low glucose levels (Chapter II – Section 3-4, and (358)). This depolarized state could be due to their higher metabolic state at low glucose concentrations (Chapter IV – Section 3-4). This observation suggests that greater concentrations of ATP are expected in α-cells, as reported in (347). Thus, more α-cell K_{ATP} channels should be closed at low glucose levels, compared to β-cells. In addition, α-cell K_{ATP} channels are more sensitive to ATP compared to β-cell K_{ATP} (353).

Pharmacological modulation of α-cell K_{ATP} channel activity suggests that K_{ATP} channels are important for setting the membrane potential to a level allowing activation of calcium channels. Thus, K_{ATP} channels represent a possible way whereby glucagon secretion could be regulated. In particular, opening of these channels (diazoxide-like effect) by paracrine effectors could underlie the suppression of glucagon secretion by glucose. The effect of glucose and paracrine inhibitors on α-cell calcium activity and glucagon secretion is presented in Chapter V.

CHAPTER IV

α-CELL METABOLISM

DURING GLUCOSE INHIBITION OF GLUCAGON SECRETION

1- Introduction

Pancreatic islets are responsive to variations in blood glucose concentration in such a way that α-cells increase their secretion of glucagon in hypoglycemic conditions, whereas β-cells release insulin at higher glucose levels. The β-cell response to glucose relies on its glucose-sensor composed of GLUT-2, a passive glucose transporter allowing maximal glucose uptake at ~5-15 mM (127-129), and glucokinase, an enzyme with a K_M for glucose phosphorylation of ~8 mM (130-132). Phosphorylation of glucose to glucose-6-phosphate by glucokinase is the first step of the glycolytic pathway. Breakdown of glucose generates disposable energy (increase in ATP to ADP ratio) that will mediate the exocytosis of insulin granules via closure of K_{ATP} channels (133-135), plasma membrane depolarization and L-type voltage-gated calcium channels activation, respectively (136-138). Glucokinase is the rate-limiting enzyme of β-cell glycolysis, thus the half-maximal secretory response to glucose closely matches the apparent K_M of glucokinase (470, 471). This low affinity for glucose explains why insulin is mostly released at concentrations greater than 7 mM.

In contrast to β-cells, glucose inhibits α-cell secretory activity in intact islets. However, it is widely debated whether the suppression of glucagon secretion is mediated

by a direct effect of the sugar or by inhibitory paracrine effects from β- and/or δ-cells. The expression of glucokinase in α-cells, as well as the expression of GLUT-1, an isoform of GLUT-2 with greater affinity for glucose, suggest that glucose is also dose-dependently metabolized in this cell-type (282, 283). As expected, biochemical experiments on α-cells describe glucose-dependent elevation in the rate of glucose oxidation (282, 345-347), and greater ATP to ADP ratios (339, 348, 349). However, previous attempts to measure any changes in α-cell NADH and NADPH (referred to as NAD(P)H) or flavoprotein autofluorescence by single-photon excitation have been unsuccessful (415, 420, 350, 351). The conjunction of two-photon excitation of NAD(P)H autofluorescence and fluorescence-based identification of mouse α-cells (described in Chapter II – Section 3-1) allows the dynamic measurement of their metabolic redox state. Our study confirms that glucose is metabolized in α-cells and compares α-cell NAD(P)H response with β-cells. In addition, measurements of glucagon secretion from pure populations of flow-sorted α-cells show that contrary to its effect on intact islets, glucose does stimulate glucagon secretion from isolated α-cells. This observation argues against a direct inhibition of glucagon secretion by glucose and supports the paracrine inhibition model.

2- Materials and methods

2-1 Materials – Transgenic mice - Islet isolation and culture (Chapter II- Section 2).

Accutase, propidium iodide and tetramethylrhodamine-ethyl-ester-perchlorate (TMRE) were purchased from Invitrogen (Carlsbad, CA). For imaging purposes, isolated

islets and sorted α-cells were attached on gelatin (0.1%)-coated 35-mm glass-bottomed dishes (MatTek Corp., Ashland, MA).

2-2 Cell dispersion and cell flow-sorting

~200 islets were extracted per pancreas and cultured overnight in suspension in islet medium. They were washed in PBS at pH7.4 without calcium and magnesium chloride. Then, they were digested in Accutase for 15 minutes at 37ºC (gentle shaking) and resuspended in imaging solution (i.e. filtered aqueous solution containing: 125 mM NaCl, 5.7 mM KCl, 2.5 mM $CaCl_2 – 2H_2O$, 1.2 mM $MgCl_2$, 10 mM HEPES and 0.1% bovine serum albumin (BSA), pH7.4), at 11 mM glucose. One to two hours after Accutase dispersion, fluorescent cells were isolated by fluorescence-activated cell-sorting (FACS). For this purpose, we used the BD FACSAria cell sorter (BD Biosciences, San Jose, CA) in the Vanderbilt Flow Sorting Core. EYFP, GFP and propidium iodide (1 μg/ml) were excited at 488nm, fluorescence was collected using a 500-560 band-pass filter for EYFP and GFP, and a 593-639nm filter for propidium iodide.

Cells were sorted in presence of propidium iodide, a viability dye, and cells positive for propidium iodide signal were excluded from the sorting. Doublet cells were discriminated by pulse geometry gating, looking at the area, height and width of the voltage pulses. We were able to sort ~500 viable α-cells per pancreas from EYFP-expressing islets, and ~3,000 β-cells from MIP-GFP mice (443).

2-3 Glucagon and insulin secretion assays from islets and isolated α-cells

Overnight cultured islets were pre-incubated for one hour in basal imaging

solution containing 1 mM glucose at 37ºC. Islets were placed into tubes (10 islets per tube) and exposed to different conditions at 37ºC for one hour. Samples containing secreted hormones were analyzed by radio-immunoassays in the Vanderbilt Hormone Assay Core. Islet hormone content was measured after overnight freezing of the islets in 1% Triton X-100. Each measurement was duplicated. Hormone secretion was expressed as fractional release, i.e. the percentage of total hormone content released over a one-hour incubation period.

Isolated α-cells collected by flow-sorting were resuspended and pre-incubated in imaging solution (1 mM glucose) for one hour at 37ºC. α-cells were then placed into tubes (50 α-cells per tube) and exposed to different conditions at 37ºC during one hour.

2-4 NAD(P)H measurements

Prior to imaging, islets were equilibrated in imaging buffer at 1 mM glucose for one hour and placed in a microfluidic device for imaging purposes, as described in Chapter II – Section 2-5. We used a two-photon excitation LSM710 laser scanning microscope with a Fluar 40x/1.3NA oil immersion lens (Zeiss) to measure cellular redox state (470, 472, 473), using a Coherent Chameleon laser tuned to 710 nm (Coherent Inc., Santa Clara, CA). The laser power was kept below 3.5 mW at the sample; at this laser power, no observable damage is caused to the islet (472). NAD(P)H fluorescence was collected by non-descanned detectors through a custom 380–500nm filter (Chroma Inc., Rockingham, VT).

Two-photon imaging was sequentially used with single-photon confocal imaging to localize the EYFP-expressing α-cells (pinhole diameter = 1.89 airy unit). EYFP was

excited at 514nm, and the emission was collected through a 520-560nm band-pass filter. For the dose-response curve at steady-state concentrations of glucose, a z-stack of an islet was acquired at 1 mM glucose, and another z-stack was collected 15 minutes after glucose stimulation, after NAD(P)H signal reaches a plateau. For a given α-cell, optical sections with the greatest EYFP fluorescence (i.e. the middle of the cell) were used as references for comparing NAD(P)H signals before and after glucose application. This strategy was used to overcome any cell movement. Non-EYFP cells were considered to represent β-cells.

2-5 Mitochondrial membrane potential imaging

TMRE was added in the imaging solution at 10 nM. After waiting 15 minutes for TMRE to equilibrate across the mitochondrial membrane, a z-stack of images was collected. 15 minutes after glucose stimulation, another z-stack was acquired and compared to the TMRE signals obtained previously. TMRE was excited at 543nm, and the fluorescence collected through a 560nm long-pass filter.

3- Results

3-1 Glucose effects on hormone secretion from islets and sorted α-cells

The glucose-dependent insulin and glucagon responses from EYFP-expressing islets are shown in Fig. IV-1A, and are similar to wild-type islets (420). The results confirm that glucagon is mostly released at low glucose concentrations (< 4 mM) when the release of insulin is minimal. Higher glucose levels (> 7 mM) stimulate insulin

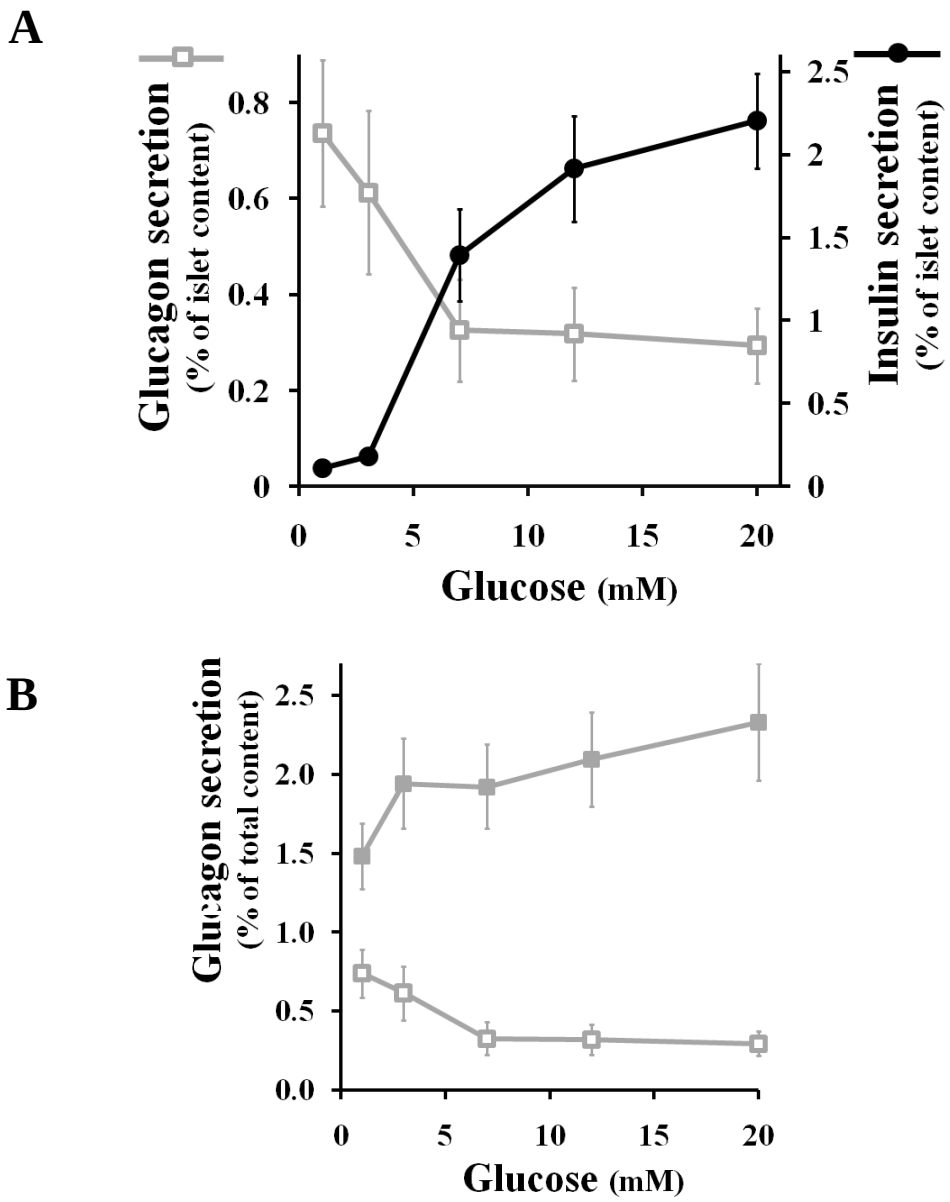

Figure IV-1: Glucose effects on hormone secretion from intact islets and sorted α-cells. A, percent of islet glucagon (solid squares) and insulin (solid circles) content secreted per hour in response to glucose. When glucose levels are greater or equal than 7 mM, both insulin and glucagon secretion are statistically different from baseline release at 1 mM (n=7 islets, $p<0.01$, ANOVA-independent samples). B, percent of glucagon content secreted from sorted α-cells (solid squares) and intact islets (open squares, reproduced from A). Secretion from sorted cells is significantly greater at 12 and 20 mM than at 1 mM ($p<0.05$, ANOVA). Between 14 and 30 assays were performed at any given glucose concentration. Error bars represent the standard error of the mean.

secretion and inhibit glucagon release, as previously reported in the literature (292, 319, 337, 474). Even at higher glucose levels, though, α-cells retain an active secretory activity representing ~40% of the maximal response observed at low glucose, a number similar to that reported from our islet perifusion assays (Chapter III – Section 3-1). In addition, application of arginine (10 mM), a potent glucagon secretagogue (316), leads to an ~1.8-fold enhancement over basal glucagon release (from 0.74 ±0.15%, n=7, to 1.35 ±0.26% of total cellular glucagon content, n=5, $p<0.05$, Student's *t* test – unpaired samples, from Fig. V-1A).

While we were primarily interested in the behavior of α-cells in their native islet environment, the specific expression of EYFP within α-cells allows for efficient cell sorting by flow cytometry (FACS). Cells were sorted in presence of propidium iodide, a viability dye, and cells positive for propidium iodide signal were excluded from the sorting. Post-sorting measurements of cell viability show that over 95% of sorted cells were viable, and these cells retain their ability to attach to gelatin-coated dishes for imaging purposes. Purity was determined to be >90% both by re-sorting samples of isolated cells and by counting the number of EYFP cells attached on the dishes after being cultured for one day. We also measured the insulin content in each assay to confirm that β-cells were absent in our purified α-cell preparations, and found no detectable traces of insulin. Figure IV-1B presents the glucagon secretion response to glucose from these pure populations of α-cells. We found that glucagon secretion is ~2-fold greater than that from intact islets at low glucose levels (1 mM). Importantly, glucose does not inhibit glucagon secretion from isolated α-cells. Actually, glucose stimulates glucagon release: application of 12 mM glucose increases basal secretion by 38.0 ±3.8% (n=25, $p<0.05$,

ANOVA). As it does in intact islets, arginine strongly stimulates glucagon secretion from sorted cells. Glucagon secretion at 1 mM glucose increases 2.8-fold after application of 10 mM of arginine (from 1.66 ±0.20%, n=30, to 4.71 ±0.9% of total cellular glucagon content, n=10, $p<0.001$ - from Fig. V-1B).

3-2 NAD(P)H measurements as an indicator of cellular metabolic redox state

Fluorescence from pyridine nucleotides (NADH and NADPH) can be used as an intrinsic probe to study cellular metabolism. The absorption and fluorescence spectra of NADH and NADPH being indistinguishable, we refer to both as NAD(P)H. Because NADH and NADPH are both fluorescent, whereas NAD^+ and NAD^+P are not, changes in the cellular redox state lead to changes in the autofluorescence signal. NAD(P)H fluorescence is normally excited with ultra-violet light (320-380 nm) and emits in the region of 400-500 nm. Two-photon excitation NAD(P)H microscopy is preferred over single-photon excitation because it reduces cell photodamage, and provides a good spatial resolution thanks to its inherent optical-sectioning ability. Two-photon excitation relies on the absorption of two photons of red light (at 710nm) to provide the same amount of energy as one photon of half the wavelength (355nm). Variations in NAD(P)H autofluorescence intensity and NAD(P)H concentration are linear (473).

Typically, glucose catabolism leads to an increase in NAD(P)H autofluorescence. This effect is mediated by reduction of NAD^+ and/or NAD^+P into NADH and NADPH, respectively. NADH comes from the glycolysis (cytosol) and the tricarboxylic acid cycle (mitochondria), whereas NADPH comes from the pentose phosphate pathway (cytosol). NADH produced during glycolysis is transferred into the mitochondria thanks to the

malate-asparte and glycerol 3-phosphate shuttles. Pyruvate, the end product of glycolysis, enters into the mitochondria by the mitochondrial pyruvate transporter. Pyruvate is further metabolized by the tricarboxylic acid cycle, hence producing more NADH. NADH will eventually be oxidized by the respiratory chain in the inner mitochondrial membrane, resulting in the production of ATP.

3-3 Time-series acquisition of NAD(P)H response to a step-increase in glucose

Figure IV-2A illustrates how fluorescence-based identification of α-cells allows precise spatio-temporal NAD(P)H measurements in single cells. For intact islets, a step-increase in glucose from 1 to 20 mM augments the intensity of islet NAD(P)H signals in both α- and β-cells (Fig. IV-2B). The time course of the NAD(P)H response is similar from both cell types and begins ~ 2 minutes after glucose application, reaching a plateau 30 to 60 seconds after the start of the response. In contrast, we observed biphasic NAD(P)H responses in both cell-types at low glucose levels. The sharp response of the first phase (Fig. IV-2C) declines to a lower plateau (not shown in figure) by 5 minutes.

3-4 Determination of basal metabolic redox states

As shown in the time-series plot from Fig. IV-2B, basal α-cell NAD(P)H at 1 mM glucose is greater than in the central part of the islet (consisting of mostly if not all β-cells). On average, NAD(P)H autofluorescence intensity was 40.8 ±2.4% greater in α-cells (n=263). Since this difference could result from greater basal metabolic state or from brighter non-NAD(P)H autofluorescence, we determined the minimal NAD(P)H intensity by fully oxidizing NAD(P)H into non-fluorescent NAD^+(P). We used the mitochondrial uncoupler FCCP (carbonyl cyanide 4-(trifluoromethoxy)

A

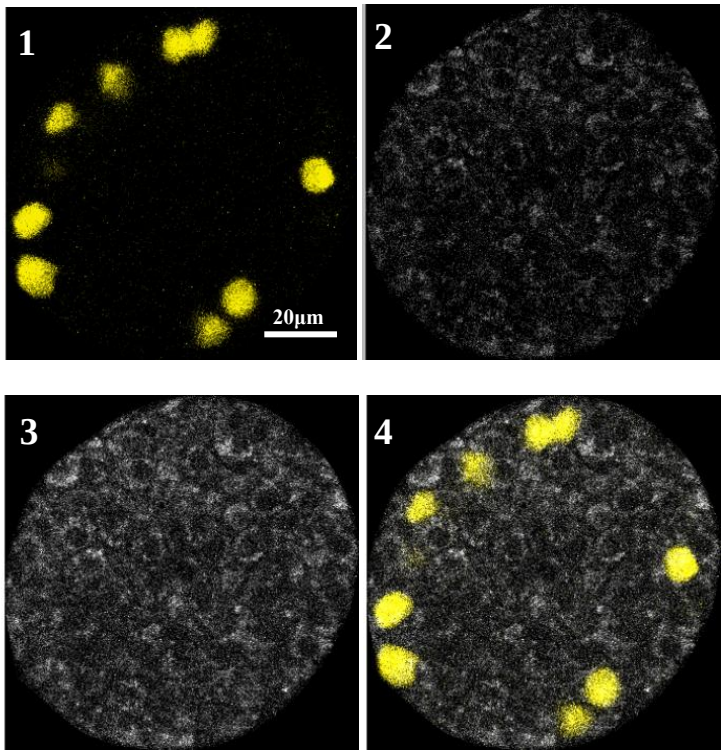
1
2
20μm
3
4

B

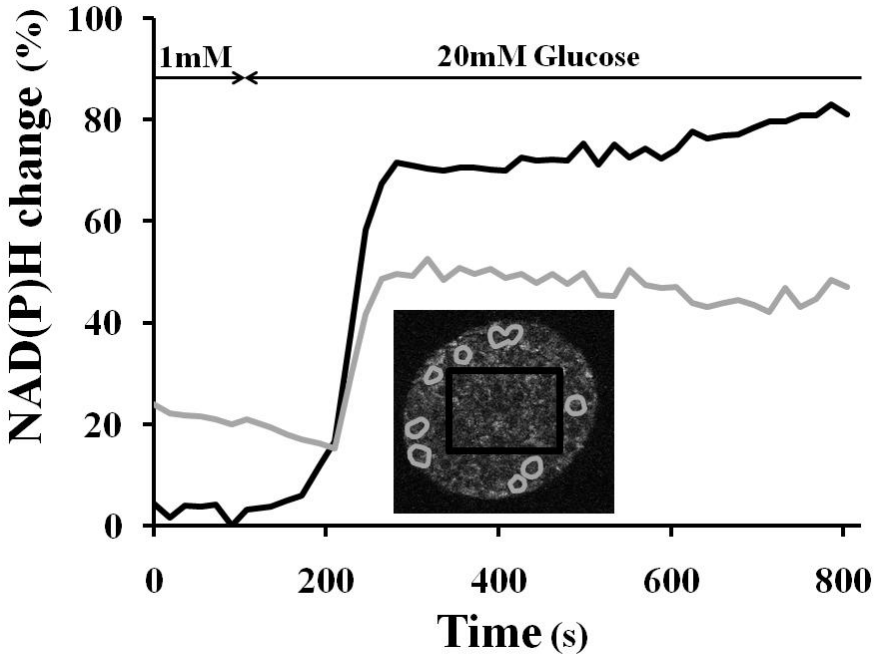
NAD(P)H change (%)
100
80
60
40
20
0
1mM
20mM Glucose
0
200
400
600
800
Time (s)

C

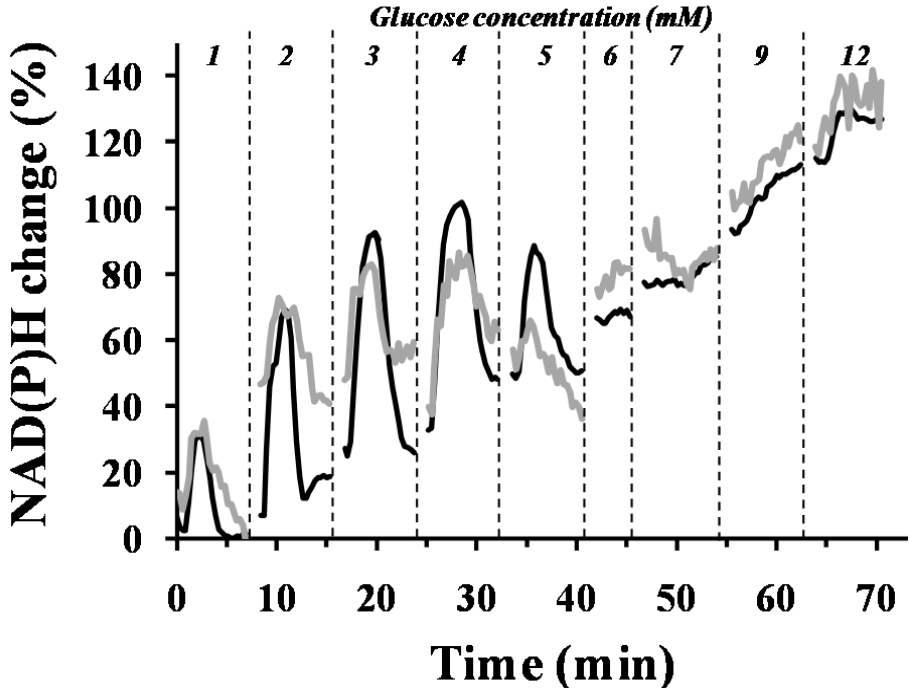

Figure IV-2: Time-series acquisition of glucose-dependent NAD(P)H responses from intact islets. A, confocal section of an intact islet showing EYFP-labeled α-cells (panel 1). Panel 2 presents the NAD(P)H autofluorescence signal from the same plane at 1 mM glucose (Glc) and Panel 3 presents the same plane after an incubation period of 10 minutes with 20 mM glucose. Panel 4 is an overlay of EYFP and NAD(P)H signals at 20 mM glucose. B, representative time-course of the NAD(P)H response from the same islet exposed to a step-increase in glucose from 1 to 20 mM. Black traces indicate β-cells, gray traces indicate α-cells. The plot is expressed in percent change relative to minimal β-cell NAD(P)H values at 1 mM glucose. NAD(P)H emission was collected every 15 seconds. Inset NAD(P)H islet image denotes α-cell locations by gray circles based on EYFP signal, and β-cell region of interest by the black rectangle. C, another islet exposed to small increases in glucose concentrations. Below 6 mM, step-increases in glucose led to transient increases in NAD(P)H signal followed by a plateau that starts from the nadir of the acute response. The plot is expressed in percent NAD(P)H change relative to baseline values from each cell-type.

phenylhydrazone) to dissipate the proton gradient across the inner mitochondrial membrane. As a result, the tight coupling between the electron transport chain and the ATP synthase is disrupted. ATP is no longer produced aerobically and cell metabolism is stopped. NAD(P)H is rapidly oxidized by the respiratory chain into non-fluorescent $NAD^+(P)$, and is not regenerated (475).

Fig. IV-3A presents the time-series acquisition of both α- and β-cell NAD(P)H responses to FCCP. As expected, addition of 1 μM FCCP rapidly reduces the NADH autofluorescence intensity which reaches a plateau after ~ 5-6 minutes. Addition of more FCCP did not further reduce the signal, suggesting that NADH was fully oxidized. Overall, the decrease in signal was similar from both α- and β-cells (-40.3 ±3.1% and -38.0 ±2.7%, respectively; n=19 α-cells, 7 islets, $p<0.001$, Student's *t* test - paired samples). After FCCP treatment, the α-cell autofluorescence intensity was still 38.5 ±6.5% ($p<0.001$) greater than in β-cells after NADH oxidation, a value close to the one obtained without FCCP (40.8 ±2.4%). Thus, some of the greater amount of α-cell autofluorescence collected through the NADH emission filter is likely due to non-NADH autofluorescence (e.g. elastin, collagen, lipopigments and pyridoxine) (476, 477). Assuming that FCCP fully oxidizes NADH, we can subtract this "non-NADH" background from the autofluorescence intensity measured at 1 mM glucose. In this case, we found that the NAD(P)H baseline was still 51.7 ±6.2% ($p<0.001$) greater in α-cells compared to β-cells.

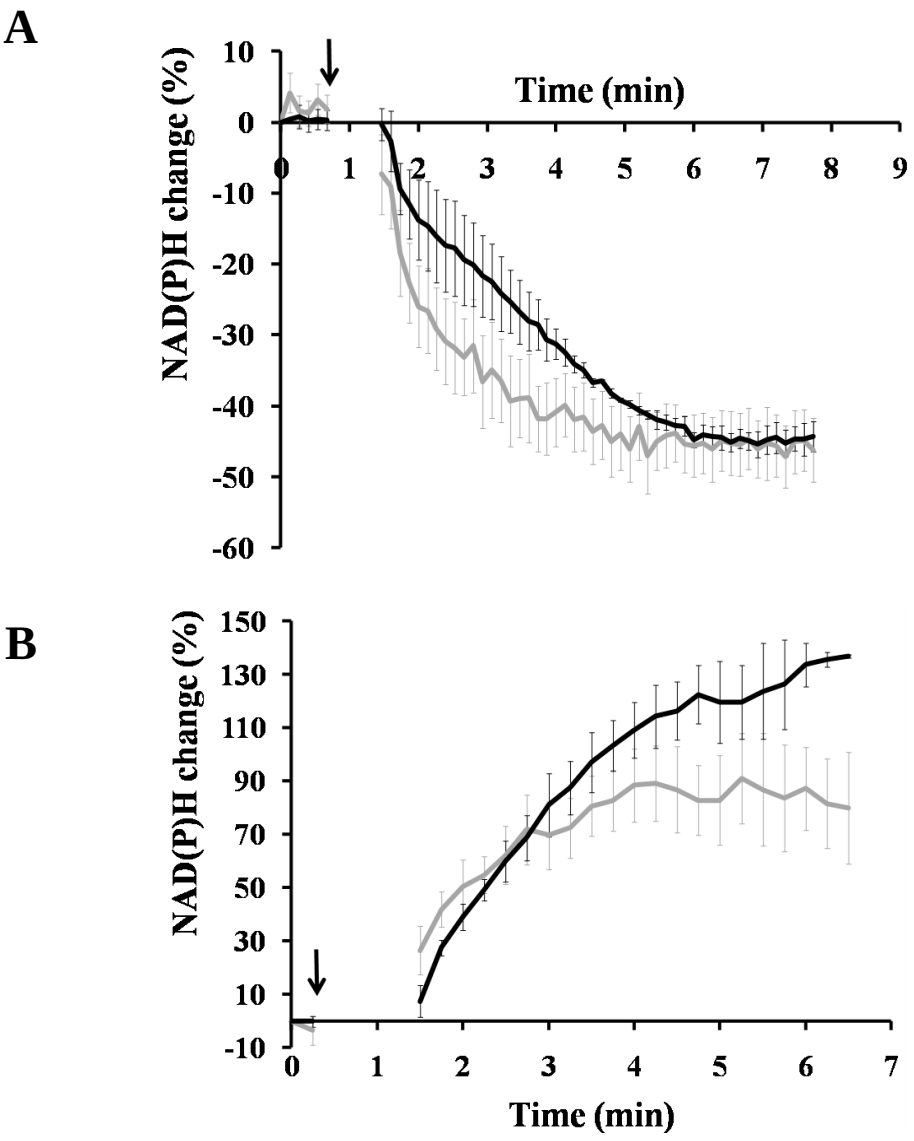

Figure IV-3: Time-series acquisition of the fluorescence intensity collected through the NAD(P)H emission filter in response to FCCP and cyanide application. Transgenic islets expressing EYP in α-cells were perifused at 1 mM glucose. Black traces indicate β-cells (from 3 islets), gray traces indicate α-cells (12 α-cells from 3 islets for A and 13 α-cells from 3 islets for B). A, application of 1 μM FCCP (black arrow) reduces the amount of autofluorescence collected in both α- and β-cells ($p<0.01$ comparing the baseline with values after 5 minutes of FCCP exposure, paired Student's *t* test). B, application of 3 mM NaCN (black arrow) elevates both α- and β-cell NAD(P)H redox state ($p<0.01$ after 5 minutes of NaCN exposure, paired Student's *t* test). Error bars represent the standard error of the mean.

3-5 Determination of maximal metabolic redox states

As previously described, exposure of the islets to FCCP yields a minimal NAD(P)H signal. To determine the maximal dynamic range of the NAD(P)H response, we fully reduced NAD^+(P) into NAD(P)H, its fluorescent counterpart. For this purpose, we perifused the islets with cyanide anion (CN^-) which is an inhibitor of cytochrome c oxidase. As a consequence, the electron transport chain is disrupted, NAD(P)H can no longer be oxidized by the respiratory chain and accumulates in the mitochondria (475). As expected, exposure to cyanide induces an increase in NAD(P)H autofluorescence in both α- and β-cells, meaning that more NAD(P)H is being produced (Fig. IV-3B). NAD(P)H accumulation reaches a plateau after ~ 5-6 minutes.

Fig. IV-3B suggests that cyanide has a greater effect on β-cells. However, this result is misleading because α-cells contains more non-NAD(P)H autofluorescence, as previously discussed. By subtracting the autofluorescence not related to NAD(P)H and normalizing the result to the maximal signal obtained from β-cells after cyanide addition, we found that both α-and β-cell maximal NAD(P)H concentrations are indeed very similar (maximal α-cell NAD(P)H level represents 93.8 ±7.8% of maximal β-cell NAD(P)H).

3-6 Glucose-dependent NAD(P)H responses from intact islets and isolated α-cells

To determine the glucose-dependent NAD(P)H responses from intact islets, we acquired z-stack images of an islet, beginning at 1 mM glucose, and then 10 minutes after each change in glucose concentration, when NAD(P)H signal has reached a plateau. The islet NAD(P)H response to step-increases in glucose concentration (Fig. IV-4A) was

A

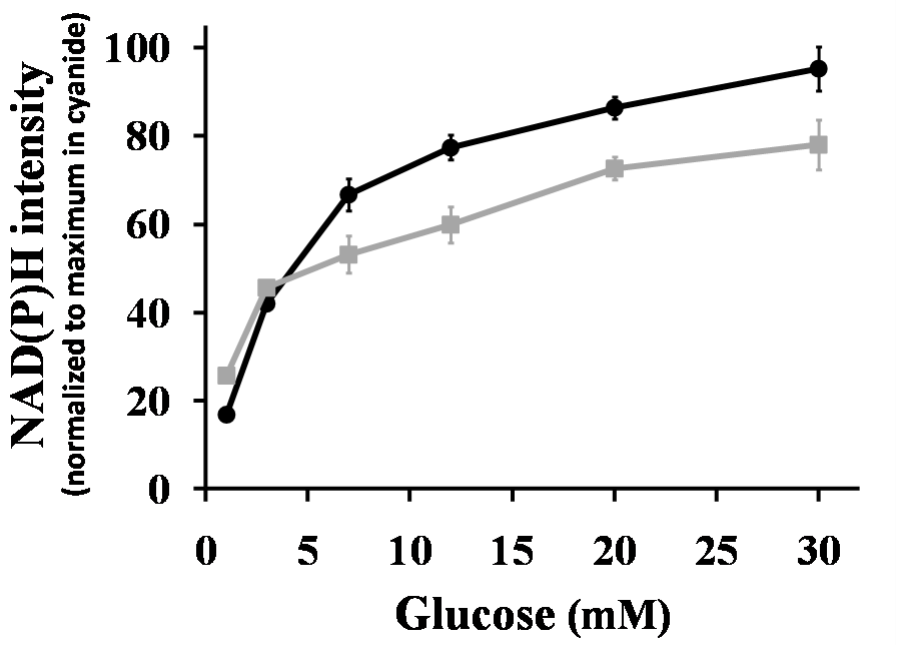
NAD(P)H intensity
(normalized to maximum in cyanide)
100
80
60
40
20
0
0
5
10
15
20
25
30
Glucose (mM)

B

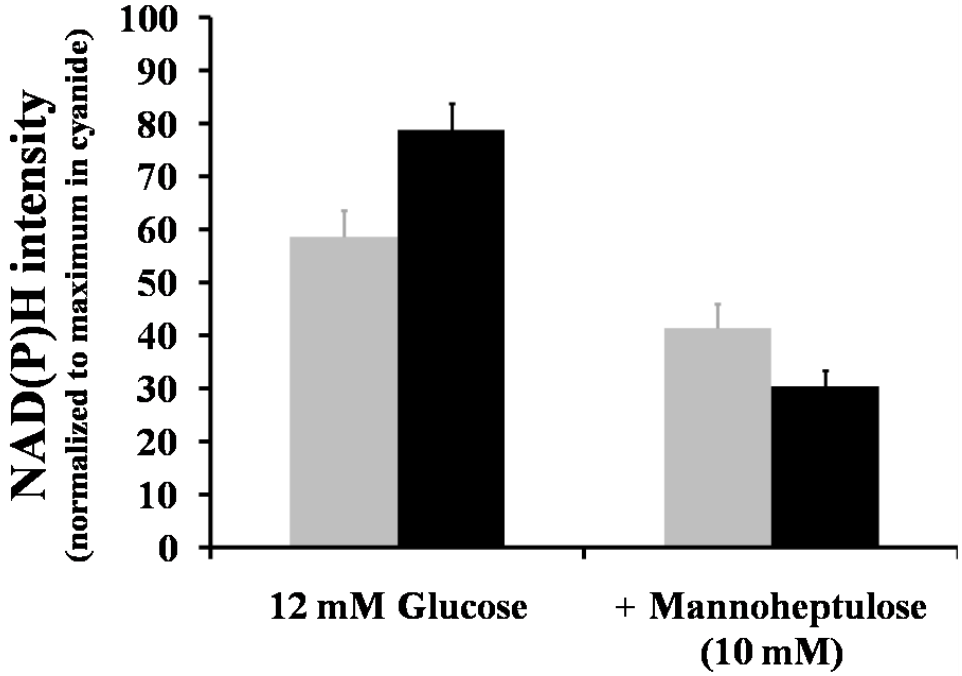
NAD(P)H intensity
(normalized to maximum in cyanide)
100
90
80
70
60
50
40
30
20
10
0
12 mM Glucose
+ Mannoheptulose
(10 mM)

C

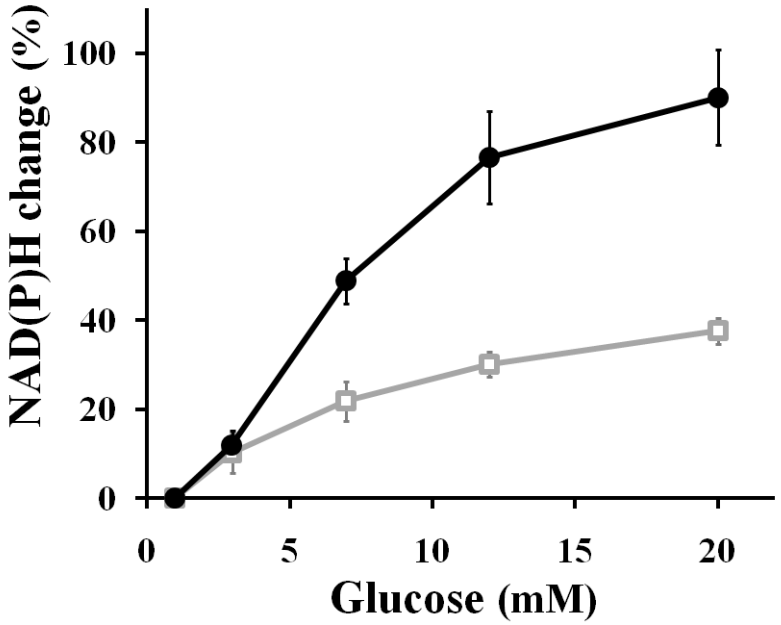

Figure IV-4: Glucose-dependent NAD(P)H responses from intact islets and isolated cells. Black traces indicate β-cells, gray traces indicate α-cells, both with SEM error bars. A, NAD(P)H responses to step-increases in glucose from islet α-cells (solid squares, n=250) and β-cells (solid circles, core regions averaged from 67 islets). The data has been normalized to minimal and maximal β-cell NAD(P)H obtained with FCCP and cyanide, respectively. B, application of 12 mM glucose increases cellular redox state in both α- and β-cells (gray and black columns, respectively). Addition of 10 mM D-mannoheptulose significantly inhibits NAD(P)H responses from both cell types ($p<0.01$, n=12 for α-cells, n=7 for β-cells). C, % change in NAD(P)H autofluorescence to step-increases in glucose from isolated α-cells compared to values at 1 mM glucose (open squares, n=146) and isolated β-cells (open circles, n=269). All the NAD(P)H responses in A and C were significantly different from baseline at 1 mM glucose ($p<0.01$, ANOVA – independent samples).

normalized to the minimal NADH redox state obtained with FCCP, and to the maximal signal following application of 3 mM sodium cyanide. Both α- and β-cells dose-dependently increased their NADH redox state with glucose. The dynamic range of the α-cell NAD(P)H response, as measured by the ratio between NAD(P)H levels at 1 mM and 30 mM, was ~ 2-fold less than for β-cells (3.1 ±0.3 vs. 5.7 ±0.5, respectively). This difference mainly arises from the greater basal NAD(P)H level in α-cells (as described in Section 3-4).

The glucose dose-response was fit to a sigmoidal curve, which yielded an EC_{50} (half maximal response) of 7.1 mM for α-cells (95% confidence interval: 1.3 to 39.2 mM) and 4.2 mM for β-cells (2.8 to 6.3 mM). These values suggest that the metabolic response of both cell types is limited by glucokinase, the hexokinase with a low affinity for glucose (471). Application of a non-metabolizable competitive inhibitor of glucokinase, D-mannoheptulose (10 mM) (478, 479), strongly reduces NAD(P)H autofluorescence in islets perifused at 12 mM glucose (Fig. IV-4B). Mannoheptulose was more potent at inhibiting β-cells than α-cells (78.2 ±5.2% reduction in β-cell NADH against 53.8 ±8.9% inhibition in α-cells).

We also measured glucose dose-dependent increases in the NAD(P)H response from sorted α- and β-cells, isolated from Glucagon-EYFP (420) and MIP-GFP (443) mice, respectively (Fig. IV-4C). These experiments were performed with our previous microscope (LSM 510) and since we did not calibrate our NAD(P)H signal with FCCP and cyanide, we cannot compare the values obtained from isolated cells with islet cells. However, the elevation in NAD(P)H intensity in response to glucose confirms that isolated cells metabolize the sugar. In addition, the NAD(P)H response to glucose was

more heterogeneous from isolated α-cells than for those within intact islets, as observed in dispersed β-cells (472). Only ~ 70% of isolated α-cells were responsive to glucose (at 12 and 20 mM) compared to over 95% of α-cells within intact islets. Also, the standard deviation of the increase from 1 to 12 mM glucose was greater in isolated α-cells (~ 70% of the mean compared to ~ 30% in islet α-cells).

Lastly, we investigated if inhibitors of glucagon release would have an effect on α-cell metabolic state, but we did not observe any deviation in NAD(P)H after addition of insulin (100 nM), zinc (30 μM), or GABA (1 mM).

3-7 Mitochondrial membrane potential measurements

In order to confirm that glucose is metabolized in α-cells, we utilized another imaging method based on the partitioning of a fluorescent dye across the inner mitochondrial membrane. Glucose metabolism induces the activation of the tricarboxylic acid cycle which coupling with the oxidative respiratory chain leads to proton extrusion from the mitochondrial matrix into the mitochondrial intermembrane space. As a result, the inner mitochondrial membrane hyperpolarizes and cationic fluorescent indicators, such as TMRE (tetramethylrhodamine-ethyl-ester), accumulate across of the inner mitochondrial membrane (480, 481). The more TMRE accumulates into the mitochondria, the brighter the cell fluorescence intensity becomes (Fig. IV-5A). As expected, glucose dose-dependently hyperpolarizes the inner mitochondrial membrane of α-cells present in intact pancreatic islets. TMRE fluorescence in α-cells increases by 61 (±7) % from 1 to 7 mM glucose, and by 125 (±17) % from 1 to 12 mM (Fig. IV-5B).

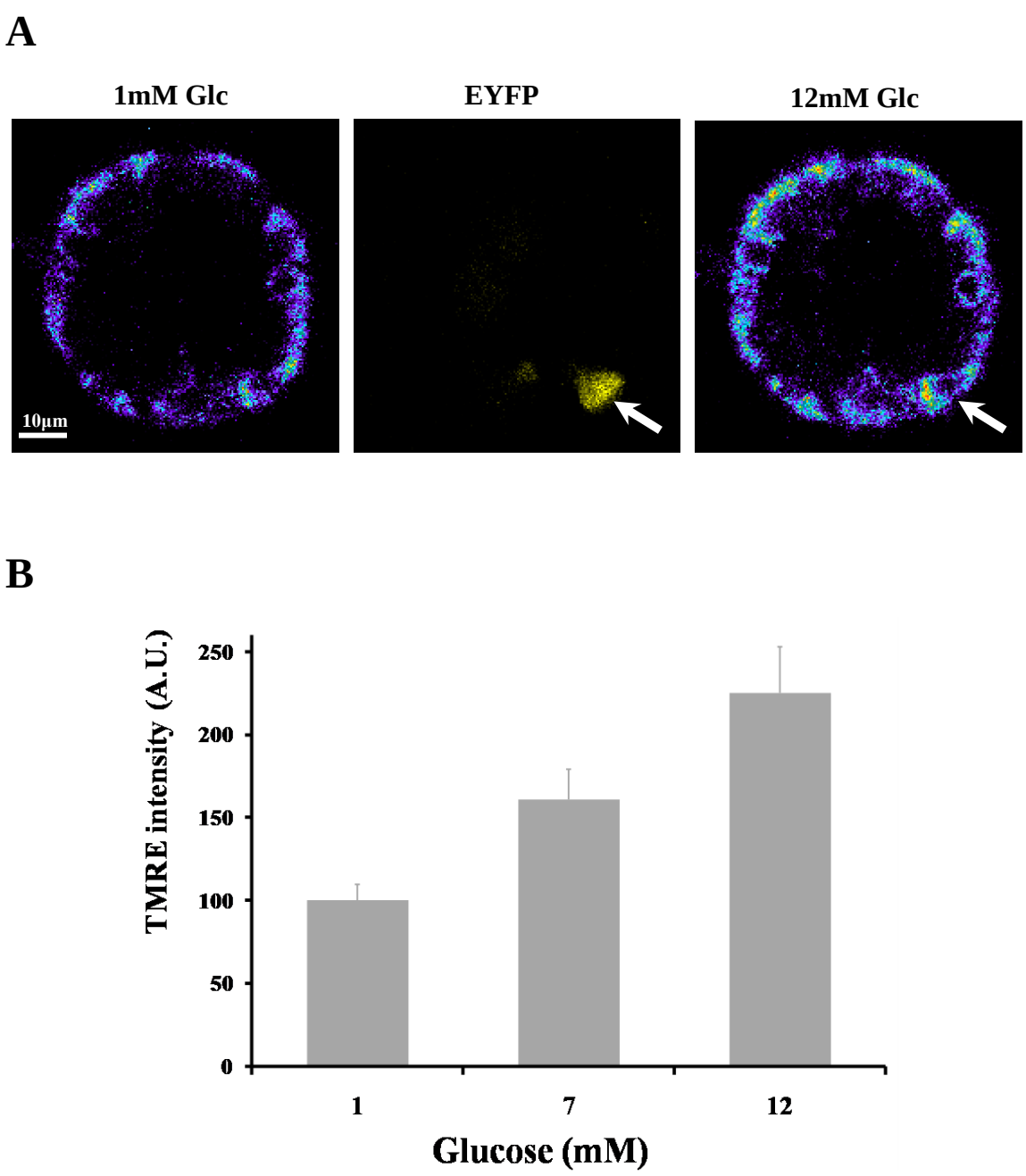

Figure IV-5: Mitochondrial membrane potential changes in response to glucose. A, left panel: confocal section of a representative intact islet incubated with 10 nM TMRE (pseudocolor scale) at 1 mM glucose. Middle panel: same confocal plane, the white arrow points to one EYFP-labeled α-cell. Right panel: TMRE intensity after 10 minutes of perifusion at 12 mM glucose. B, glucose dose-dependently elevates α-cell TMRE intensity. Differences in fluorescence intensities at 1, 7 and 12 mM were statistically significant ($p<0.01$, ANOVA, 26 α-cells measured from 7 islets). Error bars indicate the standard error of the mean.

3-8 Arginine-dependent modulation of α-cell NAD(P)H

We demonstrated that glucose, which inhibits glucagon secretion from intact islets, is metabolized in α-cells. We next sought to determine whether L-arginine is metabolized in α-cells. The amino acid arginine is a potent glucagon secretagogue (314, 315). How arginine mediates its action is still debated (Chapter I – Section 4-6-6). Arginine is transported into the cells by cationic amino acid transporters (482), and metabolized through the action of arginase which hydrolyzes arginine to urea and ornithine (483). Ornithine is then further metabolized and feeds the tricarboxylic acid cycle. Arginase is expressed and is active in pancreatic islets (484).

To determine the arginine-dependent NAD(P)H responses, we acquired z-stack images of an islet at 1 mM glucose, and another z-stack acquisition was collected 10 minutes after arginine stimulation, when NAD(P)H signal has reached a plateau (data not shown). The islet NAD(P)H response to step-increases in arginine concentration (Fig. IV-6) was normalized to the minimal NADH redox state obtained with FCCP, and to the maximal signal with sodium cyanide. Both α- and β-cells dose-dependently increased their NADH redox state with arginine. Interestingly, the α-cell NAD(P)H response to arginine was similar to glucose (Fig. IV-4A). For instance, application of 20 mM arginine or 20 mM glucose induces an increase in α-cell NAD(P)H signal corresponding to ~ 70-80% of its maximum in cyanide. In contrast, β-cells were less effective at metabolizing arginine. For instance, 20 mM arginine leads to a β-cell NAD(P)H redox state that only represents ~ 40% of its maximal in cyanide, as compared to ~ 95% with 20 mM glucose (Fig. IV-4A).

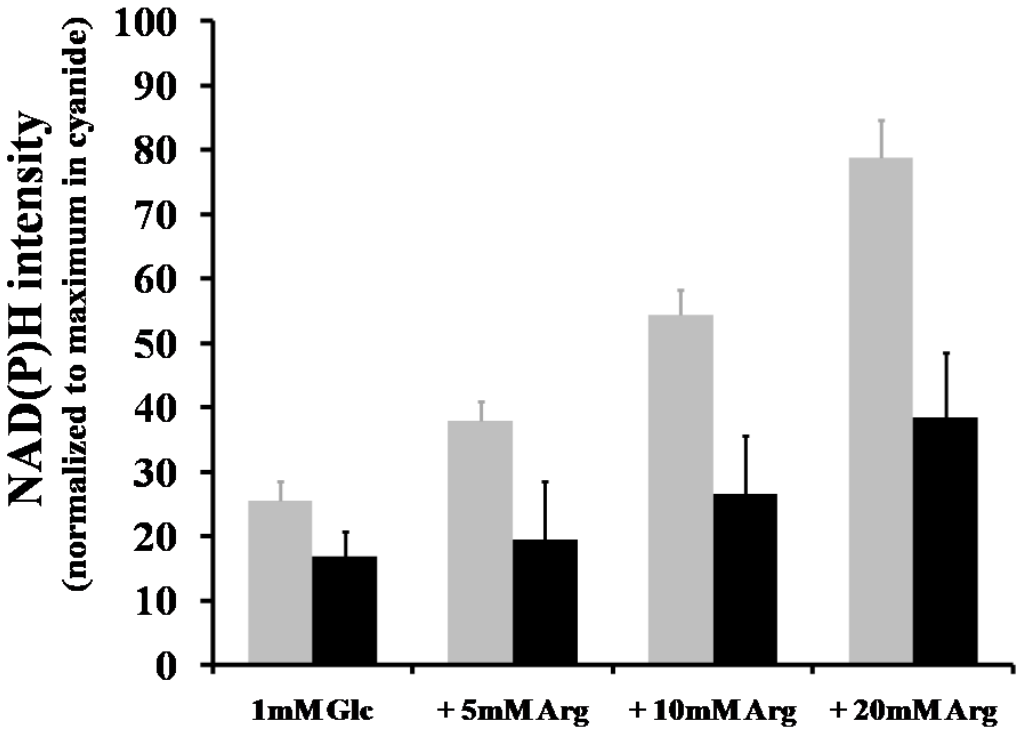

Figure IV-6: Arginine-dependent NAD(P)H responses from intact islets. Pancreatic islets from transgenic mice expressing fluorescent proteins in α-cells were perifused at 1 mM glucose and exposed to step-increases in arginine concentrations. The data has been normalized to minimal and maximal β-cell NAD(P)H obtained with FCCP and cyanide, respectively. Arginine dose-dependently enhanced the NAD(P)H levels in both α- and β-cells (gray and black columns, respectively). The α-cell NAD(P)H change to arginine was significant ($p<0.01$, ANOVA, 30 α-cells measured from 7 islets) and α-cell NAD(P)H intensity was different from β-cell intensity for each condition tested ($p<0.01$, Student's *t* test). Error bars indicate the standard error of the mean.

3-9 Pyruvate-dependent modulation of α-cell NAD(P)H

Finally, we examined the effect of pyruvate on α-cell metabolism. Pyruvate is a glycolytic intermediate that supplies energy to the cells via activation of the tricarboxylic acid cycle in the mitochondria. Exogenous pyruvate enters the cell by monocarboxylate transporters expressed on the plasma membrane and is taken up by mitochondria via mitochondrial pyruvate transporters. Pyruvate induces a biphasic glucagon response from intact islets while only transiently stimulating insulin secretion (348). This transient effect on insulin release is concomitant to a transient rise in metabolism, as measured by two-photon NAD(P)H imaging (485).

Time-series acquisition of α-cell NAD(P)H responses to pyruvate from intact islets indicates that pyruvate stimulates α-cell NAD(P)H only transiently (Fig. IV-7), similar to what is seen in β-cells. These experiments were performed with our previous microscope (LSM 510). Since we did not calibrate our NAD(P)H signal with FCCP and cyanide, we cannot compare the NAD(P)H signal from α- and β-cells. However, we did record transient NAD(P)H elevations in β-cells (not shown).

4- Discussion

4-1 Hormone secretion responses to glucose

Hormone secretion assays indicate that the intact pancreatic islet is a good model for studying the mechanisms of glucagon secretion at low glucose levels and glucagon suppression at high glucose. Glucagon release from islets is indeed maximal at concentrations below 4 mM and inhibited at increasing concentrations of glucose

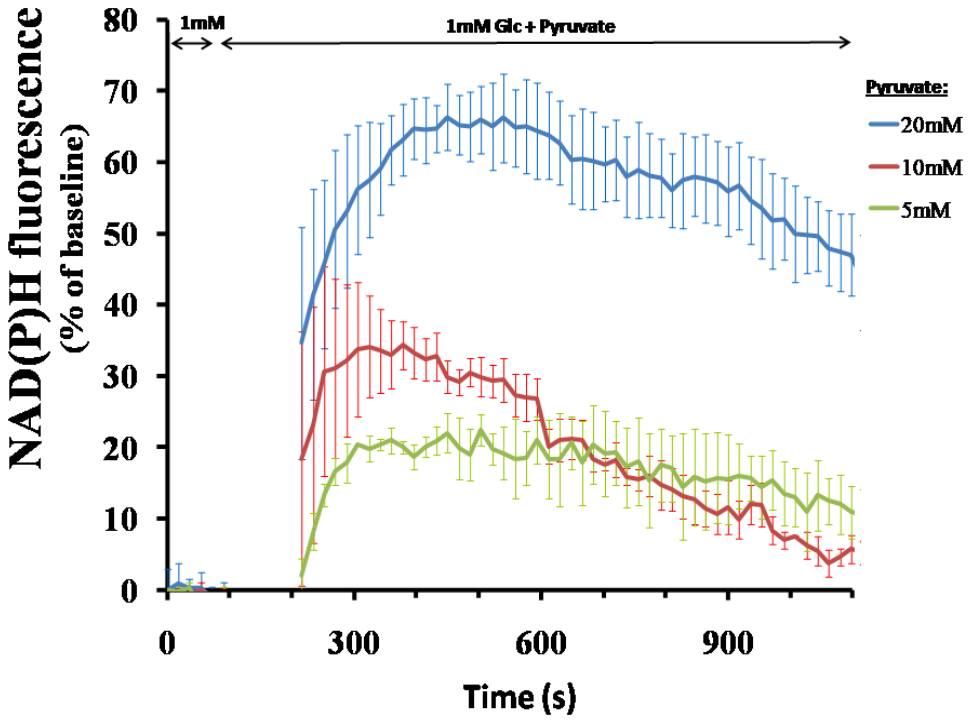

Figure IV-7: Pyruvate-dependent NAD(P)H responses from α-cells in intact pancreatic islets. Islets from transgenic mice expressing fluorescent proteins in α-cells were perifused at 1 mM glucose and exposed to step-increases in pyruvate concentrations (5, 10 or 20 mM). The α-cell NAD(P)H change to pyruvate was significant ($p<0.01$, Student's *t* test, 62 α-cells measured from 18 islets harvested from 2 mice). Error bars indicate the standard error of the mean.

(Fig. IV-1A), similar to in vivo measurements (319). However, the extent of the inhibition differs between isolated islets and perfused pancreata: high glucose almost entirely suppresses glucagon secretion from pancreata whereas it leads to a ~ 60% inhibition in perifused islets. The reduced inhibition observed in isolated islets could be attributed to lack of α-cell innervation (reviewed in Chapter I – Section 2-4) or to proteolytic damages during the isolation procedure.

To separate paracrine inhibition from possible direct suppressive effects of glucose, we studied the secretory responses of pure populations of isolated mouse α-cells. Flow-sorted α-cells are viable and arginine retains its ability to strongly stimulate glucagon secretion from these cells. However, important differences emanate from the comparison with α-cells present in intact islets. First, at basal glucose concentration (1 mM), isolated cells secrete ~ 2-fold more glucagon than do cells within intact islets. This greater basal secretion has been also reported in dispersed rat islets and flow-sorted rat α-cells (290, 418, 486, 487) and suggests that even baseline α-cell secretory activity is tonically inhibited in the islet. This observation emphasizes the importance of cell-cell contacts (juxtacrine signaling) or paracrine effectors for normal glucagon response. Second, glucose does not inhibit the glucagon secretion from α-cells removed from the islet environment. In fact, glucose has a stimulatory effect on isolated mouse α-cells. We found that 12 mM glucose enhances basal glucagon release by ~ 40% (Fig. IV-1B). This result supports previous studies on isolated rat α-cells describing a ~ 65% increase from 1 to 12 mM glucose (311, 341). The lack of inhibition of glucagon secretion from pure populations of α-cells argues against a direct suppressive action of glucose and supports a paracrine model.

4-2 Metabolic responses to glucose

β-cell glucose metabolism plays a pivotal role in insulin secretion (129, 132, 133, 135-138, 442). In contrast, the role of α-cell metabolism in glucagon secretion remains to be determined. Biochemical studies report glucose-dependent increases in the rates of glucose oxidation (282) (345-347), and greater ATP to ADP ratios (339, 348, 349). However, these results were recently challenged because fluorescence microscopic techniques were unable to detect any α-cell metabolic responses to glucose (350, 351, 415, 420). These experiments were based on single-photon excitation of NAD(P)H and flavoprotein autofluorescence. We successfully report dose-dependent changes in α-cell metabolic redox state in response to glucose, as measured by two-photon excitation of NAD(P)H autofluorescence in well-identified α-cells in intact islets and from pure populations of isolated cells (Fig. IV-2). We confirmed this result by measuring glucose-dependent changes in mitochondrial membrane potential, as indicated by TMRE imaging (Fig. IV-5).

NAD(P)H levels measured in islets incubated at 1 mM glucose were ~ 50% greater in α-cells than in β-cells. This enhanced metabolic redox state is consistent with greater basal α-cell ATP to ADP ratio (347) and likely illustrates the metabolic potential needed for maximal glucagon secretion at low glucose levels. This difference in basal metabolic state could arise from cell differences in the expression of high-affinity hexokinases that are already saturated at 1 mM glucose (283). From 1 to 30 mM glucose, the NAD(P)H levels were increased ~ 3-fold in α-cells and ~ 6-fold in β-cells. This observation is in agreement with previous studies reporting lower dynamic ranges in the rates of glucose oxidation and in ATP/ADP ratio, as compared to β-cells (345-348). Our

results indicate that the reduced dynamic range in α-cell NAD(P)H response was mostly explained by the ~ 50% greater baseline level in this cell-type.

Glucokinase (hexokinase IV) is an allosteric enzyme that displays a sigmoidal steady-state kinetic response to increasing glucose concentrations in the millimolar range. Glucokinase is established as the rate-limiting step for β-cell glycolysis (132) and NAD(P)H response to glucose follows glucokinase kinetics (Fig. IV-2, (472)). Glucokinase is also expressed in α-cells (283) and the time course of the α-cell NAD(P)H response, EC_{50}, and inhibition by D-mannoheptulose (a non-metabolized glucokinase inhibitor), suggest that glucokinase is also the rate-limiting step for α-cell glycolysis (Fig. IV-2 and IV-4). The half maximal glucose response obtained from islet α-cells is slightly right-shifted as compared to β-cells (7 and 4 mM, respectively) and could indicate cell-specific differences in the regulation of glucokinase. Furthermore, we noticed that glucokinase inhibition by mannoheptulose was more effective in β-cells, as indicated by our NAD(P)H measurements. This difference could potentially arise from cell differences in the rate of mannoheptulose uptake because β-cell transporters GLUT-2 are more specific at transporting heptose than α-cell GLUT-1 (488).

As opposed to the typical monophasic NAD(P)H response induced by a switch from low to high glucose concentrations, some islets responded by a biphasic response at concentrations below 6 mM (Fig. IV-2C). To our knowledge, this observation has not been described in the literature and could reflect a feedback inhibition in the glycolytic pathway. Further studies would be necessary to determine the origin of the inhibition at low glucose.

In addition, we confirmed that glucose dose-dependently enhances α-cell

NAD(P)H on cells purified by fluorescence-activated cell sorting. However, we noticed more variability in the NAD(P)H response from isolated α-cells compared to cells in intact islets, as observed in dispersed β-cells (472). This heterogeneity in NAD(P)H responses and the opposite secretory activity to glucose exposure stress the fact that α-cells need the 3D cytoarchitecture of the islet for normal physiology. Loss of juxtacrine and paracrine effects, or proteolytic damage during islet dispersion could explain why isolated cells behave differently (418, 486, 487, 489).

4-3 Relationship between metabolism and secretion

The mechanisms underlying the suppression of α-cell secretory activity are poorly understood, but two general types of models have been proposed: direct inhibition by glucose, or paracrine inhibition from non α-cells within the islet of Langerhans. Models supporting a direct inhibition by glucose propose that the elevation in α-cell metabolic state mediates the inhibition of α-cell secretory activity (352, 357, 490). The reduction in glucagon secretion from intact islets occurs between 3 and 7 mM of glucose (Fig. IV-1A) but α-cell metabolic redox state only increases by 16.4 ±1.4% over the same concentrations (Fig. IV-4A). It seems unlikely that such a small change in metabolism accounts for the suppressive effect of glucose observed in islets. In contrast, a rise in NAD(P)H levels in isolated α-cells is translated into an increase in glucagon secretion, meaning that an increase in metabolism stimulates glucagon secretion when α-cells are retrieved from their islet environment. It is worth noting that this stimulatory effect of glucose on glucagon secretion is also observed in type-I and advanced type-II diabetes when the β-cell population is depleted (Chapter I – Section 1-2-2). Such an effect could

possibly arise from loss of cell-cell contacts between α- and β-cells, or from loss of paracrine effects.

The NAD(P)H elevation to the glucagon secretagogue arginine was greater in α-cells compared to β-cells (Fig. IV-6). Although we did not investigate this observation further, it is possible that the difference originates from cell-specific variations in arginase expression. The sharp NAD(P)H response to arginine is concomitant with an acute secretory activity from both islet α-cells and isolated α-cells, and supports a mechanism whereby arginine mediates its effect by stimulating α-cell metabolism (317, 491, 492).

Pyruvate is another glucagon secretagogue that induces a biphasic glucagon response (acute first phase follows by a plateau at a lower level) (348). Similarly to β-cells, pyruvate is only transiently metabolized in α-cells (Fig. IV-7, (485)). Possible mechanisms for this transient effect involve inhibition of either mitochondrial pyruvate metabolism or transport (485). For instance, the mitochondrial pyruvate symporter present in the inner membrane co-transports pyruvate with a proton. This acidification of the matrix could dissipate the proton gradient across the inner membrane and inhibit ATP synthase.

Glucose, as well as the secretagogues arginine and pyruvate, elevate islet α-cell metabolism; however their respective effect on glucagon secretion is opposite. We conclude that elevation in α-cell metabolism is not sufficient for glucagon inhibition in intact islets. In addition, our secretion assays from isolated α-cells show that glucose does stimulate glucagon secretion from α-cells retrieved from their islet environment. It is therefore likely that activation of α-cell metabolism enhances glucagon secretion, as also

observed with arginine and pyruvate. Thus, the opposite behavior to glucose exposure supports a paracrine inhibition model whereby α-cell secretory activity would be dampened by other cell-types within the islet. This paracrine effect is unlikely to be mediated by inhibition of α-cell metabolism since α-cell redox state is greater at inhibitory concentrations of glucose and since candidate paracrine inhibitors (insulin, zinc, GABA) do not modulate NAD(P)H levels. Thus, paracrine effectors likely act downstream α-cell metabolism, possibly by inhibiting intracellular calcium activity or by inhibiting exocytotic mechanisms. The effect of glucose and candidate paracrine inhibitors of glucagon secretion on α-cell calcium dynamics is presented in Chapter V.

CHAPTER V

MECHANISMS OF GLUCAGON INHIBITION UNDER HIGH GLUCOSE CONDITIONS

1- Introduction

Glucagon is a gluconeogenic hormone released from α-cells present in intact pancreatic islets at glucose concentrations below 4 mM, whereas higher glucose levels inhibit its secretion (Fig. IV-1A). The mechanisms underlying the suppression of α-cell secretory activity are poorly understood, but two general types of models have been proposed as follows: direct inhibition by glucose or paracrine inhibition from non-α-cells within the islet of Langerhans. The electrophysiological model of glucagon secretion proposes that glucose directly inhibits the secretion of glucagon (Chapter III). Glucose inhibition would be mediated by K_{ATP} channel closure, membrane depolarization and inhibition of voltage-gated calcium channels. The lack of reliable method for distinguishing α-cells within the islet has hindered the α-cell research field. To identify α-cells for analysis, we took advantage of transgenic mice expressing fluorescent proteins targeted specifically to these cells (Chapter II – Section 3-1). Imaging of cellular metabolism by two-photon excitation of NAD(P)H autofluorescence reveals that glucose is metabolized in α-cells and that glucokinase is the likely rate-limiting step in this process (Chapter IV – Section 3-6). This result indicates that glucose could potentially activate the mechanism proposed by the electrophysiological model. However, glucagon

secretagogues such as arginine and pyruvate also stimulate α-cell metabolism, meaning that an increase in α-cell redox state is not sufficient to inhibit the secretion of glucagon (Chapter IV – Sections 3-8 and 3-9). Closure of K_{ATP} channels by tolbutamide, as well as membrane depolarization by KCl or arginine, increase α-cell $[Ca^{2+}]_i$ while stimulating the secretion of glucagon (Chapter III). In addition, measurements of glucagon secretion from pure populations of flow-sorted α-cells show that contrary to its effect on intact mouse islets, glucose does stimulate the secretion of glucagon from isolated α-cells (Fig. IV-1B). Collectively, these results contradict the predictions of the electrophysiological model and argue against a direct inhibition of glucagon secretion by glucose.

The paracrine model of glucagon secretion proposes that non-α-cells, such as β-cells and δ-cells, release paracrine inhibitors of glucagon secretion under hyperglycemic conditions (a detailed review is presented in Chapter I – Section 4-6-2). Although the exact mechanisms underlying paracrine inhibition are not known, it has been proposed that paracrine inhibitors would hyperpolarize the α-cell membrane potential and thus, inactivate high-voltage sensitive calcium channels. Using diazoxide, a K_{ATP} channel opener, we found that membrane hyperpolarization inactivates calcium channels and inhibits the secretion of glucagon (Fig. III-7 and III-8). This observation suggests that a mechanism involving K_{ATP} channel opening and/or calcium channel inactivation could potentially lead to the suppression of glucagon output from pancreatic islets.

Models of glucagon suppression by glucose often postulate that $[Ca^{2+}]_i$ and calcium oscillations (either their amplitude, frequency, or both) are reduced at inhibitory concentrations of glucose. However, there is poor consensus regarding glucose-mediated calcium dynamics in the α-cell. Some studies report a decrease in calcium dynamics in

intact mouse islets (359, 360), intact human islets (415), single rat α-cells (363), dispersed guinea pig α-cells (361) and dispersed mouse α-cells (319, 337), other studies report a weak or negligible inhibitory effect of glucose in dispersed mouse α-cells (339) (296), whereas others describe glucose-mediated increases in $[Ca^{2+}]_i$ in isolated rat α-cells (311) and in a subset of α-cells within intact mouse islets (364). In this chapter, we have studied the effects of glucose on α-cell $[Ca^{2+}]_i$ dynamics in well-identified α-cells both in the intact islet and in single isolated α-cells. We have also investigated the effects of candidate paracrine inhibitors on both α-cell $[Ca^{2+}]_i$ and glucagon secretion.

2- Materials and methods

Materials, as described in Chapter II-Section 2-1.

Transgenic mice, Chapter II-2-2.

Averaged $[Ca^{2+}]_i$ changes in response to glucose were assessed by FuRed imaging on EYFP-expressing α-cells, whereas time-series measurements were obtained by Fluo-4 imaging on RFP-expressing α-cells.

Islet isolation and culture, Chapter II-2-3.

For imaging purposes, isolated islets and sorted α-cells were attached on gelatin (0.1%)-coated 35-mm glass-bottomed dishes (MatTek Corp., Ashland, MA).

Cell dispersion and cell flow-sorting, Chapter IV-2-2.

Glucagon and insulin secretion assays from islets and isolated α-cells, Chapter IV-2-4.

Intracellular free calcium measurements by confocal Fluo4-AM imaging

Time series Fluo-4 imaging was used for recording calcium oscillations within RFP islets, as described in Chapter II-2-8. Glucose and paracrine inhibitors were added at different locations on the edge of the imaging dish and mixed by gentle pipetting.

Intracellular free calcium measurements by confocal FuraRed-AM imaging

Islets were labeled with 10 μM FuraRed-AM for 1 h in imaging solution containing 1 mM glucose, at 37 °C. After washing, islets were allowed to equilibrate on the microscope stage for 15 min. FuraRed was used for measuring the calcium dose-response curve at steady-state concentrations of glucose. Sequential *z*-stack acquisitions of EYFP and FuraRed were performed at 1 mM glucose, and another z-stack was collected 15 to 30 minutes after glucose stimulation. For a given α-cell, optical sections with the greatest EYFP fluorescence (i.e. the middle of the cell) were used as references for comparing FuraRed signals before and after glucose application. This strategy was used to overcome any cell movement. Non-EYFP cells were considered to represent β-cells. FuraRed was excited at 488 nm, and its fluorescence collected through a 620–680-nm bandpass filter. Controls for photobleaching and dye leakage out of the cells were performed on separate islets (n = 7) and showed no statistically significant decrease in FuraRed fluorescence (−0.8 ± 2% for 19 α-cells and 0.06 ± 3.69% for β-cells at 1 mM glucose).

Calcium concentration values can be approximated from single wavelength

excitation of calcium dyes knowing the dissociation constant (K_D) of the probe and the basal calcium concentration (493, 494). The K_D values used for FuraRed was 1.1 μM (495) and the basal calcium concentration was 80 nM in both α- and β-cells as estimated previously (465, 496).

3- Results

3-1 Glucagon secretion assays in response to candidate paracrine inhibitors

In the islets, glucose suppresses the secretion of glucagon while stimulating β-cell secretory activity (Fig. III-2 and IV-1A). In contrast, glucose enhances the secretion of glucagon from pure populations of flow-sorted α-cells (Fig. IV-1B). Taken together, these observations support the paracrine model of glucagon inhibition in which glucose indirectly mediates its inhibition by stimulating the secretion of paracrine inhibitors from non-α-cells.

Insulin, zinc ions, and GABA are released by β-cells (341, 348, 377) and somatostatin by δ-cells (405, 497). All these compounds are candidate paracrine inhibitors of glucagon secretion from α-cells. We confirmed their inhibitory effects on glucagon secretion from intact islets incubated at 1 mM glucose (Fig. V-1A). Application of 100 nM insulin, 30 μM zinc ions, 100 nM GABA, and 100 nM somatostatin reduces basal glucagon secretion by ~ 75%. In comparison, an increase in glucose concentration to 12 mM inhibits the α-cell secretory activity by 56.8 ± 11.4%. Application of arginine (10 mM), a potent glucagon secretagogue (316), leads to an ~ 1.8-fold enhancement over

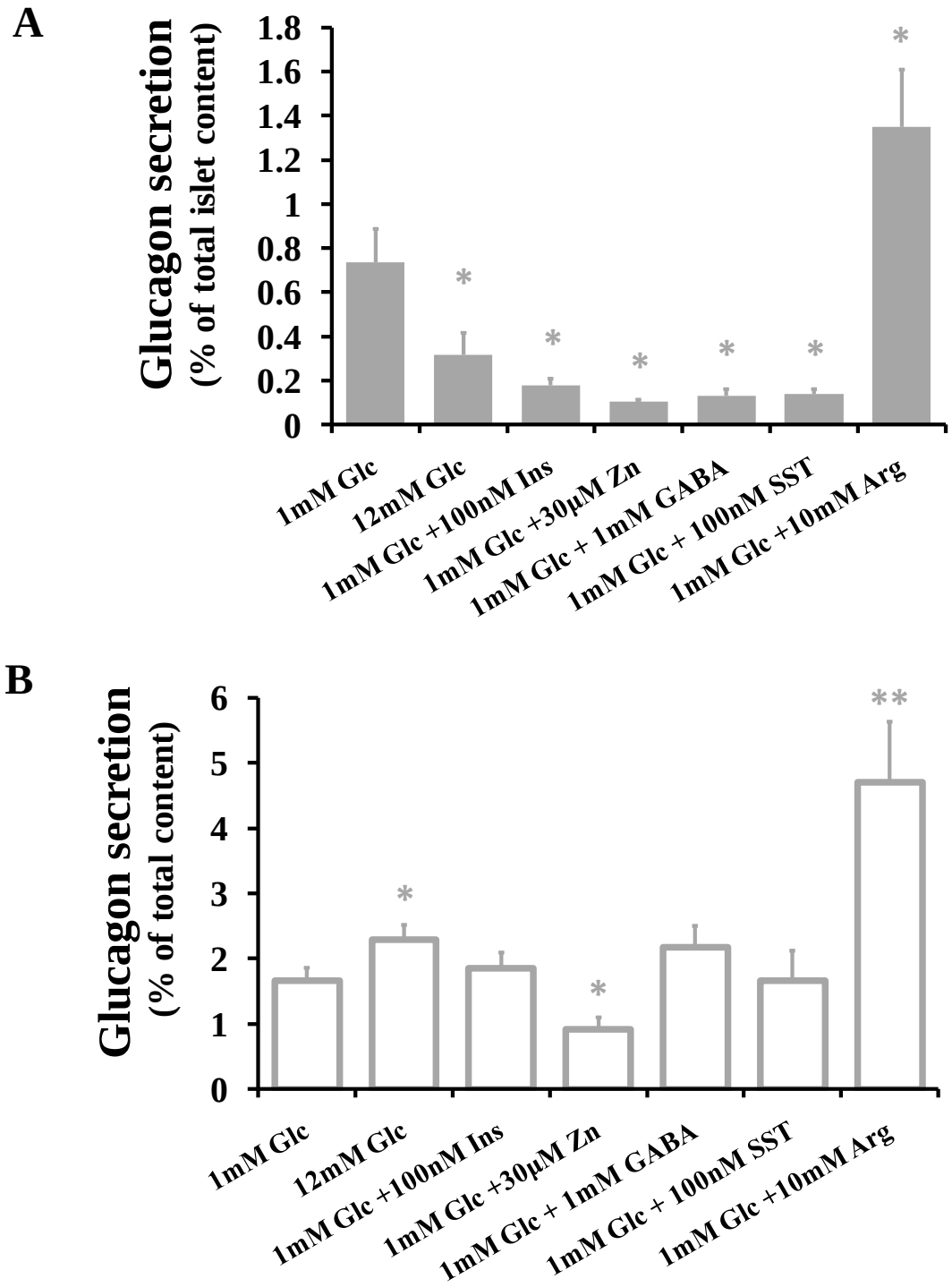

Figure V-1: Glucagon secretion from intact islets and sorted α-cells in response to candidate paracrine inhibitors. *A*, percent of islet glucagon content secreted per h. *B*, percent of glucagon content secreted from flow-sorted α-cells. *Glc*, glucose; *Ins*, insulin; *SST*, somatostatin; *Arg*, arginine. *Error bars* represent the mean ± S.E. *, $p < 0.05$, **, $p < 0.01$, ANOVA.

basal glucagon release (from 0.74 ± 0.15%, n = 7, to 1.35 ± 0.26% of total cellular glucagon content, n = 5, $p < 0.05$, Student's t test, unpaired samples).

We next investigated the effect of these inhibitors on flow-sorted α-cells. The same concentrations of insulin, GABA, and somatostatin had no significant effect on glucagon secretion (Fig. V-1B). Interestingly, only zinc retained its inhibitory effect, but its effect was muted compared to intact islets. Indeed, zinc reduced the basal glucagon secretion from sorted α-cells by 45.2 ± 5.1% (n = 17, p = 0.02, Student's t test, unpaired samples), whereas it inhibits glucagon secretion by ~ 75% in intact islets. In contrast, glucose stimulates glucagon release from sorted α-cells; application of 12 mM glucose increases basal secretion by 38.0 ± 3.8% (n = 25, $p < 0.05$, ANOVA). As it does in intact islets, arginine strongly stimulates glucagon secretion from sorted α-cells. Glucagon secretion from isolated cells at 1 mM glucose increases 2.8-fold after application of 10 mM arginine (from 1.66 ± 0.20%, n = 30, to 4.71 ± 0.9% of total cellular glucagon content, n = 10, $p < 0.001$).

3-2 Averaged α-cell $[Ca^{2+}]_i$ in response to glucose

We measured the cytoplasmic calcium concentrations in EYFP-labeled α-cells using FuraRed-AM. In intact islets, both α- and β-cells respond to glucose by increasing their averaged $[Ca^{2+}]_i$ in a dose-dependent manner (Fig. V-2A). Similar to the NAD(P)H response (Chapter IV), the dynamic range of the calcium response is less in α-cells than in β-cells. For instance, a change in glucose from 1 to 12 mM augments α-cell $[Ca^{2+}]_i$ by 45.3 ± 5.3% and β-cell $[Ca^{2+}]_i$ by 96.0 ± 6.2%. We assessed the role of glucokinase for

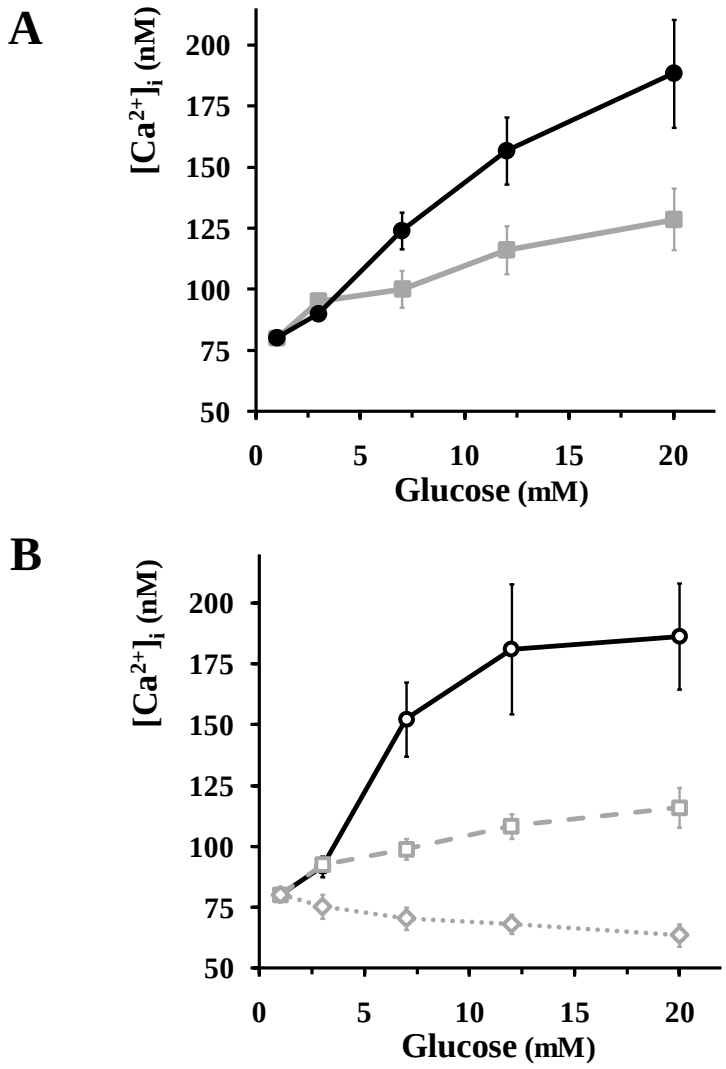

Figure V-2: Glucose-dependent changes in $[Ca^{2+}]_i$ by FuraRed imaging from intact islets and isolated cells. *Black lines* and *gray lines* with *error bars* represent β- and α-cells, respectively. *A*, glucose-dependent $[Ca^{2+}]_i$ increases from intact islets. At glucose levels greater than or equal to 7 mM, changes were statistically significant to base line at 1 mM glucose (n = 22 α-cells from 7 islets, $p < 0.01$, ANOVA). *B*, glucose-dependent $[Ca^{2+}]_i$ changes from sorted cells. Two distinct responses were apparent from sorted α-cells. The *dashed gray line* represents α-cells responding to glucose by an increase in $[Ca^{2+}]_i$ (11 of 20 cells). The *dotted gray plot* indicates α-cells that decrease their $[Ca^{2+}]_i$ (7 of 20 cells). At glucose levels greater than or equal to 7 mM, changes were statistically significant from base line (n = 9 β-cells, n = 20 α-cells, $p < 0.01$, ANOVA, correlated samples).

glucose-dependent increases in $[Ca^{2+}]_i$ by applying 10 mM of D-mannoheptulose to islets perifused with 12 mM glucose. Following treatment with the inhibitor, α-cell $[Ca^{2+}]_i$ was reduced by 19.5 ± 0.4% and β-cell $[Ca^{2+}]_i$ by 24.7 ± 0.9% (19 α-cells were analyzed from six islets, $p < 0.01$, Student's *t* test). Alternatively, we confirmed the stimulatory effect of 12 mM glucose on $[Ca^{2+}]_i$ by Fluo-4 imaging on tdRFP islets incubated at 1 mM (+62.1 ± 8.4% change in Fluo-4 intensity for α-cells and +111.0 ± 33.6% for β-cells, 15 α-cells were analyzed from seven islets, $p < 0.01$, Student's *t* test). Overall, ~ 90% (48 of 54 cells) of α-cells within intact islets elevate their average $[Ca^{2+}]_i$ after switching the glucose concentration from 1 to 12 mM.

Sorted β-cells display a similar $[Ca^{2+}]_i$ response to glucose compared with β-cells in intact islets, as measured by FuraRed imaging (Fig. V-2B). However, the calcium response from isolated α-cells is considerably more heterogeneous. Over 50% of the cells exhibit a response similar to that seen within intact islets, but one-third of the cells show decreasing $[Ca^{2+}]_i$, and 10% of the isolated α-cells are not responsive.

3-3 Effects of glucose and other glucagon inhibitors on α-cell calcium oscillations

α-cells are known to exhibit intracellular calcium oscillations at low glucose concentrations (Chapter II – Section 3-5) (359, 364, 415, 465). The specific expression of tdRFP in α-cells allows the use of Fluo-4, a sensitive calcium indicator. Islets were attached on gelatin-coated dishes for imaging purposes. At 1 mM glucose, 46% of islet α-cells (77 of 168 cells) were found to be oscillating during a typical 5-min observation period (Table V-1). Calcium oscillations are also present at inhibitory concentrations of glucose (12 mM), with a similar proportion of oscillating cells (49%, 46 of 91 cells).

	Number of cells analyzed	% of oscillating cells	Frequency (oscillation per min)	Amplitude of oscillations (%)		
				+15-30% increase	+30-60%	>60%
Islets at 1mM glucose	168	46	0.89 ±0.07	56.1 ±5.6	28.8 ±3.7	15.1 ±3.5
Islets at 12mM glucose	91	49	1.44 ±0.18**	52.4 ±7.1	30.8 ±5.3	16.8 ±5.2
Islets at 1mM glucose +100nM insulin	60	45	0.71 ±0.09	63.0 ±11.8	21.7 ±6.9	15.2 ±7.2
Islets at 1mM glucose +30µM Zn	62	40	0.84 ±0.17	56.4 ±12.8	30.8 ±9.7	12.8 ±5.7
Islets at 1mM glucose +1mM GABA	57	39	0.84 ±0.14	55.7 ±13.4	27.3 ±6.4	17.0 ±7.7
Islets at 1mM glucose +100nM somatostatin	46	50	0.78 ±0.09	60.9 ±8.1	30.5 ±8.4	8.6 ±2.9
Isolated cells at 1mM	45	53	0.89 ±0.10	55.5 ±6.6	25.6 ±6.3	18.9 ±5.6
Isolated cells at 12mM	52	52	0.97 ±0.15	64.5 ±8.9	20.7 ±5.3	14.9 ±6.9
Isolated cells at 1mM +30µM Zn	30	57	0.67 ±0.10	75.0 ±13.1	20.3 ±7.2	4.7 ±2.6

Table V-1: Comparison of α-cell calcium oscillation characteristics in response to glucose and inhibitors of glucagon secretion, as measured by Fluo-4 imaging. Each α-cell was monitored during 5 minutes for each condition. ******, $p < 0.01$, Student's *t* test.

Unlike the steady $[Ca^{2+}]_i$ oscillations seen in β-cells within intact islets, the α-cell calcium oscillations exhibit different shapes, amplitudes, and durations and random periodicity (Table V-1, Fig. V-3, Fig. V-4A). Typically, the signal to noise ratio of the Fluo-4 fluorescence was between 15 and 100 in our experiments. Defining an oscillation as a local $[Ca^{2+}]_i$ peak in time with greater than a 15% change in Fluo-4 signal, we estimated an overall frequency of 0.89 ± 0.07 oscillation/min from oscillating islet α-cells at 1 mM glucose. Interestingly, glucose application (12 mM) increases this frequency to 1.44 ± 0.18 oscillations/min ($p < 0.01$, Student's *t* test) but did not modify the amplitude distribution of the calcium events (Table V-1). The time series of Fluo-4 fluorescence is consistent with the averaged $[Ca^{2+}]_i$ changes reported with FuraRed described above. A representative time-series of the Fluo-4 response (Fig. V-3B) shows one α-cell that increases its oscillatory frequency after application of 7 mM glucose, and another responds by a sharp increase in $[Ca^{2+}]_i$. In a separate experiment, we applied a step-increase in glucose from 1 to 12 mM on 31 α-cells from 14 islets harvested from 6 mice. Islets were placed in a microfluidic device as previously described (Fig. II-2). We found that only ~10% of the α-cells responded to glucose by reducing the frequency of calcium oscillations and averaged $[Ca^{2+}]_i$. Thus, calcium imaging of intact islets suggests that glucagon inhibition by glucose is not mediated by a decrease in calcium dynamics. Actually, a majority of α-cells (~60%) exhibited an increase in calcium activity after glucose application. Similar to tolbutamide application (Fig. III-9), the effect of glucose is heterogeneous from cell to cell. Some α-cells behave like β-cells and quickly respond by a strong rise in $[Ca^{2+}]_i$, whereas others responded more slowly. We also noticed transient inhibition in the frequency/amplitude of calcium oscillations in 2 out of 31 cells.

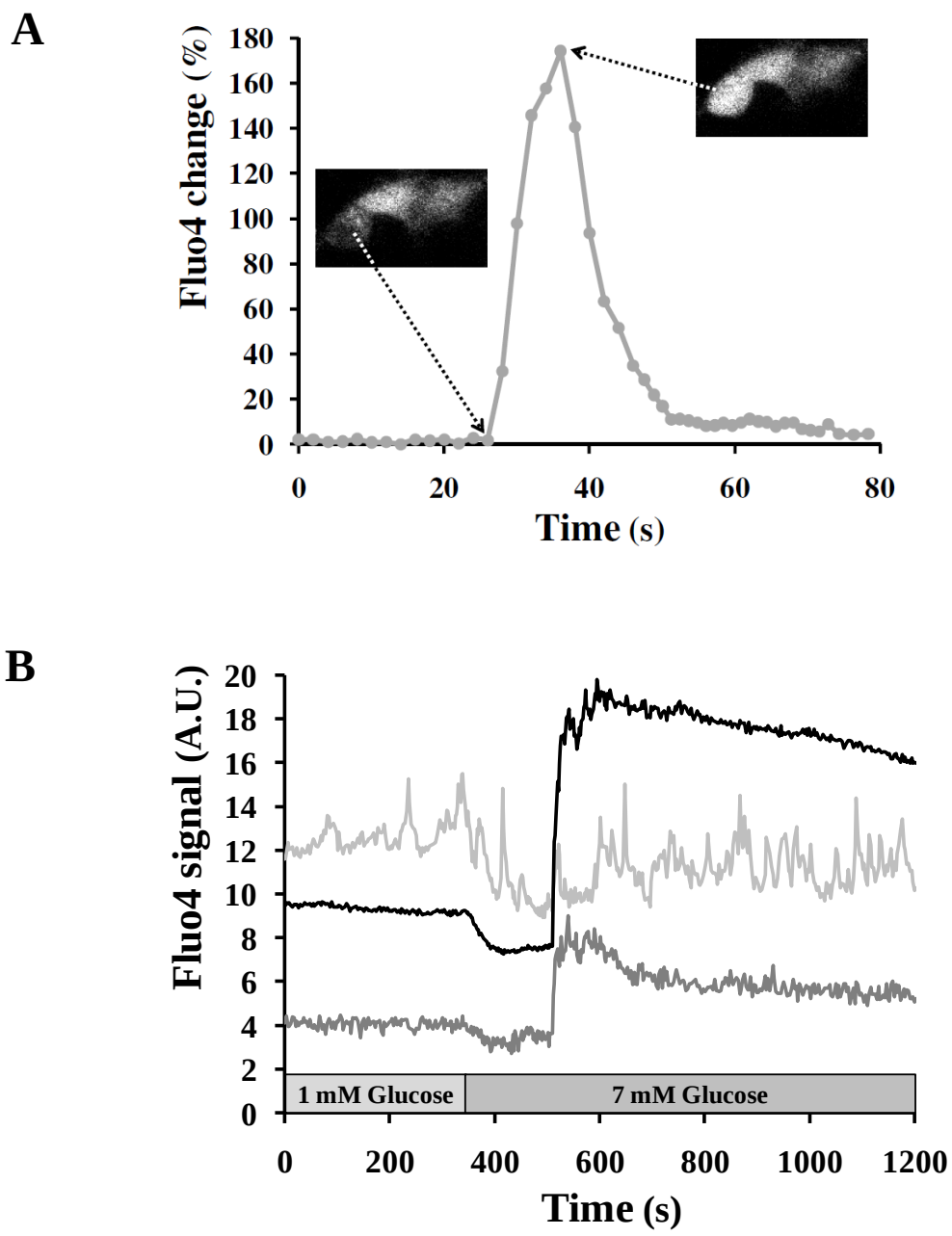

Figure V-3: Calcium oscillations from α-cells within intact islets as measured by Fluo-4. *A, B* are time series of the Fluo-4 signal relative to the minimal intensity recorded during the experiment. *A*, single calcium pulse from one islet α-cell perifused with 1 mM glucose. The *inset* images show the cell before and at the maximum of the calcium transient. B, representative time course of the Fluo-4 response from an islet exposed to a step-increase in glucose from 1 to 7 mM. The *black line* indicates a region of β-cells, and the *gray plots* show the responses of two individual α-cells. Fluo-4 signal was recorded every 2 s.

Finally, ~25% of the α-cells did not exhibit any significant response to glucose.

The oscillatory activity of isolated α-cells showed that at 1 mM glucose, 53% exhibited calcium oscillations with the same frequency as α-cells present in intact islet (0.89 ± 0.1 oscillation/min). We did not observe any significant deviation in their averaged oscillatory properties at elevated glucose levels or in the presence of zinc ions (Table V-1). We performed time-series measurements of the Fluo-4 response of sorted α-cells to a step-increase in glucose (from 1 to 12 mM). Out of 29 sorted α-cells from 6 mice, 12 cells responded by an increase in calcium activity, 10 cells were not responsive, and 7 cells reduced their calcium activity.

We assessed the effect of candidate paracrine inhibitors of glucagon secretion on islet α-cell calcium oscillations and did not observe any significant change in their oscillatory behavior. In addition, zinc did not inhibit sorted α-cell calcium oscillations either (Table V-1).

3-4 α- / β-cell synchronization during whole islet calcium waves

As shown in Figure V-4A, the calcium oscillations seen at low glucose are not synchronized between adjacent α-cells (n = 12 adjacent pairs of oscillating α-cells). However, islet α-cell $[Ca^{2+}]_i$ does sometimes approximately follow the surrounding coordinated β-cell $[Ca^{2+}]_i$ waves at glucose concentrations between 8 and 12 mM (18 of 25 α-cells, one representative example on Figure V-4B). The time course and duration of such α-cell signals show more complex oscillatory patterns compared with those in the β-cells. The α-cells signals are not likely to come from neighboring β-cells because of the following: 1) they do not always occur; 2) they follow a different time course when they

A

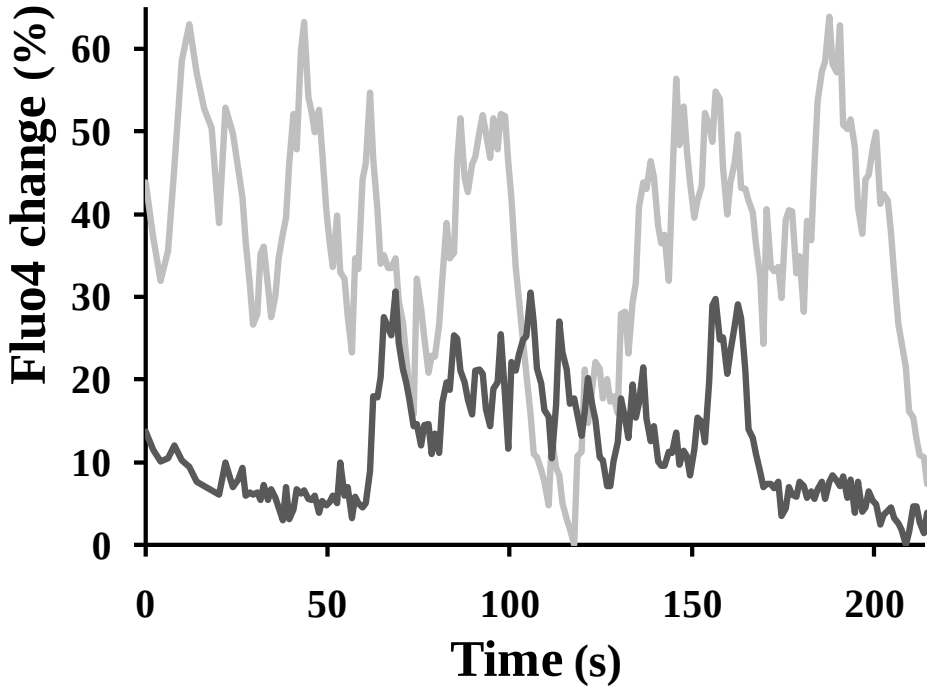
Flu04 change (%)
60
50
40
30
20
10
0
0
50
100
150
200
Time (s)

B

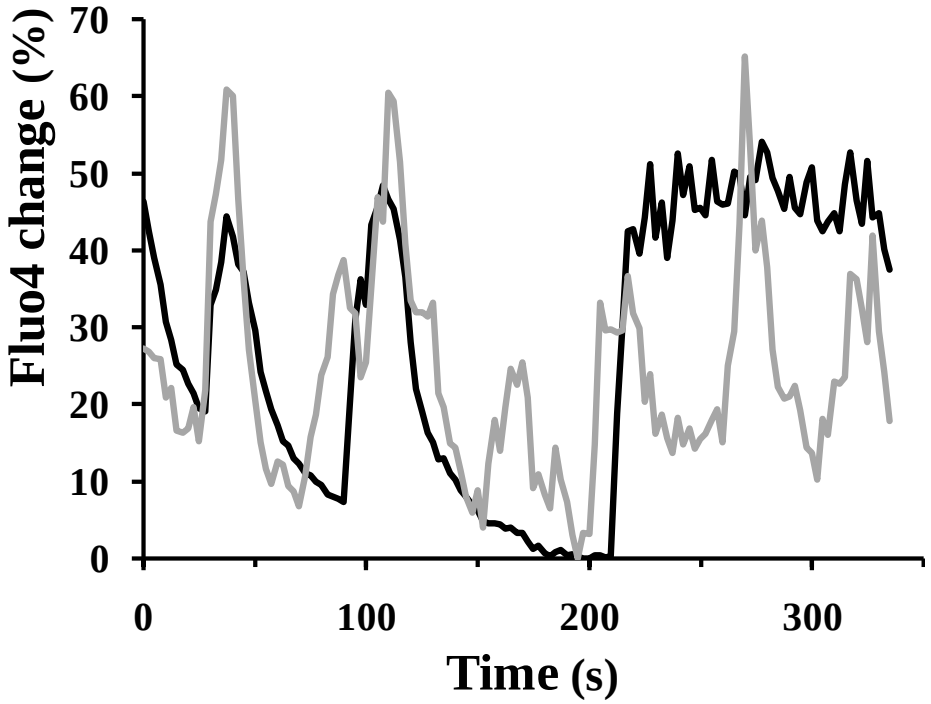
Flu04 change (%)
70
60
50
40
30
20
10
0
0
100
200
300
Time (s)

C

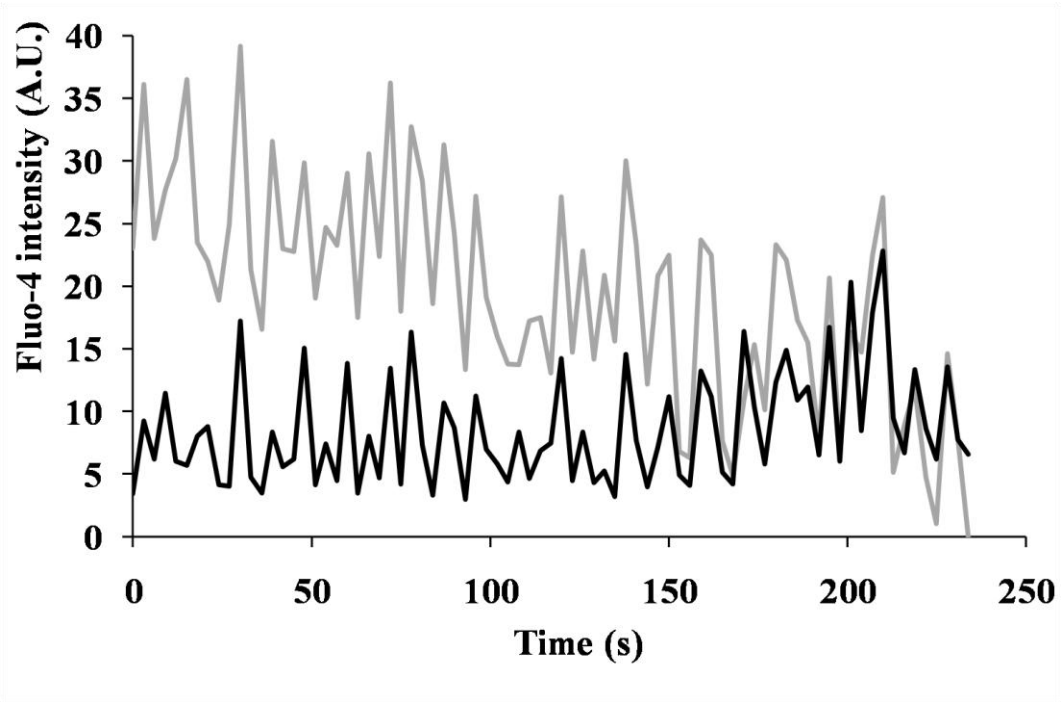

Figure V-4: α- and β- cells exhibit some coordination in their calcium oscillations. *A, B* are time series of the Fluo-4 signal relative to the minimal intensity recorded during the experiment. A, two adjacent α-cells within an islet exposed to 1 mM glucose show no synchronization between their $[Ca^{2+}]_i$ responses. B, representative time course of Fluo-4 signals from an islet exposed to 12 mM glucose. The *black line* indicates β-cells, and the *gray line* represents an α-cell. C, representative time course of Fluo-4 signals from an islet exposed to 100 μM tolbutamide. The *black and gray lines* indicate β- and α-cells, respectively. Fluo-4 signal was recorded every 2.5 s, and the confocal pinhole diameter was 1 airy unit.

do occur; and 3) there was no change in their properties as the confocal pinhole diameter was decreased down to 1 airy unit, where any out-of-focus fluorescence from beyond a couple of micrometers would be totally rejected (498). In addition, we also observed $[Ca^{2+}]_i$ synchronization between α- and β-cells at 1 mM glucose, when β-cell calcium waves were stimulated by pharmacological blockade of K_{ATP} channels, using 100 μM tolbutamide (Fig. V-4C).

4- Discussion

4-1 Effects of paracrine inhibitors on hormone secretion

Hormone secretion assays indicate that *ex vivo* islets are a relevant model for the study of the mechanisms of glucagon inhibition by glucose (Fig. III-2 and IV-1A). We investigated the effects of the candidate paracrine inhibitors, insulin, GABA, zinc ions, and somatostatin. All of these inhibited glucagon secretion from intact islets (Fig. V-1A). However, only zinc retains its ability to inhibit glucagon secretion from pure populations of mouse α-cells, but its inhibitory effect was reduced islet α-cells (Fig. V-1B). Our results support previous studies on isolated rat α-cells describing a stimulatory effect for both glucose and arginine and an inhibitory effect for zinc (311, 341). Overall, our hormone assays indicate that α-cells behave quite differently when they are retrieved from their intra-islet milieu and that it is not possible to extrapolate from isolated cells to the islet behavior. These differences in glucagon secretion could originate from loss of paracrine signals. However, the loss of response to insulin, GABA, and somatostatin from isolated cells is puzzling and might arise from proteolytic damage during cell

dispersion or from loss of cell-cell contacts (418, 486, 487, 489).

4-2 Effects of glucose on α-cell calcium activity

Influx of calcium ions is a trigger for exocytosis of endocrine vesicles, and the amount of insulin secreted from normal β-cells is closely related to $[Ca^{2+}]_i$ (Fig. IV-1A and V-2A) (137, 138, 499). Because glucagon release from islets is inhibited at elevated concentrations of glucose, one would naively expect the α-cell $[Ca^{2+}]_i$ to drop concomitantly. Several models of glucose-mediated suppression of glucagon secretion rely on this assumption; however, there is poor consensus regarding glucose-mediated calcium dynamics in the α-cell. Some studies report a decrease in cytoplasmic calcium levels or a slowing down of oscillation frequencies in response to glucose (359, 360, 415), and some report a weak or negligible effect (296, 339), although some others describe glucose-mediated increases in $[Ca^{2+}]_i$ (311, 364). Our calcium measurements on intact islets (FuraRed and Fluo-4 imaging) indicate that α-cells respond to glucose by elevating their averaged $[Ca^{2+}]_i$ (Fig. V-2A). The extent of the response is $\sim$ 50% less than in β-cells (from 1 to 12 mM glucose).

One noticeable difference between α- and β-cell calcium responses is their oscillatory pattern. α-cells exhibit apparently random, asynchronous calcium oscillations at low glucose levels, whereas β-cells display regular and synchronous calcium waves at higher glucose concentrations (> 7 mM) (170). We measured α-cell calcium oscillations and found the same proportion of oscillating α-cells at both low and high glucose levels (Table V-1). Although the shape and amplitude distribution of $[Ca^{2+}]_i$ signals do not depend on glucose, the oscillating cells do display greater frequencies at high glucose

level. Collectively, these results suggest that inhibition of glucagon secretion from intact islets is not mediated by a decrease in calcium levels or slowing down of oscillations.

Similar to β-cells, α-cell $[Ca^{2+}]_i$ is increased by glucose (Section 3-2) and tolbutamide, a K_{ATP} channel blocker (Fig. III-9), and its response to glucose is inhibited by D-mannoheptulose, a glucokinase inhibitor (Section 3-2). Together, these results suggest that the same mechanism may be responsible for both α- and β-cell calcium increases to glucose; glycolysis, increased ATP/ADP, K_{ATP} closure, membrane depolarization, and activation of voltage-gated calcium channels, as has been proposed previously (311).

4-3 Comparison of α-cell $[Ca^{2+}]_i$ responses to glucose between islet and sorted α-cells

Glucagon secretion from sorted α-cells is ~ 2-fold greater than α-cells in intact islets at 1 mM glucose (Chapter IV – Section 4-1). This observation suggests that glucagon release is tonically inhibited in the islet. This reduced basal secretion could possibly be explained by lower α-cell calcium activity. However, we did not observe any significant deviation between islet and sorted α-cells in the percent of oscillating cells at 1 mM glucose, as well as in the shape and amplitude distribution of calcium oscillations (Table V). This uncoupling between calcium activity and secretion is similar to what we report with glucose. It is therefore possible that glucose suppression of glucagon secretion and tonic α-cell inhibition in the islet involve the same mechanism.

In contrast to the $[Ca^{2+}]_i$ responses to glucose in intact islets, those in isolated α-cells are more diverse; ~ 50% respond similarly to α-cells in intact islets, and ~ 50% of these are either nonresponsive or slightly decrease their $[Ca^{2+}]_i$ (Fig. V-2B). To a lesser

extent, this pronounced heterogeneity was also seen in the metabolic responses (Chapter IV). Our experiments indicate that α-cells removed from the islet behave quite differently in terms of their NAD(P)H, calcium, and secretory responses. In other words, α-cells need the three-dimensional cytoarchitecture of the islet for normal physiology. Deviations in isolated α-cell response could be attributed to loss of cell-cell contacts, loss of paracrine communication, or proteolytic damage during islet dispersion. Most research on α-cell biology to date has been conducted on isolated cells. Besides the possible artifacts coming from the difficulty to distinguish these cells from other cell types, part of the controversy on α-cell metabolic and calcium responses could originate from the wide heterogeneity found in isolated cells. Our data show that α-cells within intact islets provide a much more physiologically relevant and robust approach to investigate these cells.

4-4 α-/β- cell calcium coordination

Intracellular calcium oscillations are not coordinated between adjacent α-cells in islets perifused at low glucose levels (Fig. V-4A). However, α-cells exhibit some synchronization with β-cells during the regular synchronous calcium waves seen between 7 and 12 mM (Fig. V-4B). The spreading of $[Ca^{2+}]_i$ waves into α-cells likely contributes to the greater $[Ca^{2+}]_i$ measured at high glucose (Fig. V-2A). The physiological significance in terms of glucagon secretion is unclear because α-/β-cell waves occur over 7 mM glucose when glucagon secretion is already inhibited. Intercellular communication through gap junctions made of connexin-36 is the consensus explanation behind the generation of periodic β-cell calcium waves and concomitant insulin pulses (170, 180,

181). Whether gap junctions are present in α-cell membrane is still a matter of debate (417, 501) but the observed α-/β-cell synchrony during calcium waves seems to hint that gap junctions might also connect these two cell types. Further studies are necessary to validate this hypothesis.

5- Conclusion

Few studies relate the effects of glucagon inhibitors on α-cell $[Ca^{2+}]_i$. One study on dispersed mouse α-cells reports a slight decrease, if any, in $[Ca^{2+}]_i$ following the addition of insulin, and no change in calcium signal was observed with zinc or GABA (296). Insulin was found to inhibit calcium signals in a clonal α-cell line, but the effect was lost at glucose levels above 1 mM (339). In addition, it was found that somatostatin does not reduce $[Ca^{2+}]_i$ in sorted rat α-cells (407) and that zinc slightly stimulates the frequency of calcium oscillations in dispersed mouse α-cells and in a clonal α-cell line (339). Our calcium measurements from intact mouse islets indicate that application of the candidate paracrine inhibitors of glucagon secretion, insulin, zinc, GABA, and somatostatin, does not significantly affect α-cell intracellular calcium dynamics. Consequently, the suppressive effect of glucose is likely to act downstream from α-cell Ca^{2+} signals, presumably at the vesicle trafficking or exocytotic machinery levels. For instance, glucagon inhibition could be mediated by a reduced likelihood of granule fusion with the plasma membrane, by depriming of docked vesicles, or by a depletion of the readily releasable pool of glucagon-containing vesicles. Very few studies provide information on the mechanisms of α-cell granule trafficking and exocytosis. Nonetheless,

inhibition of glucagon secretion by somatostatin has been shown to involve a $G\alpha_{i2}$ protein-dependent pathway where activation of the serine/threonine protein phosphatase calcineurin leads to depriming of docked secretory granules belonging to the readily releasable pool (407). In that case, no decrease in $[Ca^{2+}]_i$ was observed. Similarly, imidazoline-containing compounds are inhibitors of glucagon secretion, and glucagon suppression does not involve modulation of plasma membrane ion channel activity and inhibition of electrical activity but rather involves activation of the serine/threonine protein phosphatase calcineurin and inhibition of Ca^{2+}-dependent exocytosis of the glucagon-containing granules (500). Furthermore, it has been reported that the size of the readily releasable pool is tightly regulated and depends on cAMP levels. For instance, epinephrine, via cAMP elevation, mediates its stimulatory effect on glucagon secretion by enhancing up to 5-fold the rate of granule mobilization from a reserve pool (286), without modifying α-cell $[Ca^{2+}]_i$ (Chapter II – Section 3-6). Unraveling the precise secretory mechanisms responsible for glucose-stimulated glucagon inhibition in intact islets will require further investigations.

CHAPTER VI

IMAGING GAP JUNCTIONAL COUPLING WITHIN INTACT ISLETS

1- Introduction

1-1 Background information

Islet β-cell $[Ca^{2+}]_i$ exhibits regular and synchronized oscillations across the rodent islet between 7 to 12 mM glucose. At these concentrations, $[Ca^{2+}]_i$ waves spread throughout the islet and cause pulsatile insulin release (141, 177, 178). Interestingly, this coordinated pattern is impaired in diabetic rodent models as well as in diabetic humans (196, 502). Intercellular communication through gap junctions is the likely explanation for this coordinated behavior. Gap junctions are membrane channels usually organized by clusters near tight junctions that allow the direct diffusion of small molecules (<1 kDa) between two juxtaposing cells. Gap junctions are not specific so that a wide variety of ions, metabolites, and second messengers can pass through them (503). A gap junction is the result of the assembly of two connexons from two different cells. Each connexon contains six connexins; each connexin has four membrane-spanning α helices and intracellular N and C termini (182). Mice express at least 20 different connexin isoforms but the present consensus is that mouse β-cells are only coupled by homotypic gap junctions composed of the connexin-36kDa (Cx36). Intercellular communication through these gap junctions probably serves to synchronize electrical activity and secretion among β-cells, as demonstrated by loss of coordination in islets treated with gap junction

blockers, or in transgenic mouse islets lacking Cx36 (180, 181).

1-2 Hypothesis: *glucose modulates gap junctional coupling between β-cells*

Our group designed a microfluidic device allowing the creation of a well-defined linear gradient of extracellular glucose concentrations across an islet (172). This study demonstrates that β-cells are not sufficiently coupled to allow transmission of calcium waves into non-stimulated regions of the islet (i.e. when [Glucose] < 7 mM). This observation challenges current computational models of islet function. Indeed, these models predict that calcium waves should spread from regions above the threshold for wave generation to regions below the threshold. In order to adapt to this new observation, our collaborators, Dr. A. Sherman's group from the National Institute of Health, Bethesda MD, suggested that glucose might modulate gap junction electrical conductance between β-cells. In other words, calcium waves do not spread into regions below the threshold because β-cell coupling is reduced in these non-excited regions. Mathematical models of the islet are perfectible but successfully predicted that calcium waves should be disrupted in islets with ~ 50% reduction in gap junction conductance, such as islets from heterozygous $Cx36^{+/-}$ mice (170). The same models predict that a ~ 300% step-decrease in coupling conductance from stimulated to non-stimulated regions would be needed to explain why calcium waves do not spread into non-stimulated regions (personal communication from Dr. R. Benninger, Vanderbilt University).

To test our hypothesis, we use an innovative approach relying on the diffusion of a small fluorescent dye through gap junctions. The technique, called LAMP (Local Activation of a Molecular Fluorescent Probe), is presented in Section 3-1 and the

experimental conditions detailed in Section 2-4.

1-3 Evidence of gap junction modulation by glucose

Glucose-dependent modulation of gap junction conductance has been reported in the literature. One study found that microinjection of glycolytic substrates into one β-cell produced transient changes in NAD(P)H fluorescence in neighboring cells. This effect was only effective at high glucose concentrations (504). Also, the number of coupled cells after microinjection of non-membrane-permeable dyes is increased at high glucose concentrations (505). In addition, electrophysiological studies, via two-electrode recordings of pairs of pancreatic islet cells, suggest that β-cell coupling increases with the concentration of glucose (506). This modulation of gap junction conductance could be the consequence of structural rearrangements, as shown by freeze-fracture studies of islets reporting that gap junction clusters occur in two configurations: linear single strands and polygonal aggregates. Interestingly, a 10-minute exposure at 20 mM glucose increases the relative amount of polygonally packed connexons threefold above the basal values measured at 2.8 mM. The researchers did not notice any change in the total number of connexons in the membrane (507).

2- Materials and methods

2-1 Materials, as described in Chapter II- Section 2-1.

2-2 Islet isolation and culture, Chapter II- Section 2-1. For imaging purposes, isolated

islets were attached on gelatin (0.1%)-coated 35-mm glass-bottomed dishes (MatTek Corp., Ashland, MA).

2-3 HeLa and βTC3 cell culture condition

HeLa cells were grown in a sodium bicarbonate-buffered Dulbecco's modified Eagle medium (DMEM) supplemented with 10% FBS. βTC3 cells were maintained in DMEM containing 15% horse serum and 2.5% FBS, and 5 mM glucose. Cells were supplemented with 100 IU/ml penicillin, and 100 μg/ml streptomycin in a 95% O_2 – 5% CO_2 moist atmosphere at 37ºC. All media and culture reagents were obtained from Life Technologies, Inc.

2-4 LAMP assay

NPE-HCCC2/AM was gently provided by Dr. W-H Li from the University of Texas Southwestern Medical Center. NPE-HCCC2/AM was aliquoted in DMSO (dimethyl sulfoxide) to a final concentration of 2 mM, and stored at -20ºC. Before imaging, islets were loaded with NPE-HCCC2/AM (5 μM in imaging solution at 2 mM glucose) during 1 hour on a "belly-dancer" platform shaker at room temperature. Islets were than incubated in a NPE-HCCC2/AM-free imaging solution and transferred to the microscope stage incubator at 37ºC. Islets rested on the stage for 20 minutes to adapt to their new environment and to allow full cleavage of AM groups by intracellular esterases.

Photoactivation of the dye in a region of interest was performed at 730nm by two-photon excitation using a Coherent Chameleon laser (Coherent Inc., Santa Clara, CA). The fluorescent dye was excited at 790nm by two-photon laser excitation, and its

fluorescence collected through a 429-525nm band-pass filter (Chroma Inc., Rockingham, VT). We used a Fluar 40x/1.3NA oil immersion objective mounted on a LSM510 laser scanning microscope (Zeiss, Germany). For photoactivation, two-photon excitation was preferred over UV light to avoid damaging the cells (508). Also, diffusion of dyes is a slow process compared to diffusion of small molecules such as ions and small metabolites. Therefore, we imaged the islets for 15-20 minutes taking an image every 20-30 seconds to further reduce cell photodamage and dye photobleaching.

2-5 Measurement of junctional conductance by patch-clamp recordings

2-5-1 Methodology

The electrophysiological experiments described in Figures VI-5B and VI-6-B have been performed with the assistance of Dr. M. Zhang and Dr. L.S. Satin from the Virginia Commonwealth University (Richmond, VA). The perforated patch whole-cell recording of single β-cells in intact islet provides a reliable method to measure the strength of gap junction electrical coupling between the patched cell and its adjacent β-cells (501, 509-511). Briefly, the method takes advantage of the coordinated electrical coupling observed at high glucose levels (> 7 mM) when electrical and calcium waves spread across the islet. In current-clamp mode, it is possible to measure the change in membrane potential due to gap junction coupling to other oscillating β-cells (ΔV). Switching to voltage-clamp mode (at -65 mV, the resting potential) allows the recording of incoming ionic currents from adjacent coupled cells (ΔI). The total coupling conductance (G, in siemens) between the patched cell and its neighbors can be calculated by applying Ohm's law: $G = \Delta I / \Delta V$ (the method is presented in Figure VI-1).

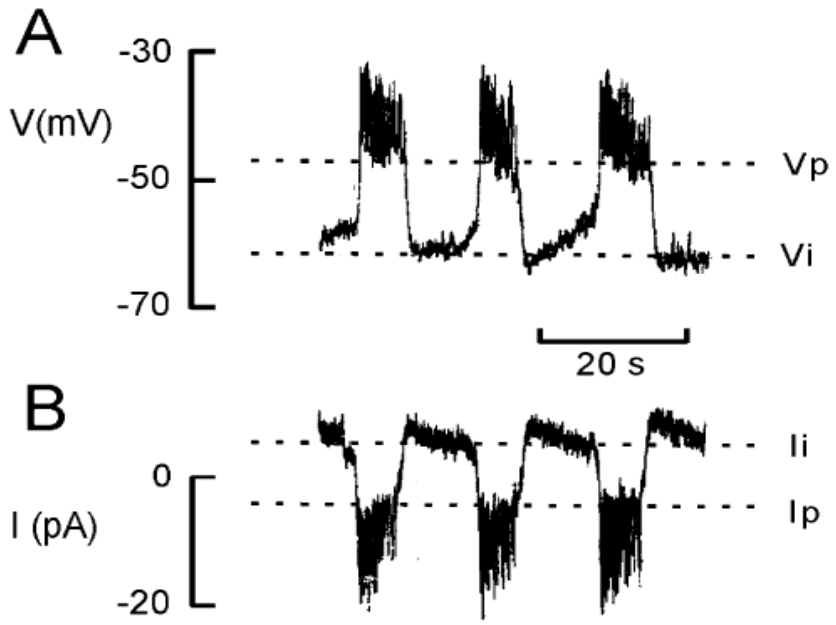

Figure VI-1: Measurements of electrical coupling conductance between β-cells. A, current-clamp recording of membrane potential from a patched β-cell in an islet perifused at 11 mM glucose. The maximally negative interburst potential (Vi) and the plateau potential (Vp) are indicated by dotted lines. B, voltage-clamp recording of inward currents from the same cell. The current levels corresponding to the repolarization of the burst of action potentials (Ii) and the plateau (Ip) are indicated by the dotted lines. The coupling conductance can be calculated according to Ohm's law (conductance=I/V, with I=Ii-Ip and V=Vi-Vp). Modified from (299).

2-5-2 Experimental conditions

Isolated islets were continually superfused with an extracellular solution containing 115 mM NaCl, 5 mM KCl, 3 mM $CaCl_2$, 2 mM $MgCl_2$, 10 mM HEPES, 2 mM glucose, pH = 7.2 (511). Pipettes were pulled from borosilicate glass using a two-stage horizontal puller (Sutter Instruments' P-97, Novato, CA) and were filled with an

intracellular solution of 11.8 mM NaCl, 28.4 mM K_2SO_4, 63.7 mM KCl, 1 mM $MgCl_2$, 20.8 mM HEPES, 0.5 mM EGTA, pH = 7.2, along with 0.1 mg/ml amphotericin B. The latter is an antibiotic that forms small perforations in the membrane patch, providing electrical access to the cell interior. Pipette resistances ranged from 5 to 8 MΩ using our internal solutions. After patching a peripheral β-cell with a stable seal resistance ranging from 2 to 10 GΩ, glucose levels were stepped from 2 to 11 mM. An Axopatch 200B patch-clamp amplifier (Axon Instruments, Union City, CA) was used in the standard tight-seal perforated patch-clamp mode to record membrane potentials or ion currents in current-clamp or voltage-clamp mode, respectively (512).

3- Results

3-1 Local Activation of a Molecular Fluorescent Probe (LAMP)

To determine whether glucose modulates gap junctional coupling, we used a new method (LAMP) that relies on the diffusion of a photoactivatable fluorescent dye. This technique was developed in 2004-2005 by Dr. W-H Li and co-workers, and applied successfully on human fibroblasts, HeLa cells transfected with Cx26 and mouse pancreatic acinar cells (508, 513, 514). Li's group provided us with NPE-HCCC2/AM, the photoactivatable probe used for LAMP assay. Similar to the calcium indicator Fluo4-AM, the probe contains acetoxymethyl (AM) ester groups that render the molecule hydrophobic and free to diffuse into the cells. Once inside the cell, cytosolic esterases cleave the AM groups revealing two negative charges that trap the now hydrophilic probe in the cell. Once the cells are loaded with the tracer, a region of interest can be

photoactivated by UV exposure (or two-photon excitation at 730nm, as described in Section 2-4) and become fluorescent (508). Because of its low molecular weight (i.e. 450 Da), the fluorescent dye permeates through gap junctions and the kinetics of dye diffusion into non-photoactivated cells provides valuable information on the strength of cell coupling (Fig. VI-2).

The LAMP assay is a non-invasive technique that provides high spatiotemporal resolution ideal for the study of dynamic fluxes through gap junctions. Its main advantage is the possibility to introduce a diffusible dye within the cells without the need of microinjection. Indeed, microinjection of non membrane permeable dyes, such as Lucifer yellow or neurobiotin, has two limitations that may affect the interpretation of the data: leakage of the dye via disruption of the cell membrane; and modification of the biophysical properties of gap junction channels potentially sensitive to the extra-volume injected. However, LAMP has never been performed on multilayered cell clusters such as pancreatic islets and LAMP has not been tested with cells connected by gap junctions made of Cx36. The first goal of the study was to validate the method in intact mouse islets.

3-2 Determination of dye transfer rates

Figure VI-3 illustrates the LAMP technique applied to intact islets. The islets were successfully loaded with the probe and photoactivation successfully converted the probe into a fluorescent dye. Similar to other AM-based indicators such as Fluo4-AM, the tracer is trapped mostly in the first cell-layer surrounding the islet where hydrophobic AM groups are cleaved. Once the LAMP probe is photoactivated, its fluorescence can be

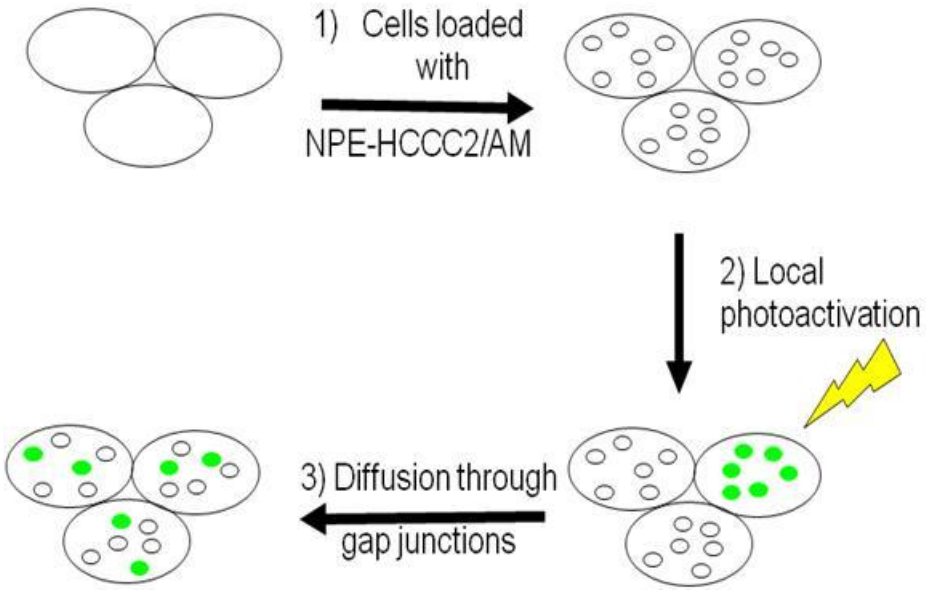

Figure VI-2: Schematic of the LAMP assay for studying gap junction coupling. LAMP is a three-step method. 1) NPE-HCCC2/AM is trapped into the cells following the cleavage of acetoxymethyl (AM) ester groups by cytosolic esterases. 2) UV light excitation (365nm or 730nm by two-photon excitation) of a region or a cell of interest photolyzes the NPE (1-(2-nitrophenyl)ethyl) groups of NPE-HCCC2 (black open circles). The resulting product, HCCC2 (green circles), is a coumarin-based fluorescent dye that is maximally excited at 425nm (790nm by two-photon excitation) and emits at 460nm (emission filter used: 429-525nm).

monitored over time. Typically, the fluorescence intensity slowly fades in the photoactivated region and reaches a minimum after 10 to 15 minutes. This slow kinetics was expected because gap junctions only guide the diffusion of molecules smaller than 1,000 Da. Thus, LAMP dye diffusion is limited by its size (450 Da), and a maximum of two molecules can theoretically pass together through one channel at any given time. The decrease in intensity in the photoactivated region can be fit to a single exponential decay function (Fig. VI-3B and 3C). The Neperian logarithm of the function produces a straight line whose slope (in absolute value) represents the decay rate, or transfer rate of the LAMP dye (514). The decay rate (k) and half-time ($t_{1/2}$) are related by the equation: $t_{1/2} = (\ln 2) / |k|$. For instance, the half-time obtained from Figure VI-3 is ~ 120s, meaning that 50% of the fluorescence vanished after 120s. The decay rate and half-time provide valuable information on the strength of gap junction coupling. Thus, an increase in gap junction permeability to the LAMP dye would account for an increase in transfer rates and reduction of half-time values.

Half-times of LAMP diffusion calculated in intact islets were ~ 2-fold greater than the ones from human fibroblasts that are connected by Cx43 (514). The slower diffusion rates reported in islets were expected, since electrophysiological measurements of electrical coupling have estimated that Cx36 channels have the smallest unitary conductance of all of the gap junction isoforms (between 5 and 15 pS). In comparison, unitary conductance from Cx43 channels is 10-times greater than from Cx36 (515). In addition, each pair of β-cells is connected by ~ 60 gap junctions, and each β-cell is coupled to 5-7 other β-cells (183, 185, 516, 517) .

As illustrated in Figure VI-3, we interpreted a decrease in fluorescence intensity

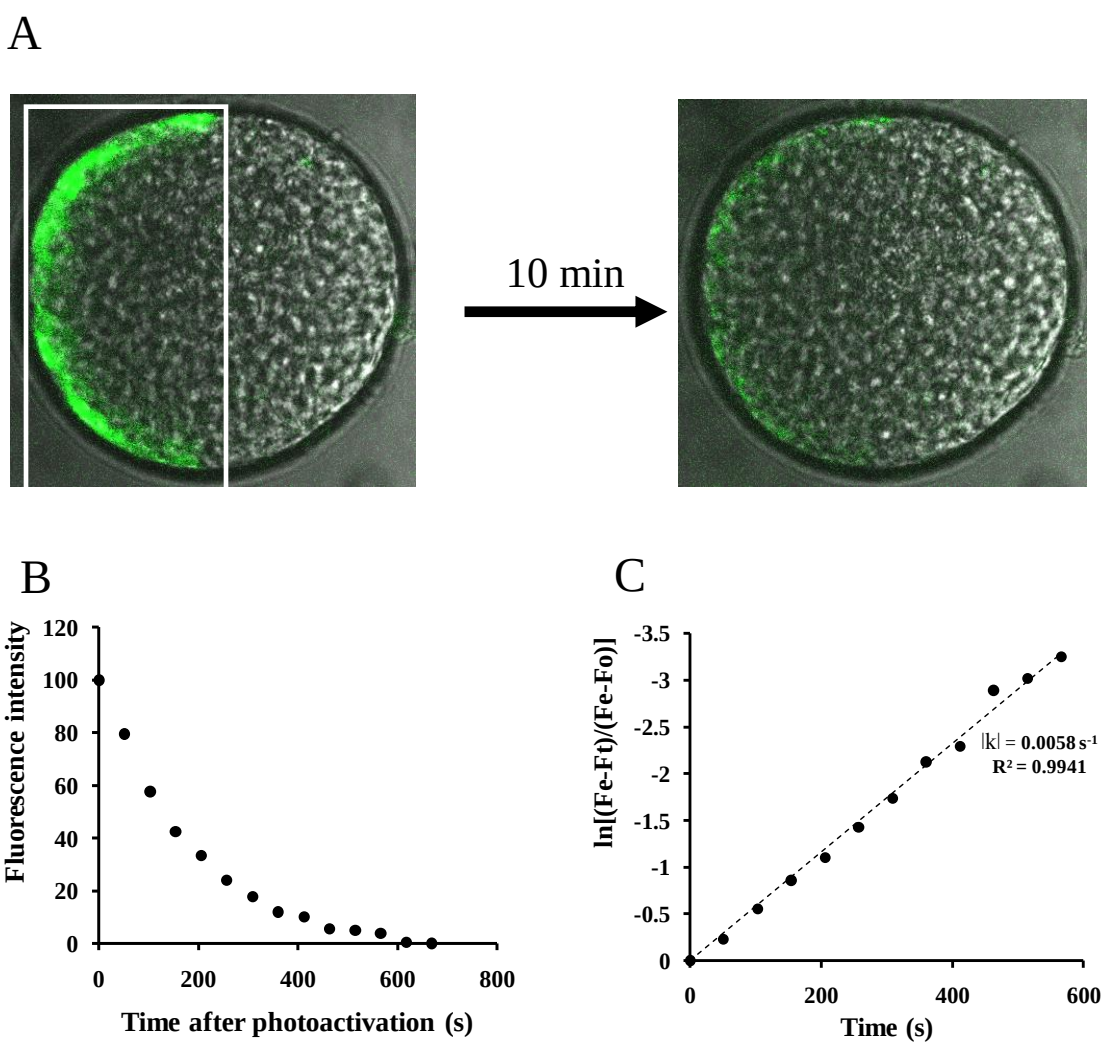

Figure VI-3 LAMP diffusion in intact islets and transfer rate calculations. A, overlay of differential interference contrast and HCCC2 fluorescence (in green) images of an islet. A region of interest (open white rectangle on the left panel) has been photoactivated by two-photon excitation at 730nm. As a result, HCCC2 becomes fluorescent when excited at 790nm by two-photon excitation. The dye slowly diffuses through gap junctions into non-fluorescent cells, resulting in a decrease in fluorescence intensity in the plane of observation (right panel). B, the plot of intensity (normalized here) over time yields a single-exponential decay that provides information on the strength of β-cell coupling. C, the rate of intercellular dye transfer (noted *k* on the graph) can be assessed by applying the Fick's equation of diffusion kinetics, F_e, F_o and F_t are the fluorescence intensities at equilibrium, zero time and time t (514). R is the correlation coefficient of the linear regression, and the slope (|k|) provides the rate of HCC2 transfer.

from photoactivated regions as an indication on how well cells were connected. A better approach would be to measure an increase in intensity from non-photoactivated regions. However, our experimental conditions did not allow the direct measurement of LAMP diffusion into non-activated regions. Indeed, two-photon imaging is intrinsically an optical sectioning technique that provides a precise spatial resolution in a 3D structure such as the islet. Thus, photo-activation and measurement of fluorescence signal only occur in a ~ 2μm-thick section of an islet (518). Therefore, most of the LAMP probe is expected to diffuse into adjacent cells located in out-of-focus planes.

To verify that LAMP dye is transferred into non-photoactivated adjacent regions, we performed the LAMP assay on single cells in an islet. I used the same experimental settings as previously described; the only modification was the use of a 63X-objective (instead of a 40X-magnification lens). As expected, a reduction in fluorescence intensity was observed in the photoactivated cell and, in some instances, we noticed an increase in fluorescence signal from adjacent cells (Fig. VI-4). However, the fluorescence intensity measured in adjacent cells was weak compared to the photoactivated cell. As a result, the laser power needed to be substantially augmented to detect a signal. Still, the signal to noise ratio was usually too small for quantification of LAMP transfer rates.

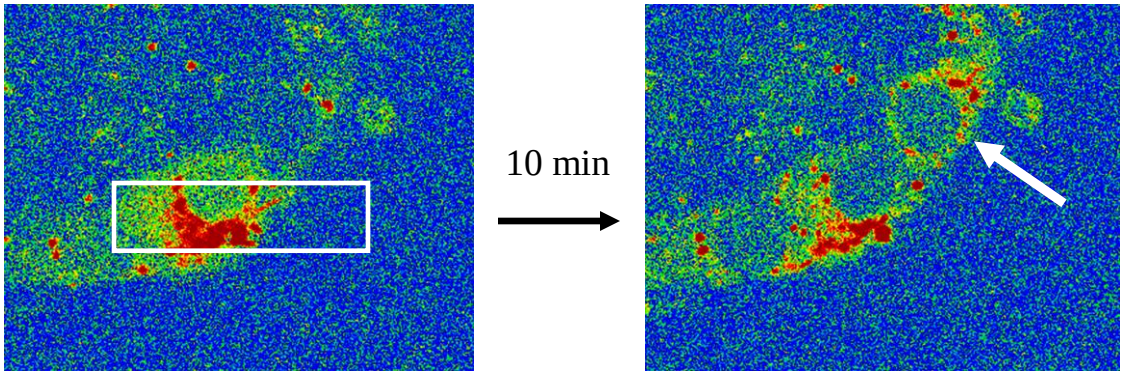

Figure VI-4: single-cell LAMP imaging in an islet. Left panel shows the region where the LAMP probe (pseudocolor) has been photoactivated (open white rectangle). The fluorescent tracer diffuses into an adjacent cell (white arrow in the right panel) and reaches equilibrium after 10 minutes.

3-3 Gap junction blocker inhibition of dye diffusion

As a control experiment to ensure that the LAMP assay is sensitive to gap junction blockade, we used two non-selective blockers of gap junctions that are not chemically related: 18α-glycyrrhetinic acid (αGA) and mefloquine (Fig. VI-5) (519, 520). As expected, LAMP diffusion was reduced in a dose-dependent manner by both blockers. High concentrations of blockers totally abolished LAMP diffusion. This observation suggests that the blockers reduced gap junction opening enough to hinder the passage of the LAMP probe.

Mefloquine was found to be more potent at reducing the gap junction permeability for the LAMP probe. The half maximal inhibitory concentration (IC_{50}) for mefloquine was 10.5 ±0.3 μM, compared to 42.1 ±0.9 μM for αGA. These values agree with previous studies reporting an IC_{50} of 15μM for mefloquine in interneurons electrically coupled via Cx36 (521), and gap junction inhibition by αGA at concentrations ranging from 50 to 100

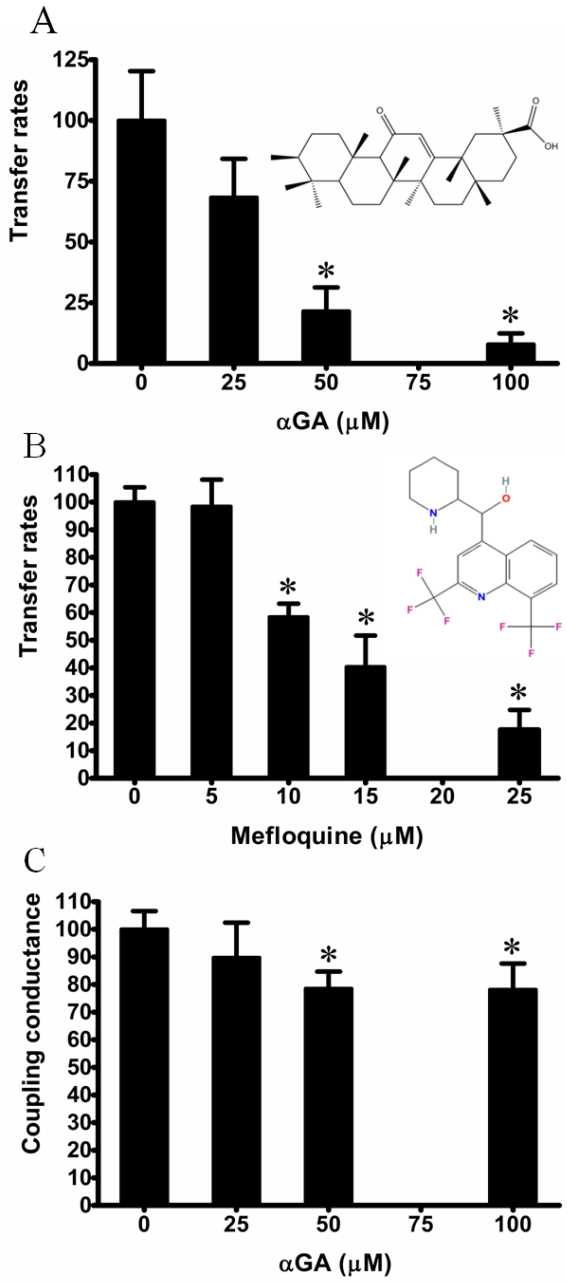

Figure VI-5: Gap junction blocker effects on LAMP permeability and gap junction coupling conductance. A & B, isolated islets were perfused at 12 mM glucose supplemented with adequate concentrations of blockers 15 min prior photoactivation. Inset chemical structures for αGA and mefloquine show that the blockers are not chemically related. C, electrophysiological measurements of β-cell coupling conductance from intact islets. Transfer rate and coupling conductance values have been normalized to the maximum obtained at 12 mM glucose without gap junction blockers. 5 to 24 assays were performed at any given blocker concentration. Error bars represent the standard error of the mean. *: $p<0.01$ compared to baseline value, ANOVA.

μM (180).

Interestingly, high levels of αGA strongly block gap junction permeability, while αGA only induces a 20% reduction in coupling conductance, as measured by patch-clamp recordings (method presented in Section 2-5). We interpreted this observation as a consequence of the size-limited diffusion of the LAMP probe. The partial obstruction of gap junctions by αGA would affect LAMP permeability more than ionic current diffusion. In conclusion, the dose-dependent reduction in dye diffusion following application of gap junction blockers appeared to confirm that the LAMP assay could be used to study gap junction coupling in intact islets.

3-4 Glucose-modulation of dye transfer rates

One physiological question we wanted to address was to determine whether glucose modulates gap junction coupling between β-cells (Section 1-2). We performed the LAMP assay in islets perifused at different glucose concentrations and noticed a ~40% increase in LAMP transfer rates at high glucose compared to low glucose levels (Fig. VI-6). Patch-clamp recordings confirmed that glucose dose-dependently increases β-cell electrical coupling conductance. Surprisingly, glucose similarly augments LAMP permeability and coupling conductance by 40 to 45% from 2 to 20 mM glucose. This result potentially provides some mechanistic insights on how glucose affects β-cell coupling. As previously discussed, LAMP permeability is limited by its size whereas coupling conductance is not, thus modulation of gap junction diameter differentially affects permeability and conductance. In contrast, modulation of the number of active gap junctions would similarly affect permeability and conductance. Since glucose leads to

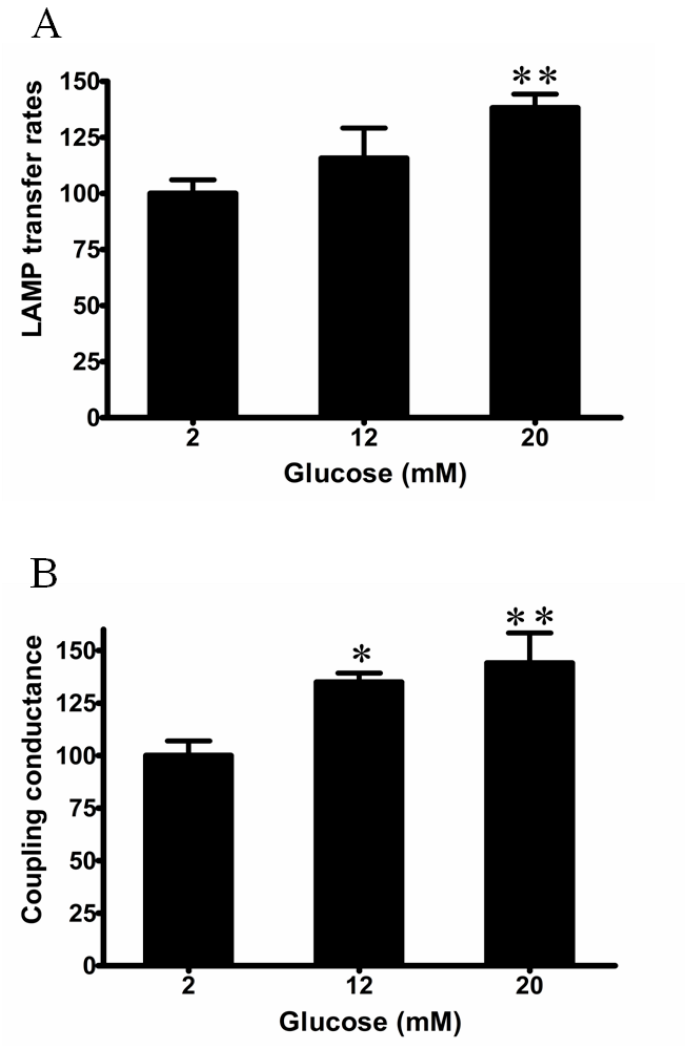

Figure VI-6: Glucose augments gap junction permeability for LAMP (A) and β-cell electrical coupling conductance in isolated islets (B). In order to measure detectable amounts of electrical coupling at low glucose, we perfused the islets with 100 μM tolbutamide, a K_{ATP} channel blocker. Tolbutamide artificially triggers electrical waves across the islet at low glucose. Tolbutamide was also present at increasing glucose concentrations. Transfer rate and coupling conductance values have been normalized to baseline at 2 mM glucose. 24 to 59 LAMP assays and 6 to 12 electrophysiological recordings were performed at any given glucose concentration. Error bars represent the standard error of the mean. *: $p<0.05$ and **: $p<0.01$compared to baseline value, ANOVA.

~40% rise in both LAMP permeability and coupling conductance, glucose likely mediates this effect by increasing the number of active gap junctions by ~ 40%.

3-5 LAMP assay in islets lacking Cx36

Transgenic mice with a knockout of both Cx36 alleles have provided strong evidence that Cx36 is integral for islet coordination and pulsatile insulin release (181). Islets from these animals do not exhibit calcium waves when stimulated by glucose. In addition, several observations suggest that Cx36 is the only gap junction isoform expressed in β-cells. First, freeze-fracture studies failed to observe any gap junction plaques in islets lacking Cx36 (181). Second, Lucifer yellow is constrained into the microinjected cell (181). Third, electrophysiological measurements of electrical communication through gap junctions failed to detect any coupling conductance (170).

We utilized islets from $Cx36^{-/-}$ mice as a negative control for the LAMP assay. The fluorescent tracer should be circumscribed into the photoactivated cells because it could not diffuse through gap junctions anymore. Figure VI-7A presents the results of the study. Surprisingly, the LAMP tracer appeared to diffuse out of the photoactivated region, and the dye transfer rates were even greater in $Cx36^{-/-}$ islets compared to wild-type islets. We performed single-cell photo-activation, and in a few instances the dye diffused into adjacent cells (Fig. VI-7B). These findings suggested that the LAMP probe was diffusing through gap junctions in $Cx36^{-/-}$ islets, indicating that another type of gap junction might be upregulated in the mutant islets. We next utilized the gap junction blocker mefloquine to confirm that dye diffusion was indeed mediated by gap junctions. As expected, mefloquine

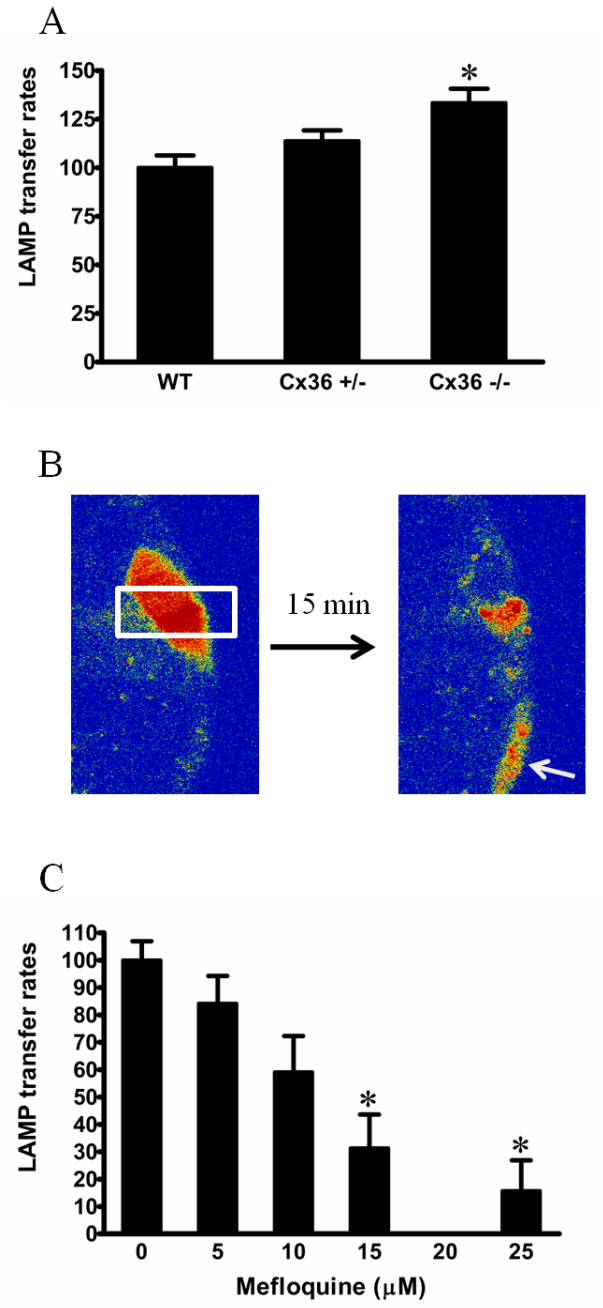

Figure VI-7: LAMP probe still diffuses in islets lacking Cx36 channels. A, LAMP transfer rates from Cx36 $^{-/-}$ islets are ~ 40% greater than wild-type islets (23 to 26 assays were achieved per condition). B, left panel, the open white rectangle represents the photoactivated region. One cell has become fluorescent (pseudocolor). The white arrow in the right panel shows an adjacent cell that has taken up the fluorescent probe. C, mefloquine dose-dependently reduces LAMP permeability in Cx36 $^{-/-}$ islets (10 to 15 assays per condition). Lamp assays were performed at 11 mM glucose. Error bars represent the standard error of the mean. *: $p<0.01$ compared to baseline value, ANOVA.

disrupted its diffusion in a dose-dependent manner (Fig. VI-7C). In summary, if the LAMP assay is a valid method to assess gap junction permeability, the results would imply that other type(s) of gap junction are upregulated in $Cx36^{-/-}$ islets and would suggest that Cx36 is not the only connexin expressed in β-cells.

3-6 LAMP leakage in βTC3 and HeLa cells

Mefloquine is thought to be relatively more effective at blocking Cx36 channels than most other types of gap junctions (520). We measured an IC_{50} of 18.4 μM in $Cx36^{-/-}$ islets, a value close to the one found in wild-type islets (10.5 μM). This result could suggest that LAMP diffusion from wild-type and mutant islets involves the same gap junction isoform. For instance, it is possible that the LAMP probe does not diffuse through Cx36 channels, but permeates through another isoform. This hypothesis could explain why dye transfer rates and mefloquine potency are similar in both wild-type and $Cx36^{-/-}$ islets.

To test if the LAMP probe can pass through Cx36 channels, we decided to perform the LAMP assay on culture cells, such as HeLa cells, a human cancer cell line that does not express any gap junctions (513). HeLa cells should provide another negative control for LAMP, and its transfection with Cx36 cDNA should determine if the LAMP dye diffuses through this isoform. We also cultured monolayers of βTC3 cells, a β-cell line that presumably expresses only Cx36 channels (522, 523). When applying the LAMP assay on βTC3 cells and non-transfected HeLa cells, we noticed that the fluorescence intensity in photoactivated cells was vanishing but we could not detect any diffusion of fluorescence in neighboring cells. Photoactivation of single isolated cells not coupled to

any adjacent cells confirmed that fluorescence intensity was literally fading. Interestingly, application of gap junction blockers was still able to block LAMP diffusion (data not shown). These surprising results seriously compromise our previous finding that glucose modulates gap junction permeability in islets. It could explain why the dye was still diffusing in Cx36$^{-/-}$ islets.

There are several ways to explain a reduction in LAMP intensity in cells that do not have gap junctions. For instance, the LAMP probe could be photo-unstable. Some fluorophores are very sensitive to laser excitation in such a way that they lose their ability to fluoresce (photobleaching). This seems unlikely because the fluorescence intensity was stable in presence of high concentrations of gap junction blockers (Fig. VI-5A). A more likely explanation to the disappearance of LAMP probe in photoactivated regions is that the dye leaks out of the cells through the plasma membrane. The dye could either diffuse directly through the lipid bilayer or be extruded out of the cell by large channels or transporters.

3-7 Effects of probenecid and sulfinpyrazone on LAMP leakage

Several candidates could be responsible for the extrusion of relatively "big" molecules such as the LAMP probe (450 Da). For instance, P2Z/P2X$_7$ purinergic receptors, voltage-dependent anion channels (VDAC), and multidrug resistance transporters (MRT) are all potentially able to extrude such a large molecule (524, 525). Drugs such as probenecid and sulfinpyrazone are non-specific inhibitors of VDAC (526) and MRT (525). To test if these channels are involved in the extrusion of the dye, we performed the LAMP assay in HeLa cells and found that application of both drugs

stopped its diffusion (data not shown). This result suggests that MRT and/or VDAC are responsible for LAMP leakage and renders possible to improve the LAMP assay by blocking the efflux of dye extrusion to the extracellular milieu. Thus, LAMP assay was applied on wild type islets perifused with the drugs, but no diffusion was observed (Fig. VI-8). Since probenecid does not inhibit connexin channels (527), we concluded that the LAMP assay was not suitable for studying gap junction communication in intact islets.

4- Conclusion and future directions

This report presents an innovative strategy to study gap junction communication by monitoring the intercellular diffusion of small fluorescent dyes. We believed the technique well-suited for investigating gap junction communication in the pancreatic islet. However, we found that the fluorescent tracer was extruded from the cells, likely via VDAC or MRT channels. Blockade of these channels by probenecid, a drug that does not inhibit connexin channels (527), circumvents the dye inside the photoactivated cells, revealing the absence of diffusion through Cx36 gap junctions. These channels have been shown to preferentially exchange cationic molecules (186). In addition, Cx36 channels are not permeable to Lucifer yellow, a small microinjected tracer that has the same molecular weight that the LAMP probe and carries two negative charges, as LAMP does (185, 528). For these reasons, the LAMP assay is not suited for studying the dynamics of islet gap junction communication. Since our report, collaborators from the University of Texas have tried to develop a cationic LAMP probe that could hopefully cross Cx36 channels.

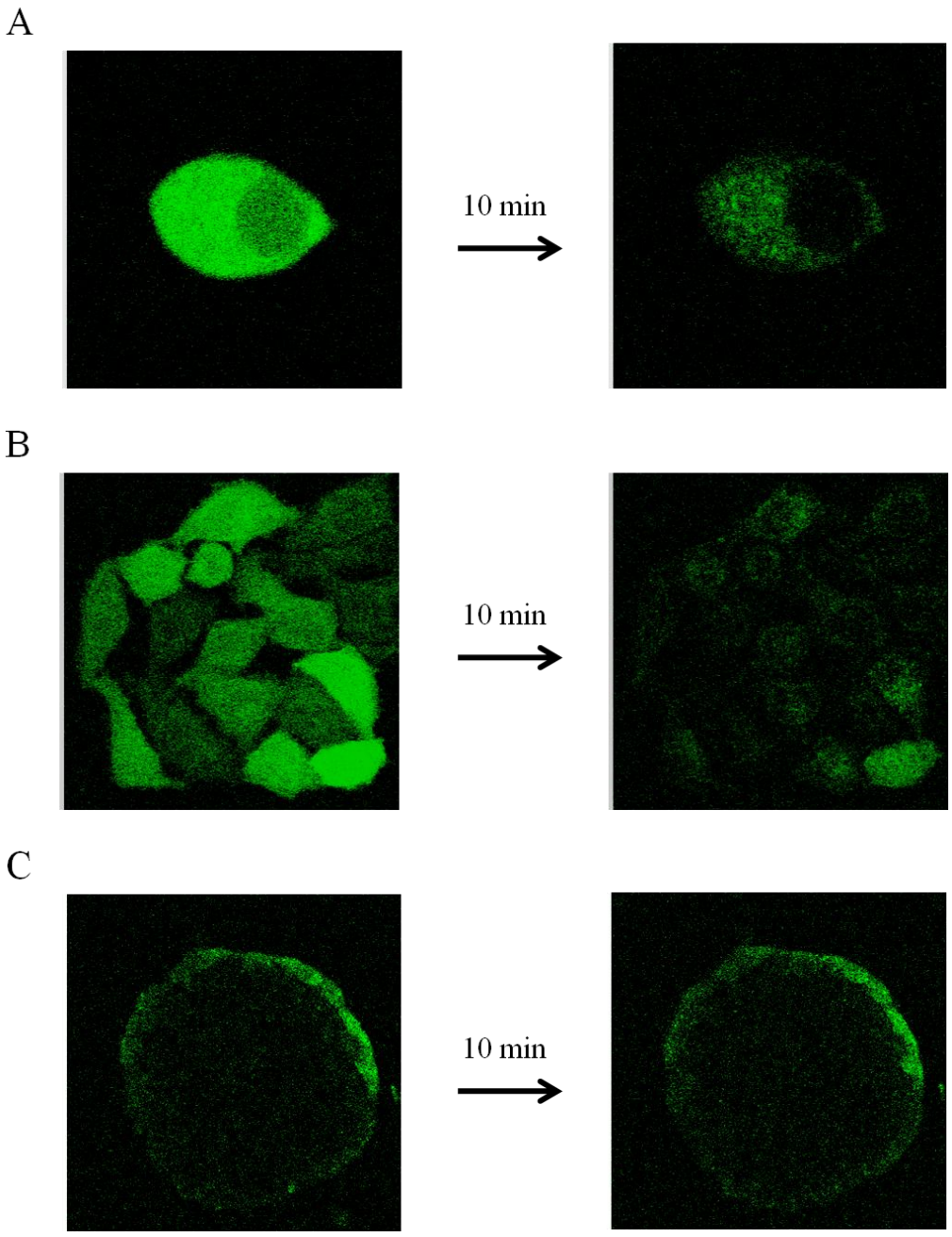

Figure VI-8: LAMP leakage out of the cells is stopped by non-specific inhibitors of VDAC and MRT. A, photoactivation of the LAMP probe into an isolated βTC3 leads to reduction in fluorescence intensity that likely represents dye leakage out of the cell. B, the same result is apparent from photoactivated clusters of HeLa cells that do not express gap junctions. C, an example of LAMP assay performed on an islet incubated with probenecid is presented. Application of probenecid (500 μM) or sulfinpyrazone (1 mM) stops dye extrusion to the extracellular milieu by blocking channels (such as VDAC or MRT) involved in the transport of large molecules. The absence of LAMP diffusion into other cells suggests that the LAMP probe does not permeate through Cx36 channels.

The decrease in LAMP intensity in loaded islets was misleading since it was not indicating intercellular dye diffusion through gap junctions but extrusion of the dye to the extracellular milieu. Controls are critical for proper interpretation of the data. The inhibition of dye diffusion by gap junction blockers constituted a strong negative control. Retrospectively, it appears that the blockers were acting on membrane channels responsible for LAMP extrusion. However, we did not find any report of such unspecific effects in the literature. As often, the best control was the simplest one: the dye was vanishing from single isolated cells that do not express gap junctions.

Patch-clamp experiments, performed by collaborators from Virginia Commonwealth University, confirmed that glucose positively modulates the coupling conductance of β-cells (+55% from low to high glucose). However, mathematical models of the islet function predict a larger increase in coupling conductance (+300%). The mechanisms of gap junction modulation by glucose as well as improvement of the models are currently under investigation in our group.

CHAPTER VII

CONCLUSION AND FUTURE DIRECTIONS

1- Conclusion

Isolated mouse pancreatic islets were used as a model for studying both the mechanisms of glucagon secretion under low-glucose conditions and glucagon suppression by glucose. Two general models have been proposed to account for this suppression: direct inhibition by glucose or indirect inhibition mediated by paracrine factors released from other islet cell-types. To easily and rigorously identify α-cells in the intact islet, we took advantage of transgenic mice expressing fluorescent proteins specifically in this cell-type (Chapter II). Glucose-dependent increases in α-cell NAD(P)H levels and inhibition by mannoheptulose (glucokinase inhibitor) demonstrate that glucose is metabolized in α-cells and suggest that glucokinase is the likely rate-limiting enzyme in this process (Fig. IV-4). Similar to glucose which is an inhibitor of glucagon secretion, the glucagon secretagogues arginine and pyruvate also enhance the α-cell metabolic redox state (Fig. IV-6 and IV-7). This result indicates that an elevation in α-cell metabolic redox state is not sufficient to suppress the secretion of glucagon.

Importantly, glucose does stimulate the glucagon output from pure populations of flow-sorted α-cells (Fig. IV-1B). This observation argues against a direct inhibition of glucagon secretion by glucose and supports the paracrine inhibition model in the islet. Interestingly, basal glucagon secretion from flow-sorted α-cells at 1 mM glucose is ~2-fold greater than from intact islets. In addition, application of the candidate paracrine

inhibitor zinc suppresses secretion from sorted-cells but the amount of glucagon released is still greater than basal secretion from intact islets (Fig. V-1). Taken together, these observations suggest that even baseline α-cell secretory activity is tonically inhibited and emphasize the importance of cell-cell contacts for normal glucagon response. For instance, baseline inhibition could be mediated by juxtacrine signaling or by intercellular communication through gap junctions. The presence of gap junctions connecting α- and β-cells is supported by the observation of calcium oscillation coordination between the two cell-types at high glucose levels (Fig. V-4).

Pharmacological modulation of ion channels under low-glucose conditions indicates that activation of L-type voltage-gated calcium channels is integral for α-cell calcium oscillations and glucagon secretion (Fig. III-3 and III-4). We further demonstrate that TTX-sensitive Na^+ channels are not necessary for calcium channel activation and glucagon secretion (Fig. III-5 and III-6). This result indicates that α-cell membrane should be fairly depolarized at low glucose concentrations (> -50mV) to allow L-type channel activation, as discussed in Chapter III- Section 4. Using a membrane potential dye, we showed that the majority of α-cells were more depolarized than β-cells at low glucose levels (Chapter II – Section 3-4). This depolarized state could be due to higher α-cell metabolic state at low glucose concentrations (Chapter IV – Section 3-4). This observation suggests that α-cells may contain greater concentrations of ATP compared to β-cells, and therefore more α-cell K_{ATP} channels should be closed at low glucose levels.

α-cell $[Ca^{2+}]_i$ and glucagon output from islets are affected by K_{ATP} channel activity in a manner similar to β-cells. Closure of the channels leads to greater $[Ca^{2+}]_i$ and hormone output (Fig. III-9 and III-10), whereas K_{ATP} channel opening has the opposite

effect (Fig. III-7 and III-8). As a result, modulation of K_{ATP} channel activity could constitute a possible mechanism for regulating the secretion of glucagon. In particular, glucose could potentially suppress the secretion of glucagon by membrane hyperpolarization (e.g. by opening α-cell K_{ATP} channels) and inhibition of L-type voltage-gated calcium channels. Indeed, because glucagon release from islets is inhibited at elevated concentrations of glucose, one would naively expect the α-cell $[Ca^{2+}]_i$ to drop concomitantly. However, our calcium imaging studies indicate that glucose elevates α-cell $[Ca^{2+}]_i$ besides inhibiting the secretion of glucagon (Fig. V-2A, Table V-1). Application of candidate paracrine inhibitors (insulin, zinc, GABA, and somatostatin) leads to reduced glucagon secretion but did not decrease the α-cell calcium activity either (Fig. V-1A and Table V-1).

Table VII-1 summarizes the main results of the study and compares the relationship between islet α-cell intracellular calcium levels, as assessed by the calcium indicator Fluo-4, and the resulting effect on glucagon secretion. Under hypoglycemic conditions, α-cell $[Ca^{2+}]_i$ and glucagon secretion are closely related. Thus, activation of L-type voltage-gated calcium channels induced by membrane depolarization (via blockade of K_{ATP} channels by tolbutamide, or uptake of the positively-charged arginine) leads to greater secretory activity. In contrast, inactivation of L-type voltage-gated calcium channels by nifedipine, or by membrane hyperpolarization (via activation of K_{ATP} channels by diazoxide), suppresses the secretion of glucagon. Importantly, α-cell secretory activity appears to uncouple with its $[Ca^{2+}]_i$ under hyperglycemic conditions since glucagon suppression occurs despite greater α-cell $[Ca^{2+}]_i$ levels.

Taken together, α-cells function similarly to β-cells, in contrast to previously

published models. In the absence of cell-cell contacts, glucagon secretion increases as a function of glucose concentration. In the islet, the data suggest that suppression by glucose occurs downstream from α-cell calcium signaling, presumably at the level of vesicle trafficking or exocytotic machinery. For instance, glucagon inhibition could be mediated by a reduced likelihood of granule fusion with the plasma membrane, by depriming of docked vesicles, or by a depletion of the readily releasable pool of glucagon-containing vesicles. Figure VII-1 presents a schematic model that summarizes the main results of the study.

	% change in Fluo-4	% change in glucagon secretion
Tolbutamide (100µM)	**+35**	**+95**
Arginine (10mM)	**+50**	**+180**
Diazoxide (100µM)	**-25**	**-45**
Nifedipine (20µM)	**-20**	**-55**
Glucose (12mM)	**+60**	**-60**

Table VII-1: Synoptic relationship between the α-cell intracellular calcium signal, as measured by Fluo-4 imaging, and the secretion of glucagon from intact mouse islets. Values are expressed in % change compared to baseline at 1 mM glucose. At low glucose levels, α-cell membrane depolarization mediated by closure K_{ATP} channels (via application of tolbutamide) or uptake of the positively charged arginine enhances α-cell $[Ca^{2+}]_i$ and glucagon secretion. In addition, inactivation of L-type voltage-gated calcium channels by nifedipine or membrane hyperpolarization mediated by activation of K_{ATP} channels, reduces glucagon output. In contrast, α-cell $[Ca^{2+}]_i$ uncouples from secretion at high glucose levels. Indeed, glucagon secretion is suppressed despite greater α-cell $[Ca^{2+}]_i$.

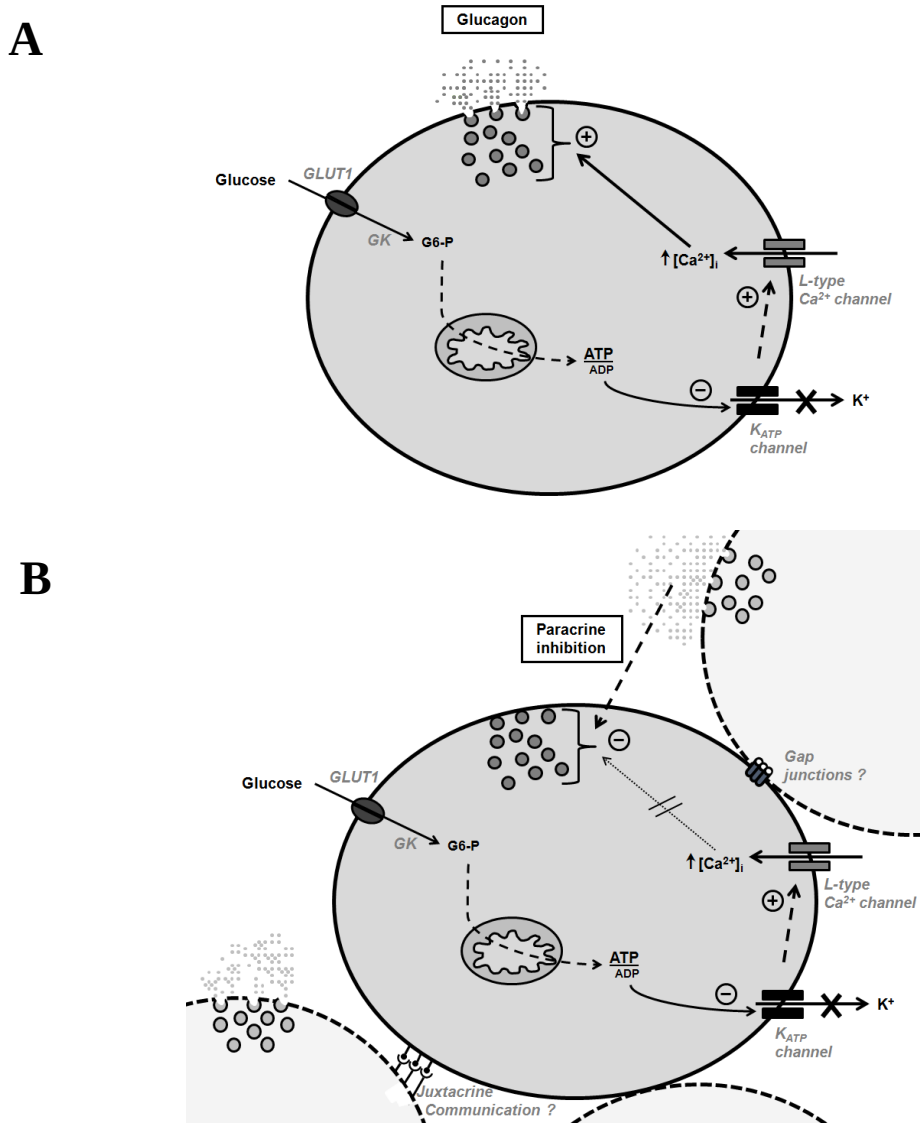

Figure VII-1: Working model of the mechanisms of glucagon secretion and its suppression by glucose. A, in single α-cells retrieved from their islet environment, glucose is transported into the cells by GLUT1 (glucose transporter- 1) and metabolized, glucokinase (GK) being the rate limiting-enzyme in this process. Glucose metabolism slightly elevates α-cell $[Ca^{2+}]_i$ and stimulates the secretion of glucagon from single cells. Similar to β-cells, this effect is likely mediated by an increase in the ATP to ADP ratio that closes K_{ATP} channels. The subsequent membrane depolarization would activate more L-type voltage-gated calcium channels that stimulate granule exocytosis. B, glucose is also metabolized and elevates the $[Ca^{2+}]_i$ in α-cells present in intact islets. However, this elevation in $[Ca^{2+}]_i$ is not translated into more glucagon being released, indicating that glucagon suppression occurs downstream from α-cell calcium signaling, presumably at the level of vesicle trafficking or exocytotic machinery. Glucagon suppression from intact islet likely involves paracrine factors from other cell-types (dotted line circle). Alternatively, juxtacrine inhibition via cell-cell contacts and suppression mediated by gap junctions are other possible inhibitory mechanisms.

2- Future directions

2-1 Effects of glucose on α-cell membrane potential

The effect of glucose on α-cell membrane potential is currently not known. Glucose has been found to slightly depolarize the α-cell membrane, as reported in intact mouse islets (285, 356) and in isolated rat α-cells (341). However, membrane hyperpolarization has also been observed in isolated mouse α-cells (352) and in islet α-cells from mice and rats (357, 358). Our study indicates that glucose is metabolized in α-cells and slightly elevates α-cell $[Ca^{2+}]_i$ (Fig. IV-4 and V-2A). Closure of K_{ATP} channels by tolbutamide also elevates α-cell $[Ca^{2+}]_i$. Taken together, these observations suggest that, similar to β-cells, glucose metabolism in α-cells leads to greater ATP to ADP ratios that close K_{ATP} channels, depolarize the plasma membrane and then activate L-type voltage-gated calcium channels (Fig. VII-1). We would like to further support this mechanism by recording a positive effect of glucose on α-cell membrane potential in intact islets. This could be done by using $DiBAC_4(3)$ to test whether glucose has a depolarizing effect on α-cells, the method is presented in Chapter II, Section 3-4. Alternatively, the membrane potential could be measured by the patch clamp technique. Electrophysiological experiments will be greatly facilitated since α-cells are easily identifiable in our transgenic animals expressing fluorescent proteins in α-cells.

2-2 Relationship between α-cell calcium oscillations and exocytosis

α-cells appear to constitute a heterogeneous cell population. For instance, calcium oscillations display a wide variety of shapes, duration and amplitude, and glucose

differentially affects these properties from cell to cell. In addition, α-cells are still oscillating while their secretory activity is inhibited by glucose (Chapter V). These observations question how single calcium pulses relate to glucagon secretion.

To rigorously assess the relationship between calcium pulses and secretion, we will use a new fluorescent protein biosensor resulting from the fusion of three proteins. A pH-dependent fluorescent protein (pHluorin) (530) is inside the lumen of glucagon granules and a mCherry (531) is outside the granule in the cytoplasm. pHluorin and mCherry are fused to phogrin, a membrane protein located in granules. Granules will be tracked thanks to the expression of mCherry. The pHluorin fluorescence is quenched by the low pH inside the granule, but, upon exocytosis, the pH is greatly increased and the fluorescence can be detected. Transgenic mice expressing this biosensor in the floxed ROSA26 promoter has been developed by our collaborators (Han lab) and could be crossed with our Glucagon-Cre mice. Simultaneous measurements of α-cell $[Ca^{2+}]_i$ could be performed by FuraRed imaging.

Thanks to this strategy, an intracellular calcium oscillation should lead to a concomitant increase in pHluorin fluorescence. This relationship should be disrupted at high glucose levels when calcium oscillations would not be translated into an elevation in pHluorin. In addition, granule trafficking from the endosomal pool to the plasma membrane, as measured by mCherry fluorescence, should be reduced at high glucose levels. Alternatively, granules could accumulate close to the membrane and be unable to undergo exocytosis.

2-3 Lentiviral-based expression of genes of interest in islet α-cells

In Chapter II, we present a successful Cre/loxP strategy for identifying α-cells. We are currently developing a complementary strategy based on lentiviral infection of isolated wild-type islets or dispersed cells. The idea is to specifically express a gene of interest in α-cells. To achieve specificity, gene expression will be driven by the same rat glucagon promoter used in the Cre/loxP strategy. Lentiviral infection of islets is a powerful tool to study β-cells via expression of proteins under the rat insulin promoter (529). The main advantage of lentiviral infection over transgenic islets is the flexibility of the method: not only can fluorescent proteins be used for α-cell identification, but also as fluorescence-based biosensors, or as fluorescent tracers fused to proteins of interest for tracking and/or knock-in studies. The possibility of recognizing α-cells within intact islets and expressing proteins of interest in these cells open the door to a wide range of experimental settings. For instance, fluorescent biosensors could be specifically express in α-cells to measure cAMP and ATP levels in response to glucagon inhibitors and glucagon secretagogues (445). One possible limitation of the lentiviral approach is the weakness of the glucagon promoter. If it appears that the promoter does not drive the expression of fluorescent reporters in sufficient amount to be detected, both the Cre/loxP and the lentiviral methods would need to be combined. The strategy consists in transducing islets isolated from transgenic Glucagon-Cre mice with lentiviruses containing a loxP-flanked stop codon cassette between a strong viral promoter (e.g. CytoMegalovirus promoter) and the gene of interest.

2-4 Gap junctional communication between α-cells and β-cells in the islet

Intercellular communication through gap junctions made of connexin-36 is the consensus explanation behind the coordination of β-cell calcium waves observed at glucose concentrations greater than 7 mM, as demonstrated by the loss of synchrony in islets treated with gap junction blockers, or in transgenic mouse islets lacking connexin-36 (170, 180, 181). Whether gap junctions are present in α-cell membrane represents an important issue in islet physiology. α-cell gap junctions were first documented by freeze fracture electron microscopy (532, 533) and later using dye microinjection (416). These studies provided evidence for both homologous (i.e. α-/α-cell coupling) and heterologous (i.e. α-/β-cell coupling) coupling. However, recent electrophysiological studies failed to obtain any evidence for coupling between β- and non- β-cells (501), challenging a previous report (417). The observed α-/β-cell synchrony during calcium waves seems to hint that gap junctions connect these two cell-types (Fig. V-4B). In addition, preliminary data from transgenic mice lacking connexin-36 indicate that the islets maintain near normal glucose-stimulated insulin secretion, but do not exhibit glucose-mediated suppression of glucagon secretion (Benninger RK, personal communication). These observations support a role for α-/β-cell gap junctional communication in α-cell function. Such a role for electrical communication would be different from the paracrine interactions proposed to date, which have focused on chemical interactions of secreted products.

The LAMP method described in Chapter VI represents an innovative strategy for assaying gap junctional permeability for small dyes. However, the method was not successful in islets, likely because islet gap junctions are permeable to cationic molecules

(186) and the LAMP probe carries two negative charges. Our collaborators from the University of Texas are developing a cationic LAMP probe that could hopefully be applied to pancreatic islets. Alternatively, RFP-labeled α-cells could be patched by filling the internal solution of the pipette with fluorescent agents of various charge and molecular weight (e.g. propidium iodide, MW= 414 Da charge= +2; ethidium bromide, MW= 314 charge= +1; Lucifer Yellow, MW=443 charge= -2; calcein, MW=623 charge= -4). Diffusion of the dye into neighboring cells could be assessed by confocal microscopy. Furthermore, the gene expression of α-cell connexins could be determined by RT-PCR (Reverse Transcriptase – Polymerase Chain Reaction) in pure populations of flow-sorted α-cells.

REFERENCES

1. Lieberman MA, Marks AD (2005). Section 5: carbohydrate metabolism. *Mark's Basic Medical Biochemistry: A Clinical Approach*. Eds. Lippincott Williams & Wilkins.

2. American Diabetes Association (2008). Standards of Medical Care in Diabetes. *Diabetes Care*, **31**(s1): 12-54.

3. Bolli GB and Fanelli CG (1999). Physiology of glucose counterregulation to hypoglycemia. *Endocrinol. Metab. Clin. North Am*., **28**(3): 467-93.

4. Cryer PE (1999). Symptoms of hypoglycemia, thresholds for their occurrence, and hypoglycemia unawareness. *Endocrinol. Metab. Clin. North Am*., **28**(3): 495-500.

5. Cryer PE (1993). Glucose counterregulation: prevention and correction of hypoglycemia in humans. *Am. J. Physiol*., **264**(2 Pt 1): E149-55.

6. Evans ML, McCrimmon RJ, Flanagan DE, Keshavarz T, Fan X, McNay EC, Jacob RJ, Sherwin RS (2004). Hypothalamic ATP-sensitive K^+ channels play a key role in sensing hypoglycemia and triggering counterregulatory epinephrine and glucagon responses. *Diabetes*, **53**: 2542-51.

7. National Institute of Health (2010). National diabetes statistics. http://diabetes.niddk.nih.gov/dm/pubs/statistics/index.htm.

8. American Diabetes Association. http://www.diabetes.org/diabetes-basics/diabetes-statistics/.

9. Wild S, Roglic G, Green A, Sicree R, and King H (2004).Global prevalence of diabetes. *Diabetes Care*, **27**:1047-53.

10. Romao I, Roth J (2008). Genetic and environmental interactions in obesity and type-II diabetes. *J. Am. Diet. Assoc*., **108**(4 Suppl 1): 24-8.

11. Unger RH, Orci L (1975). The essential role of glucagon in the pathogenesis of diabetes mellitus. *Lancet*, **1**(7897): 14-6.

12. Rudernam NB, Aoki TT, Cahill JF Jr. (1976). Gluconeogenesis and its disorders in man. In: Hanson RW, Mehlam MA, eds. *Gluconeogenesis: its regulation in mammalian species.* New York: John Wiley and Sons (517).

13. Reaven GM, Chen YD, Golay A, Swislocki AL, Jaspan JB (1987). Documentation of hyperglucagonemia throughout the day in nonobese and obese patients with noninsulin-dependent diabetes mellitus. *J. Clin. Endocrinol. Metab.*, **64**: 106-10.

14. Baron AD, Schaeffer L, Shragg P, Kolterman OG (1987). Role of hyperglucagonemia in maintenance of increased rates of hepatic glucose output in type-II diabetes. *Diabetes*, **36**: 274-83.

15. Dinneen S, Alzaid A, Turk D, Rizza R (1995). Failure of glucagon suppression contributes to postprandial hyperglycemia in IDDM. *Diabetologia*, **38**: 337-43.

16. Shah P, Vella A, Basu A, Basu R, Schwenk WF, Rizza RA (2000). Lack of suppression of glucacon contributes to postprandial hyperglycemia in subjects with type-II diabetes mellitus. *J. Clin. Endocrinol. Metab.*, **85**: 4053-59.

17. Matsuda M, Defronzo RA, Glass L, Consoli A, Giordano M, Bressler P, Delprato S (2002). Glucagon dose-response curve for hepatic glucose production and glucose disposal in type-II diabetic patients and normal individuals. *Metabolism*, 51(9): 1111-9.

18. Cryer PE (2002). Hypoglycaemia: the limiting factor in the glycaemic management of type-I and type-II diabetes. *Diabetologia*, **45**: 937-948.

19. Djuric SW, Grihalde N, Lin CW (2002). Glucagon receptor antagonists for the treatment of type-II diabetes: current prospects. *Curr. Opin. Investig. Drugs*, **3**: 1617-23.

20. Jiang G, Zhang BB (2003). Glucagon and regulation of glucose metabolism. *Am. J. Physiol. Endocrinol. Metab*., **284**: E671-E678.

21. Sloop KW, Michael MD, Moyers JS (2003). Glucagon as a target for the treatment of type-II diabetes. *Expert Opin. Ther. Targets*, **9**: 593-600.

22. Edgerton DS, Johnson KM, Cherrington AD (2009). Current strategies for the inhibition of hepatic glucose production in type-II diabetes, *Front Biosci*., **14**: 1169-81.

23. Cryer PE (2008). Hypoglycemia: still the limiting factor in the glycemic management of diabetes. *Endocr. Pract*., **14**(6): 750-56.

24. Robertson RP (2002). Islet transplantation: travels up the learning curve. *Curr. Diab. Rep.*, **2**(4): 365-70.

25. Digon BJ (2009). History of islet transplantation. *Curr. Diab. Rep*., **9**(4): 312-6.

26. Naftanel MA, Harlan DM (2004). Pancreatic islet transplantation. *PLoS Med*., **1**(3): e58.

27. Harlan DM, Kenyon NS, Korsgren O, Roep BO (2009). Current advances and travails in islet transplantation. *Diabetes*, **58**(10): 2175-84.

28. Shapiro AM, Ricordi C, Hering BJ, Auchincloss H, Lindblad R, Robertson RP, Secchi A, Brendel MD, Berney T, Brennan DC, Cagliero E, Alejandro R, Ryan EA,

DiMercurio B, Morel P, Polonsky KS, Reems JA, Bretzel RG, Bertuzzi F, Froud T, Kandaswamy R *et al*. (2006). International trial of the Edmonton protocol for islet transplantation. *N. Engl. J. Med*., **355**: 1318-30.

29. Kendall DM, Teuscher AU, Robertson RP (1997). Defective glucagon secretion during sustained hypoglycemia following successful islet allo- and autotransplantation in humans. *Diabetes*, **46**: 23-27.

30. Motta PM, Macchiarelli G, Nottola SA, Correr S (1997). Histology of the exocrine pancreas. *Microsc. Res. Tech*., **37**(5-6): 384-98.

31. Suckale J, Solimena M (2008). Pancreas islets in metabolic signaling-focus on the β-cell. *Front Biosci*., **13**: 7156-71.

32. Cabrera O, Berman DM, Kenyon NS, Ricordi C, Berggren PO, Caicedo A (2006). The unique cytoarchitecture of human pancreatic islets has implications for islet cell function. *Proc. Natl. Acad. Sci*., **103**(7): 2334-9.

33. Wierup N, Svensson H, Mulder H, Sundler F (2002). The ghrelin cell: a novel developmentally regulated islet cell in the human pancreas. *Regulatory Peptides*, **107** :63-69.

34. Bosco D, Armanet M, Morel P, Niclauss N, Sgroi A, Muller YD, Giovannoni L, Parnaud G, Berney T (2010). Unique arrangement of α- and β-cells in human islets of Langerhans. *Diabetes*, **59**(5): 1202-10.

35. Edlund H (2002). Pancreatic organogenesis: developmental mechanisms and implications for therapy. *Nat. Rev. Genet*., **3**(7): 524-32.

36. Herrera PL, Huarte J, Sanvito F, Meda P, Orci L, Vassalli JD (1991). Embryogenesis of the murine endocrine pancreas; early expression of pancreatic polypeptide gene. *Development*, **113**: 1257-65.

37. Teitelman G, Alpert S, Polak JM, Martinez A, Hanahan D (1993). Precursor cells of mouse endocrine pancreas coexpress insulin, glucagon and the neuronal proteins tyrosine hydrolase and neuropeptide Y, but not pancreatic polypeptide. *Development*, **118**: 1031-39.

38. Alpert S, Hanahan D, Teitelman G (1988). Hybrid insulin genes reveal a developmental lineage for pancreatic endocrine cells and imply a relationship with neurons. *Cell*, **53**(2): 295-308.

39. Prado CL, Pugh-Bernard AE, Elghazi L, Sosa-Pineda B, Sussel L (2004). Ghrelin cells replace insulin-producing β-cells in two mouse models of pancreas development. *Proc. Natl. Acad. Sci. USA*, **101**(9): 2924-9.

40. Jonsson J, Carlsson L, Edlund T, Edlund H (1994). Insulin-promoter-factor 1 is required for pancreas development in mice. *Nature*, **371**(6498): 606-9.

41. Stoffers DA, Zinkin NT, Stanojevic V, Clarke WL, Habener JF (1997). Pancreatic agenesis attributable to a single nucleotide deletion in the human IPF1 gene coding sequence. *Nat. Genet*., **15**(1): 106-10.

42. Ashizawa S, Brunicardi FC, Wang XP (2004). PDX-1 and the pancreas. *Pancreas*, **28**(2): 109-20.

43. Kawaguchi Y, Cooper B, Gannon M, Ray M, MacDonald RJ, Wright CV (2002). The role of the transcriptional regulator Ptf1a in converting intestinal to pancreatic progenitors. *Nat. Genet*., **32**: 128–134.

44. Ahlgren U, Pfaff S, Jessel TM, Edlund T, Edlund H (1997). Independent requirement for ISL1 in the formation of the pancreatic mesenchyme and islet cells. *Nature*, **385**: 257-60.

45. Gradwohl G, Dierich A, LeMeur M, Guillemot F (2000). Neurogenin3 is required for the development of the four endocrine cell lineages of the pancreas. *Proc. Natl. Acad. Sci. USA*, **97**: 1607-11.

46. Naya FJ, Huang HP, Qiu Y, Mutoh H, DeMayo FJ, Leiter AB, Tsai MJ (1997). Diabetes, defective pancreatic morphogenesis, and abnormal entoroendocrine differentiation in BETA2/neuroD-deficient mice. *Genes Dev*., **11**: 2323-34.

47. Sussel L, Kalamaras J, Hartigan-O'Connor DJ, Meneses JJ, Pedersen RA, Rubenstein JL, German MS (1998). Mice lacking the homeodomain transcription factor Nkx2.2 have diabetes due to arrested differentiation of pancreatic β-cells. *Development*, **125**: 2213-21.

48. Collombat P, Mansouri A, Hecksher-Sorensen J, Serup P, Krull J, Gradwohl G, Gruss P (2003). Opposing actions of Arx and Pax4 in endocrine pancreas development. *Genes Dev*., **17**: 2591-2603.

49. Heller RS, Stoffers DA, Liu A, Schedl A, Crenshaw EB, Madsen OD, Serup P (2004). The role of Brn4/Pou3f4 and Pax6 in forming the pancreatic glucagon cell identity. *Dev. Biol*., **268**: 123-34.

50. St-Onge L, Sosa-Pineda B, Chowdhury K, Mansouri A, Gruss P (1997). Pax6 is required for differentiation of glucagon-producing -cells in mouse pancreas. *Nature*, **387**: 406-9.

51. Artner I, Lay JL, Hang Y, Elghazi L, Schisler JC, Henderson E, Sosa-Pineda B, Stein R (2006). MafB: an activator of the glucagon gene expressed in developing islet α- and β-cells. *Diabetes*, **55**: 297-304.

52. Nishimura W, Kondo T, Salameh T, El Khattabi I, Dodge R, Bonner-Weir S, Sharma A (2006). A switch from MafB to MafA expression accompanies differentiation to pancreatic β-cells. *Dev. Biol*., **293**: 526-39.

53. Lee CS, Sund NJ, Behr R, Herrera PL, Kaestner KH (2005). Foxa2 is required for the differentiation of pancreatic α-cells. *Dev. Biol*., **278**(2): 484-95.

54. Stoffers DA, Ferrer J, Clarke WL, Habener JF (1997). Early-onset type-II diabetes mellitus (MODY4) linked to IPF1. *Nat. Genet*., **17**(2): 138-9.

55. Hani EH, Stoffers DA, Chèvre JC, Durand E, Stanojevic V, Dina C, Habener JF, Froguel P (1999). Defective mutations in the insulin promoter factor-1 (IPF-1) gene in late-onset type-II diabetes mellitus. *J. Clin. Invest*., **104**(9): R41-8.

56. Macfarlane WM, Frayling TM, Ellard S, Evans JC, Allen LI, Bulman MP, Ayers S, Shepherd M, Clark P, Millward A, Demaine A, Wilken T, Docherty K, Hattersley AT (1999). Missense mutations in the insulin promoter factor-1 gene predispose to type-II diabetes. *J. Clin. Invest*., **104**(9): R33-9.

57. Malecki MT, Lebrun P, Pezzolesi M, Warram JH, Krolewski AS, Jhala US (2006). A newly identified mutation in an IPF1 binding site of the insulin gene promoter may predispose to type-II diabetes mellitus. *Diabetologia*, **49**(8): 1985-7.

58. Malecki MT, Jhala US, Antonellis A, Fields L, Doria A, Orban T, Saad M, Warram JH, Montminy M, Krolewski AS (1999). Mutations in NEUROD1 are associated with the development of type-II diabetes mellitus. *Nat. Genet*., **23**(3): 323-8.

59. Madsen OD, Serup P (2006). Towards cell therapy for diabetes. *Nat. Biotechnol*., **24**(12): 1481-3.

60. Dor Y, Brown J, Martinez OI, Melton DA (2004). Adult pancreatic β-cells are formed by self-duplication rather than stem-cell differentiation. *Nature*, **429**(6987): 41-6.

61. Xu X, D'Hoker J, Stangé G, Bonné S, De Leu N, Xiao X, Van de Casteele M, Mellitzer G, Ling Z, Pipeleers D, Bouwens L, Scharfmann R, Gradwohl G, Heimberg H (2008). β-cells can be generated from endogenous progenitors in injured adult mouse pancreas. *Cell*, **132**(2): 183-4.

62. Bonner-Weir S (1993). The microvasculature of the pancreas, with emphasis on that of the islets of Langerhans: anatomy and functional implications. *The Pancreas: Biology, Pathobiology, and Disease*, 759-70.

63. Henderson MC, Moss JR (1985). A morphometric study of the endocrine and exocrine capillaries of the pancreas. *Q. J. Exp. Physiol*., **70**(3): 347-56.

64. Bendayan M (1993). Pathway of insulin in pancreatic tissue on its release by the β-cell. *Am. J. Physiol*., **264**(2 Pt 1): G187-94.

65. Moldovan FC, Brunicardi S (2001). Endocrine pancreas: summary of observations generated by surgical fellows. *World J. Surg*., **25**(4): 468-73.

66. Stagner JI, Samols E (1986). Retrograde perfusion as a model for testing the relative effects of glucose versus insulin on the α-cell. *J. Clin. Invest*., **77**(3): 1034-7.

67. Samols E, Stagner JI, Ewart RB, Marks V (1988). The order of islet microvascular cellular perfusion is β→α→δ in the perfused rat pancreas. *J. Clin. Invest*., **82**(1): 350-3.

68. Stagner JI, Samols E, Bonner-Weir S (1988). β→α→δ pancreatic islet cellular perfusion in dogs. *Diabetes*, **37**(12): 1715-21.

69. Stagner JI, Samols E, Marks V (1989). The anterograde and retrograde infusion of glucagon antibodies suggests that α-cells are vascularly perfused before δ-cells within the rat islet. *Diabetologia*, **32**(3): 203-6.

70. Stagner JI, Samols E (1992). The vascular order of islet cellular perfusion in the human pancreas. *Diabetes*, **41**(1): 93-7.

71. Stagner JI, Samols E, Koerker DJ, Goodner CJ (1992). Perfusion with anti-insulin gamma globulin indicates a β to α to δ cellular perfusion sequence in the pancreas of the rhesus monkey, Macaca mulatta. *Pancreas*, **7**(1): 26-9.

72. Wayland H (1997). Microcirculation in pancreatic function. *Microsc. Res. Tech*., **37**(5-6): 418-33.

73. Murakami T, Fujita T, Miyake T, Ohtsuka A, Taguchi T, Kikuta A (1993). The insulo-acinar portal and insulo-venous drainage systems in the pancreas of the mouse, dog, monkey and certain other animals: a scanning electron microscopic study of corrosion casts. *Arch. Histol. Cytol*., **56**(2): 127-47.

74. Miyake T, Murakami T, Ohtsuka A (1992). Incomplete vascular casting for a scanning electron microscope study of the microcirculatory patterns in the rat pancreas. *Arch. Histol. Cytol*., **55**(4): 397-406.

75. Ohtani O (1984). Review of scanning electron and light microscopic methods in microcirculation research and their application in pancreatic studies. *Scan.. Electron. Microsc.*, **2**: 653-661.

76. Liu YM, Guth PH, Kaneko K, Livingston EH, Brunicardi FC (1993). Dynamic in vivo observation of rat islet microcirculation. *Pancreas*, **8**(1): 15-21.

77. Nyman LR, Wells KS, Head WS, McCaughey M, Ford E, Brissova M, Piston DW, Powers AC (2008). Real-time, multidimensional in vivo imaging used to investigate blood flow in mouse pancreatic islets.. *J. Clin. Invest*., **118**(11): 3790-7.

78. Jansson L, Hellerström C (1983). Stimulation by glucose of the blood flow to the pancreatic islets of the rat. *Diabetologia*, **25**(1): 45-50.

79. Ahrén B (2000). Autonomic regulation of islet hormone secretion: implications for health and disease. *Diabetologia*, **43**(4): 393-410.

80. Borg WP, During MJ, Sherwin RS, Borg MA, Brines ML, Shulman GI (1994). Ventromedial hypothalamic lesions in rats suppress counterregulatory responses to hypoglycemia. *J. Clin. Invest*., **93**: 1677-82.

81. de Vries MG, Arseneau LM, Lawson ME, Beverly JL (2003). Extracellular glucose in rat ventromedial hypothalamus during acute and recurrent hypoglycemia. *Diabetes*, **52**: 2767-73.

82. Cegrell L (1968). Adrenergic nerves and monoamine-containing cells in the mammalian endocrine pancreas. *Acta. Physiol. Scand*., **314**: 17-23.

83. Ahren B, Ericson LE, Lundquist I, Loren I, Sundler F (1981). Adrenergic innervation of pancreatic islets and modulation of insulin secretion by the sympato-adrenal system. *Cell Tissue Res*., **216**: 15-30.

84. Pettersson M, Ahren B, Lundquist I, Böttcher G, Sundler F (1987). Neuropeptide Y: intrapancreatic neuronal localization and effects on insulin secretion in the mouse. *Cell Tissue Res.*, **248**: 43-8.

85. Ahren B, Böttcher G, Kowalyk S, Dunning BE, Sundler F, Taborsky GJ (1990). Galanin is co-localized with noradrenaline and neuropeptide Y in dog pancreas and celiac ganglion. *Cell Tissue Res*., **261**: 49-58.

86. Coupland RE (1958). The innervation of the pancreas of the rat, cat and rabbit as revealed by the cholinesterase technique. *J. Anat*., **92**: 143-9.

87. Bishop AE, Polak JM, Green IC, Bryant MG, Bloom SR (1980). The location of VIP in the pancreas of man and rat. *Diabetologia*, **18**: 73-8.

88. Havel PJ, Dunning BE, Verchere CB, Baskin DG, O'Dorisio T, Taborsky GJ (1997). Evidence that vasoactive intestinalpolypeptide is a parasympathetic neurotransmitter in the endocrine pancreas in the dog. *Regul. Pept*., **71**: 163-170.

89. Winzell MS, Ahrén B (2007). Role of VIP and PACAP in islet function. *Peptides*, **28**(9): 1805-13.

90. Knuhtsen S, Holst JJ, Baldissera FG, Skak-Nielsen T, Poulsen SS, Jensen SL, Nielsen OV (1987). Gastrin-releasing peptide in the porcine pancreas. *Gastroenterology*, **92**(5 Pt 1): 1153-8.

91. Pettersson M, Ahrén B (1988). Gastrin-releasing peptide (GRP): effects on basal and stimulated insulin and glucagon secretion in the mouse. *Peptides*, **8**: 55-60.

92. Wood SM, Jung RT, Webster JD, Ghatei MA, Adrian TE, Yanaihara N, Yanaihara C, Bloom SR (1983). The effect of the mammalian neuropeptide, gastrin releasing peptide (GRP), on gastrointestinal and pancreatic hormone secretion in man. *Clin. Sci*., **65**: 365-71.

93. Fridolf T, Sundler F, Ahren B (1992). Pituitary adenylate cyclase-activating polypeptide (PACAP): occurrence in rodent pancreas and effects on insulin and glucagon secretion in the mouse. *Cell Tissue Res*., **269**: 275-9.

94. Tornoe K, Hannibal J, Fahrenkrug J, Holst JJ (1997). PACAP-(1-38) as neurotransmitter in pig pancreas: receptor activation revealed by the antagonist PACAP-(6-38). *Am. J. Physiol*., **273**: G436-46.

95. Filipsson K, Tornoe K, Holst J, Ahren B (1997). Pituitary adenylate cyclase-activating polypeptide stimulates insulin and glucagon secretion in humans. *J. Clin. Endocrinol. Metab.*, **82**: 3093-8.

96. Karlsson S, Sundler F, Ahren B (1992). Neonatal capsaicin-treatment in mice: effects on pancreatic peptidergic nerves and 2-deoxy-D-glucose-induced insulin and glucagon secretion. *J. Auton. Nerv. Syst*., **39**: 51-60.

97. Rosenfeld MG, Mermod JJ, Amara SG, Swanson LW, Sawchenko PE, Rivier J, Vale WW, Evans RM (1983). Production of a novel neuropeptide encoded by the calcitonin gene via tissue-specific RNA processing. *Nature*, **304**(5922): 129-35.

98. Sorenson RL, Garry DG, Brelje TC (1991). Structural and functional considerations of GABA in islets of Langerhans: β-cells and nerves. *Diabetes*, **40**: 1365-74.

99. Ekblad E, Alm P, Sundler F (1994). Distribution, origin, and projections of nitric oxide synthase-containing neurons in gut and pancreas. *Neuroscience*, 63: 233-48.

100. Rehfeld JF, Larsson LI, Goltermann NR, Schwartz TW, Holst JJ, Jensen SL, Morley JS (1980). Neural regulation of pancreatic hormone secretion by the C-terminal tetrapeptide of CCK. *Nature*, **284**(5751): 33-8.

101. Coutinho-Silva R, Parsons M, Robson T, Burnstock G (2001). Changes in expression of P2 receptors in rat and mouse pancreas during development and ageing. *Cell Tissue Res*., **306**(3): 373-83.

102. Hayashi M, Otsuka M, Morimoto R, Hirota S, Yatsushiro S, Takeda J, Yamamoto A, Moriyama Y (2001). Differentiation-associated Na^+-dependent inorganic phosphate cotransporter (DNPI) is a vesicular glutamate transporter in endocrine glutamatergic systems. *J. Biol. Chem*., **276**(46): 43400-6.

103. Gammelsaeter R, Frøyland M, Aragón C, Danbolt NC, Fortin D, Storm-Mathisen J, Davanger S, Gundersen V (2004). Glycine, GABA and their transporters in pancreatic islets of Langerhans: evidence for a paracrine transmitter interplay. *J. Cell Sci*., **117**(Pt 17): 3749-58.

104. Zern RT, Bird JL, Feldman JM (1980). Effect of increased pancreatic islet norepinephrine, dopamine and serotonin concentration on insulin secretion in the golden hamster. *Diabetologia*, **18**(4): 341-6.

105. Kirchgessner AL, Gershon MD (1990). Innervation of the pancreas by neurons in the gut. *J. Neurosci*., **10**(5): 1626-42.

106. Porte D Jr, Williams RH (1966). Inhibition of insulin release by norepinephrine in man. *Science*, **152**: 1248-50.

107. Ahren B, Veith R, Taborsky GJ Jr (1987). Sympathetic nerve stimulation versus pancreatic norepinephrine infusion in the dog: 1. Effects on basal release of insulin and glucagon. *Endocrinology*, **121**: 323-31.

108. Holst JJ, Jensen SL, Knuhtsen S, Nielsen OV (1983). Autonomic nervous control of pancreatic somatostatin secretion. *Am. J. Physiol*., **245**: E542-8.

109. Ahren B, Veith RC, Paquette TL, Taborsky GJ Jr. (1987). Sympathetic nerve stimulation versus pancreatic norepinephrine infusion in the dog: 2. Effects on basal release of somatostatin and pancreatic polypeptide. *Endocrinology*, **121**: 332-9.

110. Kurose T, Seino Y, Nishi S, Tsuji K, Taminato T, Tsuda K, Imura H (1990). Mechanism of sympathetic neural regulation of insulin, somatostatin, and glucagon secretion. *Am. J. Physiol*., **258**(1 Pt 1): E220-7.

111. Dunning BE, Ahren B, Veith RC, Böttcher G, Sundler F, Taborsky GJ Jr. (1986). Galanin: a novel pancreatic neuropeptide. *Am. J. Physiol*., **251**: E127-33.

112. Morgan DG, Kulkarni RN, Hurley JD, Wang ZL, Wang RM, Ghatei MA, Karlsen AE, Bloom SR, Smith DM (1998). Inhibition of glucose stimulated insulin secretion by neuropeptide Y is mediated via the Y1 receptor and inhibition of adenylyl cyclase in RIN 5AH rat insulinoma cells. *Diabetologia*, **41**(12): 1482-91.

113. Schwartz NS, Clutter WE, Shah SD, Cryer PE (1987). Glycemic thresholds for activation of glucose counterregulatory systems are higher than the threshold for

symptoms. *J. Clin. Invest.*, **79**(3): 777-81.

114. Mitrakou A, Ryan C, Veneman T, Mokan M, Jenssen T, Kiss I, Durrant J, Cryer P, Gerich J (1991). Hierarchy of glycemic thresholds for counterregulatory hormone secretion, symptoms, and cerebral dysfunction. *Am. J. Physiol*., **260**(1 Pt 1): E67-74.

115. Diem P, Redmon JB, Abid M, Moran A, Sutherland DE, Halter JB, Robertson RP (1990). Glucagon, catecholamine and pancreatic polypeptide secretion in type-I diabetic recipients of pancreas allografts. *J. Clin. Invest*., **86**(6): 2008-13.

116. Sherck SM, Shiota M, Saccomando J, Cardin S, Allen EJ, Hastings JR, Neal DW, Williams PE, Cherrington AD (2001). Pancreatic response to mild non-insulin-induced hypoglycemia does not involve extrinsic neural input. *Diabetes*, **50**: 2487-96.

117. Ahrén B, Taborsky GJ Jr. (1986). The mechanism of vagal nerve stimulation of glucagon and insulin secretion in the dog. *Endocrinology*, **118**(4): 1551-7.

118. Ahrén B, Paquette TL, Taborsky GJ Jr. (1986). Effect and mechanism of vagal nerve stimulation on somatostatin secretion in dogs. *Am. J. Physiol*., **250**(2 Pt 1): E212-7.

119. Song SH, McIntyre SS, Shah H, Veldhuis JD, Hayes PC, Butler PC (2000). Direct measurement of pulsatile insulin secretion from the portal vein in human subjects. *J. Clin. Endocrinol. Metab.*, **85**: 4491-9.

120. Porksen N, Munn S, Steers J, Vore S, Veldhuis J, Butler P (1995). Pulsatile insulin secretion accounts for 70% of total insulin secretion during fasting. *Am J. Physiol. Endocrinol. Metab.*, **269**: E478-88.

121. Matveyenko AV, Veldhuis JD, Butler PC (2008). Measurement of pulsatile insulin secretion in the rat: direct sampling from the hepatic portal vein. *Am J. Physiol. Endocrinol. Metab*., **295**(3): E569-74.

122. Ritzel RA, Veldhuis JD, Butler PC (2003). Glucose stimulates pulsatile insulin secretion from human pancreatic islets by increasing secretory burst mass: dose-response relationship. *J. Clin. Endocrinol. Metab.*, **88**(2): 742-7.

123. Stagner JI, Samols E (1985). Role of intrapancreatic ganglia in regulation of periodic insular secretions. *Am. J. Physiol*., **248**(5 Pt 1): E522-30.

124. Pørksen N, Munn S, Ferguson D, O'Brien T, Veldhuis J, Butler P (1994). Coordinate pulsatile insulin secretion by chronic intraportally transplanted islets in the isolated perfused rat liver. *J. Clin. Invest*., **94**(1): 219-27.

125. Fendler B, Zhang M, Satin L, Bertram R (2009). Synchronization of pancreatic islet oscillations by intrapancreatic ganglia: a modeling study. *Biophys. J.*, **97**(3): 722-9.

126. Zhang M, Fendler B, Peercy B, Goel P, Bertram R, Sherman A, Satin L (2008). Long lasting synchronization of calcium oscillations by cholinergic stimulation in isolated pancreatic islets. *Biophys. J.*, **95**(10): 4676-88.

127. Thorens B, Sarkar HK, Kaback HR, Lodish HF (1988). Cloning and functional expression in bacteria of a novel glucose transporter present in liver, intestine, kidney, and β-pancreatic islet cells. *Cell*, **55**(2): 281-90.

128. Johnson JH, Newgard CB, Milburn JL, Lodish HF, Thorens B (1990). The high Km glucose transporter of islets of Langerhans is functionally similar to the low affinity transporter of liver and has an identical primary sequence. *J. Biol. Chem.*, **265**(12): 6548-51.

129. Hughes SD, Quaade C, Johnson JH, Ferber S, Newgard CB (1993). Transfection of AtT-20ins cells with GLUT-2 but not GLUT-1 confers glucose-stimulated insulin secretion. Relationship to glucose metabolism. *J. Biol. Chem.*, **268**(20): 15205-12.

130. Iynedjian PB, Pilot PR, Nouspikel T, Milburn JL, Quaade C, Hughes S, Ucla C, Newgard CB (1989). Differential expression and regulation of the glucokinase gene in liver and islets of Langerhans. *Proc. Natl. Acad. Sci. USA*, **86**(20): 7838-42.

131. Magnuson MA, Shelton KD (1989). An alternate promoter in the glucokinase gene is active in the pancreatic β-cell. *J. Biol. Chem.*, **264**(27): 15936-42.

132. Matschinsky FM (1990). Glucokinase as glucose sensor and metabolic signal generator in pancreatic beta-cells and hepatocytes. *Diabetes*, **39**(6): 647-52.

133. Cook DL, Hales CN (1984). Intracellular ATP directly blocks K^+ channels in pancreatic β-cells. *Nature*, **311**(5983): 271-3.

134. Ashcroft FM, Harrison DE, Ashcroft SJ (1984). Glucose induces closure of single potassium channels in isolated rat pancreatic β-cells. *Nature*, **312**(5993): 446-8.

135. Detimary P, Van den Berghe G, Henquin JC (1996). Concentration dependence and time course of the effects of glucose on adenine and guanine nucleotides in mouse pancreatic islets. *J. Biol. Chem.*, **271**(34): 20559-65.

136. Wollheim CB, Sharp GW (1981). Regulation of insulin release by calcium. *Physiol. Rev.*, **61**(4): 914-73.

137. Hoenig M, Sharp GW (1986). Glucose induces insulin release and a rise in cytosolic calcium concentration in a transplantable rat insulinoma. *Endocrinology*, **119**(6): 2502-7.

138. Satin LS, Cook DL (1985). Voltage-gated Ca^{2+} current in pancreatic β-cells. *Pflugers Arch.*, **404**(4): 385-7.

139. MacDonald PE, Wheeler MB (2003). Voltage-dependent K^+ channels in pancreatic β-cells: role, regulation and potential as therapeutic targets. *Diabetologia*, **46**(8): 1046-62.

140. Göpel SO, Kanno T, Barg S, Eliasson L, Galvanovskis J, Renström E, Rorsman P (1999). Activation of Ca^{2+}-dependent K^+ channels contributes to rhythmic firing of action potentials in mouse pancreatic β-cells. *J. Gen. Physiol*., **114**: 759-69.

141. Bertram R, Sherman A., Satin LS (2007). Metabolic and electrical oscillations: partners in controlling pulsatile insulin secretion. *Am. J. Physiol. Endocrinol. Metab*., **293**: E890-900.

142. van Haeften TW, Boonstra E, Veneman TF, Gerich JE, van der Veen EA (1990). Dose-response characteristics for glucose-stimulated insulin release in man and assessment of influence of glucose on arginine-stimulated insulin release. *Metabolism*, **39**(12): 1292-9.

143. Zawalich WS, Yamazaki H, Zawalich KC (2008). Biphasic insulin secretion from freshly isolated or cultured, perifused rodent islets: comparative studies with rats and mice. *Metabolism*, **57**(1): 30-9.

144. Nunemaker CS, Wasserman DH, McGuinness OP, Sweet IR, Teague JC, Satin LS (2006). Insulin secretion in the conscious mouse is biphasic and pulsatile. *Am. J. Physiol. Endocrinol. Metab*., **290**(3): E523-9.

145. Efendić S, Luft R, Wajngot A (1984). Aspects of the pathogenesis of type-II diabetes. *Endocr. Rev*., **5**(3): 395-410.

146. Del Prato S (2003). Loss of early insulin secretion leads to postprandial hyperglycaemia. *Diabetologia*, **46**(Suppl 1): M2-8.

147. Barg S, Eliasson L, Renstrom E and Rorsman P (2002). A subset of 50 secretory granules in close contact with L-type Ca^{2+} channels accounts for first-phase insulin secretion in mouse β-cells. *Diabetes*, S74-S82.

148. Straub SG, Sharp GW (2002). Glucose-stimulated signaling pathways in biphasic insulin secretion. *Diabetes Metab. Res. Rev*., **18**(6): 451-63.

149. Bratanova-Tochkova TK, Cheng H, Daniel S, Gunawardana S, Liu YJ, Mulvaney-Musa J, Schermerhorn T, Straub SG, Yajima H, Sharp GW (2002). Triggering and augmentation mechanisms, granule pools, and biphasic insulin secretion. *Diabetes*, **51**(Suppl. 1): S83-90.

150. Wang Z, Thurmond DC (2009). Mechanisms of biphasic insulin-granule exocytosis: roles of the cytoskeleton, small GTPases and SNARE proteins. *J. Cell Sci*., **122**: 893-903.

151. Henquin JC (2009). Regulation of insulin secretion: a matter of phase control and amplitude modulation. *Diabetologia*, **52**(5): 739-51.

152. Eliasson L, Renström E, Ding WG, Proks P, Rorsman P (1997). Rapid ATP-dependent priming of secretory granules precedes Ca^{2+}-induced exocytosis in mouse pancreatic β-cells. *J. Physiol*., **503**(Pt 2): 399-412.

153. Takahashi N, Kadowaki T, Yazaki Y, Ellis-Davies GC, Miyashita Y, Kasai H (1999). Post-priming actions of ATP on Ca^{2+}-dependent exocytosis in pancreatic β-cells. *Proc. Natl. Acad. Sci. USA*, **96**(2): 760-5.

154. Dyachok O, Idevall-Hagren O, Sagetorp J, Tian G, Wuttke A, Arrieumerlou C, Akusjärvi G, Gylfe E, Tengholm A (2008). Glucose-induced cyclic AMP oscillations regulate pulsatile insulin secretion. *Cell Metab.*, **8**(1): 26-37.

155. Jensen MV, Joseph JW, Ronnebaum SM, Burgess SC, Sherry AD, Newgard CB (2008). Metabolic cycling in control of glucose-stimulated insulin secretion. *Am. J. Physiol. Endocrinol Metab*., **295**(6): E1287-97.

156. Rorsman P, Renström E (2003). Insulin granule dynamics in pancreatic β-cells. *Diabetologia*, **46**(8): 1029-45.

157. Varadi A, Ainscow EK, Allan VJ, Rutter GA (2002). Involvement of conventional kinesin in glucose-stimulated secretory granule movements and exocytosis in clonal pancreatic β-cells. *J. Cell Sci*., **115**(Pt 21): 4177-89.

158. Nenquin M, Szollosi A, Aguilar-Bryan L, Bryan J, Henquin JC (2004). Both triggering and amplifying pathways contribute to fuel-induced insulin secretion in the absence of sulfonylurea receptor-1 in pancreatic β-cells. *J. Biol. Chem*., **279**(31): 32316-24.

159. Ravier MA, Nenquin M, Miki T, Seino S, Henquin JC (2009). Glucose controls cytosolic Ca^{2+} and insulin secretion in mouse islets lacking adenosine triphosphate-sensitive K^+ channels owing to a knockout of the pore-forming subunit Kir6.2. *Endocrinology*, **150**(1): 33-45.

160. Szollosi A, Nenquin M, Aguilar-Bryan L, Bryan J, Henquin JC (2007). Glucose stimulates Ca^{2+} influx and insulin secretion in 2-week-old β-cells lacking ATP-sensitive K^+ channels. *J. Biol. Chem*., **282**(3): 1747-56.

161. Grodsky GM, Curry D, Landahl H, Bennett L (1969). Further studies on the dynamic aspects of insulin release in vitro with evidence for a two-compartmental storage system. *Acta. Diabet. Lat*., **6**(Suppl. 1): 554 -78.

162. Ma X, Zhang Y, Gromada J, Sewing S, Berggren PO, Buschard K, Salehi A,

Vikman J, Rorsman P, Eliasson L (2005). Glucagon stimulates exocytosis in mouse and rat pancreatic α-cells by binding to glucagon receptors. *Mol. Endocrinol.*, **19**(1): 198-212.

163. Sharp GW (1979). The adenylate cyclase-cyclic AMP system in islets of Langerhans and its role in the control of insulin release. *Diabetologia*, **16**: 287-96.

164. Prentki M, Matschinsky F (1987). Ca^{2+}, cAMP, and phospholipid-derived messengers in coupling mechanisms of insulin secretion. *Physiol. Rev*., **67**: 1185-1248.

165. Nolan CJ, Madiraju MS, Delghingaro-Augusto V, Peyot ML, Prentki M (2006). Fatty acid signaling in the β-cell and insulin secretion. *Diabetes*, **55**(Suppl. 2): S16-23.

166. Yaney GC, Corkey BE (2003). Fatty acid metabolism and insulin secretion in pancreatic β-cells. *Diabetologia*, **46**(10): 1297-312.

167. Zawalich WS, Yamazaki H, Zawalich KC, Cline G (2004). Comparative effects of amino acids and glucose on insulin secretion from isolated rat or mouse islets. *J. Endocrinol.*, **183**(2): 309-19.

168. Nolan CJ, Prentki M (2008). The islet β-cell: fuel responsive and vulnerable. *Trends Endocrinol. Metab.*, **19**(8): 285-91.

169. Valdeolmillos M, Santos RM, Contreras D, Soria B, Rosario LM (1989). Glucose-induced oscillations of intracellular Ca^{2+} concentration resembling bursting electrical activity in single mouse islets of Langerhans. *FEBS Lett.*, **259**(1): 19-23.

170. Benninger RK, Zhang M, Head WS, Satin LS, Piston DW (2008). Gap junction coupling and calcium waves in the pancreatic islet. *Biophys. J.*, **95**(11): 5048-61.

171. Bergsten P, Grapengiesser E, Gylfe E, Tengholm A, Hellman B (1994). Synchronous oscillations of cytoplasmic Ca^{2+} and insulin release in glucose-stimulated pancreatic islets. *J. Biol. Chem*., **269**: 8749-53.

172. Rocheleau JV, Walker GM, Head WS, McGuinness OP, Piston DW (2004). Microfluidic glucose stimulation reveals limited coordination of intracellular Ca^{2+} activity oscillations in pancreatic islets. *Proc. Natl. Acad. Sci. USA*, **101**(35): 12899-903.

173. Nunemaker CS, Bertram R, Sherman A, Tsaneva-Atanasova K, Daniel CR, Satin LS (2006). Glucose modulates $[Ca^{2+}]_i$ oscillations in pancreatic islets via ionic and glycolytic mechanisms. *Biophys. J.*, **91**(6): 2082-96.

174. Longo EA, Tornheim K, Deeney JT, Varnum BA, Tillotson D, Prentki M, Corkey BE (1991). Oscillations in cytosolic free Ca^{2+}, oxygen consumption, and insulin secretion in glucose-stimulated rat pancreatic islets. *J. Biol. Chem*., **266**: 9314-19.

175. Bertram R, Previte J, Sherman A, Kinard TA, Satin LS (2000). The phantom burster model for pancreatic β-cells. *Biophys. J.*, **79**(6): 2880-92.

176. Nunemaker CS, Bertram R, Sherman A, Tsaneva-Atanasova K, Daniel CR, Satin LS (2006). Glucose modulates $[Ca^{2+}]_i$ oscillations in pancreatic islets via ionic and glycolytic mechanisms. *Biophys. J.*, **91**(6): 2082-96.

177. Beauvois MC, Merezak C, Jonas JC, Ravier MA, Henquin JC, Gilon P (2006). Glucose-induced mixed $[Ca^{2+}]$c oscillations in mouse β-cells are controlled by the membrane potential and the SERCA3 Ca^{2+}-ATPase of the endoplasmic reticulum. *Am. J. Physiol. Cell Physiol*., **290**: C1503-11.

178. Gilon P, Shepherd RM, Henquin JC (1993). Oscillations of secretion driven by oscillations of cytoplasmic Ca^{2+} as evidenced in single pancreatic islets. *J. Biol. Chem*., **268**: 22265-8.

179. Easley CJ, Rocheleau JV, Head WS, Piston DW (2009). Quantitative measurement of zinc secretion from pancreatic islets with high temporal resolution using droplet-based microfluidics. *Anal. Chem.*, **81**(21): 9086-95.

180. Rocheleau JV, Remedi MS, Granada B, Head WS, Koster JC, Nichols CG, Piston DW (2006). Critical role of gap junction coupled K_{ATP} channel activity for regulated insulin secretion. *PLoS Biol.*, **4**(2): e26.

181. Ravier MA, Güldenagel M, Charollais A, Gjinovci A, Caille D, Söhl G, Wollheim CB, Willecke K, Henquin JC, Meda P (2005). Loss of connexin36 channels alters β-cell coupling, islet synchronization of glucose-induced Ca^{2+} and insulin oscillations, and basal insulin release. *Diabetes*, **54**(6): 1798-807.

182. Harris AL (2001). Emerging issues of connexin channels: biophysics fills the gap. *Q. Rev. Biophys*., **34**(3): 325-472.

183. Srinivas M, Rozental R, Kojima T, Dermietzel R, Mehler M, Condorelli DF, Kessler JA, Spray DC (1999). Functional properties of channels formed by the neuronal gap junction protein connexin36. *J. Neurosci.*, **19**(22): 9848-55.

184. Teubner B, Degen J, Söhl G, Güldenagel M, Bukauskas FF, Trexler EB, Verselis VK, De Zeeuw CI, Lee CG, Kozak CA, Petrasch-Parwez E, Dermietzel R, Willecke K (1999). Functional expression of the murine connexin-36 gene coding for a neuron-specific gap junctional protein. *J. Membr. Biol.*, **176**(3):249-62.

185. Zhang Q, Galvanovskis J, Abdulkader F, Partridge CJ, Göpel SO, Eliasson L, Rorsman P (2008). Cell coupling in mouse pancreatic β-cells measured in intact islets of Langerhans. *Philos. Transact. A. Math. Phys. Eng. Sci*., **366**(1880): 3503-23.

186. Charpantier E, Cancela J, Meda P (2007). β-cells preferentially exchange cationic molecules via connexin-36 gap junction channels. *Diabetologia*, **50**(11): 2332-41.

187. Bergsten P, Westerlund J, Liss P, Carlsson PO (2002). Primary in vivo oscillations of metabolism in the pancreas. *Diabetes*, **51**(3): 699-703.

188. Nunemaker CS, Zhang M, Wasserman DH, McGuinness OP, Powers AC, Bertram R, Sherman A, Satin LS (2005). Individual mice can be distinguished by the period of their islet calcium oscillations: is there an intrinsic islet period that is imprinted in vivo? *Diabetes*, **54**(12): 3517-22.

189. Lang DA, Matthews DR, Peto J, Turner RC (1979). Cyclic oscillations of basal plasma glucose and insulin concentrations in human beings. *N. Engl J. Med.*, **301**(19): 1023-7.

190. Song SH, McIntyre SS, Shah H, Veldhuis JD, Hayes PC, Butler PC (2000). Direct measurement of pulsatile insulin secretion from the portal vein in human subjects. *J. Clin. Endocrinol. Metab.*, **85**(12): 4491-9.

191. Quesada I, Todorova MG, Alonso-Magdalena P, Beltrá M, Carneiro EM, Martin F, Nadal A, Soria B (2006). Glucose induces opposite intracellular Ca^{2+} concentration oscillatory patterns in identified α- and β-cells within intact human islets of Langerhans. *Diabetes*, **55**(9): 2463-9.

192. Serre-Beinier V, Bosco D, Zulianello L, Charollais A, Caille D, Charpantier E, Gauthier BR, Diaferia GR, Giepmans BN, Lupi R, Marchetti P, Deng S, Buhler L, Berney T, Cirulli V, Meda P (2009). Cx36 makes channels coupling human pancreatic β-cells, and correlates with insulin expression. *Hum. Mol. Genet*., **18**(3): 428-39.

193. Pileggi A, Fenjves ES, Klein D, Ricordi C, Pastori RL (2004). Protecting pancreatic β-cells. I*UBMB Life*, **56**(7): 387-94.

194. Yamamoto T, Horiguchi A, Ito M, Nagata H, Ichii H, Ricordi C, Miyakawa S (2009). Quality control for clinical islet transplantation: organ procurement and preservation, the islet processing facility, isolation, and potency tests. *J. Hepatobiliary Pancreat. Surg.*, **16**(2): 131-6.

195. Bingley PJ, Matthews DR, Williams AJ, Bottazzo GF, Gale EA (1992). Loss of regular oscillatory insulin secretion in islet cell antibody positive non-diabetic subjects. *Diabetologia*, **35**(1): 32-8.

196. Lang DA, Matthews DR, Burnett M, Turner RC (1981). Brief, irregular oscillations of basal plasma insulin and glucose concentrations in diabetic man. *Diabetes*, **30**(5): 435-9.

197. Matthews DR, Lang DA, Burnett MA, Turner RC (1983). Control of pulsatile insulin secretion in man. *Diabetologia*, **24**(4): 231-7.

198. Reza Mirbolooki M, Taylor GE, Knutzen VK, Scharp DW, Willcourt R, Lakey JR (2009). Pulsatile intravenous insulin therapy: the best practice to reverse diabetes complications? *Med. Hypotheses*, **73**(3): 363-9.

199. Bratusch-Marrain PR, Komjati M, Waldhäusl WK. (1986). Efficacy of pulsatile versus continuous insulin administration on hepatic glucose production and glucose utilization in type-I diabetic humans. *Diabetes*, **35**(8): 922-6.

200. Sima AA (2006). Pathological mechanisms involved in diabetic neuropathy: can we slow the process? *Curr. Opin. Investig. Drugs*, **7**(4): 324-37.

201. Langerhans P (1869). Beitrage zur mikroskopischen Anatomie der Bauchspeicheldruse., *Inaug. Diss.*

202. Renaut (1879), *Compte rendus*, **89**: 247.

203. Kuhne and Heidelgerg (1882). *Untersuch. aus. d. Physiol. Institut*, **2**: 448.

204. Harris G (1894). *J. Physiol*., **15**: 349.

205. Podwysozzki (1882). *Arch. f. Mikr. Anat*. , **21**: 765.

206. Lane MA (1907). The cytological characters of the areas of Langerhans. *Am. J. Anat*., **7**: 409-22.

207. Dale HH (1905). On the "Islets of Langerhans" in the Pancreas. *Philosophical Transactions of the Royal Society of London*. *Series B, Containing Papers of a Biological Character*, **197**: 25-46.

208. Opie (1901). *Journ. of Experim. Medecine*: 397-527.

209. von Mering JV and Minkowski O (1889). Diabetes mellitus nach Pankreasextirpation. *Zbl. Klin. Med.*, **10**: 393.

210. Banting F, Best C (1922). The internal secretion of the pancreas. *J. Lab. Clin. Med*., **7**: 251.

211. Best C (1962). *Canad. Med. Ass. J*., **87**: 1046-51.

212.. Murlin JR, Clough HD, Gibbs CBF, and Stokes AM (1923). Aqueous extracts of pancreas I. Influence on the carbohydrate metabolism of depancreatized animals. *J. Biol. Chem*., 56: 253-96.

213. Kimball CP, Murlin JR (1923). Aqueous extracts of pancreas. III: Some precipitation reaction of insulin. *J. Biol. Chem*., **58**: 337.

214. Sutherland EW, de Duve C (1948). Origin and distribution of the hyperglycemic-glycogenolytic factor of the pancreas. *J. Biol. Chem*., **175**: 663-74.

215. Foa PP, Santamaria S, Weinstein HR, Berger S, Smith JA (1952). Secretion of the hyperglycemic-glycogenolytic factor in normal dogs. *Am. J. Physiol*., **171**(1): 32-6.

216. Staub A, Sinn L, Behrens OK (1955). Purification and crystallization of glucagon. *J. Biol. Chem*., **214**: 619-32.

217. Bromer WW, Sinn LG, Staub A, Behrens OK (1957). The amino acid sequence of glucagon. *Diabetes*, **6**(3): 234-8.

218. Unger RH, Eisentraut AM, McCall MS, Madison LL (1961). Glucagon antibodies and immunoassay for glucagon. *J. Clin. Invest*., **40**: 1280-89.

219. Baum J, Simons BE Jr, Unger RH, Madison LL (1962). Localization of glucagon in the α cells in the pancreatic islet by immunofluorescent technics. *Diabetes*, **11**: 371-4.

220. Lacy PE, Kostianovsky M (1967). Method for the isolation of intact islets of Langerhans from the rat pancreas. *Diabetes*, **16**: 35-9.

221. Jin T (2008). Mechanisms underlying proglucagon gene expression. *J. Endocrin*., **198**: 17-28.

222. Herzig S, Fuzesi L, Knepel W (2000). Heterodimeric Pbx-Prep1 homeodomain protein binding to the glucagon gene restricting transcription in a cell type-dependent manner. *J. Biol. Chem*., **275**(36): 27989-99.

223. Morel C, Cordier-Bussat M, Philippe J (1995). The upstream promoter element of the glucagon gene G1 confers pancreatic cell-specific expression. *J. Biol. Chem*., **270**: 3046-55.

224. Ritz-Laser B, Estreicher A, Klages N, Saule S, Philippe J (1999). Pax-6 and Cdx-2/3 interact to activate glucagon gene expression on the G1 control element. *J. Biol. Chem*., **274**: 4124-32.

225. Wang M, Drucker DJ (1995). The LIM domain homeobox gene isl-1 is a positive regulator of islet cell-specific proglucagon gene transcription. *J. Biol. Chem*., **270**(21): 12646-52.

226. Hussain MA, Lee J, Miller CP, Habener JF (1997). POU domain transcription factor brain 4 confers pancreatic α-cell-specific expression of the proglucagon gene through

interaction with a novel proximal promoter G1 element. *Mol. Cell. Biol*., **17**: 7186-94.

227. Gauthier BR, Schwitzgebel VM, Zaiko M, Mamin A, Ritz-Laser B, and Philippe J (2002). Hepatic Nuclear Factor-3 (HNF-3 or Foxa2) Regulates Glucagon Gene Transcription by Binding to the G1 and G2 Promoter Elements. *Mol. Endocrinol.*, **16**: 170-83.

228. Knepel W, Chafitz J, Habener JF (1990). Transcriptional activation of the rat glucagon gene by the cyclic AMP-responsive element in pancreatic islet cells. *Mol. Cell. Biol*., **10**(12): 6799-6804.

229. Bell GI, Santerre RF, Mullenbach GT (1983). Hamster preproglucagon contains the sequence of glucagon and two related peptides. *Nature*, **302**: 716-8.

230. Bell GI, Sanchez-Pescador R, Laybourn PJ, Najarian RC (1983). Exon duplication and divergence in the human preproglucagon gene. *Nature*, **304**: 368-71.

231. Lund PK, Goodman RH, Dee PC, Habener JF (1982). Pancreatic preproglucagon cDNA contains two glucagon-related coding sequences arranged in tandem. *Proc. Natl. Acad. Sci. USA*, **79**: 345-9.

232. Patzelt C, Tager HS, Carroll RJ, Steiner DF (1979). Identification and processing of proglucagon in pancreatic islets. *Nature*, **282**: 260-6.

233. Mojsov S, Heinrich G, Wilson IB, Ravazzola M, Orci L, Habener JF (1986). Proglucagon gene expression in pancreas and intestine diversifies at the level of post-translational processing. *J. Biol. Chem*., **261**: 11880-9.

234. Larsen PJ, Tang-Christensen M, Holst JJ, Orskov C (1997). Distribution of glucagon-like peptide-1 and other preproglucagon-derived peptides in the rat hypothalamus and brainstem. *Neuroscience*, **77**: 257-70.

235. Egea JC, Hirtz C, Deville de Periere D (2003). Preproglucagon mRNA expression in adult rat submandibular glands. *Diabetes Nutr. Metab*., **16**: 130-3.

236. Dey A, Lipkind GM, Rouillé Y, Norrbom C, Stein J, Zhang C, Carroll R, Steiner DF (2005). Significance of prohormone convertase-2, PC2, mediated initial cleavage at the proglucagon interdomain site, Lys70-Arg71, to generate glucagon. *Endocrinology*, **146**(2): 713-27.

237. Steiner DF (1998). The proprotein convertases. *Curr. Opin. Chem. Biol*., **2**(1): 31-9.

238. Rouille Y, Westermark G, Martin SK, Steiner DF (1994). Proglucagon is processed to glucagon by prohormone convertase 2 in αTC1–6 cells. *Proc. Natl. Acad. Sci. USA*, **91**: 3242-6.

239. Furuta M, Zhou A, Webb G, Carroll R, Ravazzola M, Orci L, Steiner DF (2001). Severe defect in proglucagon processing in islet α-cells of prohormone convertase-2 null mice. *J. Biol. Chem*., **276**: 27197-202.

240. Scopsi L, Gullo M, Rilke F, Martin S, Steiner DF (1995). Proprotein convertases (PC1/PC3 and PC2) in normal and neoplastic human tissues: their use as markers of neuroendocrine differentiation. *J. Clin. Endocrinol. Metab.*, **80**(1): 294-301.

241. Jansen E, Ayoubi TA, Meulemans SM, van De Ven WJ (1997). Regulation of human prohormone convertase 2 promoter activity by the transcription factor EGR-1. *Biochem. J*., **328**: 69-74.

242. Mbikay M, Raffin-Sanson ML, Sirois F, Kalenga L, Chretien M, Seidah NG (2002). Characterization of a repressor element in the promoter region of proprotein convertase 2 (PC2) gene. *Brain Res. Mol. Brain Res*., **102**: 35-47.

243. Shen X, Li QL, Brent GA, Friedman TC (2005). Regulation of regional expression in rat brain PC2 by thyroid hormone/characterization of novel negative thyroid hormone response elements in the PC2 promoter. *Am. J. Physiol. Endocrinol. Metab*., **288**: E236-45.

244. Yatoh S, Akashi T, Chan PP, Kaneto H, Sharma A, Bonner-Weir S, Weir GC (2007). NeuroD and reaggregation induce β-cell specific gene expression in cultured hepatocytes. *Diabetes Metab. Res. Rev*., **23**: 239-49.

245. Katz LS, Gosmain Y, Marthinet E, Philippe J (2009). Pax6 regulates the proglucagon processing enzyme PC2 and its chaperone 7B2. *Mol. Cell. Biol*., **29**(8): 2322-34.

246. Steiner DF (1998). The proprotein convertases. *Curr. Opin. Chem. Biol*., **2**(1): 31-9.

247. Rodbell M, Krans HM, Pohl SL, Birnbaumer L (1971). The glucagon-sensitive adenyl cyclase system in plasma membranes of rat liver. 3. Binding of glucagon: method of assay and specificity. *J. Biol. Chem*., **246**(6): 1861-71.

248. Jelinek LJ, Lok S, Rosenberg GB, Smith RA, Grant FJ, Biggs S, Bensch PA, Kuijper JL, Sheppard PO, Sprecher CA, O'Hara PJ, Foster D, Walker KM, Chen LHJ, McKernan PA, Kindsvogel W (1993). Expression cloning and signaling properties of the rat glucagon receptor. *Science*, **259**: 1614-6.

249. Segre GV, Goldring SR (1993). Receptors for secretin, calcitonin, parathyroid hormone (PTH)/PTH-related peptide, vasoactive intestinal peptide, glucagonlike peptide 1, growth hormone-releasing hormone, and glucagon belong to a newly discovered G-protein-linked receptor family. *Trends Endocrinol. Metab.*, **4**(10): 309-14.

250. Laburthe M, Couvineau A, Gaudin P, Maoret JJ, Rouyer-Fessard C, Nicole P (1996). Receptors for VIP, PACAP, secretin, GRF, glucagon, GLP-1, and other members of their new family of G protein-linked receptors: structure-function relationship with special reference to the human VIP-1 receptor. *Ann. N. Y. Acad. Sci*., **805**: 94-109.

251. Authier F, Desbuquois B (2008). Glucagon receptors. *Cell. Mol. Life Sci*., **65**(12): 1880-99.

252. Xu Y, Xie X (2009). Glucagon receptor mediates calcium signaling by coupling to Gαq/11 and Gα i/o in HEK293 cells. *J. Recept. Signal. Transduct. Res*., **29**(6): 318-25.

253. Authier F, Desbuquois B, De Galle B (1992). Ligand-mediated internalization of glucagon receptors in intact rat liver. *Endocrinology*, **131**: 447-57.

254. Abrahamsen N, Lundgren K, Nishimura E (1995). Regulation of glucagon receptor mRNA in cultured primary rat hepatocytes by glucose and cAMP. *J. Biol. Chem*., **270**(26): 15853-7.

255. Dunphy JL, Taylor RG, Fuller PJ (1998). Tissue distribution of rat glucagon receptor and GLP-1 receptor gene expression. *Mol. Cell. Endocrinol*., **141**(1-2): 179-86.

256. Ahloulay M, Bouby N, Machet F, Kubrusly M, Coutaud C, Bankir L (1992). Effects of glucagon on glomerular filtration rate and urea and water excretion. *Am. J. of Physiol. Renal Physiol*., **263**: F24-36.

257. Chiba S (1975). Positive chronotropic and inotropic effects of glucagon on the canine isolated atrium. *Tohoku J. Exp. Med*., **115**(1): 61-5.

258. Carlson MG, Snead WL, Campbell PJ (1993). Regulation of free fatty acid metabolism by glucagon. *J. Clin. Endocrinol. Metab.*, **77**: 11-5.

259. Geary N (1990). Pancreatic glucagon signals postprandial satiety. *Neurosci. Biobehav. Rev*., **14**(3): 323-38.

260. Charlton MR, Adey DB, Nair KS (1996). Evidence for a catabolic role of glucagon during an amino acid load. *J. Clin. Invest*., **98**(1): 90-9.

261. Brunicardi FC, Kleinman R, Moldovan S, Nguyen TH, Watt PC, Walsh J, Gingerich R (2001). Immunoneutralization of somatostatin, insulin, and glucagon causes alterations in islet cell secretion in the isolated perfused human pancreas. *Pancreas*, **23**(3): 302-8.

262. Vincent M, Guz Y, Rozenberg M, Webb G, Furuta M, Steiner D, Teitelman G (2003). Abrogation of protein convertase 2 activity results in delayed islet cell differentiation and maturation, increased α-cell proliferation, and islet neogenesis. *Endocrinology*, **144**: 4061-9.

263. Gelling RW, Du XQ, Dichmann DS, Romer J, Huang H, Cui L, Obici S, Tang B, Holst JJ, Fledelius C, Johansen PB, Rossetti L, Jelicks LA, Serup P, Nishimura E, Charron MJ (2003). Lower blood glucose, hyperglucagonemia, and pancreatic α-cell hyperplasia in glucagon receptor knockout mice. *Proc. Natl. Acad. Sci. USA*, **100**: 1438-43.

264. Jaspan JB, Polonsky KS, Lewis M, Pensler J, Pugh W, Moossa AR, Rubenstein AH (1981). Hepatic metabolism of glucagon in the dog: contribution of the liver to overall metabolic disposal of glucagon. *Am. J. Physiol*., **240**(3): E233-44.

265. Kervran A, Dubrasquet M, Blache P, Martinez J, Bataille D (1990). Metabolic clearance rates of oxyntomodulin and glucagon in the rat: contribution of the kidney. *Regul. Pept..*, **31**(1): 41-52.

266. Pospisilik JA, Hinke SA, Pederson RA, Hoffmann T, Rosche F, Schlenzig D, Glund K, Heiser U, McIntosh CH, Demuth H (2001). Metabolism of glucagon by dipeptidyl peptidase IV (CD26). *Regul. Pept..*, **96**(3): 133-41.

267. Mallat A, Pavoine C, Dufour M, Lotersztajn S, Bataille D, Pecker F (1987). A glucagon fragment is responsible for the inhibition of the liver Ca^{2+} pump by glucagon. *Nature*, **325**: 620-2.

268. Dalle S, Fontés G, Lajoix AD, LeBrigand L, Gross R, Ribes G, Dufour M, Barry L, LeNguyen D, Bataille D (2002). Miniglucagon (glucagon 19-29): a novel regulator of the pancreatic islet physiology. *Diabetes*, **51**(2): 406-12.

269. Masharani U and German MS (2007). Chapter 18. Pancreatic Hormones & Diabetes Mellitus. *Greenspan's Basic & Clinical Endocrinology*, *8th edition*.

270. Weir GC, Knowlton SD, Martin DB (1974). Glucagon secretion from the perfused rat pancreas. Studies with glucose and catecholamines. *J. Clin. Invest*., **54**(6): 1403-12.

271. Raum WJ, Swerdloff RS, Garner D, Laks H, Laks MM (1984). Chronic norepinephrine infusion and insulin and glucagon secretion in the dog. *Am. J. Physiol*., **246**(3 Pt 1): E232-6.

272. Santiago JV, Clarke WL, Shah SD, Cryer PE (1980). Epinephrine, norepinephrine, glucagon, and growth hormone release in association with physiological decrements in the plasma glucose concentration in normal and diabetic man. *J. Clin. Endocrinol. Metab.*, **51**(4): 877-83.

273. Leclercq-Meyer V, Marchand J, Malaisse WJ (1977). An arginine-like effect of the "fumarate + glutamate + pyruvate" mixture on glucagon release. *Life Sci.*, **20**(7): 1193-8.

274. Goodner CJ, Walike BC, Koerker DJ, Ensinck JW, Brown AC, Chideckel EW,

Palmer J, Kalnasy L (1977). Insulin, glucagon, and glucose exhibit synchronous, sustained oscillations in fasting monkeys. *Science*, **195**(4274): 177-9.

275. Stagner JI, Samols E, Weir GC (1980). Sustained oscillations of insulin, glucagon, and somatostatin from the isolated canine pancreas during exposure to a constant glucose concentration. *J. Clin. Invest.*, **65**(4): 939-42.

276. Goodner CJ, Koerker DJ, Stagner JI, Samols E (1991). In vitro pancreatic hormonal pulses are less regular and more frequent than in vivo. *Am. J. Physiol.*, **260**(3 Pt 1): E422-9.

277. Hellman B, Salehi A, Gylfe E, Dansk H, Grapengiesser E (2009). Glucose Generates coincident insulin and somatostatin pulses and antisynchronous glucagon pulses from human pancreatic islets. *Endocrinology*, **150**(12): 5334-40.

278. Grapengiesser E, Salehi A, Qader SS, Hellman B (2006). Glucose induces glucagon release pulses antisynchronous with insulin and sensitive to purinoceptor inhibition. *Endocrinology*, **147**(7): 3472-7.

279. Weigle DS, Koerker DJ, Goodner CJ (1984). Pulsatile glucagon delivery enhances glucose production by perifused rat hepatocytes. *Am. J. Physiol.*, **247**(4 Pt 1): E564-8.

280. Weigle DS, Goodner CJ (1986). Evidence that the physiological pulse frequency of glucagon secretion optimizes glucose production by perifused rat hepatocytes. *Endocrinology*, **118**(4): 1606-13.

281. Goodner CJ, Koerker DJ, Weigle DS, McCulloch DK (1989). Decreased insulin- and glucagon-pulse amplitude accompanying β-cell deficiency induced by streptozocin in baboons. *Diabetes*, **38**(7): 925-31.

282. Heimberg H, De Vos A, Pipeleers D, Thorens B, Schuit F (1995). Differences in glucose transporter gene expression between rat pancreatic α- and β-cells are correlated to differences in glucose transport but not in glucose utilization. *J. Biol. Chem.*, **270**(15): 8971-5.

283. Heimberg H, De Vos A, Moens K, Quartier E, Bouwens L, Pipeleers D, Van Schaftingen E, Madsen O, Schuit F (1996). The glucose sensor protein glucokinase is expressed in glucagon-producing α-cells. *Proc. Natl. Acad. Sci. USA*, **93**(14): 7036-41.

284. Bokvist K, Olsen HL, Høy M, Gotfredsen CF, Holmes WF, Buschard K, Rorsman P, Gromada J (1999). Characterisation of sulphonylurea and ATP-regulated K^+ channels in rat pancreatic α-cells. *Pflugers Arch.*, **438**(4): 428-36.

285. Göpel SO, Kanno T, Barg S, Weng XG, Gromada J, Rorsman P (2000). Regulation of glucagon release in mouse α-cells by K_{ATP} channels and inactivation of TTX-sensitive

Na^+ channels. *J. Physiol*., **528**(Pt 3): 509-20.

286. Gromada J, Bokvist K, Ding WG, Barg S, Buschard K, Renström E, Rorsman P (1997). Adrenaline stimulates glucagon secretion in pancreatic α-cells by increasing the Ca^{2+} current and the number of granules close to the L-type Ca^{2+} channels. *Gen. Physiol*., **110**(3): 217-28.

287. Vignali S, Leiss V, Karl R, Hofmann F, Welling A (2006). Characterization of voltage-dependent sodium and calcium channels in mouse pancreatic α- and β-cells. *J. Physiol*., **572**(Pt 3): 691-706.

288. Yoshimoto Y, Fukuyama Y, Horio Y, Inanobe A, Gotoh M, Kurachi Y (1999). Somatostatin induces hyperpolarization in pancreatic islet α-cells by activating a G protein-gated K^+ channel. *FEBS Lett.*, **444**(2-3): 265-9.

289. Gromada J, Høy M, Olsen HL, Gotfredsen CF, Buschard K, Rorsman P, Bokvist K (2001). G_{i2} proteins couple somatostatin receptors to low-conductance K^+ channels in rat pancreatic α-cells. *Pflugers Arch*., **442**(1): 19-26.

290. Gromada J, Franklin I, Wollheim CB (2007). α-cells of the endocrine pancreas: 35 years of research but the enigma remains. *Endocr. Rev*., **28**(1): 84-116.

291. MacDonald PE, De Marinis YZ, Ramracheya R, Salehi A, Ma X, Johnson PR, Cox R, Eliasson L, Rorsman P (2007). A K_{ATP} channel-dependent pathway within α-cells regulates glucagon release from both rodent and human islets of Langerhans. *PLoS Biol.*, **5**(6): e143.

292. Göpel S, Zhang Q, Eliasson L, Ma XS, Galvanovskis J, Kanno T, Salehi A, Rorsman P (2004). Capacitance measurements of exocytosis in mouse pancreatic α-, β- and δ-cells within intact islets of Langerhans. *J. Physiol*., **556**(Pt 3): 711-26.

293. Wendt A, Birnir B, Buschard K, Gromada J, Salehi A, Sewing S, Rorsman P, Braun M (2004). Glucose inhibition of glucagon secretion from rat α-cells is mediated by GABA released from neighboring β-cells. *Diabetes*, **53**(4): 1038-45.

294. Liu YJ, Vieira E, Gylfe E (2004). A store-operated mechanism determines the activity of the electrically excitable glucagon-secreting pancreatic α-cell. *Cell Calcium*, **35**(4): 357-65.

295. Vignali S, Leiss V, Karl R, Hofmann F, Welling A (2006). Characterization of voltage-dependent sodium and calcium channels in mouse pancreatic α- and β-cells. *J. Physiol*., **572**: 691-706.

296. Quoix N, Cheng-Xue R, Mattart L, Zeinoun Z, Guiot Y, Beauvois MC, Henquin JC, Gilon P (2009)., Glucose and pharmacological modulators of ATP-sensitive K^+ channels

control [Ca^{2+}]*c* by different mechanisms in isolated mouse α-cells. *Diabetes*, **58**(2): 412-21.

297. Muñoz A, Hu M, Hussain K, Bryan J, Aguilar-Bryan L, Rajan AS (2005). Regulation of glucagon secretion at low glucose concentrations: evidence for adenosine triphosphate-sensitive potassium channel involvement. *Endocrinology*, **146**(12): 5514-21.

298. Leung YM, Ahmed I, Sheu L, Tsushima RG, Diamant NE, Gaisano HY (2006). Two populations of pancreatic islet α-cells displaying distinct Ca^{2+} channel properties. *Biochem. Biophys. Res. Commun*., **345**(1): 340-4.

299. Kanno T, Gopel SO, Rorsman P, Wakui M (2002). Cellular function in multicellular system for hormone-secretion: electrophysiological aspect of studies on α-, β- and δ-cells of the pancreatic islet. *Neurosci. Res. Rev*., **42**(2): 79-90.

300. Zhang Y, Zhang N, Gyulkhandanyan AV, Xu E, Gaisano HY, Wheeler MB, Wang Q (2008). Presence of functional hyperpolarisation-activated cyclic nucleotide-gated channels in clonal α cell lines and rat islet α cells. *Diabetologia*, **51**(12): 2290-8.

301. Banarer S, McGregor VP, Cryer PE (2002). Intraislet hyperinsulinemia prevents the glucagon response to hypoglycemia despite an intact autonomic response. *Diabetes*, **51**: 958-65.

302. Zhou H, Tran PO, Yang S, Zhang T, LeRoy E, Oseid E, Robertson RP (2004). Regulation of α-cell function by the β-cell during hypoglycemia in wistar rats: the "switch-off" hypothesis. *Diabetes*, **53**: 1482-7.

303. Hope KM, Tran PO, Zhou H, Oseid E, Leroy E, Robertson RP (2004). Regulation of α-cell function by the β-cell in isolated human and rat islets deprived of glucose: the "switch-off" hypothesis. *Diabetes*, **53**:1488-95.

304. Kawamori D, Kurpad AJ, Hu J, Liew CW, Shih JL, Ford EL, Herrera PL, Polonsky KS, McGuinness OP, Kulkarni RN (2009). Insulin signaling in α-cells modulates glucagon secretion in vivo. *Cell. Metab*., **9**(4): 350-61.

305. Diao J, Asghar Z, Chan CB, Wheeler MB (2005). Glucose-regulated glucagon secretion requires insulin receptor expression in pancreatic α-cells. *J. Biol. Chem*., **280**(39): 33487-96.

306. Slucca M, Harmon JS, Oseid EA, Bryan J, Robertson RP (2010). ATP-sensitive K^+ channel mediates the zinc switch-off signal for glucagon response during glucose deprivation. *Diabetes*, **59**(1): 128-34.

307. Zhou H, Zhang T, Harmon JS, Bryan J, Robertson RP (2007). Zinc, not insulin, regulates the rat α-cell response to hypoglycemia in vivo. *Diabetes*, **56**(4): 1107-12.

308. Farhy LS, Du Z, Zeng Q, Veldhuis PP, Johnson ML, Brayman KL, McCall AL (2008). Amplification of pulsatile glucagon counterregulation by switch-off of α-cell-suppressing signals in streptozotocin-treated rats. *Am. J. Physiol. Endocrinol. Metab*., **295**(3): E575-85.

309. Farhy LS, McCall AL (2009). Pancreatic network control of glucagon secretion and counterregulation. *Methods Enzymol*., **467**: 547-81.

310. Westphal SA, Gannon MC, Nuttall FQ (1990). Metabolic response to glucose ingested with various amounts of protein. *Am. J. Clin. Nutr*., **52**(2):267-72.

311. Olsen HL, Theander S, Bokvist K, Buschard K, Wollheim CB, Gromada J (2005). Glucose stimulates glucagon release in single rat α-cells by mechanisms that mirror the stimulus-secretion coupling in β-cells. *Endocrinology*, **146**: 4861-70.

312. Pagliara AS, Stillings SN, Hover B, Martin DM, Matschinsky FM (1974). Glucose modulation of amino acid-induced glucagon and insulin release in the isolated perfused rat pancreas. *J. Clin. Invest*., **54**(4): 819-32.

313. Unger RH, Ohneda A, Aguilar-Parada E, Eisentraut AM (1969). The role of aminogenic glucagon secretion in blood glucose homeostasis. *J. Clin. Invest*., **48**(5): 810-22.

314. Gerich JE, Charles MA, Grodsky GM (1974). Characterization of the effects of arginine and glucose on glucagon and insulin release from the perfused rat pancreas. *J. Clin. Invest*., **54**(4): 833-41.

315. Gerich JE, Charles MA, Grodsky GM (1976). Regulation of pancreatic insulin and glucagon secretion. *Annu. Rev. Physiol*., **38**: 353-88.

316. Pipeleers DG, Schuit FC, Van Schravendijk CF, Van de Winkel M (1985). Interplay of nutrients and hormones in the regulation of glucagon release. *Endocrinology*, **117**(3): 817-23.

317. Henningsson R, Lundquist I (1998). Arginine-induced insulin release is decreased and glucagon increased in parallel with islet NO production. *Am. J. Physiol*., **275**(3 Pt 1): E500-6.

318. Berts A, Gylfe E, Hellman B (1997). Cytoplasmic Ca^{2+} in glucagon-producing pancreatic α-cells exposed to carbachol and agents affecting Na^{+} fluxes. *Endocrine*, **6**: 79-83.

319. Shiota C, Rocheleau JV, Shiota M, Piston DW, Magnuson MA (2005). Impaired glucagon secretory responses in mice lacking the type-1 sulfonylurea receptor. *Am. J. Physiol. Endocrinol. Metab*., **289**(4): E570-7.

320. Zhou YP, Grill VE (1994). Long-term exposure of rat pancreatic islets to fatty acids inhibits glucose-induced insulin secretion and biosynthesis through a glucose fatty acid cycle. *J. Clin. Invest*., **93**(2): 870-6.

321. Edwards JC, Taylor KW (1970). Fatty acids and the release of glucagon from isolated guinea-pig islets of Langerhans incubated in vitro. *Biochim. Biophys. Acta*., **215**(2): 310-5.

322. Edwards JC, Howell SL, Taylor KW (1969). Fatty acids as regulators of glucagon secretion. *Nature*, **224**(5221): 808-9.

323. Bollheimer LC, Landauer HC, Troll S, Schweimer J, Wrede CE, Schölmerich J, Buettner R (2004). Stimulatory short-term effects of free fatty acids on glucagon secretion at low to normal glucose concentrations. *Metabolism*, **53**(11): 1443-8.

324. Olofsson CS, Salehi A, Göpel SO, Holm C, Rorsman P (2004). Palmitate stimulation of glucagon secretion in mouse pancreatic α-cells results from activation of L-type calcium channels and elevation of cytoplasmic calcium. *Diabetes*, **53**: 2836-43.

325. Hong J, Abudula R, Chen J, Jeppesen PB, Dyrskog SE, Xiao J, Colombo M, Hermansen K (2005). The short-term effect of fatty acids on glucagon secretion is influenced by their chain length, spatial configuration, and degree of unsaturation: studies in vitro. *Metabolism*, **54**(10): 1329-36.

326. Gremlich S, Bonny C, Waeber G, Thorens B (1997). Fatty acids decrease IDX-1 expression in rat pancreatic islets and reduce GLUT2, glucokinase, insulin, and somatostatin levels. *J. Biol. Chem*., **272**(48): 30261-9.

327. Hong J, Chen L, Jeppesen PB, Nordentoft I, Hermansen K (2005). Stevioside counteracts the cell hypersecretion caused by long-term palmitate exposure. *Am. J. Physiol. Endocrinol. Metab*., **290**: E416-22.

328. Ichiba T, Tanaka A, Ohta Y (1988). Adrenergic control of the glucagon response to ammonia in the perfused rat pancreas. *Diabetes Res. Clin. Pract*., **5**(3): 177-84.

329. Ozaki N, Shibasaki T, Kashima Y, Miki T, Takahashi K, Ueno H, Sunaga Y, Yano H, Matsuura Y, Iwanaga T, Takai Y, Seino S (2000). cAMP-GEFII is a direct target of cAMP in regulated exocytosis. *Nat. Cell. Biol*., **2**: 805-11.

330. Vikman J, Svensson H, Huang YC, Kang Y, Andersson SA, Gaisano HY, Eliasson L (2009). Truncation of SNAP-25 reduces the stimulatory action of cAMP on rapid exocytosis in insulin-secreting cells. *Am. J. Physiol. Endocrinol. Metab*., **297**(2): E452-61.

331. Hayashi M, Yamada H, Uehara S, Morimoto R, Muroyama A, Yatsushiro S, Takeda

J, Yamamoto A, Moriyama Y (2003). Secretory granule-mediated co-secretion of L-glutamate and glucagon triggers glutamatergic signal transmission in islets of Langerhans. *J. Biol. Chem*., **278**(3): 1966-74.

332. Weaver CD, Yao TL, Powers AC, Verdoorn TA (1996). Differential expression of glutamate receptor subtypes in rat pancreatic islets. *J. Biol. Chem*., **271**: 12977-84.

333. Tong Q, Ouedraogo R, Kirchgessner AL (2002). Localization and function of group III metabotropic glutamate receptors in rat pancreatic islets. *Am. J. Physiol. Endocrinol. Metab*., **282**: E1324-33.

334. Uehara S, Muroyama A, Echigo N, Morimoto R, Otsuka M, Yatsushiro S, Moriyama Y (2004). Metabotropic glutamate receptor type 4 is involved in autoinhibitory cascade for glucagon secretion by α-cells of islet of Langerhans. *Diabetes*, **53**: 998-1006.

335. Bertrand G, Gross R, Puech R, Loubatières-Mariani MM, Bockaert J (1993). Glutamate stimulates glucagon secretion via an excitatory amino acid receptor of the AMPA subtype in rat pancreas. *Eur. J. Pharmacol*., **237**(1): 45-50.

336. Cabrera O, Jacques-Silva MC, Speier S, Yang SN, Köhler M, Fachado A, Vieira E, Zierath JR, Kibbey R, Berman DM, Kenyon NS, Ricordi C, Caicedo A, Berggren PO (2008). Glutamate is a positive autocrine signal for glucagon release. *Cell. Metab*., **7**(6): 474-5.

337. Vieira E, Salehi A, Gylfe E (2007). Glucose inhibits glucagon secretion by a direct effect on mouse pancreatic α-cells. *Diabetologia*, **50**(2): 370-9.

338. Asplin C, Raghu P, Dornan T, Palmer JP (1983). Glucose regulation of glucagon secretion independent of β-cell activity. *Metabolism*, **32**(3): 292-5.

339. Ravier MA, Rutter GA (2005). Glucose or insulin, but not zinc ions, inhibit glucagon secretion from mouse pancreatic α-cells. *Diabetes*, **54**(6): 1789-97.

340. Dunbar JC, Brown A (1984). Glucagon secretion by dispersed α cell enriched islets from streptozotocin treated hamsters in perifusion. *Horm. Metab. Res*., **16**(5): 221-5.

341. Franklin I, Gromada J, Gjinovci A, Theander S, Wollheim CB (2005). β-cell secretory products activate α-cell ATP-dependent potassium channels to inhibit glucagon release. *Diabetes*, **54**(6): 1808-15.

342. Iezzi M, Kouri G, Fukuda M, Wollheim CB (2004). Synaptotagmin V and IX isoforms control Ca^{2+}-dependent insulin exocytosis. *J. Cell Sci*., **117**: 3119-27.

343. Hamaguchi K, Leiter EH (1990). Comparison of cytokine effects on mouse pancreatic α-cell and β-cell lines. Viability, secretory function, and MHC antigen

expression. *Diabetes*, **39**(4): 415-25.

344. Powers AC, Efrat S, Mojsov S, Spector D, Habener JF, Hanahan D (1990). Proglucagon processing similar to normal islets in pancreatic α-like cell line derived from transgenic mouse tumor. *Diabetes*, **39**(4): 406-14.

345. Gorus FK, Malaisse WJ, Pipeleers DG (1984). Differences in glucose handling by pancreatic α- and β-cells. *J. Biol. Chem*., **259**: 1196-200.

346. Schuit F, De Vos A, Farfari, Moens K, Pipeleers D, Brun T, Prentki M (1997). Metabolic fate of glucose in purified islet cells. Glucose-regulated anaplerosis in β-cells. *J. Biol. Chem*., **272**:18572-9.

347. Detimary P, Dejonghe S, Ling Z, Pipeleers D, Schuit F, Henquin JC (1998). The changes in adenine nucleotides measured in glucose-stimulated rodent islets occur in β cells but not in cells and are also observed in human islets. *J. Biol. Chem*., **273**: 33905-8.

348. Ishihara H, Maechler P, Gjinovci A, Herrera PL, Wollheim CB (2003). Islet β-cell secretion determines glucagon release from neighboring α-cells. *Nat. Cell Biol*., **5**: 330-5.

349. Ostenson CG (1979). Regulation of glucagon release: effects of insulin on the pancreatic A2-cell of the guinea pig. *Diabetologia*, **17**(5): 325-30.

350. Mercan D, Kadiata MM, Malaisse WJ (1999). Differences in the time course of the metabolic response of β- and non-β pancreatic islet cells to D-glucose and metabolized or non-metabolized hexose esters. *Biochem. Biophys. Res. Commun*., **262**(2): 346-9.

351. Martens GA, Cai Y, Hinke S, Stangé G, Van de Casteele M, Pipeleers D (2005). Glucose suppresses superoxide generation in metabolically responsive pancreatic β-cells. *J. Biol. Chem*., **280**(21): 20389-96.

352. Barg S, Galvanovskis J, Göpel SO, Rorsman P, Eliasson L (2000). Tight coupling between electrical activity and exocytosis in mouse glucagon-secreting α-cells. *Diabetes*, **49**: 1500-10.

353. Leung YM, Ahmed I, Sheu L, Tsushima RG, Diamant NE, Hara M, Gaisano HY (2005). Electrophysiological characterization of pancreatic islet cells in the MIP-GFP mouse. *Endocrinology*, **146**: 4766-75.

354. Rajan AS, Aguilar-Bryan L, Nelson DA, Nichols CG, Wechsler SW, Lechago J, Bryan J (1993). Sulfonylurea receptors and ATP-sensitive K^+ channels in clonal pancreatic α-cells. *J. Biol. Chem*., **268**: 15221-8.

355. Rorsman P, Hellman B (1988). Voltage-activated currents in guinea pig pancreatic A2 cells. Evidence for Ca^{2+}-dependent action potentials. *J. Gen. Physiol*., **91**: 223-42.

356. Gromada J, Ma X, Høy M, Bokvist K, Salehi A, Berggren PO, Rorsman P (2004). ATP-sensitive K^+ channel-dependent regulation of glucagon release and electrical activity by glucose in wild-type and $SUR1^{-/-}$ mouse α-cells. *Diabetes*, **53**(Suppl 3): S181-9.

357. Manning Fox JE, Gyulkhandanyan AV, Satin LS, Wheeler MB (2006). Oscillatory membrane potential response to glucose in islet β-cells: a comparison of islet-cell electrical activity in mouse and rat. *Endocrinology*, **147**(10): 4655-63.

358. Hjortoe GM, Hagel GM, Terry BR, Thastrup O, Arkhammar PO (2004). Functional identification and monitoring of individual α- and β-cells in cultured mouse islets of Langerhans. *Acta. Diabetol*., **41**(4): 185-93.

359. Nadal A, Quesada I, Soria B (1999). Homologous and heterologous asynchronicity between identified α-, β- and δ-cells within intact islets of Langerhans in the mouse. *J. Physiol*., **517**(Pt 1): 85-93.

360. Quesada I, Nadal A, Soria B (1999). Different effects of tolbutamide and diazoxide in α, β-, and δ-cells within intact islets of Langerhans. *Diabetes*, **48**(12): 2390-7.

361. Johansson H, Gylfe E, Hellman B (1987). The actions of arginine and glucose on glucagon secretion are mediated by opposite effects on cytoplasmic Ca^{2+}. *Biochem. Biophys. Res. Commun.*, **147**(1): 309-14.

362. Rorsman P, Salehi SA, Abdulkader F, Braun M, MacDonald PE (2008). K_{ATP}-channels and glucose-regulated glucagon secretion. *Trends Endocrinol. Metab.*, **19**(8): 277-84.

363. Kalkhoff RK, Siegesmund KA (1981). Fluctuations of calcium, phosphorus, sodium, potassium, and chlorine in single α- and β-cells during glucose perifusion of rat islets. *J. Clin. Invest*., **68**(2): 517-24.

364. Asada N, Shibuya I, Iwanaga T, Niwa K, Kanno T (1998). Identification of α- and β-cells in intact isolated islets of Langerhans by their characteristic cytoplasmic Ca^{2+} concentration dynamics and immunocytochemical staining. *Diabetes*, **47**(5): 751-7.

365. Takahashi N, Kishimoto T, Nemoto T, Kadowaki T, Kasai H (2002). Fusion pore dynamics and insulin granule exocytosis in the pancreatic islet. *Science*, **297**(5585): 1349-52.

366. Greenbaum CJ, Prigeon RL, D'Alessio DA (2002). β-cell function, incretin effect, and glucagon suppression in patients with type-I diabetes who have normal fasting glucose. *Diabetes*, **51**: 951-7.

367. Braaten JT, Faloona GR, Unger RH (1974). The effect of insulin on the α-cell

response to hyperglycemia in long-standing alloxan diabetes. *J. Clin. Invest*., **53**(4): 1017-21.

368. Hutton JC, Penn EJ, Peshavaria M (1983). Low-molecular-weight constituents of isolated insulin-secretory granules. Bivalent cations, adenine nucleotides and inorganic phosphate. *Biochem. J*., 210(2): 297-305.

369. Unger RH (1985). Glucagon physiology and pathophysiology in the light of new advances. *Diabetologia*, **28**: 574-8.

370. Raskin P, Fujita Y, Unger RH (1975). Effect of insulin-glucose infusions on plasma glucagon levels in fasting diabetics and nondiabetics. *J. Clin. Invest*., **56**(5): 1132-8.

371. Honey RN, Fallon MB, Weir GC (1980). Effects of exogenous insulin, glucagon, and somatostatin on islet hormone secretion in the perfused chicken pancreas. *Metabolism*, **29**(12): 1242-6.

372. Weir GC, Knowlton SD, Atkins RF, McKennan KX, Martin DB (1976). Glucagon secretion from the perfused pancreas of streptozotocin-treated rats. *Diabetes*, **25**: 275-82.

373. Greenbaum CJ, Havel PJ, Taborsky GJ, Klaff LJ (1991). Intra-islet insulin permits glucose to directly suppress pancreatic α-cell function. *J. Clin. Invest*., **88**: 767-73.

374. Buchanan KD, Mawhinney WA (1973). Insulin control of glucagon release from insulin-deficient rat islets. *Diabetes*, **22**(11): 801-3.

375. Kisanuki K, Kishikawa H, Araki E, Shirotani T, Uehara M, Isami S, Ura S, Jinnouchi H, Miyamura N, Shichiri M (1995). Expression of insulin receptor on clonal pancreatic cells and its possible role for insulin-stimulated negative regulation of glucagon secretion. *Diabetologia*, **38**: 422-9.

376. Maruyama H, Hisatomi A, Orci L, Grodsky GM, Unger RH (1984). Insulin within islets is a physiologic glucagon release inhibitor. *J. Clin. Invest*., **74**(6): 2296-9.

377. Xu E, Kumar M, Zhang Y, Ju W, Obata T, Zhang N, Liu S, Wendt A, Deng S, Ebina Y, Wheeler MB, Braun M, Wang Q (2006). Intra-islet insulin suppresses glucagon release via GABA-$GABA_A$ receptor system. *Cell Metab.*, **3**(1): 47-58.

378. Gyulkhandanyan AV, Lu H, Lee SC, Bhattacharjee A, Wijesekara N, Fox JE, MacDonald PE, Chimienti F, Dai FF, Wheeler MB (2008). Investigation of transport mechanisms and regulation of intracellular Zn^{2+} in pancreatic α-cells. *J. Biol. Chem*., **283**(15): 10184-97.

379. Franklin IK, Wollheim CB (2004). GABA in the endocrine pancreas: its putative role as an islet cell paracrine-signalling molecule. *J. Gen. Physiol*., **123**: 185-90.

380. Thomas-Reetz AC and De Camilli P (1994). A role for synaptic vesicles in non-neuronal cells: clues from pancreatic β-cells and from chromaffin cells. *FASEB J.*, **8**: 209-16.

381. Sorenson RL, Garry DG, Brelje TC (1991). Structural and functional considerations of GABA in islets of Langerhans. *Diabetes*, **40**: 1365-74.

382. MacDonald PE, Obermüller S, Vikman J, Galvanovskis J, Rorsman P, Eliasson L (2005). Regulated exocytosis and kiss-and-run of synaptic-like microvesicles in INS-1 and primary rat β-cells. *Diabetes,* **54**:736-43.

383. Braun M, Wendt A, Birnir B, Broman J, Eliasson L, Galvanovskis J, Gromada J, Mulder H, Rorsman P (2004). Regulated exocytosis of GABA-containing synaptic-like microvesicles in pancreatic β-cells. *J. Gen. Physiol*., **123**(3): 191-204.

384. Gaskins HR, Baldeon ME, Selassie L, Beverly JL (1995). Glucose modulates gamma-aminobutyric acid release from the pancreatic βTC6 cell line. *J. Biol. Chem*., **270**: 30286-9.

385. Nagamatsu ST, Watanabe T, Nakamichi Y, Yamamura C, Tsuzuki K, Matsushima S (1999). α-Soluble N-ethylmaleimide-sensitive factor attachment protein is expressed in pancreatic β-cells and functions in insulin but not γ-aminobutyric acid secretion. *J. Biol. Chem*., **274**: 8053-60.

386. Winnock F, Ling Z, De Proft R, Dejonghe S, Schuit F, Gorus F, Pipeleers D (2001). Correlation between GABA release from rat islet β-cells and their metabolic state. *Am. J. Physiol. Endocrinol. Metab*., **282**: E937-42.

387. Wang C, Kerckhofs K, Van de Casteele M, Smolders I, Pipeleers D, Ling Z (2006). Glucose inhibits GABA release by pancreatic β-cells through an increase in GABA shunt activity. *Am. J. Physiol. Endocrinol. Metab*., **290**(3): E494-9.

388. Smismans A, Schuit F, Pipeleers D (1997). Nutrient regulation of gamma-aminobutyric acid release from islet β-cells. *Diabetologia,* **40**(12): 1411-5.

389. Rorsman P, Berggren PO, Bokvist K, Ericson H, Möhler H, Ostenson CG, Smith PA (1989). Glucose-inhibition of glucagon secretion involves activation of $GABA_A$-receptor chloride channels. *Nature*, **341**(6239): 233-6.

390. Gilon P, Bertrand G, Loubatières-Mariani MM, Remacle C, Henquin JC (1991). The influence of gamma-aminobutyric acid on hormone release by the mouse and rat endocrine pancreas. *Endocrinology*, **129**(5): 2521-9.

391. Bailey SJ, Ravier MA, Rutter GA (2007). Glucose-dependent regulation of gamma-aminobutyric acid ($GABA_A$) receptor expression in mouse pancreatic islet α-cells.

Diabetes, **56**: 320-7.

392. Tudurí E, Filiputti E, Carneiro EM, Quesada I (2008). Inhibition of Ca^{2+} signaling and glucagon secretion in mouse pancreatic α-cells by extracellular ATP and purinergic receptors. *Am. J. Physiol. Endocrinol. Metab*., **294**(5): E952-60.

393. Hazama A, Hayashi S, Okada Y (1998). Cell surface measurements of ATP release from single pancreatic β-cells using a novel biosensor technique. *Pflugers Arch*., **437**(1): 31-5.

394. Fields RD, Burnstock G (2006). Purinergic signalling in neuron-glia interactions. *Nat. Rev. Neurosci*., **7**: 423-36.

395. Chapal J, Loubatieres-Mariani MM, Petit P, Roye M (1985). Evidence for an A2-subtype adenosine receptor on pancreatic glucagon secreting cells. *Br. J. Pharmacol*., **86**: 565-9.

396. Poulsen CR, Bokvist K, Olsen HL, Hoy M, Capito K, Gilon P, Gromada J (1999). Multiple sites of purinergic control of insulin secretion in mouse pancreatic β-cells. *Diabetes*, **48**: 2171-81.

397. Brazeau P, Vale W, Burgus R, Ling N, Butcher M, Rivier J, Guillemin R (1973). Hypothalamic polypeptide that inhibits the secretion of immunoreactive pituitary growth hormone. *Science*, **179**(4068): 77-9.

398. Patel YC (1999). Somatostatin and its receptor family. *Front Neuroendocrinol*., **20**(3): 157-98.

399. Dubois MP (1975). Immunoreactive somatostatin is present in discrete cells of the endocrine pancreas. *Proc. Natl. Acad. Sci. USA*, **72**: 1340-3.

400. Koerker DJ, Ruch W, Chideckel E, Palmer J, Goodner CJ, Ensinck J, Gale CC (1974). Somatostatin: hypothalamic inhibitor of the endocrine pancreas. *Science*, **184**(135): 482-4.

401. Strowski MZ, Parmar RM, Blake AD, Schaeffer JM (2000). Somatostatin inhibits insulin and glucagon secretion via two receptors subtypes: an in vitro study of pancreatic islets from somatostatin receptor 2 knockout mice. *Endocrinology*, **141**: 111-7.

402. Ludvigsen E, Olsson R, Stridsberg M, Janson ET, Sandler S (2004). Expression and distribution of somatostatin receptor subtypes in the pancreatic islets of mice and rats. *J. Histochem. Cytochem.*, **52**: 391-400.

403. Kumar U, Sasi R, Suresh S, Patel A, Thangaraju M, Metrakos P, Patel SC, Patel YC (1999). Subtype-selective expression of the five somatostatin receptors (hSSTR1-5) in

human pancreatic islet cells: a quantitative double-label immunohistochemical analysis. *Diabetes*, **48**: 77–85.

404. Singh V, Brendel MD, Zacharias S, Mergler S, Jahr H, Wiedenmann B, Bretzel RG, Plöckinger U, Strowski MZ (2007). Characterization of somatostatin receptor subtype-specific regulation of insulin and glucagon secretion: an in vitro study on isolated human pancreatic islets. *J. Clin. Endocrinol. Metab.*, **92**(2): 673-80.

405. Hauge-Evans AC, King AJ, Carmignac D, Richardson CC, Robinson IC, Low MJ, Christie MR, Persaud SJ, Jones PM (2009). Somatostatin secreted by islet δ-cells fulfills multiple roles as a paracrine regulator of islet function. *Diabetes*, **58**(2): 403-11.

406. Yoshimoto Y, Fukuyama Y, Horio Y, Inanobe A, Gotoh M, Kurachi Y (1999). Somatostatin induces hyperpolarization in pancreatic islet α-cells by activating a G protein-gated K^+ channel. *FEBS Lett.*, **444**: 265-9.

407. Gromada J, Høy M, Buschard K, Salehi A, Rorsman P (2001). Somatostatin inhibits exocytosis in rat pancreatic α-cells by G_{i2}-dependent activation of calcineurin and depriming of secretory granules. *J. Physiol*., **535**: 519-32.

408. Fehmann HC, Strowski M, Göke B (1995). Functional characterization of somatostatin receptors expressed on hamster glucagonoma cells. *Am. J. Physiol*., **268**(1 Pt 1): E40-7.

409. Kadowaki S, Taminato T, Chiba T, Goto Y, Nozawa M, Seino Y, Matsukura S, Fujita T (1980). Somatostatin release from the isolated, perfused diabetic rat pancreas: inverse relationship between pancreatic somatostatin and insulin. *Diabetes*, **29**(12): 960-3.

410. Schusdziarra V, Rouiller D, Harris V, Unger RH (1981). Origin of peripheral venous hypersomatostatinemia in alloxan-diabetic dogs. *Endocrinology*, **109**(4): 1107-16.

411. Orci L, Baetens D, Rufener C, Amherdt M, Ravazzola M, Studer P, Malaisse-Lagae F, Unger RH (1976). Hypertrophy and hyperplasia of somatostatin-containing δ-cells in diabetes. *Proc. Natl. Acad. Sci. USA*, **73**(4): 1338-42.

412. Ruggere MD, Patel YC (1984). Somatostatin, glucagon, and insulin secretion from perfused pancreas of BB rats. *Am. J. Physiol*., **247**(2 Pt 1): E221-7.

413. Tabata M, Shima K, Tanaka R, Tanaka A, Ota T, Sawazaki N, Kumahara Y (1981). Changes in somatostatin release from perfused pancreas of streptozotocin-induced diabetic rats. *Endocrinol. Jpn*., **28**(2): 101-9.

414. Hara M, Patton G, Gerich J (1979). Increased somatostatin release from pancreases of alloxan diabetic rats perfused in vitro. *Life Sci.*, **24**(7): 625-8.

415. Quesada I, Todorova MG, Alonso-Magdalena P, Beltrá M, Carneiro EM, Martin F, Nadal A, Soria B (2006). Glucose induces opposite intracellular Ca^{2+} concentration oscillatory patterns in identified α- and β-cells within intact human islets of Langerhans. *Diabetes*, **55**(9): 2463-9.

416. Michaels RL, Sheridan JL (1981). Islets of Langerhans: dye coupling among immunocytochemically distinct cell types. *Science*s, **214**(4522):801-3.

417. Meda P, Santos RM, Atwater I (1986). Direct identification of electrophysiologically monitored cells within intact mouse islets of Langerhans. *Diabetes*, **35**(2): 232-6.

418. Fletcher DJ, Grogan WM, Barras E, Weir GC (1983). Hormone release by islet β-cell-enriched, and α- and δ-cell-enriched populations prepared by flow cytometry. *Endocrinology*, **113**(5): 1791-8.

419. Vignali S, Leiss V, Karl R, Hofmann F, Welling A (2006). Characterization of voltage-dependent sodium and calcium channels in mouse pancreatic α- and β-cells. *J. Physiol*., **572**(Pt 3): 691-706.

420. Quoix N, Cheng-Xue R, Guiot Y, Herrera PL, Henquin JC, Gilon P (2007). The GluCre-ROSA26EYFP mouse: a new model for easy identification of living pancreatic α-cells. *FEBS Lett.*, **581**(22): 4235-40.

421. Gee KR, Brown KA, Chen WN, Bishop-Stewart J, Gray D, Johnson I (2000). Chemical and physiological characterization of Fluo-4 Ca^{2+}-indicator dyes. *Cell Calcium*, **27**(2): 97-106.

422. Luche H, Weber O, Nageswara Rao T, Blum C, Fehling HJ (2007). Faithful activation of an extra-bright red fluorescent protein in "knock-in" Cre-reporter mice ideally suited for lineage tracing studies. *Eur. J. Immunol*., **37**(1): 43-53.

423. van Suylichem PT, Wolters GH, van Schilfgaarde R (1992). Peri-insular presence of collagenase during islet isolation procedures. *J. Surg. Res*., **53**(5): 502-9.

424. McDonald JC, Duffy DC, Anderson JR, Chiu DT, Wu H, Schueller OJ, Whitesides GM (2000). Fabrication of microfluidic systems in poly(dimethylsiloxane). *Electrophoresis*, **21**(1): 27-40.

425. Bräuner T, Hülser DF, Strasser RJ (1984). Comparative measurements of membrane potentials with microelectrodes and voltage-sensitive dyes. *Biochim. Biophys. Acta*., **771**(2): 208-16.

426. Yamada A, Gaja N, Ohya S, Muraki K, Narita H, Ohwada T, Imaizumi Y (2001). Usefulness and limitation of $DiBAC_4(3)$, a voltage-sensitive fluorescent dye, for the

measurement of membrane potentials regulated by recombinant large conductance Ca^{2+}-activated K^+ channels in HEK293 cells. *Jpn J. Pharmacol*., **86**(3): 342-50.

427. Herrera PL (2000). Adult insulin- and glucagon-producing cells differentiate from two independent cell lineages. *Development*, **127**(11): 2317-22.

428. Sauer B (1998). Inducible gene targeting in mice using the Cre/lox system. *Methods*, **14**(4): 381-92.

429. Takahashi R, Ishihara H, Tamura A, Yamaguchi S, Yamada T, Takei D, Katagiri H, Endou H, Oka Y (2006). Cell type-specific activation of metabolism reveals that β-cell secretion suppresses glucagon release from α-cells in rat pancreatic islets. *Am. J. Physiol. Endocrinol. Metab*., **290**(2): E308-16.

430. Soriano P (1999). Generalized lacZ expression with the ROSA26 Cre reporter strain. *Nat. Genet*., **21**(1): 70-1.

431. Srinivas S, Watanabe T, Lin CS, William CM, Tanabe Y, Jessell TM, Costantini F (2001). Cre reporter strains produced by targeted insertion of EYFP and ECFP into the ROSA26 locus. *BMC Dev. Biol*., **1**: 4.

432. Postic C, Shiota M, Niswender KD, Jetton TL, Chen Y, Moates JM, Shelton KD, Lindner J, Cherrington AD, Magnuson MA (1999). Dual roles for glucokinase in glucose homeostasis as determined by liver and pancreatic β-cell-specific gene knock-outs using Cre recombinase. *J. Biol. Chem*., **274**(1): 305-15.

433. A monomeric red fluorescent protein. Campbell RE, Tour O, Palmer AE, Steinbach PA, Baird GS, Zacharias DA, Tsien RY. 2002, *Proc. Natl. Acad. Sci. USA*, **99**(12): 7877-82.

434. Bowman BJ, Draskovic M, Freitag M, Bowman EJ (2009). Structure and distribution of organelles and cellular location of calcium transporters in Neurospora crassa. *Eukaryot. Cell*, **8**(12): 1845-55.

435. Martin DIK, Whitelaw E (1996). The vagaries of variegating transgenes. *BioEssays*, **18**: 919-23.

436. Herbert J, Wilcox JN, Pham KT, Fremeau RT Jr, Zeviani M, Dwork A, Soprano DR, Makover A, Goodman DS, Zimmerman EA, Roberts JL, Schon EA (1986). Transthyretin: a choroid plexus-specific transport protein in human brain. *Neurology*, **36**(7): 900-11.

437. Jacobsson B, Collins VP, Grimelius L, Pettersson T, Sandstedt B, Carlström A (1989). Transthyretin immunoreactivity in human and porcine liver, choroid plexus, and pancreatic islets. *J. Histochem. Cytochem*., **37**(1): 31-7.

438. Jacobsson T, Pettersson T, Sandstedt B and Carlström A (1979). Prealbumin in the islets of Langerhans. *IRCS Med. Sci*., **7**: 590.

439. Itoh N, Hanafusa T, Miyagawa J, Tamura S, Inada M, Kawata S, Kono N, Tarui S (1992). Transthyretin (prealbumin) in the pancreas and sera of newly diagnosed type-I (insulin-dependent) diabetic patients. *J. Clin. Endocrinol. Metab.*, **74**(6): 1372-7.

440. Westermark GT, Westermark P (2008). Transthyretin and amyloid in the islets of Langerhans in type-II diabetes. *Exp. Diabetes Res*., **2008**: 429274.

441. Yamada K, Nakata M, Horimoto N, Saito M, Matsuoka H, Inagaki N (2000). Measurement of glucose uptake and intracellular calcium concentration in single, living pancreatic β-cells. *J. Biol. Chem*., **275**(29): 22278-83.

442. De Vos A, Heimberg H, Quartier E, Huypens P, Bouwens L, Pipeleers D, Schuit F (1995). Human and rat β-cells differ in glucose transporter but not in glucokinase gene expression. *J. Clin. Invest*., **96**(5): 2489-95.

443. Hara M, Wang X, Kawamura T, Bindokas VP, Dizon RF, Alcoser SY, Magnuson MA, Bell GI (2003). Transgenic mice with green fluorescent protein-labeled pancreatic β-cells. *Am. J. Physiol. Endocrinol. Metab*., **284**(1): E177-83.

444. Kawamori D, Kurpad AJ, Hu J, Liew CW, Shih JL, Ford EL, Herrera PL, Polonsky KS, McGuinness OP, Kulkarni RN (2009). Insulin signaling in α-cells modulates glucagon secretion in vivo. *Cell Metab.*, **9**(4): 303-5.

445. VanEngelenburg SB, Palmer AE (2008). Fluorescent biosensors of protein function. *Curr. Opin. Chem. Biol*., **12**(1): 60-5.

446. Grapengiesser E (1998). Glucagon amplifies tetrodotoxin-resistant Na^+ oscillations in glucose-stimulated pancreatic β-cells. *Exp. Clin. Endocrinol. Diabetes*, **106**(4): 303-9.

447. Braun M, Ramracheya R, Bengtsson M, Zhang Q, Karanauskaite J, Partridge C, Johnson PR, Rorsman P (2008). Voltage-gated ion channels in human pancreatic β-cells: electrophysiological characterization and role in insulin secretion. *Diabetes*, **57**(6): 1618-28.

448. Muñoz A, Hu M, Hussain K, Bryan J, Aguilar-Bryan L, Rajan AS (2005). Regulation of glucagon secretion at low glucose concentrations: evidence for adenosine triphosphate-sensitive potassium channel involvement. *Endocrinology*, **146**(12): 5514-21.

449. Ricordi C, Gray DW, Hering BJ, Kaufman DB, Warnock GL, Kneteman NM, Lake SP, London NJ, Socci C, Alejandro R, Zeng Y, Scharp DW, Viviani G, Falqui L, Tzakis A, Bretzel RG, Federlin K, Pozza G, James RFL, Rajotte RV, Di Carlo V, MOrris PJ, Sutherland DER (1990). Islet isolation assessment in man and large animals. *Acta.*

Diabetol. Lat., **27**(3): 185-95.

450. Burgoyne RD, Morgan A (2003). Secretory granule exocytosis. *Physiol. Rev.*, **83**(2): 581-632.

451. Barclay JW, Morgan A, Burgoyne RD (2005). Calcium-dependent regulation of exocytosis. *Cell Calcium*, **38**(3-4): 343-53.

452. Berts A, Gylfe E, Hellman B (1995). Ca^{2+} oscillations in pancreatic islet cells secreting glucagon and somatostatin. *Biochem. Biophys. Res. Commun.*, **208**(2): 644-9.

453. Kasai H, Aosaki T, Fukuda J (1987). Synaptic Ca-antagonist ω-conotoxin irreversibly blocks N-type Ca-channels in chick sensory neurons. *Neurosci. Res.*, **4**(3): 228-35.

454. Yamada H, Otsuka M, Hayashi M, Nakatsuka S, Hamaguchi K, Yamamoto A, Moriyama Y (2001). Ca^{2+}-dependent exocytosis of L-glutamate by αTC6, clonal mouse pancreatic α-cells. *Diabetes*, **50**(5): 1012-20.

455. Randriamampita C, Bismuth G, Debré P, Trautmann A (1991). Nitrendipine-induced inhibition of calcium influx in a human T-cell clone: role of cell depolarization. *Cell Calcium*, **12**(4): 313-23.

456. Lewis RS, Cahalan MD (1995). Potassium and calcium channels in lymphocytes. *Annu. Rev. Immunol.*, **13**: 623-53.

457. Kanno T, Suga S, Wu J, Kimura M, Wakui M (1998). Intracellular cAMP potentiates voltage-dependent activation of L-type Ca^{2+} channels in rat islet β-cells. *Pflugers Arch.*, **435**(4): 578-80.

458. Henquin JC (2000). Triggering and amplifying pathways of regulation of insulin secretion by glucose. *Diabetes*, **49**(11): 1751-60.

459. Ronner P, Matschinsky FM, Hang TL, Epstein AJ, Buettger C (1993). Sulfonylurea-binding sites and ATP-sensitive K^+ channels in α-TC glucagonoma and β-TC insulinoma cells. *Diabetes*, **42**(12): 1760-72.

460. Rajan AS, Aguilar-Bryan L, Nelson DA, Nichols CG, Wechsler SW, Lechago J, Bryan J (1993). Sulfonylurea receptors and ATP-sensitive K^+ channels in clonal pancreatic α-cells. Evidence for two high affinity sulfonylurea receptors. *J. Biol. Chem.*, **268**(20): 15221-8.

461. Nichols CG (2006). K_{ATP} channels as molecular sensors of cellular metabolism. *Nature*, **440**(7083): 470-6.

462. Doliba NM, Qin W, Vatamaniuk MZ, Buettger CW, Collins HW, Magnuson MA, Kaestner KH, Wilson DF, Carr RD, Matschinsky FM (2006). Cholinergic regulation of fuel-induced hormone secretion and respiration of $SUR1^{-/-}$ mouse islets. *Am. J. Physiol. Endocrinol. Metab.*, **291**(3): E525-35.

463. Miki T, Liss B, Minami K, Shiuchi T, Saraya A, Kashima Y, Horiuchi M, Ashcroft F, Minokoshi Y, Roeper J, Seino S (2001). ATP-sensitive K^+ channels in the hypothalamus are essential for the maintenance of glucose homeostasis. *Nat. Neurosci.*, **4**(5): 459-60.

464. Proks P, Reimann F, Green N, Gribble F, Ashcroft F (2002). Sulfonylurea stimulation of insulin secretion. *Diabetes*, **51**(Suppl 3): S368-76.

465. Berts A, Ball A, Gylfe E, Hellman B (1996). Suppression of Ca^{2+} oscillations in glucagon-producing α-cells by insulin/glucose and amino acids. *Biochim. Biophys. Acta.*, **1310**(2): 212-6.

466. Loubatières AL, Loubatiéres-Mariani MM, Alric R, Ribes G (1974). Tolbutamide and glucagon secretion. *Diabetologia*, **10**(4): 271-6.

467. Hermansen K (1982). Tolbutamide, glucose, calcium, and somatostatin secretion. *Acta. Endocrinologica*, **99**(1): 86-93.

468. Høy M, Olsen HL, Bokvist K, Buschard K, Barg S, Rorsman P, Gromada J (2000). Tolbutamide stimulates exocytosis of glucagon by inhibition of a mitochondrial-like ATP-sensitive K^+ (K_{ATP}) conductance in rat pancreatic α-cells. *J. Physiol.*, **527**(Pt 1): 109-20.

469. Singh V, Brendel MD, Zacharias S, Mergler S, Jahr H, Wiedenmann B, Bretzel RG, Plöckinger U, Strowski MZ (2007). Characterization of somatostatin receptor subtype-specific regulation of insulin and glucagon secretion: an in vitro study on isolated human pancreatic islets. *J. Clin. Endocrinol. Metab.*, **92**(2): 673-80.

470. Bennett BD, Jetton TL, Ying G, Magnuson MA, Piston DW (1996). Quantitative subcellular imaging of glucose metabolism within intact pancreatic islets. *J. Biol. Chem.*, **271**(7): 3647-51.

471. Magnuson MA and Matschinsky FM (2004). Glucokinase and glycemic disease: from basics to novel therapeutics. *Frontiers in Diabetes*, **16**: 1-17.

472. Piston DW, Knobel SM (1999). Quantitative imaging of metabolism by two-photon excitation microscopy. *Methods Enzymol.*, **307**: 351-68.

473. Patterson GH, Knobel SM, Arkhammar P, Thastrup O, Piston DW (2000). Separation of the glucose-stimulated cytoplasmic and mitochondrial NAD(P)H responses

in pancreatic islet β-cells. *Proc. Natl. Acad. Sci. USA*, **97**(10): 5203-7.

474. Unger RH (1971). Glucagon physiology and pathophysiology. *N. Engl. J. Med.*, **285**(8): 443-9.

475. Eng J, Lynch RM, Balaban RS (1989). Nicotinamide adenine dinucleotide fluorescence spectroscopy and imaging of isolated cardiac myocytes. *Biophys. J.*, **55**(4): 621-30.

476. Manjunath BK, Kurein J, Rao L, Murali Krishna C, Chidananda MS, Venkatakrishna K and Kartha VB (2004). Autofluorescence of oral tissue for optical pathology in oral malignancy . *J. Photochem. and Photobiol*., **73**(1-2): 49-58.

477. Wagnieres GA, Star WM and Wilson BC (1998). In vivo fluorescence spectroscopy and imaging for oncological applications. *Photochem. and Photobiol*., **68**(5): 603-32.

478. Coore HG, Randle PJ (1964). Inhibition of glucose phosphorylation by mannoheptulose. *Biochem. J*., **91**(1): 56-9.

479. Sweet IR, Li G, Najafi H, Berner D, Matschinsky FM (1996). Effect of a glucokinase inhibitor on energy production and insulin release in pancreatic islets. *Am. J. Physiol*., **271**(3 Pt 1): E606-25.

480. Ehrenberg B, Montana V, Wei MD, Wuskell JP, Loew LM (1988). Membrane potential can be determined in individual cells from the nernstian distribution of cationic dyes. *Biophys. J.*, **53**(5): 785-94.

481. Wikstrom JD, Katzman SM, Mohamed H, Twig G, Graf SA, Heart E, Molina AJ, Corkey BE, de Vargas LM, Danial NN, Collins S, Shirihai OS (2007). β-Cell mitochondria exhibit membrane potential heterogeneity that can be altered by stimulatory or toxic fuel levels. *Diabetes*, **56**(10): 2569-78.

482. Hellman B, Sehlin J, Täljedal I (1971). Uptake of alanine, arginine and leucine by mammalian pancreatic β-cells. *Endocrinology*, **89**(6): 1432-9.

483. Morris SM (2009). Recent advances in arginine metabolism: roles and regulation of the arginases. *Br. J. Pharmacol*., **157**(6): 922-30.

484. Stickings P, Mistry SK, Boucher JL, Morris SM, Cunningham JM (2002). Arginase expression and modulation of IL-1β-induced nitric oxide generation in rat and human islets of Langerhans. *Nitric Oxide*, **7**(4): 289-96.

485. Rocheleau JV, Head WS, Nicholson WE, Powers AC, Piston DW (2002). Pancreatic islet β-cells transiently metabolize pyruvate. *J. Biol. Chem*., **277**(34): 30914-20.

486. Weir GC, Halban PA, Meda P, Wollheim CB, Orci L, Renold AE (1984). Dispersed adult rat pancreatic islet cells in culture: α-, β-, and δ-cell function. *Metabolism*, **33**(5): 447-53.

487. Weir GC, Leahy JL, Barras E, Braunstein LP (1986). Characteristics of insulin and glucagon release from the perfused pancreas, intact isolated islets, and dispersed islet cells. *Horm. Res*., **24**(1): 62-72.

488. Malaisse WJ (2001). On the track to the β-cell. *Diabetologia*, **44**(4): 393-406.

489. Konstantinova I, Nikolova G, Ohara-Imaizumi M, Meda P, Kucera T, Zarbalis K, Wurst W, Nagamatsu S, Lammert E (2007). EphA-Ephrin-A-mediated β-cell communication regulates insulin secretion from pancreatic islets. *Cell*, **129**(2): 359-70.

490. Hahn HJ, Ziegler M (1977). Investigations on isolated islets of Langerhans in vitro. 16. Modification of the glucose-dependent inhibition of glucagon secretion. *Biochim. Biophys. Acta*., **499**(3): 362-72.

491. Malaisse WJ, Blachier F, Mourtada A, Camara J, Albor A, Valverde I, Sener A (1989). Stimulus-secretion coupling of arginine-induced insulin release. Metabolism of L-arginine and L-ornithine in pancreatic islets. *Biochim. Biophys. Acta*., **1013**(2): 133-43.

492. Blachier F, Mourtada A, Sener A, Malaisse WJ (1989). Stimulus-secretion coupling of arginine-induced insulin release. Uptake of metabolized and nonmetabolized cationic amino acids by pancreatic islets. *Endocrinology*, **124**(1): 134-41.

493. Grynkiewicz G, Poenie M, Tsien RY (1985). A new generation of Ca^{2+} indicators with greatly improved fluorescence properties. *J. Biol. Chem*., **260**(6): 3440-50.

494. Cannell MB, Cheng H, Lederer WJ (1994). Spatial non-uniformities in $[Ca^{2+}]_i$ during excitation-contraction coupling in cardiac myocytes. *Biophys. J.*, **67**(5): 1942-56.

495. Kurebayashi N, Harkins AB, Baylor SM (1993). Use of Fura red as an intracellular calcium indicator in frog skeletal muscle fibers. *Biophys. J.*, **64**(6): 1934-60.

496. Gilon P, Henquin JC (1992). Influence of membrane potential changes on cytoplasmic Ca^{2+} concentration in an electrically excitable cell, the insulin-secreting pancreatic β-cell. *J. Biol. Chem*., **267**(29): 20713-20.

497. Cejvan K, Coy DH, Efendic S (2003). Intra-islet somatostatin regulates glucagon release via type-II somatostatin receptors in rats. *Diabetes*, **52**(5): 1176-81.

498. Sandison DR, Piston DW, Williams RM, Webb WW (1995). Quantitative comparison of background rejection, signal-to-noise ratio, and resolution in confocal and full-field laser scanning microscopes. *Applied Optics*, **34**(19): 3576-88.

499. Wollheim CB, Sharp GW (1981). Regulation of insulin release by calcium. *Physiol. Rev*., **61**(4): 914-73.

500. Høy M, Bokvist K, Xiao-Gang W, Hansen J, Juhl K, Berggren PO, Buschard K, Gromada J (2001). Phentolamine inhibits exocytosis of glucagon by G_{i2} protein-dependent activation of calcineurin in rat pancreatic α-cells. *J. Biol. Chem*., **276**(2): 924-30.

501. Göpel S, Kanno T, Barg S, Galvanovskis J, Rorsman P (1999). Voltage-gated and resting membrane currents recorded from β-cells in intact mouse pancreatic islets. *J. Physiol*., **521**(3): 717-28.

502. Sturis J, Pugh WL, Tang J, Ostrega DM, Polonsky JS, Polonsky KS (1994). Alterations in pulsatile insulin secretion in the Zucker diabetic fatty rat. *Am. J. Physiol*., **267**(2 Pt 1): E250-9.

503. Harris AL (2007). Connexin channel permeability to cytoplasmic molecules. *Prog. Biophys. Mol. Biol*., **94**(1-2): 120-43.

504. Kohen E, Kohen C, Thorell B, Mintz DH, Rabinovitch A (1979). Intercellular communication in pancreatic islet monolayer cultures: a microfluorometric study. *Science*, **204**(4395): 862-5.

505. Meda P, Michaels RL, Halban PA, Orci L, Sheridan JD (1983). In vivo modulation of gap junctions and dye coupling between β-cells of the intact pancreatic islet. *Diabetes*, **32**(9): 858-68.

506. Eddlestone GT, Gonçalves A, Bangham JA, Rojas E (1984). Electrical coupling between cells in islets of Langerhans from mouse. *J. Membr. Biol*., **77**(1): 1-14.

507. In't Veld PA, Pipeleers DG, Gepts W (1986). Glucose alters configuration of gap junctions between pancreatic islet cells. *Am. J. Physiol*., **251**(2 Pt 1): C191-6.

508. Dakin K, Li WH (2006). Infrared-LAMP: two-photon uncaging and imaging of gap junctional communication in three dimensions. *Nat. Methods*, **3**(12): 959.

509. Mears D, Sheppard NF Jr, Atwater I, Rojas E (1995). Magnitude and modulation of pancreatic β-cell gap junction electrical conductance in situ. *J. Membr. Biol*., **146**(2): 163-76.

510. Sherman A, Xu L, Stokes CL (1995). Estimating and eliminating junctional current in coupled cell populations by leak subtraction. A computational study. *J. Membr. Biol*., **143**(1): 79-87.

511. Zhang M, Goforth P, Bertram R, Sherman A, Satin L (2003). The Ca^{2+} dynamics of

isolated mouse β-cells and islets: implications for mathematical models. *Biophys. J.*, **84**(5): 2852-70.

512. Hamill OP, Marty A, Neher E, Sakmann B, Sigworth FJ (1981). Improved patch-clamp techniques for high-resolution current recording from cells and cell-free membrane patches. *Pflugers Arch.*, **391**(2): 85-100.

513. Zhao Y, Zheng Q, Dakin K, Xu K, Martinez ML, Li WH (2004). New caged coumarin fluorophores with extraordinary uncaging cross sections suitable for biological imaging applications. *J. Am. Chem. Soc.*, **126**(14): 4653-63.

514. Dakin K, Zhao Y, Li WH (2005). LAMP, a new imaging assay of gap junctional communication unveils that Ca2+ influx inhibits cell coupling. *Nat. Methods*, **2**(1): 55-62.

515. Goldberg GS, Moreno AP, Lampe PD (2002). Gap junctions between cells expressing connexin-43 or -32 show inverse permselectivity to adenosine and ATP. *J. Biol. Chem.*, **277**(39): 36725-30.

516. Teubner B, Degen J, Söhl G, Güldenagel M, Bukauskas FF, Trexler EB, Verselis VK, De Zeeuw CI, Lee CG, Kozak CA, Petrasch-Parwez E, Dermietzel R, Willecke K (2000). Functional expression of the murine connexin-36 gene coding for a neuron-specific gap junctional protein. *J. Membr. Biol.*, **176**(3): 249-62.

517. Moreno AP, Berthoud VM, Pérez-Palacios G, Pérez-Armendariz EM (2005). Biophysical evidence that connexin-36 forms functional gap junction channels between pancreatic mouse β-cells. *Am. J. Physiol. Endocrinol. Metab.*, **288**(5): E948-56.

518. Piston DW (1999). Imaging living cells and tissues by two-photon excitation microscopy. *Trends Cell Biol.*, **9**(2): 66-9.

519. Davidson JS, Baumgarten IM (1988). Glycyrrhetinic acid derivatives: a novel class of inhibitors of gap-junctional intercellular communication. Structure-activity relationships. *J. Pharmacol. Exp. Ther.*, **246**(3): 1104-7.

520. Cruikshank SJ, Hopperstad M, Younger M, Connors BW, Spray DC, Srinivas M (2004). Potent block of Cx36 and Cx50 gap junction channels by mefloquine. *Proc. Natl. Acad. Sci. USA*, **101**(33): 12364-9.

521. Veruki ML, Hartveit E (2009). Meclofenamic acid blocks electrical synapses of retinal AII amacrine and on-cone bipolar cells. *J. Neurophysiol.*, **101**(5): 2339-47.

522. D'Ambra R, Surana M, Efrat S, Starr RG, Fleischer N (1990). Regulation of insulin secretion from β-cell lines derived from transgenic mice insulinomas resembles that of normal β-cells. *Endocrinology*, **126**(6): 2815-22.

523. Calabrese A, Zhang M, Serre-Beinier V, Caton D, Mas C, Satin LS, Meda P (2003). Connexin 36 controls synchronization of Ca^{2+} oscillations and insulin secretion in MIN6 cells. *Diabetes*, **52**(2): 417-24.

524. Di Virgilio F (1995). The P2Z purinoceptor: an intriguing role in immunity, inflammation and cell death. *Immunol. Today*, **16**(11): 524-8.

525. Diena T, Melani R, Caci E, Pedemonte N, Sondo E, Zegarra-Moran O, Galietta LJ (2007). Block of CFTR-dependent chloride currents by inhibitors of multidrug resistance-associated proteins. *Eur. J. Pharmacol.*, **560**(2-3): 127-31.

526. Di Virgilio F, Steinberg TH, Silverstein SC (1990). Inhibition of Fura-2 sequestration and secretion with organic anion transport blockers. *Cell Calcium*, **11**(2-3): 57-62.

527. Silverman W, Locovei S, Dahl G (2008). Probenecid, a gout remedy, inhibits pannexin-1 channels. *Am. J. Physiol. Cell Physiol.*, **295**(3): C761-7.

528. Quesada I, Fuentes E, Andreu E, Meda P, Nadal A, Soria B (2003). On-line analysis of gap junctions reveals more efficient electrical than dye coupling between islet cells. *Am. J. Physiol. Endocrinol. Metab.*, **284**(5): E980-7.

529. Kilkenny DM, Rocheleau JV (2008). Fibroblast growth factor receptor-1 signaling in pancreatic islet β-cells is modulated by the extracellular matrix. *Mol. Endocrinol.*, **22**(1): 196-205.

530. Miesenböck G, De Angelis DA, Rothman JE (1998). Visualizing secretion and synaptic transmission with pH-sensitive green fluorescent proteins. *Nature*, **394**(6689): 192-5.

531. Rizzo MA, Davidson MW and Piston DW (2010). Fluorescence protein tracking and detection in live cells. *Cold Spring Harbor Lab Press*, 3-34.

532. Orci L, Malaisse-Lagae F, Amherdt M, Ravazzola M, Weisswange A, Dobbs R, Perrelet A, Unger RH (1975). Cell contacts in human islets of Langerhans. *J. Clin. Endocrinol. Metab.*, **41**(5): 841-4.

533. Orci L, Malaisse-Lagae F, Ravazzola M, Rouiller D, Renold AE, Perrelet A, Unger R (1975). A morphological basis for intercellular communication between α- and β-cells in the endocrine pancreas. *J. Clin. Invest.*, **56**(4): 1066-70.

534. Ahmed M, Nuttall FQ, Gannon MC, Lamusga RF (1980). Plasma glucagon and alpha-amino acid nitrogen response to various diets in normal humans. *Am. J. Clin. Nutr.*, **33**(9):1917-24.

535. Rojdmark S, Bloom G, Chou MC, Jaspan JB, Field JB (1978). Hepatic insulin and glucagon extraction after their augmented secretion in dogs. *Am. J. Physiol*., **235**(1):E88-E96.

536. Eaton RP, Kipnis DM, Karl I, Eisenstein AB (1974). Effects of glucose feeding on insulin and glucagon secretion and hepatic gluconeogenesis in the rat. *Am. J. Physiol*., **227**(1):101-4.

537. Narahashi T, Tsunoo A, Yoshii M (1987). Characterization of two types of calcium channels in mouse neuroblastoma cells. *J. Physiol*., **383**:231-49.

538. Falke LC, Gillis KD, Pressel DM, Misler S (1989). 'Perforated patch recording' allows long-term monitoring of metabolite-induced electrical activity and voltage-dependent Ca2+ currents in pancreatic islet β-cells. *FEBS Lett*. **251**(1-2):167-72.